**University of Bath**

**PHD**

# Endothelial colony forming cells (ECFCs) and biomaterials: a synergy for next-generation cardiovascular implants

Fortunato, Tiago

*Award date:*
2017

*Awarding institution:*
University of Bath

Link to publication

## Alternative formats
If you require this document in an alternative format, please contact:
openaccess@bath.ac.uk

Copyright of this thesis rests with the author. Access is subject to the above licence, if given. If no licence is specified above, original content in this thesis is licensed under the terms of the Creative Commons Attribution-NonCommercial 4.0 International (CC BY-NC-ND 4.0) Licence (https://creativecommons.org/licenses/by-nc-nd/4.0/). Any third-party copyright material present remains the property of its respective owner(s) and is licensed under its existing terms.

**Take down policy**
If you consider content within Bath's Research Portal to be in breach of UK law, please contact: openaccess@bath.ac.uk with the details. Your claim will be investigated and, where appropriate, the item will be removed from public view as soon as possible.

Download date: 05. May. 2023

# Endothelial colony forming cells (ECFCs) and biomaterials: a synergy for next-generation cardiovascular implants

Tiago Fortunato

A thesis submitted for the degree of Doctor of Philosophy

University of Bath

Department of Pharmacy and Pharmacology

September 2016

**COPYRIGHT**

Attention is drawn to the fact that copyright of this thesis/portfolio rests with the author and copyright of any previously published materials included may rest with third parties. A copy of this thesis/portfolio has been supplied on condition that anyone who consults it understands that they must not copy it or use material from it except as permitted by law or with the consent of the author or other copyright owners, as applicable.

This thesis may be made available for consultation within the University Library and may be photocopied or lent to other libraries for the purposes of consultation.

## Table of Contents

**Abstract**

Endothelial colony forming cells (ECFCs) are circulating cells able to differentiate into mature endothelial cells and replenish the endothelial lining at the sites of vascular damage. Their utilization for cell therapies aiming to restore healthy endothelial lining of blood vessels and stimulate neovascularization of ischemic tissues has been the object of intense investigation. The overall aim of this project was to investigate and develop novel approaches for the promotion of vasculogenesis and endothelisation of vascular grafts by ECFCs.

First, protease-activated receptors (PARs) were investigated as potential targets to stimulate in ECFC-driven vasculogenesis and promote therapeutic revascularization. Our data showed that PAR-1 and PAR-2 are both expressed in ECFCs and functionally coupled to the ERK1/2 pathway. Specific stimulation of PAR-1, but not PAR-2, significantly inhibits *in vitro* tube formation by ECFCs, and this effect is due to the down-regulation of VEGFR-2. Although the role of PAR-2 remains elusive, this study sheds new light on the regulation of the vasculogenic activity of ECFCs and suggests a potential link between adult vasculogenesis and the coagulation cascade.

Secondly, we investigated the use of human platelet lysate gel (hPLG) as an animal product-free and patient-specific tool to isolate, amplify, differentiate and deliver endothelial progenitor cells. This extracellular matrix (ECM) was able to support the proliferation of ECFCs in 2D cultures and the formation of a complete microvascular network *in vitro* in 3D cultures. Interestingly, the culture of ECFCs on hPLG led to the upregulation of several angiogenic genes, such as VEGFR-2 and PDGFR-β, and also induced the robust sprouting of existing vessels in an *ex vivo* model. This discovery has the potential to accelerate the development of regenerative medicine applications based on implantation of microvascular networks expanded *ex vivo* or the generation of fully vascularised organs.

Finally, the biomimetic and pro-angiogenic properties of human platelet lysate (hPL) were utilised to facilitate adhesion and proliferation of ECFCs on polymeric materials. hPL was shown to promote endothelisation of biomaterials, which can be utilised for tissue engineering purposes. Novel electrospun polymeric tubular scaffolds were developed and their surface properties enhanced using plasma treatment. These scaffolds exhibit increased adsorption of proteins from hPL, which acted as an interfacial layer to promote the adhesion and proliferation of ECFCs on their surface. Such findings demonstrate that the pro-angiogenic and pro-vasculogenic properties of

platelet-derived factors can be transferred to scaffolds to stimulate endothelial growth on synthetic scaffolds for tissue engineering without the use of recombinant or animal products.

In conclusion, we propose the use of ECFCs with platelet-derived products as an ideal synergy for the vascularization of tissue engineered constructs.

**Acknowledgements**

I would like to express my gratitude to my supervisors, Dr Giordano Pula and Dr Paul De Bank, for giving me the possibility of doing my PhD in their laboratories but also for their support and guidance throughout these years. I am sincerely thankful for their help and attention to make the most of my PhD. I would also like to acknowledge the University of Bath for providing me with a scholarship.

I am especially grateful to the staff in the Microscopy Analysis Suite (Adrian, Ursula, Phil and Diana) for all that the technical support and company during my last year there. The technical staff in Pharmacy and Pharmacology, namely Jo Carter, Rod Murray and Stephen Phillips, were always extremely helpful and I would like to thank them too.

I would also like to thank the staff at RUH, especially Dave Fisher for their collaboration in my project.

I thank my fellow lab members Dina, Aisha and Kim for the good times and their help in the lab too.

Special thanks go to my friends Cristina, João, Fabiana, Ricardo and Christian.

Finally, I want to say the greatest thanks to my family. Because they are always next to me, even if we are in two different countries. Without them I could had never got here.

## List of Figures

## List of Tables

## Abbreviations

| | |
|---|---|
| ANOVA | Analysis of Variance |
| ATR | Attenuated Total Reflectance |
| BCA | Bicichoninic acid |
| BSA | Bovine serum albumin |
| CXCR4 | C-X-C chemokine receptor type 4 |
| DAPI | 4',6-diamidino-2-phenylindole |
| DMSO | Dimethyl sulfoxide |
| DTT | Dithiothreitol |
| ECFC | Endothelial Colony Forming Cell |
| ECL | Enhanced chemiluminescence |
| ECM | Extracellular matrix |
| EDTA | Ethylenediaminetetraacetic acid |
| EGF | Epidermal growth factor |
| eNOS | Endothelial Nitric Oxide Synthase |
| ELISA | Enzyme-linked immunosorbent assay |
| EPC | Endothelial Progenitor Cell |
| ERK | Extracellular signal–regulated kinase |
| ESC | Embryonic stem cell |
| FBS | Foetal Bovine Serum |
| FGF | Fibroblast Growth Factor |
| FGFR | Fibroblast Growth Factor Receptor |
| FITC | Fluorescein isothiocyanate |
| FTIR | Fourier transform infrared spectroscopy |
| GAPDH | Glyceraldehyde 3-phosphate dehydrogenase |
| GDA | Glutaraldehyde |
| GF | Growth Factor |
| GFR | Growth Factor Reduced |
| hPL | Human Platelet Lysate |
| hPLG | Human Platelet Lysate Gel |
| HUVEC | Human Umbilical Vein Endothelial Cell |
| IGF | Insulin-like Growth Factor |
| IL-8 | Interleukin 8 |
| LDL | Low-density lipoprotein |
| MSC | Mesenchymal stem cell |

| | |
|---|---|
| PAR | Protease-activated receptor |
| PBMNC | Peripheral Blood Mononuclear Cell |
| PBS | Phosphate-buffered saline |
| PCL | Polycaprolactone |
| PDGF | Platelet-derived growth factor |
| PDGFR | Platelet-derived growth factor receptor |
| PFA | Paraformaldehyde |
| PLGA | Poly(lactic-co-glycolic acid) |
| PRP | Platelet-rich plasma |
| qPCR | Quantitative Polymerase Chain Reaction |
| RIPA | Radioimmunoprecipitation assay |
| RPM | Revolutions per minute |
| RT | Room temperature/Real time |
| SDF-1 | Stromal cell–derived factor-1 |
| SDS | Sodium dodecyl sulfate |
| SDS-PAGE | Sodium dodecyl sulfate polyacrylamide gel electrophoresis |
| SEM | Scanning electron microscopy |
| TBS | Tris-Buffered Saline |
| TEM | Transmission electron microscopy |
| TRITC | Tetramethylrhodamine isothiocyanate |
| UEA | *Ulex europaeus* agglutinin |
| VEGF | Vascular Endothelial Growth Factor |
| VEGFR | Vascular Endothelial Growth Factor Receptor |
| vWF | Von Willebrand Factor |
| XPS | X-Ray Photoelectron Spectroscopy |

# Chapter 1: Introduction

## 1.1. Tissue engineering and regenerative medicine

The tissue engineering field has exponentially grown over the last decade and has progressively moved from being exclusively a lab-bench discipline to an emerging part of today's medical care. It has largely evolved from the pre-existent field of biomaterials and consists in the *de novo* engineering of tissues and organs by combining scaffolds, cells and biological molecules, often drawing cues from the most up-to-date knowledge in developmental biology (Berthiaume, Maguire and Yarmush, 2011). Although, this field is focused mainly on the replacing damaged or lost tissues, it is often somewhat misnamed by the term "regenerative medicine", which has a broader meaning. The latter encompasses research on self-healing – where the emphasis is rather placed on inducing the healing of a target tissue by potentiating the body's own ability to regenerate, through the delivery of biologically active agents, such as nucleic acids or proteins (Koria, 2012). In addition, tissue engineering has revolutionized the study of human diseases and drug toxicity by supporting the development of three-dimensional *in vitro* models that can mimic far more realistically tissue- and organ-level structures and functions that are at the root of disease (Benam et al., 2015).

While our complex immune system performs remarkably well at keeping us safe from disease, its inherent ability to protect us from any foreign agent is also the main reason why the replacement of body tissues and organs is so challenging (Starzl et al., 1993). Although, the surgical techniques for transplanting organs have improved tremendously, it is simply not possible to cope with the overwhelming demand for tissues and organs by retrieving them from volunteering donors (Orlando, Soker and Stratta, 2013). Moreover, even in cases where a suitable donor is found and an organ is successfully transplanted, the therapeutic efficacy is only partial and temporary. The most important limitation is that the immune response against the implanted organ requires permanent immunosuppression and ensues a lifelong struggle against immune rejection (Katabathina et al., 2016). Thus, tissue engineering aims at overcoming these hurdles by creating new tissues or organs from the cells of the same patient who receives the treatment. This would eliminate the necessity of either finding a compatible donor or using immunosuppressant drugs.

There are four important factors that need to be considered in order to successfully engineer a tissue *in vitro*: an appropriate cell population, a scaffold that can support the cells, the right biomolecules, such as growth factors, and physical and mechanical stimulus to influence the proper development of the construct into the target tissue (Hansmann et al., 2013) (Figure 1.1). Engineering such tissue surrogates at a scale

that is clinically relevant brings about a major challenge: the diffusion of oxygen, nutrients and waste products. In the human body, most cells are found within 100-200 µm from the nearest capillary, which allows for that exchange to happen, and in the lab this can be simulated - or at least compensated for - through the use of perfusion bioreactors (Fiedler et al., 2014). Without its own vascular network, any areas of a construct that are beyond the referred diffusional limit will not be sufficiently oxygenated resulting in cell death and, most likely, overall scaffold failure soon after implantation (Fiedler et al., 2014). Therefore, the engineering of artificial blood vessels and capillary networks is not only a major area of interest within the field, but it is also one from which the future success of the whole tissue engineering endeavour depends upon (Laschke and Menger, 2016).

This introduction will address the potential cell sources and scaffold types, with particular focus on vascular tissue engineering.

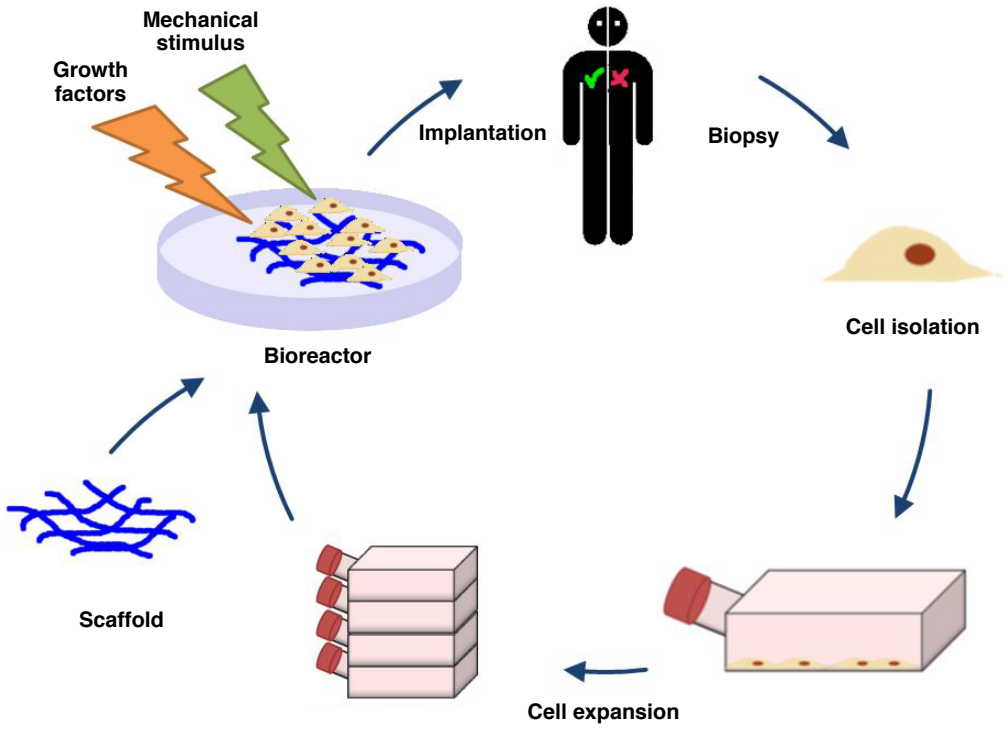


**Figure 1.1. Key stages in the tissue engineering cycle.** Cells are harvested from a patient, and expanded ex vivo. These are then seeded on an appropriate scaffold and cultured with biochemical and mechanical stimuli. The engineered tissue or organ is then implanted back into the patient to substitute or repair the diseased organ.

## 1.2. Cell sources for vascular tissue engineering

Each tissue engineering strategy faces its own specific challenges and considerations with regards to the choice of cells, but a number of these are common to all, independently of the target tissue. Firstly, it must be feasible to either directly obtain the required number of cells, or devise a method of inducing the proliferation of the starting population to expand these to the necessary numbers, either *in vitro* or *in situ* (Kumar and Starly, 2015). Next, these cells should be as easy to isolate as possible. In this context, applications based on cells originating from peripheral blood or from relatively non-vital superficial tissues (e.g. skin or adipose tissue) are more likely to be translated to the clinic than those created with cells that require more complicated surgical interventions (e.g. bone marrow or vascular tissue). Cells also need to possess the correct phenotype or be able to permanently differentiate into it, in order to perform the desired cellular functions, such as ECM deposition, cytokine release, etc. Other requirements may include the ability of these cells to integrate in a seamless manner with the native cells and tissue, as well as to connect with the existent neural and/or vascular networks. Lastly, cells should be amenable to the chosen delivery method. For example, endothelial cells must be delivered using a material that is permissive to their adhesion via surface integrins as their survival is known to be intimately linked to this process (Chavakis and Dimmeler, 2002). Depending on the nature of the approach and its specifications, a number of different sources of cells can be used for the engineering of vascular tissues. Most patients with vascular disorders are elders, thus mature vascular cells from these patients are not suitable for tissue engineering. As an example, smooth muscle cells (SMCs) isolated from the walls of blood vessels have been shown to suffer from aging-associated cellular changes, such as decreased proliferation and collagen synthesis (McKee et al., 2003). Therefore, alternative cell sources with a more proliferative and healthy profile are needed, and these are summarized bellow.

### 1.2.1. Embryonic stem cells (ESCs)

Embryonic stem cells are derived from the inner cell mass of the pre-implantation blastocyst and are capable of differentiation into all mature cell types. In addition to their pluripotency, ESCs can also replicate indefinitely while in their undifferentiated state, mainly due to their high telomerase activity. Originally, ES cell lines were derived by co-culture on growth arrested mouse embryonic fibroblasts (Skottman and Hovatta, 2006), but more recently they have also been derived under Good Manufacturing Practices (GMP) conditions using human fibroblasts or amnion epithelial cells and avoiding also the use of animal products in the culture medium (Tannenbaum et al., 2012; Lai et al., 2015), which reduces the risk of animal-borne disease transmission and improves their clinical applicability.

Several groups have managed to differentiate human ECSs into ECs, with various degrees of success, and demonstrate their ability to form capillary networks *in vivo* using murine ischaemic hindlimb models (Levenberg et al., 2002) (Wang et al., 2007). The differentiation of ESCs has also been guided towards a smooth muscle cell (SMC) phenotype (Huang et al., 2006; Xie et al., 2007; Cheung et al., 2012), which could be valuable for the *in vitro* generation of arterial vessels.

Although ESCs constitute a suitable cell source for *in vitro* disease and drug toxicity modelling and also provide useful insight into the *de novo* formation of blood vessels (i.e. vasculogenesis) (Nakagami et al., 2006), their clinical use is severally hampered by ethical issues that arise from the necessary destruction of human embryos (Vats, Tolley, Bishop and Polak, 2005). In addition, another major hurdle has been the potential for teratoma formation as a result of administering patients with pluripotent cells. However, in recent reports of long-term patient following, no adverse effects of this nature were shown, despite the immunosuppressant regimen that these were on (Schwartz et al., 2015). Crucially, just like with transplanted organs, ESCs need to be matched to individual patients to avoid immune rejection, thus their future application in the engineering of organs and tissues is dependent on the creation of vast stem cell banks.

### 1.2.2. Mesenchymal stem cells (MSCs)

Among adult stem cells, mesenchymal stem cells (MSCs) exhibit unique characteristics, which make them of great interest for regenerative purposes (Mo et al., 2016). MSCs appear to reside in niches in a variety of tissues and can differentiate into numerous lineages to repair damaged tissues, including connective tissue, bone, cartilage or fat (Kern et al., 2006). These undifferentiated cells were isolated originally from the bone marrow, but have been since detected and isolated in many other adult tissues such as muscle (Young et al., 2001), dental pulp (Perry et al., 2008), lung (Martin et al., 2008; Majka et al., 2005), saphenous vein (Covas et al., 2005), liver or adipose tissue (Heidari et al., 2013), thus providing less invasive sources of MSCs for therapy. As with ESCs, these cells have greater *in vitro* expansion capacity, but are also known for actively secreting trophic factors that promote tissue regeneration and regulate the immune system (Squillaro, Peluso and Galderisi, 2016; Castro-Manrreza and Montesinos, 2015).

MSCs from bone marrow have been extensively investigated in vascular tissue engineering (Li, Sengupta and Chien, 2014), especially to study the interplay between ECM, growth factors and mechanical forces in the differentiation these cells into SMCs during their seeding in vascular grafts (Kurpinski et al., 2010; Gong and Niklason, 2008). Equally, MSCs from adipose tissue (often called AD-SCs) and muscle have been differentiated into contractile SMCs (Rodríguez et al., 2006; Nieponice et al., 2008), proliferating on both decellularised veins (Harris et al., 2011) and artificial scaffolds which had satisfactory mechanical strength (Heydarkhan-Hagvall et al., 2008; Zambon et al., 2014; Nieponice et al., 2008).

Nevertheless, MSCs appear to be unable to differentiate into ECs *in vitro* or *in situ*, as necessary for the lumenisation of grafts or the formation of microvascular networks. Researchers have implanted vascular grafts loaded with GFP-labelled BM-MSCs and shown that, despite the beneficial effect of MSCs on the formation of an endothelial lining, this layer had its origin in the host tissue and not from the implanted stem cells (Mirza et al., 2008). Accordingly, BM-MSCs injected into immunodeficient mice cannot form capillary networks on their own but are able to assist in the stabilisation of networks formed by endothelial progenitor cells (EPCs) through the secretion of a plethora of a pro-angiogenic factors (Melero-Martin et al., 2008; Lin et al., 2012). This lack of differentiation ability towards an endothelial phenotype may be due to the epigenetic methylation of CD31 and VE-cadherin promoters, as observed in AD-SCs (Boquest et al., 2007).

A hypothesis that has been gaining increasing support suggests that most tissue resident MSCs originate within the perivascular space and not directly from the bone marrow (Corselli et al., 2013), being often labelled as pericyte/adventitial progenitor cells (Spencer et al., 2015; Katare et al., 2011). As blood vessels are ubiquitously present throughout the body, these MSCs can be rapidly recruited to areas in need of repair in their vicinity (da Silva Meirelles, Caplan and Nardi, 2008).

### 1.2.3. Induced pluripotent stem cells (iPSCs)

In the last decade, the discovery of a method for reprogramming mature cells into pluripotent stem cells by Shinya Yamanaka's lab (Takahashi and Yamanaka, 2006) has provided a new cell source for tissue engineering that bypasses the immunogenic and ethical issues of other stem cell types. This reprogramming is based on the introduction of four specific genes encoding transcription factors (also known as Yamanaka factors) and prompts adult cells to regress into a stem cell-like state, with comparable self-renewal ability and differentiation potential as ESCs. Similar to the latter, iPSCs can be differentiated into ECs (Li et al., 2011), SMCs (Bajpai et al., 2012; Wang et al., 2012) and pericytes (Orlova et al., 2014). Zanotelli et al. have shown that ECs obtained this way can self-assemble into capillary networks when cultured in peptide-functionalized poly(ethylene glycol) (PEG) hydrogels in a manner that is representative of the physiological vascular morphogenesis (Zanotelli et al., 2016). Additionally, Wang et al. has shown that human iPSC-derived SMCs can be successfully cultured onto macroporous poly(L-lactide) (PLLA) scaffolds and maintain their phenotype after subcutaneous implantation for at least 2 weeks (Wang et al., 2014a).

In recent years, a new line of research has emerged which is focused on the direct conversion of adult cells into other cell types, including ECs (Margariti et al., 2012; Ginsberg et al., 2012) and SMCs (Karamariti et al., 2013), while avoiding an intermediate pluripotency stage (Kelaini, Cochrane and Margariti, 2014). This shorter process can be achieved through transdifferentiation, in which lineage-specific factors are ectopically expressed, or through direct reprogramming, that includes an initial partial reprogramming towards the pluripotent state. ECs generated using this partial-iPS technology improved neovascularization and blood flow recovery when injected in a hindlimb ischaemia model, and could re-establish the endothelial lining of decelularized vessels *in vitro*, maintaining their patency (Margariti et al., 2012). In

addition, co-seeding of these vascular grafts with SMCs obtained from partial-iPSCs (PiPSCs) led to improved survival following implantation in mice, when compared with cell-free grafts (Karamariti et al., 2013).

Besides the potential of the iPS technology in providing autologous cell sources for regenerative purposes, it is also ideally suited for disease modeling, as the cells generated with these techniques maintain the genetic mutations that were already present in the starting cell population (Kim, 2014).

### 1.2.4. Endothelial Progenitor Cells (EPCs)

#### *Early endothelial progenitor cells (eEPCs)*

The first putative kind of circulating progenitor was proposed by Asahara and colleagues in 1997 and was derived by culturing the adherent $CD34^+$ mononuclear cell (MNC) fraction from peripheral blood on to fibronectin coated plates (Asahara et al., 1997). After 3-7 days, they differentiate and express a number of endothelial/progenitor cell surface markers such as CD133, CD34 and vascular endothelial growth factor receptor (VEGFR-2), and were thus labelled as early endothelial progenitor cells (eEPCs). Although these cells were shown to enhance angiogenesis in a mouse model of hindlimb ischaemia (Asahara et al., 1997; Kalka et al., 2000), their capacity to differentiate into ECs was questioned in subsequent studies implying an haematopoietic origin and showing that these cells did not exhibit a cobblestone morphology typical of endothelial cells or formed vascular networks (Case et al., 2007; Yoder et al., 2007; Rohde et al., 2006). Accordingly, a later study by Medina et al. has determined that eEPCs share a greater extent of their proteome with monocytes than with mature ECs, based on transcriptional and protein profiling of different endothelial progenitors (Medina et al., 2010b). Moreover, in the same study, caveolae and adherens junctions typical of ECs could not be detected in these cells. It is now fairly agreed in the field that these short-lived eEPCs contribute to neovascularization by secreting angiogenic growth factors and cytokines, such as VEGF or interleukin 8, rather than forming themselves new blood vessels (Hur et al., 2004)

Therefore, it appears to be more correct to consider these cells as pro-angiogenic monocytes rather than true endothelial progenitors and, for this reason, they should be used with caution in therapeutic angiogenesis (van der Pouw Kraan, van der Laan, Piek and Horrevoets, 2012; Medina et al., 2010b).

***Endothelial colony forming cells (ECFCs)***

Differently to eEPCs, the so-called endothelial colony forming cells (ECFCs) are regarded as a true type of endothelial progenitor and show a lack of expression of hematopoietic markers (Ingram et al., 2004). These cells are also derived from the MNC fraction of blood but are instead obtained as large colonies of adherent endothelial $CD45^-$ cells with cobblestone morphology, after 2-3 weeks of culture on dishes coated with matrix proteins (e.g. collagen) (Yoder, 2009). For this reason, these cells are also referred as late EPCs or outgrowth endothelial cells (OECs) in some research groups, which often generates some confusion in the field (Fadini, Losordo and Dimmeler, 2012). This isolation method, which is detailed in Chapter 2.1, was first described by Ingram et al. and is believed to induce the differentiation of a rare population of $CD34^+/CD133^-/CD146^+$ progenitors into ECs, as these cells can be obtained from both the total MNC fraction as well as from the referred MNC subsets from peripheral blood (PB) and cord blood (CB) (Timmermans et al., 2007; Mund et al., 2012). Although the expression of $CD34^+$ at their surface points to the bone marrow as their probable source, it is not known with certainty if these progenitors are released directly from this tissue into the bloodstream or if they originate from the wall of bigger vessels, with conflicting reports suggesting both origins (Tura et al., 2013; Lin, Weisdorf, Solovey and Hebbel, 2000). ECFCs are characterized by the expression of EC markers, such as CD31, VEGFR-2, CD146 and von Willebrand factor (vWF) and absence of leukocyte markers expression (i.e. CD14 or CD45) (Ingram et al., 2004). Functionally, ECFCs are known for taking up acetylated low-density lipoprotein (Ac-LDL) and being able to form tubes *in vitro* on Matrigel as well as capillary networks *in vivo* (Critser and Yoder, 2010; Critser, Kreger, Voytik-Harbin and Yoder, 2010; Mead, Prater, Yoder and Ingram, 2008). Additionally, these cells exhibit a highly proliferative profile and considerable self-renewal capacity, but unlike stem cells, their fate is already committed, thus do not present any risk of teratoma formation (Hirschi, Ingram and Yoder, 2008).

As with iPSCs, ECFCs can be isolated from any person, hence they are ideally suited for autologous therapies aimed at treating ischaemic diseases or for the generation of vascular grafts (Medina et al., 2010a), as well as tool for studying vascular diseases (Medina et al., 2012). However, these applications have also been hampered due their low frequency in blood, with less than 1 colony obtained per 20 mL of blood (Ingram et al., 2004). Fortunately, due to the relatively non-invasive nature of blood cell collection, this procedure can be repeated several times to improve the

likelihood of successfully isolating these cells. Some researchers have alternatively attempted to increase the number of circulating EPCs prior to blood drawing by promoting their release into the bloodstream with a variety of compounds, such as with the CXCR4 antagonist AMD3100 (Yin et al., 2007; Sun et al., 2016; Chao et al., 2016). Of interest to the prospective utilization of these cells for human therapeutic purposes, an animal product-free ECFC isolation and culture method was developed by replacing the foetal bovine serum in the endothelial growth medium (EGM) with pooled human platelet lysate (hPL), getting one step closer to the GMP requirements for clinical use (Reinisch et al., 2009).

In summary, blood constitutes a source of both EPCs and pro-angiogenic hematopoietic cells, which can be exploited to synergistically promote vascular repair and overall healing of damaged tissues (Yoon et al., 2005).

### 1.3. Scaffold-based approaches for vascular tissue engineering

The engineering of vascular tissues is subdivided into two main development areas: microvascular networks and vascular grafts. The first involves the creation of capillary networks with the aim of improving blood perfusion and reducing ischaemia in damaged tissues (Rouwkema and Khademhosseini, 2016). Some examples are myocardial infarction, where the promotion of local blood supply is necessary to match the considerable oxygen demand of the infarcted myocardium and guarantee its survival (Ardehali and Ports, 1990), and chronic wounds, where insufficient blood vessel network has been shown to hinder full tissue repair (Gordillo and Sen, 2003). The second comprises the development of replacements for greater calibre vessels to be used in bypass surgeries in alternative to the use of autologous venous or arterial grafts.

### 1.3.1. Microvascular network formation

In order to promote the formation of capillary-like tubes through self-organization of ECs, a scaffold material should meet a set of requirements:

- Allow the encapsulation either *in vitro* or *in situ* of the target cells.
- Provide a 3D architecture for cell growth.
- Be biocompatible (i.e. not eliciting an inflammatory response).
- Allow the diffusion of oxygen and nutrients.
- Possess similar mechanical properties to the targeted tissue.
- Allow the quick adhesion of cells.
- Be biodegradable either naturally or by the direct action of the cells.
- Allow the establishment of a growth factor gradient.

Hydrogels present several advantages that make them the ideal material type to fulfil these demands. The gelation process through which these hydrophilic networks are formed allows them to be moulded *in vitro* into any desired shape, while permitting the homogenous dispersion of cells throughout it, or be injected without damaging the targeted and surrounding tissues during delivery (Johnson and Christman, 2013). Due their high water content and permeability, the diffusion of oxygen, nutrients as well as secreted molecules is greatly facilitated, which is essential for cell survival. The mechanical profile of these materials also resembles that of most vascularized soft tissues, thus are able to flex in concert with deformations of host tissue (Zhu and Marchant, 2011). Their application is not restricted to soft tissues though, as their mouldable nature allows them to be combined with harder materials into bi-phasic scaffolds in order to meet the required stiffness parameters, as for example in the case of engineered bone implants (Daculsi et al., 2010). Hydrogels can be derived from synthetic polymers, such as polyethylene glycol, (PEG) and poly(lactic-co-glycolic acid) (PLGA), or from both natural materials, including silk fibroin, alginate, Matrigel, chitosan, collagen or fibrin, and have been extensively reviewed by others (Johnson and Christman, 2013; El-Sherbiny and Yacoub, 2013; Rufaihah and Seliktar, 2016). Depending on the specific type of origin, natural hydrogels have a number of advantages, including a natural ability to bind biomolecules (e.g. growth factors), low cost, improved cell adhesion due to inclusion of integrin-binding sequences or susceptibility to cell-mediated proteolytic degradation (Munarin, Petrini, Bozzini and Tanzi, 2012). However, there are also drawbacks linked to the use of these natural materials, which include issues with purification and batch replicability, immunogenicity or pathogen transmission.

For example, collagen is one of the most popular hydrogels used for tissue engineering, as it is one of the main constituents of the native ECM. However, it is usually sourced from animal tissue, which carries a risk of disease transmission and may elicit an immune response due to being recognized as a non-human protein, which hinder the approval for clinical use. On the other hand, fibrin has proven to be a material which can overcome most of these issues and has been object of increasing interest (Ceccarelli and Putnam, 2014). For example, in a study by Birla and coworkers, fibrin hydrogels supported the formation of a densely vascularized cardiac tissue by seeded neonatal cardiomyocytes 3 weeks post-implantation in rats (Birla, Borschel, Dennis and Brown, 2005). This human-derived polymer acts as a provisional matrix during wound healing and tissue remodeling and is endowed with an excellent safety record regarding pathogen transmission, which grants it a superior degree of biocompatibility and great potential of approval for medical use (Dunn and Goa, 1999). Unfortunately, the cost arising from its purification from human blood and its poor mechanical properties have limited its widespread therapeutic application.

Synthetic hydrogels are advantageous compared to collagen- or fibrin-based hydrogels due to the greater control over material characteristics (including mechanical properties), reduced batch-to-batch variability and absence of disease transmission risk (Zhu and Marchant, 2011). Their superior tunability also allows the design of hydrogels that can react to environmental conditions, changing properties depending on the factors such as temperature or pH (Klouda et al., 2011). Nevertheless, these polymers need to be modified in order to promote cell adhesion or degradation, through coupling of integrin-binding domains (e.g. RGD peptides) and sequences cleavable by matrix metaloproteases (MMPs) respectively. In addition, while ECM proteins can naturally bind to most angiogenic GFs, synthetic polymers can only efficiently achieve that following chemical modification (Reed and Wu, 2014). As a consequence, the final cost of synthetic hydrogels for tissue engineering is usually considerably higher than that of natural ones. Finally, any new synthetic polymer needs to go through a rigorous process of safety assessment, as many synthetic polymers are potentially cytotoxic (Tian et al., 2012).

Therefore, synthetic and natural materials can be combined, exploiting the unique properties of each type to obtain a hydrogel with superior overall properties compared to its individual constituents. Such synergistic effect has been recently shown by mixing fibrin and PEG hydrogels in the delivery stem cell-derived ECs in an animal model (Benavides et al., 2015). The fibrin component allowed the formation of a vascular

network and infiltration of supporting pericytes, while PEG increased the stability and longevity of the injectable scaffolds. In a similar manner, Deng et al. showed that the crosslinking of collagen hydrogels with chitosan improves their mechanical properties and increases the *in vivo* vascular growth into this matrices (Deng et al., 2010).

### 1.3.2. Artificial vascular grafts

Synthetic grafts for large-caliber arterial replacement (internal diameter > 6 mm) have already proven rather successful in the clinical setting and are usually produced out of non-degradable poly(ethylene terephthalate) (Dacron®), expanded poly(tetrafluoroethylene) (Teflon®) or polyurethane (Chlupác, Filová and Bacáková, 2009; Spadaccio et al., 2013). The lower shear stress near the walls of bigger vessels (e.g. aorta), limits thrombogenicity and leads to satisfactory results with these grafts in terms of patency and durability, despite incomplete endothelisation. However, in the case of small-diameter artery (e.g. coronary arteries) grafts made of the same materials, the shear stress is higher resulting in thrombus formation and intimal hyperplasia at the anastomotic site (Binns et al., 1989; Bennion et al., 1985). Coating of these Teflon-based grafts with heparin has also been attempted with a partial improvement in patency rates (Dorrucci et al., 2008). Nonetheless, this surface treatment is likely to provide short-lasting benefits for the period immediately following implantation. Because of the limitation of artificial blood vessel implants, most of the vascular interventions are performed using autologous grafts, such as the saphenous vein. In spite of being the current gold standard, the performance of these veins is still not at a satisfactory level, mainly due to the mechanical mismatch. Veins have thinner walls than arteries and are not prepared for the higher arterial pressure. This leads to aneurism formation, followed by thickening of the vessel wall (intimal hyperplasia) and accelerated atherosclerosis (Owens et al., 2009; Sur, Sugimoto and Agrawal, 2014). Additionally, one third of the patients with peripheral artery disease do not have suitable veins that can be used as autografts and the harvesting of these veins may also result in donor site morbidity (Li, Sengupta and Chien, 2014), thus there is a great demand for an artificial alternative.

There have been two main strategies for engineering vascular grafts: *in vitro* and *in situ*. The first aims at generating functional constructs in the laboratory by using cells, scaffolds and bioreactors (Isenberg, Williams and Tranquillo, 2006). In this case a biodegradable synthetic or naturally derived scaffold is seeded with ECs, SMCs, MSCs

or a combination of these. Before being implanted, constructs are cultured in a pulsatile flow bioreactor to mimic the physiological conditions and stimulate cells to remodel the scaffold into the different layers of the blood vessel. Due to its long *in vitro* culture period, this approach is not suitable for urgent interventions. Nevertheless, a great number of vascular interventions can be planned with sufficient time to fabricate such kind of graft. The other approach is to engineer a cell-free graft that can selectively recruit cells from the host and allow the remodelling to happen *in situ*. Because no *in vitro* incubation is necessary, these grafts can be made available immediately to surgeons as well as at a lower cost. In recent example of this type of approach, an electrospun vascular graft was modified with recombinant mussel adhesive protein fused to RGD peptides to promote cellular recruitment *in situ* (Kang et al., 2015). This led to enhanced re-endothelisation by mobilized ECs/EPCs and lower graft failure in an *in vivo* rabbit model.

Independently of the approach followed, lab-engineered grafts are designed with a set of specifications in mind, with the final goal of mimicking the native tissue. The most important mechanical requirements are a burst pressure ≥1,700 mmHg (similar to that of saphenous vein) and to be able to resist the cyclic strain of the hemodynamic environment for 30 days *in vitro* without dilating (Seifu, Purnama, Mequanint and Mantovani, 2013). It is crucial that the elasticity of the graft is as close as possible to that of the native vessel, as any compliance mismatch leads to turbulence in the blood flow near anastomoses, which in turn increases platelet activation and thrombus formation (Mitchell and Niklason, 2003). Strategies aimed at reducing the thrombogenicity of the surface are often based on the chemical modification the surface with clotting inhibitors or through seeding/capture of ECs/EPCs (de Mel, Cousins and Seifalian, 2012). In order to be properly integrated over time, the implanted scaffold should also allow the ingrowth of cells from the host, while modulating their cell fate and differentiation to form new tissue. This could be controlled by the microscopic properties, such as porosity, topography, surface chemistry and bioactivity (Fioretta et al., 2012) and applies not only to vascular specific cell types but also to immune cells that mediate the inflammatory response to the implant. For example, it has been shown, that the polarization of macrophages towards the tissue remodelling (M2) phenotype on vascular grafts can be promoted by increasing the fibre thickness and porosity of the scaffolds, leading to enhanced ECM deposition by the invading cells (Wang et al., 2014b). The newly synthetized ECM gradually takes over the mechanical integrity of the graft, whilst the scaffold materials are degraded.

Therefore, the scaffold's degradation rate is another essential parameter to be considered and should be in tune with ECM deposition (Bouten et al., 2011). In this context, synthetic biodegradable polymers are the first choice for vascular grafts as, compared to natural materials, they provide a much greater control over the degradation rate and other parameters such as porosity, elasticity or microscopic structure (Kim and Mooney, 1998). Degradable polyesters, including poly(glycolic acid) (PGA), PLA, poly(caprolactone) (PCL) and their co-polymers, are the most frequently used in this approach. These polymers are known for being degraded at considerably distinct speeds, thus are often combined in the same scaffold to achieve the ideal degradation rate for the different graft layers. An interesting example is the work by Lim et al., in which a vascular graft was fabricated using poly(lactide-co-epsilon-caprolactone) (PLCL) and further reinforced with PGA fibers (Lim et al., 2008). Following seeding of vascular cells differentiated from autologous BM stem cells, grafts were implanted into the abdominal aorta of dogs and remained patent for the whole duration of the study (8 weeks). In summary, scaffolds for vascular grafts should be designed so that they act as an anti-thrombotic interface with the blood, providing a provisional template for the regeneration of the new arterial vessel, while preventing inflammatory processes that can lead to thrombosis and intimal hyperplasia, especially at the graft anastomoses.

***Methods of scaffold fabrication***

Tubular scaffolds for vascular tissue engineering can be produced from synthetic polymers via several methods. The most common ones are electrospinning, solvent casting and particulate leaching, gas foaming, freeze drying and 3D printing, with respective pros and cons, as extensively reviewed by (Fioretta et al., 2012). Among these, electrospinning is probably the most promising and widely used for this purpose, as it allows the fabrication of fibrous scaffolds with interconnected pores and tuneable fibre architecture that resemble the native ECM. This method produces fibres by applying a high-voltage to a liquid droplet in order to draw charged threads of polymer solutions, which are collected onto a grounded conductive target (Figure1.2).

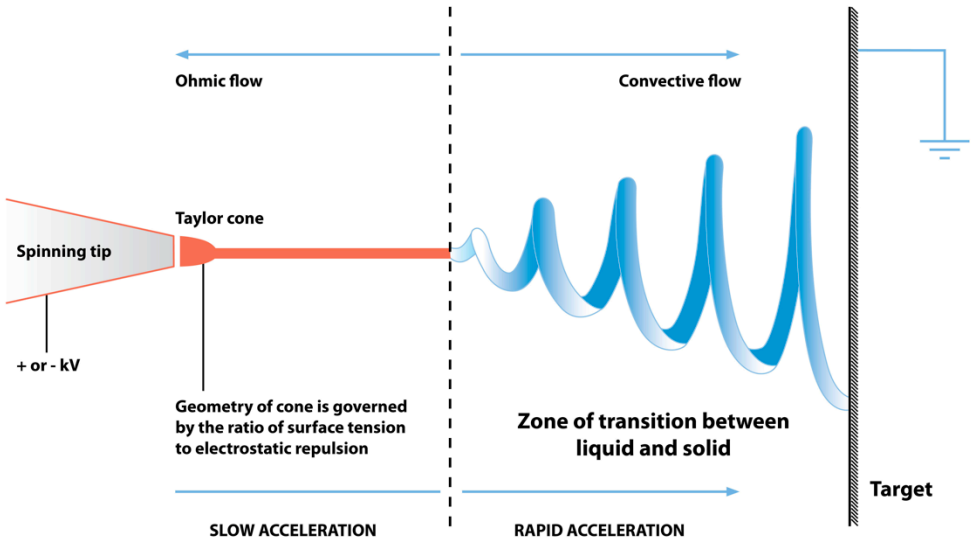


**Figure 1.2. Diagram of the electrospinning process.** The application of voltage to a liquid droplet stretches it, forming a Taylor cone. Due to electrostatic repulsion the jet is then elongated in a whipping process, during which the solvent evaporates. Solid fibres are finally deposited on the grounded collector (Diagram by Joanna Gatford at The New Zealand Institute for Plant and Food Research Ltd, distributed under a CC BY 3.0 License, Wikimedia Commons).

The most commonly used setup for producing tubular scaffolds includes a rotating mandrel as fibre collector, allowing polymeric fibres to be arranged in a cylindrical construct (Ercolani, Del Gaudio and Bianco, 2013). The operating conditions, e.g. voltage, flow rate, needle-to-target distance, mandrel speed rotation, can be controlled to tailor the fibre diameter, organization, microstructural and mechanical properties. Therefore, the layers of the scaffold can be produced with different porosities to induce the differential migration and differentiation of specific cell populations, this way accurately replicating the microstructure of a normal arterial wall (Bonani et al., 2011). Exploiting this concept, Soletti et al. developed an electrospun small-diameter scaffold made of a single polymer with a highly porous inner layer, to allow cell ingrowth, and an external densely packed fibrous layer, to mechanically reinforce it (Soletti et al., 2010). Two or more different polymers can also be electrospun in sequence to produce bilayered grafts that can mimic the biomechanical characteristics of the different vessel wall layers (Montini-Ballarin et al., 2016).

***Scaffold surface modification***

In order to mimic native cell-ECM interactions and increase adhesion and/or proliferation of cells, the surface scaffolds can be modified and functionalized with bioactive molecules (Marklein and Burdick, 2010).

Methods of modifying the surface chemistry of electrospun fibres include includes plasma treatment, wet chemical methods or surface graft polymerization (Yoo, Kim and Park, 2009). Wet chemical modification consist in the random chemical scission of ester bonds on the polymer backbones, giving origin to carboxylic and hydroxyl groups (Ercolani, Del Gaudio and Bianco, 2013), while surface graft polymerization is performed with plasma and UV-irradiation to deposit a layer of polymeric chains on scaffolds made of another polymer (Xu, Wan and Huang, 2009). Plasma treatment is employed to introduce various functional groups on a scaffold surface, modifying the surface energy and hydrophilicity to improve biocompatibility and immobilization of molecules, such as ECM peptides or GFs (Duque Sánchez et al., 2016).

Bioactive molecules can be incorporated into scaffolds either via covalent binding or physical adsorption. The first requires the surface to be modified (e.g. wet chemical method) to add a linker molecule, prior to incubation with the desired moiety (Gabriel et al., 2016). Although this method allows molecules to be bound permanently and with relative specificity, the binding efficiency is generally low due to the several reaction steps that are needed. Conversely, physical adsorption is based on non-covalent interactions (e.g. Van der Walls or hydrogen bonds) between proteins and biomaterial surfaces, and does not require the use of additional linkers (Wei et al., 2014). These methods can be used for example to load scaffolds with GFs, which direct cell differentiation or growth over their release period (Perets et al., 2003), or to coat their surface with antibodies that can capture the cells of interest from circulation (e.g. ECs) (Su et al., 2014; Petersen et al., 2014).

### 1.4. Platelets in angiogenesis and regenerative medicine

Complete tissue repair occurs as a series of four overlapping phases - haemostasis, inflammation, proliferation and remodelling – and is highly dependent on the restoration of the vascular system (Martin and Nunan, 2015). An important event leading to tissue repair is revascularisation, which occurs via angiogenesis (i.e. branching of existing blood vessels) or vasculogenesis (i.e. *de novo* formation of endothelial networks by mobilized EPCs) (Balaji, King, Crombleholme and Keswani, 2013). Both events rely on the efficient stimulation of endothelial cell proliferation, migration and differentiation, in a process that is greatly influenced by platelets (Rhee et al., 2004). Following trauma, activated platelets are accumulated and retained at the injury site and initiate the formation of a fibrin-based plug that stops the haemorrhage (Golebiewska and Poole, 2015). Platelets are anucleate cells produced by megakaryocytes in the bone marrow in a process called proplatelet formation, during which genomic DNA is lost (Italiano, Lecine, Shivdasani and Hartwig, 1999). Therefore, although platelets remain partially capable of synthetizing proteins via translation of remnant cytoplasmic mRNA in response to specific conditions and stimuli (Sim, Poncz, Gadue and French, 2016), the majority of the proteome of platelets is received from the megakaryocyte at the moment of proplatelet formation. This may account for the limited lifespan of platelets in circulation (i.e. 7-10 days) (Lebois and Josefsson, 2016). The majority of platelet regulatory proteins and growth factors are stored in the alpha granules and released upon stimulation (Nurden, 2011; Peterson et al., 2010). PDGF, VEGF, FGF-2 and EGF are some of the main growth factors released and are known as potent stimulators of angiogenesis and other reparative processes (Burnouf, Strunk, Koh and Schallmoser, 2016). In addition, fibrous proteins such as fibrinogen, fibronectin and vitronectin that potentiate the effect of the GFs are also contained in the platelet clot and are regarded as ideal for the preparation of tissue engineering scaffolds (Wang, Gallant and Ni, 2016). Therefore, the local application of platelet-derived materials have been proposed as a way of delivering GFs and ECM proteins to enhance wound healing and organ regeneration, as recently reviewed in depth by other researchers (Piccin et al., 2016; Martínez, Smith and Palma Alvarado, 2015; Burnouf et al., 2013).

Platelet-based materials are initially prepared as platelet-rich plasma (PRP), collected by single-donor autologous donation or by pooling of allogeneic donations (Greppi et al., 2011). The most common method for PRP application consists in the gelation via stimulation of the coagulation cascade with thrombin and/or $CaCl_2$ to

convert fibrinogen into fibrin (Piccin et al., 2016). Because this gel has little tensile strength, it is sometimes combined with stiffer materials or further enriched with human fibrinogen, depending on the target application. As expected, various studies performed in animal models have reported a stimulatory effect on angiogenesis by platelet products. An example of that is the work by Roy and colleagues, where PRP gel was shown to significantly increase wound vascularization in an ischaemic pig model (Roy et al., 2011). Since then, several reports have further evidenced the beneficial effect of using platelet gels for chronic and acute wound healing (Serra et al., 2013; Shan et al., 2013) and a recent systematic review has concluded in favour of the use of these materials for various clinical applications, such as adipose and bone tissue graft implantations (Sommeling et al., 2013). In addition, these platelet-derived materials appear to possess antimicrobial and anti-inflammatory properties, which further increases their therapeutic potential (Edelblute, Donate, Hargrave and Heller, 2015; Andía and Maffulli, 2013).

A modification of the use of PRP is the introduction of cell lysis, which releases the full platelet content into the plasma (Schallmoser and Strunk, 2012). Membrane fragments can then be removed, creating an entirely acellular product with even less immunogenic risk. Although this material has not been yet properly investigated for *in vivo* vascularization, it has provided a much-needed alternative to foetal bovine serum (FBS) for the expansion of MSCs and ECFCs (Schallmoser et al., 2007; Reinisch et al., 2009). Platelet lysates (PL) were shown to support the expansion of MSCs form various sources, including bone marrow, fat or cord blood, while maintaining their full differentiation potential. Lysed PRP can find important translational applications and represent a valid alternative to animal products, which would reduce the risk of viral/prion disease transmission and find easier approval for clinical use (Doucet et al., 2005).

## 1.5. Polymeric materials for vascular engineering

The ECM is composed of a number of structural proteins and polysaccharides that can provide three-dimensional support to cells. While naturally derived polymers, such as collagen or gelatin, are inherently superior as scaffolds with regard to adhesion and proliferation of cells, they possess weak mechanical properties when processed by electrospinning. In addition, concerns over the risk of immunogenic responses and disease transmission, have propelled the development of synthetic polymers for tissue engineering. Biodegradable synthetic polymers offer key advantages such as the control over their mechanical and degradation profiles to tailor for specific applications. These materials can be processed into scaffolds by variety methods and can also be chemically modified to modulate their bioactivity (Kai, Liow and Loh, 2014).

### 1.5.1. Polycaprolactone (PCL)

PCL (figure 1.3) is an hydrophobic biodegradable polyester, with a glass-transition temperature of -60 ºC and melting point around 59–64 C, due to the crystalline nature of PCL, which allows its manipulation at relatively low temperatures (Woodruff and Hutmacher, 2010). It has been approved by the Food and Drug Administration (FDA) for biomedical applications, such as drug delivery or sutures, and is particularly suited for long-term applications due to its degradation time (~2 years). PCL has low tensile strength, but a very high elongation at break (700%) (Woodruff and Hutmacher, 2010; Ercolani, Del Gaudio and Bianco, 2013).

Several groups have used this polymer (pure or blended with other polymers) to fabricate vascular scaffolds by electrospinning, as previously reviewed (Ercolani, Del Gaudio and Bianco, 2013). Such vascular grafts were characterized by mechanical properties (i.e. burst pressure and compliance) comparable with those of native vessels (McClure et al., 2009). In addition, small-diameter electrospun PCL grafts exhibited superior endothelialization in rat arterial model when compared to PTFE vascular grafts (Pektok et al., 2008).

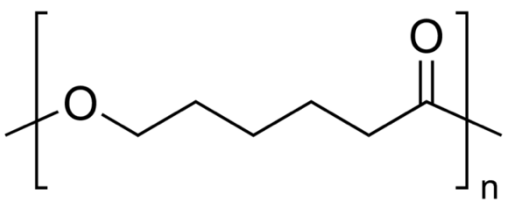


**Figure 1.3. Chemical structure of PCL.**

### 1.5.2. Poly(lactic-co-glycolic acid) (PLGA)

PLGA is a biodegradable polymer made from two monomers, lactic acid and glycolic acid (Figure 1.4). Since both of these occur naturally, PLGA has a minimal toxicity and as been approved by the FDA for human use. It has attracted considerable interest in tissue engineering owing to its biocompatibility, as well as due to the relatively tuneable degradation rate and mechanical properties (Astete and Sabliov, 2006). These vary according to the molar ratio of the individual monomers the co-polymer chain, as the hydrophilicity and speed of degradation increases with increasing glycolic acid content (BaoLin and Ma, 2014).

This polymer has also been extensively investigated for the development of tubular scaffolds, showing great improvements compared to poly(glycolic acid) (PGA) scaffolds (Ercolani, Del Gaudio and Bianco, 2013). One group investigated the engineering of small-diameter tubular scaffolds with pre-seeded ECs and SMCs an tested these as arterial substitutes in adult dogs (Kim et al., 2008). These seeded grafts could induce the formation of neointima and maintain patency for 3 weeks, while cell-free grafts became occluded within 1 week.

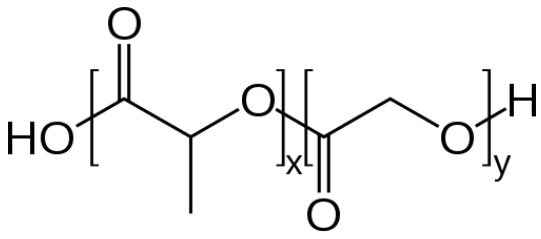


**Figure 1.4. Chemical structure of PLGA.** The structure of this linear copolymer varies with the ratio of its constituent monomers. X (lactic acid) and Y (glycolic acid) indicate the number of times each unit repeats.

### 1.5. Aims & Objectives

The aim of this project was to investigate and develop novel approaches for the promotion of vasculogenesis and endothelisation of vascular grafts by ECFCs. For this purpose, three different lines of research were pursued. The first will dissect the role of protease-activated receptors (PARs) in ECFC-driven vasculogenesis as potential therapeutic targets in tissue engineering. The second explores the utilization of human platelet lysate gel (hPLG) as an angiogenic support for the *ex vivo* expansion of ECFCs and formation of microvascular networks. Finally, the last research chapter is focused on the development of polymer-based tubular scaffolds with increased endothelial adhesion and proliferation as potential tool to generate artificial vascular grafts.

Consequently, the main objectives of this work were:

- Establish the isolation of ECFCs and phenotypically characterize them.
- Investigate the expression of PARs in ECFCs and assess the effect of stimulation of these receptors on cell proliferation and vasculogenic response.
- Characterize hPLG as a human substrate for culture of ECFCs.
- Evaluate the ability of hPLG to induce the formation of capillary networks following encapsulation in this three-dimensional matrix.
- Develop a new method of fabrication of tubular scaffolds by electrospinning with improved surface properties.
- Assess the adhesion, proliferation and morphology of ECFCs on the vascular scaffolds and their modulation by different biochemical treatments.

# Chapter 2: Materials & Methods

## 2.1. Isolation and culture of peripheral blood Endothelial Colony Forming Cells (ECFCs)

50 mL of blood were collected by venepuncture from the median cubital vein of healthy, drug-free volunteers after obtaining their written consent. The donor consent procedure and venepuncture protocol were approved by the Ethics Committee of the University of Bath. ECFCs were obtained from the peripheral blood mononuclear cell (PBMNC) fraction of whole human blood, which was separated by density gradient centrifugation, as previously described (Ingram et al., 2004). Heparinized blood (2.5 U/mL) was diluted with an equal volume of $Ca^{2+}$/$Mg^{2+}$-free Phosphate-buffered saline (PBS; Gibco, Thermo Fisher Scientific, Paisley, UK) and carefully overlaid onto a layer of Ficoll-Paque PLUS (GE Healthcare, Uppsala, Sweden), with a density of 1.077 g/mL at 20 ºC, in conical tubes which were centrifuged at 400 x *g* (with low deceleration) for 30 min at room temperature. The intermediate layer, corresponding to the PBMNC fraction (i.e. buffy coat), was collected, resuspended in serum-free medium (EBM-2, cat. no. CC-3156, Lonza, Walkersville, US), centrifuged for 5 min at 500 x *g*, washed in EBM-2 and, finally, centrifuged at 250 x *g* to remove any remaining Ficoll-Paque and excess plasma. Tissue culture plastic was coated with collagen I from rat tail (50 µg/mL in 0.02 N acetic acid; Corning, Bedford, MA, US) at a final concentration of 5 µg/$cm^2$ of growth surface. Plates were then incubated at room temperature for 1 h, after which the collagen solution was carefully aspirated and the surfaces washed with PBS. Cells were seeded at a density of 2 x $10^5$ cells/$cm^2$ on the collagen-coated plastic in complete medium (EGM-2, Lonza), which contained 10% v/v FBS and the supplier's growth factor supplement (i.e. human basic Fibroblast Growth Factor, Vascular Endothelial Growth Factor, human Epidermal Growth Factor and long R3 Insulin-like Growth Factor 1; cat. no. CC-4176, Lonza) and incubated at 37 ºC under a humidified atmosphere with 5% $CO_2$. Cell culture medium was replaced every 2 days to maintain adequate nutrient levels and remove non-adherent cells. Plates were regularly inspected for 3 weeks for colony appearance. Colonies with a distinct endothelial morphology (i.e. tightly packed cobblestone shaped cells) could be found between days 14 and 21 amongst non-proliferating spindle shaped cells (Figure 2.1). Colonies were selectively detached using TrypLE Express (Gibco) and separately expanded. For subsequent passaging, every semi-confluent flask or well was washed with pre-warmed PBS and cells detached with TrypLE through incubation at 37 ºC for 5 min or until fully detached. The cell suspension pelleted by centrifugation at 220 x *g*

for 3 min in the presence of EGM-2 medium and cells were then seeded in new culture vessels at a sub-culture ratio of 1:3.

For cryopreservation, early passage cells were detached and pelleted in the same manner as for regular passaging, but were instead resuspended in cold EGM-2 containing 20% v/v FBS and 10% v/v DMSO. After transferring into cryovials, cells were gradually cooled at 1 ºC/min to -80 ºC in a freezing container (i.e. Mr Frosty) and transferred to liquid nitrogen storage after 24 h.

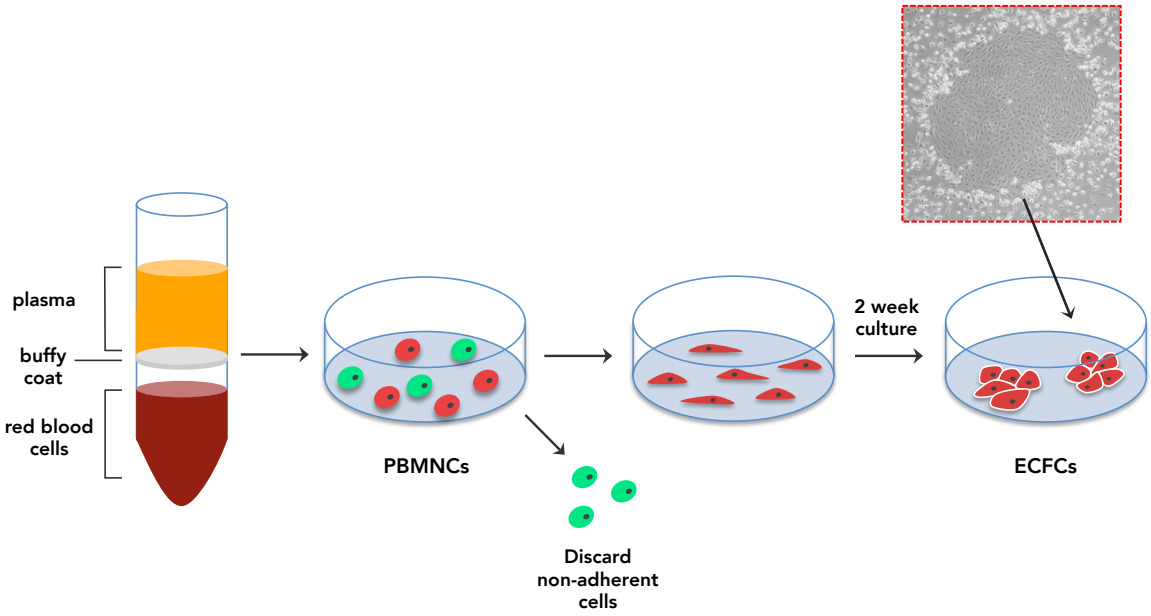


**Figure 2.1. Method of isolation of ECFCs.** Summary of method for isolating ECFCs from peripheral blood, as first described by Ingram *et al.* (2004).

## 2.2. Preparation of human platelet lysate (hPL)

Units of leukocyte-depleted platelet-rich plasma (PRP), prepared by cytapheresis, were kindly provided by the Blood Bank at the Royal United Hospitals (RUH) Bath NHS Foundation Trust. The bags were anonymised and released for research purposes under the ethical approval of the South West - Central Bristol Research Ethics Committee (REC) after their expiry (5 days after harvesting). Preparation and handling were performed in accordance with the guidelines approved by the Ethics Committee of the University of Bath. The platelet count for each unit was >2.40 x $10^{11}$ in an average volume of 200 mL plasma (supplemented with citrate to prevent platelet activation and coagulation). Platelets from 5 or more donors were pooled and lysed by ultrasonication using a Model 150VT Ultrasonic Homogenizer (BioLogics, Manassas, VA, US). A stepped titanium micro tip was used and sonication was performed at 40% amplitude (power) output and 75% pulse for 4 minutes per sample of 25 mL of PRP. Aliquots were then centrifuged at 4,000 x *g* (15 min, 4 ºC) to remove platelet fragments and sequentially filtered through 0.45 µm and 0.2 µm pore filters (Millipore, Watford, UK) to obtain human platelet lysate (hPL; Figure 2.2).

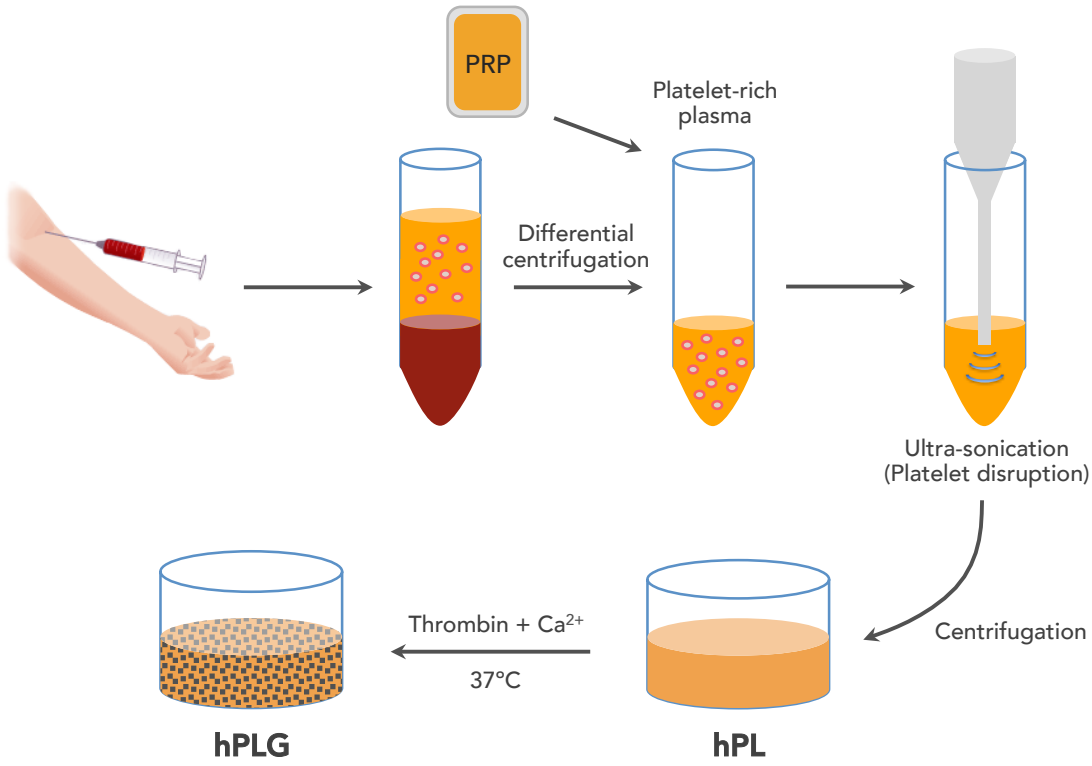


**Figure 2.2. Production of platelet lysate.** Overview of the procedure for the production of human platelet lysate (hPL) and human platelet lysate gel (hPLG).

## 2.3. Preparation of collagen, fibrin and platelet lysate gels

*Preparation of rat tail collagen I gels*

For the formation of collagen gels, rat-tail collagen I (Corning) was diluted to a final concentration of 1.5 mg/mL in acetic acid (0.02 N) and polymerized by neutralizing the pH using 1 M NaOH followed by incubation at 37 ºC for 10 min, as previously described (Koh, Stratman, Sacharidou and Davis, 2008).

*Preparation of human fibrin gels*

Fibrinogen from human plasma (Sigma-Aldrich) was dissolved in EBM-2 (Lonza) at 2 mg/mL and filter-sterilized through a 0.2 µm pore filter (Millipore). Human thrombin (Sigma-Aldrich) was then added at a concentration of 0.5 U/mL and the mixture incubated at 37 ºC for 10 min, causing the polymerization of fibrinogen into fibrin.

*Preparation of human platelet lysate gels (hPLG)*

As hPLG consists mainly of a fibrin network with additional ECM proteins, for its polymerization the same concentration of thrombin was used as for pure fibrin gels. Therefore, hPL was diluted in basal medium (20% v/v) (EBM-2, Lonza) and human thrombin (Sigma-Aldrich) was added to a final concentration of 0.5 U/mL, after which it was incubated at 37 ºC. Formation of hPLG (i.e. gelation) was observed within 5 minutes of thrombin addition.

## 2.4. Fabrication of scaffolds via electrospinning

Poly(D,L-lactic-co-glycolic acid) (PLGA; ester terminated, lactide:glycolide 75:25, molecular weight 76-115 kDa, Resomer® RG 756S, Boehringer Ingelheim) and polycaprolactone (PCL; number average molecular weight 80 kDa, Sigma-Aldrich) were dissolved at a concentration of 20% w/v in 9:1 2,2,2-trifluoroethanol (TFE) / hexafluoroisopropanol (HFIP) by stirring for 24 h at 20 ºC. Three different polymer blends were used: PLGA 25:75 PCL, PLGA 50:50 PCL and PLGA 75:25 PCL. The polymer solution was transferred to a 5 mL glass syringe (Hamilton) and electrospun at 15 kV (73030P high voltage power supply; Genvolt) through a 20G stainless steel needle at room temperature. A constant flow rate (Table 2.1) was maintained using a syringe infusion pump (Cole Parmer, London, UK) and a total of 1 mL was electrospun per scaffold. Fibres were collected in an ethanol bath (6 cm deep) with a round copper earthed collector (10 cm diameter) at its bottom, and wound around a Teflon cylinder

(1 cm diameter, 5 cm length) rotating at 200 rpm powered by a DC motor (part no. 919D501, Como Drills, Deal, UK). Prior to being removed from the tubular mold, each scaffold was washed three times in $dH_2O$ over a 2-hour period to elute any absorbed ethanol/solvent, and dried overnight. The electrospinning procedure is summarized in Figure 2.3.

***Table 2.1.*** *Electrospinning parameters*

| Polymer blend | Voltage (kV) | Flow rate (mL/h) |
|---|---|---|
| *PLGA 25:75 PCL* | 15 | 2.90 |
| *PLGA 50:50 PCL* | 15 | 2.25 |
| *PLGA 75:25 PCL* | 15 | 1.60 |

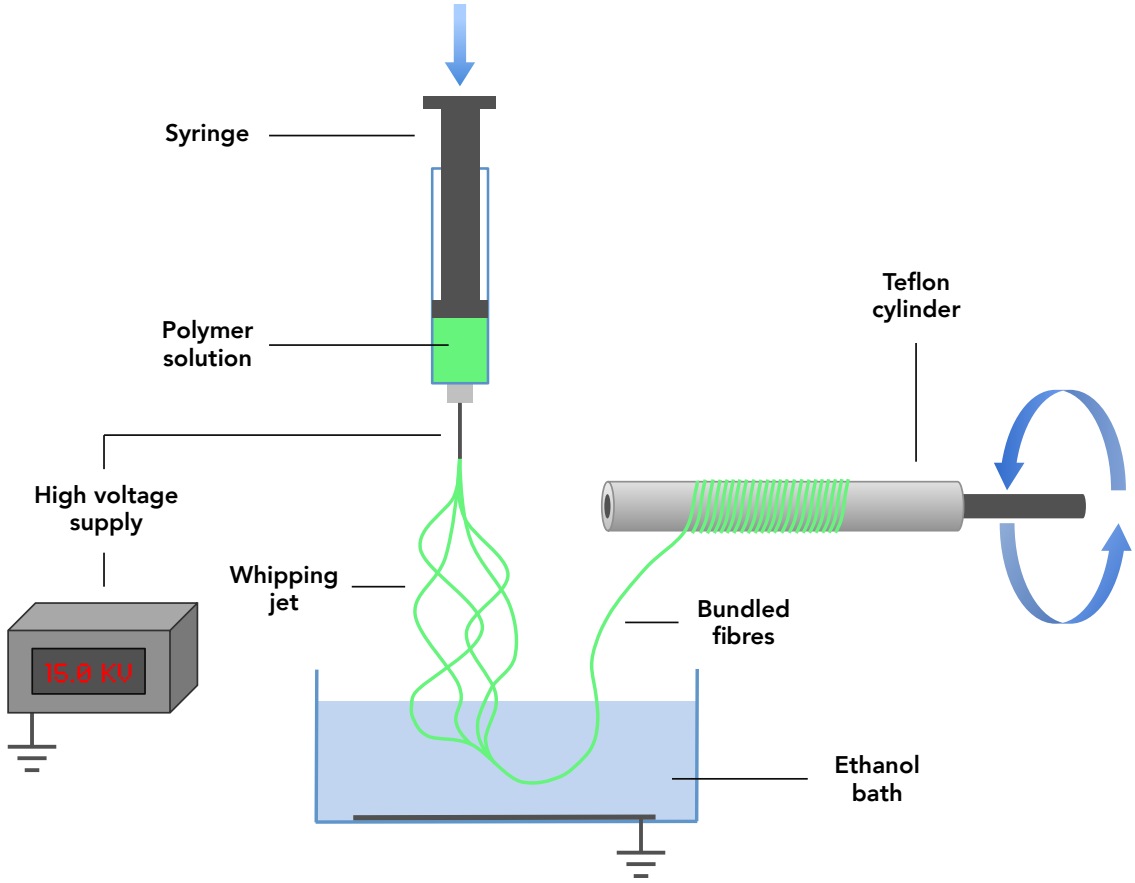


**Figure 2.3. Electrospinning method.** Overview of electrospinning apparatus for the production of tubular scaffolds.

### 2.5. Nitrogen gas plasma treatment

Scaffold samples made of the different polymer blends of PLGA/PCL were exposed to nitrogen ($N_2$) plasma in a ZEPTO low-pressure capacitively coupled radio-frequency glow discharge plasma reactor (Diener Electronic, Ebhausen, Germany) at 13.56 MHz. Plasma treatment was performed for 30 s, 60 s or 120 s, at 50% power setting (i.e. 25 W) with an inlet $N_2$ pressure of 1 bar.

### 2.6. Preparation and cell seeding on electrospun scaffold samples

For the evaluation of ECFC adhesion, proliferation, viability and morphology onto differently treated PLGA/PCL scaffolds, circular samples were cut using a 7 mm punch. Scaffolds were plasma-treated or left untreated, and sterilized by UV irradiation (30 min) followed by incubation in PBS containing 1% Gentamicin/Amphotericin B (Lonza) and 3% Penicillin/Streptomycin (Gibco) for 2 h. After sterilization, scaffolds were rinsed in sterile PBS and incubated with either FBS or hPL (diluted 1:1 in PBS containing 0.1% Gentamicin/Amphotericin B) for 1 h at room temperature. Subsequently, scaffold discs were rinsed three times in PBS, to remove any unbound constituents of FBS or hPL, and centrally placed onto 48-well culture plates. To prevent cell adhesion to the bottom of the plates, these were coated with 200 µL of sterile ultra-pure agarose (2% w/v in EBM-2; Invitrogen). ECFCs were then seeded at 7,000 cells/disc by dispensing a 20 µL droplet of cell suspension onto the centre of the scaffolds. Samples were incubated for 1 h at 37 ºC under a 5% $CO_2$ atmosphere after which time a further 250 µL of EGM-2 medium (10% FBS) was added to each well before samples were returned to the incubator for the desired time course.

### 2.7. Immunoblotting

For the phenotypic characterization of ECFCs, cells were lysed in radioimmunoprecipitation assay (RIPA) buffer (50 mM Tris, 150 mM NaCl, 0.1% w/v SDS, 0.5% v/v deoxycholic acid, 1% v/v Triton X-100) in the presence of protease inhibitors (cOmplete ULTRA, Roche, Burgess Hill, UK) and phosphatase inhibitors (PhosSTOP, Roche). Protein samples from ECFCs and PBMNCs were quantified through a colorimetric Micro BCA assay (Thermo Fisher Scientific) to enable loading of equal amounts per lane. Gel loading buffer (50 mM Tris-HCl, 2% w/v SDS, 20 mM DTT, 0.002% w/v bromophenol blue) was added to each sample at ratio of 1:5 v/v, and boiled for 5 minutes. Samples (10 µg) were then electrophoresed through sodium dodecyl sulfate polyacrylamide gels (SDS-PAGE) using 8%-12% w/v gels (depending

on target protein size) in electrophoresis Tris-glycine buffer (25 mM Tris, 192 mM glycine, 0.1% w/v SDS, pH 8.3), then transferred to PVDF membranes in wet transfer buffer (25 mM Tris, 192 mM glycine, 20% v/v methanol). Blots were blocked in either 5% w/v non-fat milk or 5% w/v bovine serum albumin (BSA) in TBST (50 mM Tris, 150 mM NaCl, 0.05% v/v Tween 20, pH 7.6) and probed with antibodies raised against the target protein (Table 2.2), diluted in TBST containing 5% w/v non-fat milk or BSA, overnight at 4 ºC. The primary antibody solution was then removed and blots were washed several times in TBST.

***Table 2.2.*** *List of primary antibodies used for immunoblotting*

| Antibody | Species | Manufacturer | Catalogue number |
|---|---|---|---|
| *β-Actin* | Mouse | Sigma-Aldrich | A5316 |
| *CD31* | Mouse | Cell Signaling | 89C2 |
| *ERK1/2* | Rabbit | Santa Cruz | sc-94 |
| *Phospho-ERK1/2* | Rabbit | Cell Signaling | 9101S |
| *PAR-1 (N19)* | Goat | Santa Cruz | sc-8203 |
| *PAR-2 (SAM11)* | Mouse | Santa Cruz | sc-13504 |
| *VE-cadherin* | Goat | Santa Cruz | sc-6458 |
| *VEGFR-2* | Rabbit | Cell Signaling | 55B11 |
| *vWF* | Rabbit | Dako | A0082 |

For enhanced chemiluminescence (ECL) based detection, blots were blocked for 30 min in TBST-milk, and then incubated in a species-appropriate horseradish peroxidase conjugated secondary antibody solution (1:2,000; Table 2.3) for 60 min. After washing in TBST, protein bands were detected by ECL and developed into photographic film (Fujifilm, Bedford, UK).

For fluorescence-based detection, blots were blocked for 30 min in PBS-based Odyssey Blocking Buffer (LI-COR), and then incubated in a species-appropriate fluorescently conjugated secondary antibody (1:20,000; Table 2.3) for 60 min. After washing three times in TBST and once in PBS, membranes were scanned with a LI-COR Odyssey CLx infrared imaging system. Densitometric analyses were performed using Image Studio Lite v5.0.21 (LI-COR).

***Table 2.3.*** *List of secondary antibodies used for immunoblotting*

| Antibody | Species | Manufacturer | Catalogue number |
|---|---|---|---|
| *Mouse IgG-HRP* | Sheep | GE Healthcare | NXA931 |
| *Goat IgG-HRP* | Donkey | Santa Cruz | sc-2020 |
| *Rabbit IgG IRDye 800CW* | Goat | LI-COR | 926-32211 |
| *Goat IgG IRDye 800CW* | Donkey | LI-COR | 926-32214 |
| *Rabbit IgG IRDye 680RD* | Goat | LI-COR | 926-68071 |
| *Mouse IgG IRDye 680RD* | Goat | LI-COR | 926-68070 |

## 2.8. Fluorescence staining

### 2.8.1. Immunofluorescence

*Staining of cells grown on coverslips*

Cells grown on coverslips were fixed and permeabilized in ice-cold 100% v/v methanol for 10 min. Following fixation, cells were washed in PBS and blocked with 1% w/v BSA/PBS for 30 min. Subsequently, samples were incubated overnight at 4 ºC with primary antibody (Table 2.4) diluted in blocking buffer (1:100). After three washing steps, samples were incubated for 1 h at room temperature with an appropriate fluorescently-conjugated secondary antibody (Table 2.5), diluted in blocking buffer (1:200) and with 1 µg/mL 4',6-diamidino-2-phenylindole (DAPI, Sigma-Aldrich) in PBS for 20 min to label cell nuclei, followed by three additional washes in PBS. Incubation with secondary antibodies and DAPI at the same concentration with no prior incubation with primary antibodies was used as a negative control. Samples were mounted on microscope slides with Vectashield HardSet Mounting Medium (Vector Laboratories, Peterborough, UK). Epifluorescence images were obtained using a Leica DMI4000B microscope (Leica, Wetzlar, Germany) with a 10x objective, while confocal images were acquired on a LSM 510 META microscope (Zeiss, Cambridge, UK) using a 63x oil-immersion objective. Images were analysed using ImageJ software (National Institutes of Health, Bethesda, MD; https://rsb.info.nih.gov/ij/).

*Staining of cells grown on ECM-based substrates*

ECFCs were grown to confluence on either collagen I-coated plates or hPLG and fixed in 4% v/v paraformaldehyde (PFA)/PBS for 15 min at room temperature. Following fixation, cells were washed three times in PBS and permeabilized in 0.1% v/v Triton X-100/PBS for 15 min. Following, blocking with 1% w/v BSA/PBS for 30 min,

samples were incubated overnight at 4 ºC with primary antibody (Table 2.4) diluted in blocking buffer (1:100). After washing with PBS, slides were incubated for 1 h at room temperature with fluorescently conjugated secondary antibody (1:200; Table 2.5) in blocking buffer and with 1 µg/mL Hoechst 33342 (Thermo Fisher Scientific) in PBS for 20 min to label nuclei. Epifluorescence images were obtained using a Leica DMI4000B microscope with a 10x objective.

*Staining of cells grown on fibrous scaffolds*

Cells were grown on synthetic fibrous scaffolds for 5 days and then fixed in 4% v/v PFA/PBS for 15 min at room temperature. Following fixation, samples were washed three times with PBS and cells permeabilized in 0.1% v/v Triton X-100/PBS for 15 min. Cellular F-actin and nuclei were labelled by incubating the samples for 20 minutes with 5 units/mL of TRITC-conjugated phalloidin (Molecular Probes, Thermo Fisher Scientific) and 1 µg/mL DAPI in 1% BSA/PBS, respectively. Samples were mounted on microscope slides with Vectashield HardSet Mounting Medium and z-stacked images were acquired with LSM 510 META confocal microscope (Zeiss) with a 20x objective. Images were analysed using ImageJ software.

***Table 2.4.*** *List of primary antibodies used for immunofluorescence*

| Antibody | Species | Manufacturer | Catalogue number |
|---|---|---|---|
| *CD31* | Mouse | Cell Signaling | 89C2 |
| *PAR-1 (N-19)* | Goat | Cell Signaling | sc-8203 |
| *PAR-2 (SAM11)* | Mouse | Santa Cruz | sc-13504 |
| *VE-cadherin* | Goat | Santa Cruz | sc-6458 |
| *vWF* | Rabbit | Dako | A0082 |

***Table 2.5.*** *List of secondary antibodies used for immunofluorescence*

| Antibody | Species | Manufacturer | Catalogue number |
|---|---|---|---|
| *Mouse IgG, Alexa Fluor 488* | Rabbit | Invitrogen | A11059 |
| *Goat IgG, Alexa Fluor 546* | Donkey | Invitrogen | A11056 |
| *Mouse, FITC* | Goat | Invitrogen | F-2761 |
| *Rabbit, FITC* | Goat | Invitrogen | F-2765 |

### 2.8.2. Lectin staining of cultured cells

ECFCs were grown to ~70% confluence on coverslips and fixed in 4% v/v PFA in TBS-based lectin buffer (50 mM Tris, 149 mM NaCl, 2.1 mM $MgCl_2$, 1 mM $CaCl_2$, pH 7.6) for 15 min, following a previously described protocol (Brooks and Hall, 2012). Samples were then washed three times in lectin buffer, followed by permeabilization in 0.1% v/v Triton X-100 for 15 min, and then blocked with 1% w/v BSA for 30 min (all solutions were prepared in lectin buffer). Cells were then incubated with FITC-labelled *Ulex europaeus* agglutinin (UEA) at a final concentration of 10 µg/mL and with DAPI (1 µg/mL) for 1 h. Coverslips were mounted in Vectashield HardSet Mounting Medium and epifluorescence images were obtained using a Leica DMI4000B microscope with a 10x objective.

### 2.8.3. Acetylated LDL (Ac-LDL) uptake

Uptake of Acetylated Low Density Lipoprotein (Ac-LDL) by ECFCs was tested using a commercially available kit (cat. no. 022K, Cell Applications, San Diego, US). ECFCs were grown on coverslips to near confluency and 1,1'-dioctadecyl–3,3,3',3'-tetramethyl-indocarbocyanine perchlorate-labelled acetylated low-density lipoprotein (DiI-Ac-LDL) was then added at a concentration of 10 µg/mL in medium. Cells were incubated at 37 ºC, 5% $CO_2$ for 4 h. Culture medium was then removed and samples were washed three times with wash buffer (proprietary composition) and nuclei stained with 1 µg/mL DAPI, followed by an additional wash. Cells were mounted in Vectashield HardSet Mounting Medium and epifluorescence images were obtained using a Leica DMI4000B microscope with a 10x objective using a standard rhodamine excitation/emission filter (552 nm excitation and 570 nm emission).

### 2.8.4. Live/dead assay

The identification of live and dead cells on scaffolds was performed using Viability/Cytotoxicity Assay Kit (Biotium, Hayward, CA, US). This assay uses calcein AM to label viable cells green and ethidium homodimer III (EthD-III) to label dead cells red. Scaffolds were prepared and seeded with 7,000 ECFCs/sample as described in 2.62 µM calcein AM and 4 µM EthD-III in reduced serum medium (2% v/v FBS) for 45 min at 37 ºC. Nuclei of all cells were stained using Hoechst 33342 (1 µg/mL) at the same time. At the end of the incubation period, the staining solution was removed and

fresh medium was added for subsequent imaging. Epifluorescence images were obtained using a Leica DMI4000B microscope at 10x magnification.

### 2.9. RNA analysis

#### 2.9.1. RNA isolation

RNA was extracted using two different techniques in order to obtain the best yield and purity:

1) For the evaluation of PARs expression, and detection of genes regulated through PAR-activation, total RNA was prepared with TRI Reagent (Ambion, Thermo Fisher Scientific) from ECFCs, human lung fibroblasts, glomerular endothelial cells, human myofibroblasts, and HK2 human renal proximal tubule epithelial cells (kindly donated by Cristina Beltrami and Dr Donald Fraser, Cardiff University). Cells were seeded at a density of $3 \times 10^4$ cells/well in 24-well plates and, after 24 h, were lysed in 500 µL of TRI Reagent solution then incubated at room temperature for 5 min to allow for nucleoprotein complexes to completely dissociate. The homogenate was then separated into aqueous and organic phases by adding 120 µL of chloroform and centrifuging at 12,000 x *g* for 15 min at 4 ºC. RNA was then precipitated from the aqueous phase by adding 250 µL of isopropanol and repeating the centrifugation step after 10 min of incubation at room temperature. The samples were then washed 3 times with 75% v/v ethanol and centrifuged for 5 min at 12,000 x *g*. RNA was then eluted in 15 µL of nuclease-free water.

2) To assess the effect on gene expression induced by hPLG, ECFCs were isolated from 3 different donors and cultured in triplicate on collagen I-coated plates or hPLG for 24 h followed by RNA extraction. Total RNA was extracted with TRIzol (Ambion) and further purified with the RNeasy Micro Kit (Qiagen, Venlo, Netherlands). ECFCs were lysed with 1 mL of TRIzol, then vortexed and kept at room temperature for 5 min. A volume of 200 µL of chloroform was added to the homogenate before centrifugation at 12,000 x *g* for 15 min at 4 ºC. The aqueous phase containing the RNA was collected and mixed with 1.5 volumes of 70% v/v ethanol. Each sample was then transferred to an RNeasy spin column and spun for 30 s at 12,000 x *g*. After

washing each spin column with a series of buffers supplied by the manufacturer, RNA was eluted by addition of 50 µL nuclease-free water.

Purity and concentration of RNA samples were assessed with the NanoDrop ND-1000 Spectrophotometer (Thermo Scientific). 1 µL of each sample was measured at 260 nm and 280 nm. Peak absorbance wavelengths for RNA and protein are 260 nm and 280 nm, respectively. The nucleic acid concentration is calculated using the Beer-Lambert law. The 260/280 ratio is used to assess the purity of RNA in terms of protein contamination and a ratio of 2.0 is usually indicative of "pure" RNA.

### 2.9.2. Reverse Transcription-Quantitative Polymerase Chain Reaction (RT-qPCR)

*cDNA synthesis*

Total RNA was converted into cDNA using one of the following protocols:

1) For the assessment of the expression of PARs and related target genes, cDNA was generated using High Capacity cDNA Reverse Transcription Kit (Applied Biosystems, Thermo Fisher Scientific). Reverse transcription (RT) master mix for one reaction was composed of 2 µL of 10X RT Buffer, 0.8 µL of 25X dNTP Mix (100 mM), 2 µL of 10X RT Random Primers, 1 µL of MultiScribe™ and 1 µL of RNAse Inhibitor. The 10 µL of 2X RT master mix was added to 10 µL of nuclease-free water containing 1 µg total RNA. The RT no template control contained only 10 µL of nuclease-free water. The following thermal cycler profile was used: 10 min at 25 °C, 120 min at 37 °C, 5 min at 85 °C, followed by cooling to 4 °C.

2) For samples relating to the study of hPLG's effect on ECFCs, cDNA was generated from 250 ng of total RNA using QuantiTect Reverse Transcription kit (Qiagen). Any possible contaminations from genomic DNA was removed by adding 2 µL of gDNA Wipeout buffer (supplied with the kit) and incubating for 2 min at 42 ºC. Each sample was then placed immediately on ice and mixed with the RT master mix containing 1 µL of reverse transcriptase, 4 µL of 5X Quantiscript RT buffer and 1 µL of RT primer mix (total reaction volume of 20 µL). The RT no template control contained only 12 µL of nuclease-free water. Samples were incubated for 30 min at 42 ºC followed by 3 min at 95 ºC to inactivate the reverse transcriptase.

The cDNA was stored at 4 ºC for a maximum of 1 week or at -20 ºC for up to 1 year.

*Quantitative PCR (qPCR)*

The qPCR master mix (final volume 20 µL) was prepared by combining 10 µL of Power SYBR® Green PCR Master Mix (Applied Biosystems), 300 nM of gene specific primers and cDNA. The amplification of a single PCR product for the genes of interest was confirmed by melting curve analysis. The nucleotide sequences of the primer pairs can be found in the table 2.6 The thermal cycling parameters used were: 10 min at 95 °C followed by 40 cycles at 95 °C for 15 s and 60 °C for 1 min. qPCR was carried out on a ViiA™7 or a QuantStudio™ 6 Flex Real-Time PCR System (Applied Biosystems). Gene-specific mRNA levels were estimated by the $2^{-\Delta\Delta Ct}$ method and normalized against GAPDH levels to obtain relative changes in gene expression, as previously described (Livak and Schmittgen, 2001).

The primers were designed using Primer-BLAST (NCBI, Bethesda, US) against mRNA sequences taken from the NCBI database. In order to avoid amplification of genomic DNA, when possible, primers were designed to span exon-exon junctions. PCR product length was ideally around 100-150 bp and the annealing temperature around 60 °C.

***Table 2.6.*** *List of primers used for qPCR*

| Gene | Primer Reverse | Primer Forward |
|---|---|---|
| *GAPDH* | 5'-TGACGAACATGGGGGCATCA | 5'-AGCCGCATCTTCTTTTGCGT |
| *Angiogenin* | 5'-CTGGGCGTTTTGTTGTTGGTC | 5'-GGTTTGGCATCATAGTGCTGG |
| *CD31* | 5'-TCGGAAGGATAAAACGCGGTC | 5'-CCAAGGTGGGATCGTGAGG |
| *CXCR4* | 5'-CCCACAATGCCAGTTAAGAAGA | 5'-ACTACACCGAGGAAATGGGCT |
| *eNOS* | 5'-TGATGGCGAAGCGAGTGAAG | 5'-ACTCATCCATACACAGGACCC |
| *FGFR-1* | 5'-AATGAGTACGGCAGCATCAAC | 5'-ACCTCGATGTGCTTTAGCCAC |
| *IL-8* | 5'-AACCCTCTGCACCCAGTTTTC | 5'-ACTGAGAGTGATTGAGAGTGGAC |
| *PAR-1* | 5'-GTAATGCGCAATCAGGAGGACG | 5'-GTATCCCATGCAGTCCCTCTCC |
| *PAR-2* | 5'-TGAAGATGGTCTGCTTCACG | 5'-TCTGCATCTGTCCTCACTGG |
| *PDGFR-β* | 5'-AGACACGGGAGAATACTTTTGC | 5'-AGTTCCTCGGCATCATTAGGG |
| *SDF-1* | 5'-ATTCTCAACACTCCAAACTGTGC | 5'-ACTTTAGCTTCGGGTCAATGC |
| *VE-cadherin* | 5'-TCTCCAGGTTTTCGCCAGTG | 5'-AAGCGTGAGTCGCAAGAATG |
| *VEGFA* | 5'-AGGGTCTCGATTGGATGGCA | 5'-AGGGCAGAATCATCACGAAGT |
| *VEGFR-2* | 5'-CCAGTGTCATTTCCGATCACTTT | 5'-GGCCCAATAATCAGAGTGGCA |
| *vWF* | 5'-GCCCTGGTTGCCATTGTAATTC | 5'-AGCCTTGTGAAACTGAAGCAT |

## 2.10. Quantification of growth factor (GF) concentrations in hPL and hPLG-conditioned medium

The concentrations of VEGF-A, EGF, PDGF-BB and FGF-2 in three separate batches of 20% v/v hPLG preparations, and GF release from hPLG into basal medium were determined by enzyme-linked immunosorbent assay (ELISA) using the Human Growth Factor II ELISA Strip Kit (Signosis, Santa Clara, US) according to the manufacturer's instructions. 100 µL of sample were used per well and absorbance was measured spectrophotometrically at 450 nm. The concentrations of the growth factors in each sample are directly proportional to its colour intensity and were calculated using a standard curve obtained with the supplied GF protein standards.

For the time course GF release experiment, hPLG was prepared as previously described in 12-well plates, and 1 mL of medium was added immediately after polymerization. Samples of conditioned medium in the absence of cells were collected after 1, 3 and 5 days incubation at 37 ºC, and kept at -80 ºC. As above, 100 µL of sample were used per well and absorbance was measured spectrophotometrically at 450 nm to quantify the GF concentrations in each sample, with the use of a standard curve.

## 2.11. Cell proliferation

### 2.11.1. Nuclei quantification assay

ECFCs were seeded at a density of 12,000 cells/well in 24-well plates on collagen I-coated wells or hPLG, and cultured in complete medium (EGM-2, Lonza) with 10% v/v FBS with or without pharmacological treatments. Cells were fixed after 24 h in 4% v/v PFA/PBS and nuclei stained with Hoechst 33342 as above. Fluorescent images were acquired using a Leica DMI4000B microscope (5x objective) and nuclei were manually counted using ImageJ software to quantify cell numbers.

### 2.11.2. Resazurin-based cell viability assay

Viability of cells seeded onto scaffolds was measured using a resazurin-based assay as an indicator of cell proliferation (Sittampalam et al., 2004). Scaffolds were prepared and seeded with 7,000 ECFCs/sample as described in section 2.6. PrestoBlue Cell Viability reagent (Molecular Probes, Thermo Fisher Scientific) was diluted 1:10 v/v in cell culture medium and added to cells at 200 µL per well, followed by incubation at 37 ºC for 3 h. At this point, medium was collected and transferred into

a 96-well plate and fluorescence intensity was read with excitation at 560/10 nm and emission at 590/10 nm using a CLARIOstar microplate reader (BMG Labtech, Aylesbury, UK). The fluorescence values of the no-cell control wells was averaged and subtracted from the fluorescence value of each experimental well. After each reading, fresh medium was added to the cells and plates were returned to the incubator. The assay was performed at 1, 3 and 5 days post-seeding on the same samples and was repeated a total of four independent times with three replicates per condition.

### 2.11.3. Double stranded DNA (dsDNA) quantification assay

The amount of dsDNA in each scaffold after 5 days of culture was quantified using the Quant-iT™ PicoGreen assay kit as an indicator of cell proliferation (Ng, Leong and Hutmacher, 2005). Scaffolds were prepared and seeded with 7,000 ECFCs/sample as described in section 2.6. A working solution was prepared by diluting the PicoGreen dsDNA reagent (1:200) in TE buffer (10 mM Tris-HCl, 1 mM EDTA, pH 7.5). Scaffolds were transferred to microtubes and 150 µL of lysis buffer (10 mM Tris pH 8, 1 mM EDTA, 0.1 % v/v Triton X-100) was added to each tube. Samples were vortexed for 10 seconds every five minutes for 30 min on ice and homogenized using a 21-gauge needle to ensure the efficient disruption of all cellular content. 100 µL of cell lysate samples (previously diluted 1:10 in TE buffer) were mixed with 100 µL of PicoGreen working reagent and incubated in microplate wells for 5 min at room temperature in the dark. Following incubation, fluorescence was measured with excitation at 483/15 nm and emission at 530/30 nm using a CLARIOstar microplate reader (BMG Labtech) with a dichroic filter at 502.8 nm. The fluorescence values of the blank control wells were averaged and subtracted from the fluorescence value of each experimental well. The assay was repeated a total of four times with three replicates per condition.

## 2.12. Angiogenesis/vasculogenesis assays

### 2.12.1. *In vitro* network formation assay

The procedure followed a protocol previously described (Arnaoutova and Kleinman, 2010) and is outlined in figure 2.4. Growth Factor Reduced (GFR)-Matrigel™ (BD Biosciences, Oxford, UK) was used to provide an extracellular matrix for cell culture by adding 65 µL of Matrigel into each well of a 96-well microplate and incubating at 37 ºC for 30 min to achieve gelation. ECFCs were detached using Accutase (Life Technologies) and plated at 7,500 cells/well in 100 µL of basal medium containing 2% v/v FBS and respective pharmacological treatments. Cells were cultured

at 37 ºC, 5% $CO_2$ for 4 hours. Phase contrast pictures were taken on an EVOS FL Cell Imaging System (Life Technologies, Thermo Fisher Scientific) with an UPlan FL N 4X/0.13 objective. Images were processed with ImageJ.

The vasculogenic coefficient was calculated by measuring the number of tubes, total tube length and number of nodes normalized to control using ImageJ with Angiogenesis Analyzer plugin (Gilles Carpentier, Faculté des Sciences et Technologie, Université Paris Est, Creteil Val de Marne, France).

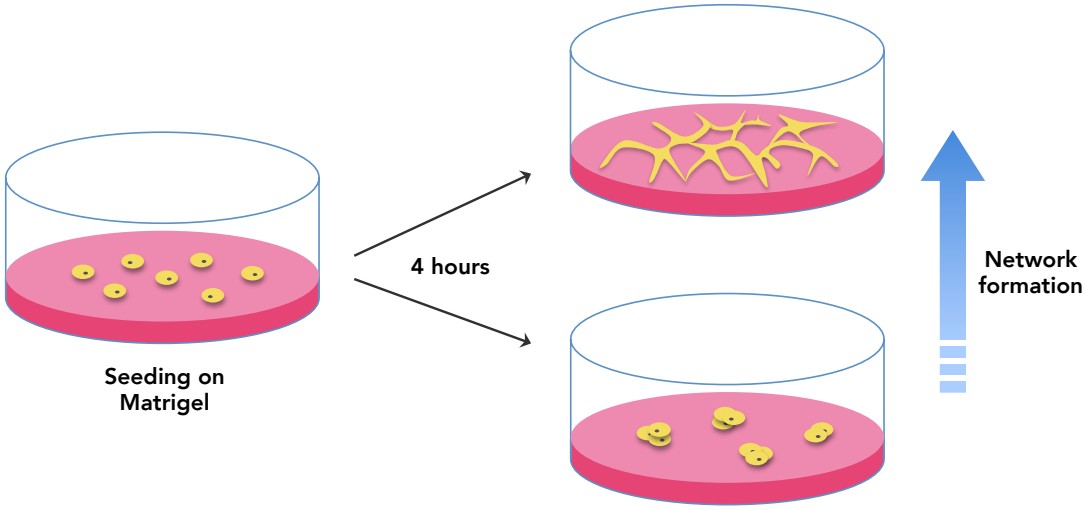


**Figure 2.4. Summary of *in vitro* network formation assay on basement membrane matrix (Matrigel).** Cells were seeded on GFR-Matrigel and cultured for 4 h before being imaged. Higher network formation was characterized by increased connections between cells (i.e. number of tubes and tube length).

### 2.12.2. *In vitro* 3D vasculogenesis assay

Encapsulation of ECFCs was performed in three different gel matrices: collagen I, fibrin and hPLG, which were prepared as described in section 2.3. Cells were mixed with the three gel precursors at a density of 2 x $10^5$ cells/mL and 70 µL of each cell suspension was added per well of a 96-well plate. Gelation was completed by incubation at 37 ºC for 10 min. Cells were then cultured for 3 days in serum-free basal medium for hPLG, and with complete medium (containing 10% v/v FBS plus recombinant GFs specified in the cell culture method – i.e. hFGF2, VEGF, hEGF and R3-IGF1) for cells in collagen and fibrin gels. For assessment of endothelial growth, constructs were fixed in 4% v/v PFA in TBS-based lectin buffer (see section 2.8.2) for 20 min, permeabilized in 0.1% v/v Triton X-100 for 15 min and blocked with 1% w/v

BSA for 30 min. Samples were then double stained with FITC-conjugated Ulex europaeus agglutinin (UEA) (10 µg/mL, overnight, 4 ºC) and Hoechst 33342 (1 µg/mL, 30 min, room temperature). For live cell imaging of lumenized networks in hPLG, gels with encapsulated ECFCs were formed inside plastic cloning rings (of equivalent diameter to a well of 96-well plate) which were placed on top of a thin glass bottom 35 mm imaging dish (*µ*-Dish, Ibidi, Martinsried, Germany) and cells were cultured in basal medium for 3 days. Cells were then incubated with Calcein AM (10 µM, 1 h) and Hoechst 33342 (1 µg/mL, 15 min) to stain their cytoplasms and nuclei, respectively. After replacing the medium, epifluorescence images were obtained using an EVOS FL microscope (Life Technologies) with 4x and 10x objectives whereas confocal live microscopy was performed with a LSM 510 META confocal microscope (Zeiss) with 10x and 20x objectives under 37 ºC, 5% $CO_2$ atmosphere. Image analysis and quantification of length of the capillary network in the different conditions were performed using ImageJ.

### 2.12.3. Aortic ring/ECFC co-culture assays

The aortic ring angiogenic assay was performed as previously described by Nicosia *et al*. (Nicosia and Ottinetti, 1990) with some modifications. 4 to 6-week-old Wistar rats, euthanatized by cervical dislocation, were obtained from Emma Robson and Prof. Roland Jones. Procedures were approved by the University's Animal Welfare and Ethical Review Body Committee and performed in conformity with the U.K. Animals (Scientific Procedures) Act 1986, the European Communities Council Directive 1986 (86/609/EEC) and were further subject to conformity with the University of Bath ethical review document. Each animal was surface-sterilized with 70% v/v ethanol and laid, back down, on a dissecting board in a laminar flow tissue culture hood to ensure sterility. With the use of a dissection microscope, aortas were harvested and the surrounding fibro-adipose tissues were removed. After rinsing with EBM-2 culture medium, aortas were sectioned into 1 mm ring segments. Rings were serum-starved for 24 h in EBM-2 supplemented with gentamicin (30 µg/mL) and amphotericin (15 ng/mL) at 37 ºC and 5% $CO_2$. These were then embedded in collagen I, fibrin or hPLG and cultured for 3 days in EBM-2 (with 2% v/v FBS, except for hPLG). Phase contrast images were acquired with an EVOS FL microscope (Thermo Fisher Scientific), and sprouting (area and length) was quantified manually using ImageJ software.

For the co-culture assay, $2 \times 10^5$ ECFCs/mL were encapsulated in hPLG surrounding the aortic rings and cultured as above. After 3 days, constructs were fixed in 4% v/v PFA in TBS-based lectin buffer (see section 2.8.2) for 20 min, permeabilized in 0.1% v/v Triton X-100 for 15 min and blocked with 1% w/v BSA for 30 min. Differential staining of human and rat endothelial cells was performed by incubating constructs overnight with FITC-UEA (10 µg/mL) and TRITC-conjugated Isolectin GS-IB4 (10 µg/mL), respectively, in addition to Hoechst 33342 (1 µg/mL) for staining of nuclei from both species. Epifluorescence images were obtained using an EVOS FL microscope with 4x and 10x objectives.

### 2.13. Electron Microscopy

#### 2.13.1. Scanning electron microscopy (SEM)

Encapsulated ECFCs (see section 2.12.2) or cell-free fibrin and hPLG samples were fixed with 2.5% v/v glutaraldehyde (GDA) in serum-free medium overnight at 4 ºC, followed by post-fixation with 1% v/v osmium tetroxide containing 1% w/v potassium ferrocyanide for 1 h. The samples were washed three times in PBS for 15 min, stained in 1% aqueous uranyl acetate solution for 1 h in the dark and dehydrated in the following acetone series: 50%, 70%, 90%, 95% v/v for 10 min each, and then in 100% acetone for 20 min. Subsequently, samples were dried by evaporation with hexamethyldisilazane and adhered to aluminium stubs using carbon tape.

Samples of ECFC-seeded PLGA/PCL scaffolds were fixed in 4% v/v PFA/PBS at 4 ºC overnight. These were further fixed in 2.5% v/v GDA in 0.1 M sodium cacodylate buffer (pH 7.3) for 2 h at room temperature. Samples were then rinsed three times in sodium cacodylate buffer and post-fixed with 1% v/v osmium tetroxide containing 1% w/v potassium ferrocyanide for 1 h at room temperature. After washing in distilled water three times over 15 min, samples were snap-frozen and freeze-dried. For the preparation of cell-free polymer fibre scaffolds, samples were adhered to aluminium stubs using carbon tape, and immediately degassed in vacuum overnight.

All samples were coated with gold using a Sputter Coater S150B system (Edwards, Crawley, UK). Images were captured with a JSM-6480LV Scanning Electron Microscope (JEOL, Tokyo, Japan).

### 2.13.2. Transmission electron microscopy (TEM)

ECFCs, encapsulated in hPLG (see section 2.12.2), were cultured for 3 days, after which they were fixed with 2.5% v/v GDA in serum-free medium overnight at 4 ºC, followed by post-fixation with 1% osmium tetroxide containing 1% potassium ferrocyanide for 1 h. The samples were then washed three times in 0.1 M sodium cacodylate buffer for 15 min, stained in 1% aqueous uranyl acetate solution for 1 h in the dark and dehydrated in an acetone series: 50%, 70%, 90%, 95% for 10 min each at 4 ºC and then in 100% acetone for 20 min at room temperature. Samples were then infiltrated with Spurr's Epoxy Resin by immersion in 1:1 v/v resin/dry acetone for 2 h and then overnight in 100% resin. The samples were then embedded in 100% resin and polymerized at 70 ºC for 8 h. Electron micrographs of 100 nm sections were taken using a JEM-1200EX II transmission electron microscope (JEOL).

### 2.14. Fibre diameter measurement

The average fibre diameter of electrospun PLGA/PCL scaffolds was determined by measuring 100 randomly selected individual fibres per scaffold type using ImageJ software. SEM images, at 1,500x magnification for PLGA 25:75 PCL scaffolds and at 3,000x for the other blends, were analysed using ImageJ. Data were plotted as a frequency distribution histogram with a bin width of 0.2 µm for PLGA 25:75 PCL scaffolds and of 0.1 µm for the other blends to which a gaussian non-linear regression was then fitted using Prism 5 (GraphPad Software, La Jolla, US).

### 2.15. Contact angle analysis

Untreated and plasma-treated (see section 2.19) PCL/PLGA electrospun scaffolds were cut into rectangles of 0.5 x 1 cm and held flat on glass slides using masking tape. A 10 µL droplet of distilled water was automatically dispensed from a Hamilton glass syringe onto each specimen using an OCA 15Pro (DataPhysics Instruments, Filderstadt, Germany) contact angle analysis system. A video was captured for 60 s at 3 frames/s for each drop using the built-in USB camera coupled to a 6x zoom lens directly opposite a light source. Right and left water contact angles of individual frames were determined using the SCA software (DataPhysics) by applying tangents at the intersections of the drop outline and the baseline. Three replicates were performed for each of the triplicate scaffolds.

## 2.16. Surface analysis

### 2.16.1. Fourier transform infrared spectroscopy (FTIR)

Platelet lysate (hPL), native and plasma-treated (see section 2.5) PLGA/PCL scaffolds and hPL-treated scaffolds were assessed with regards to their surface chemistry by Fourier transform infrared spectroscopy (FTIR). Samples of hPL-incubated scaffolds were rinsed three times in PBS and then freeze-dried prior to analysis. Spectra were obtained using a FTIR spectrometer (PerkinElmer Frontier) with an Attenuated Total Reflectance (ATR) accessory. For each sample, 10 scans were performed over a wavelength range of 4,000-600 $cm^{-1}$ at a resolution of 2 $cm^{-1}$, and spectra then normalized using advanced ATR correction.

### 2.16.2. X-ray photoelectron spectroscopy (XPS)

The surface functionalization of the electrospun scaffolds following nitrogen gas plasma treatment was studied by X-ray photoelectron spectroscopy. Spectra were obtained at the XPS Surface Analysis Facility (Cardiff Catalysis Institute) at Cardiff University. Untreated and freshly plasma-treated samples (see section 2.5) were analysed in a K-Alpha$^+$ XPS instrument (Thermo Scientific), using monochromatic Al Kα X-rays over a 400 µm area. For all samples, a pass energy of 150 eV and a step size of 1 eV were employed for survey spectra, while a pass energy of 40 eV and a step size of 0.1 eV were used for high resolution spectra of the elements of interest (carbon, oxygen and nitrogen). One sample was analysed per condition, and in each, three spots were investigated. Quantification was performed using CasaXPS v2.3.17 (Casa Software) using Scofield elemental sensitivity factors and an energy dependence of -0.6.

## 2.17. Quantification of protein adsorption by electrospun scaffolds

Samples cut from the three different PLGA/PCL blend scaffolds using a 7 mm diameter punch and plasma-treated for 30 s, 60 s or 120 s (as described in section 2.5), or left untreated. These discs were then placed in 48-well plates and incubated with 1:1 hPL/PBS for 1 h at room temperature. Scaffold samples were then rinsed three times in PBS to remove any unbound protein, followed by protein extraction using 150 µL of RIPA buffer with added protease inhibitors (cOmplete ULTRA, Roche) for 2 h at 4 ºC. The amount of protein from hPL adsorbed onto scaffolds was quantified through a colorimetric Micro BCA assay (Thermo Fisher Scientific).

### 2.18. Statistical analysis

Data are expressed throughout as mean values ± standard error of the mean (SEM). Statistical analysis was performed using Prism 6 (GraphPad Software). Statistical significance was analysed by one-way ANOVA with Bonferroni post-test (when comparing experimental conditions versus a control) or Tukey's (when comparing all conditions in between them) for experiments with three or more conditions and Student's T-test for experiments with two conditions. For grouped experiments, data was analysed by two-way ANOVA with Tukey's post-test. Normality and equality of group variances were tested by Shapiro-Wilk and Brown-Forsythe tests respectively. A statistically significant difference was accepted if $p<0.05$.

# Chapter 3: Protease-activated receptors in ECFC vasculogenesis

### 3.1. Background

Protease-activated receptors (PARs) are a group of G protein-coupled receptors that are essential to coagulation and are involved in the regulation of vascular tone, permeability and secretory activity in mature endothelial cells (Hamilton, Nguyen and Cocks, 1998; Roy et al., 1998; Ballerio et al., 2007). PARs are irreversibly activated by cleavage of their extracellular domain by extracellular proteases, which include thrombin (Vu, Hung, Wheaton and Coughlin, 1991), trypsin (Nystedt, Emilsson, Wahlestedt and Sundelin, 1994), tryptase (Molino et al., 1997) and coagulation factors VIIa and Xa (Camerer et al., 2002). The cleavage by proteases unmasks a 'peptide agonist' domain of the extracellular domain of the receptors. When unmasked, the ‘peptide agonist’ domain interacts in an intramolecular manner with the extracellular portion of the receptor, inducing receptor activation and its coupling with intracellular signalling pathways (Figure 3.1a) (Coughlin, 2005). Therefore, short synthetic peptide sequences corresponding to the tethered ligand motif of the proteolytically generated new N-terminal region can be used to selectively activate these receptors (Figure 3.1b), mimicking the effect of the activating enzymes (e.g. thrombin and trypsin) without cleaving other proteins which are also substrates (Hollenberg, Saifeddine, Al-Ani and Kawabata, 1997).

A number of studies have corroborated the role of PAR-1 and PAR-2 in the promotion or regulation of angiogenesis, in both reparative and pathological states. A significant increase in the expression of thrombin has been observed in the retinas of patients with proliferative diabetic retinopathy, which is characterized by excessive neovascularization, and an increase in the levels of cleaved PAR-1 in rat retinas following induction of diabetes (Abu El-Asrar et al., 2016). Evidence points to platelets as the main intermediaries in this phenomenon, with several authors reporting a significant release of vascular endothelial growth factor (VEGF) and stromal cell–derived factor-1 (SDF-1) in platelets following activation of PAR-1 on their surface (Etulain, Mena, Negrotto and Schattner, 2015; Chatterjee et al., 2011). In this sense, the local release of alpha-granules following thrombin-dependent PAR-1 activation could represent one of the main mechanisms by which platelets promote angiogenesis. Although not expressed by platelets, PAR-2 has been shown to play a role in blood vessel formation. It is known that this receptor is involved in the downstream signalling of tissue factor (TF)-VIIa protease complex that regulates angiogenesis (Belting et al., 2004) and that its activation increases VEGF expression in human glioblastoma cell lines through ERK phosphorylation (Dutra-Oliveira, Monteiro and Mariano-Oliveira,

2012). Also of relevance, the injection of PAR-2 activating peptide in mice stimulated capillary formation and enhanced recovery in a mouse model of limb ischaemia (Milia et al., 2002), but unfortunately no studies have followed up on these findings and investigated the outcome of such approach in human subjects.

While it has been shown that PAR-1 is expressed in ECFCs (Smadja et al., 2009), the expression of PAR-2 has not been investigated in this cell type. If PAR-2 is expressed in ECFCs, the local accumulation of active proteases following stimulation of the coagulation cascade by tissue damage could play a relevant role in the recruitment and activation of these progenitors at the site of vascular injury. Additionally, since PAR-2 is not expressed in platelets and is activated mainly by trypsin (not directly by thrombin, like PAR-1), it could represent a possible selective target for manipulation of ECFCs and their utilisation in cell therapy and tissue engineering without interfering with the normal coagulation process.

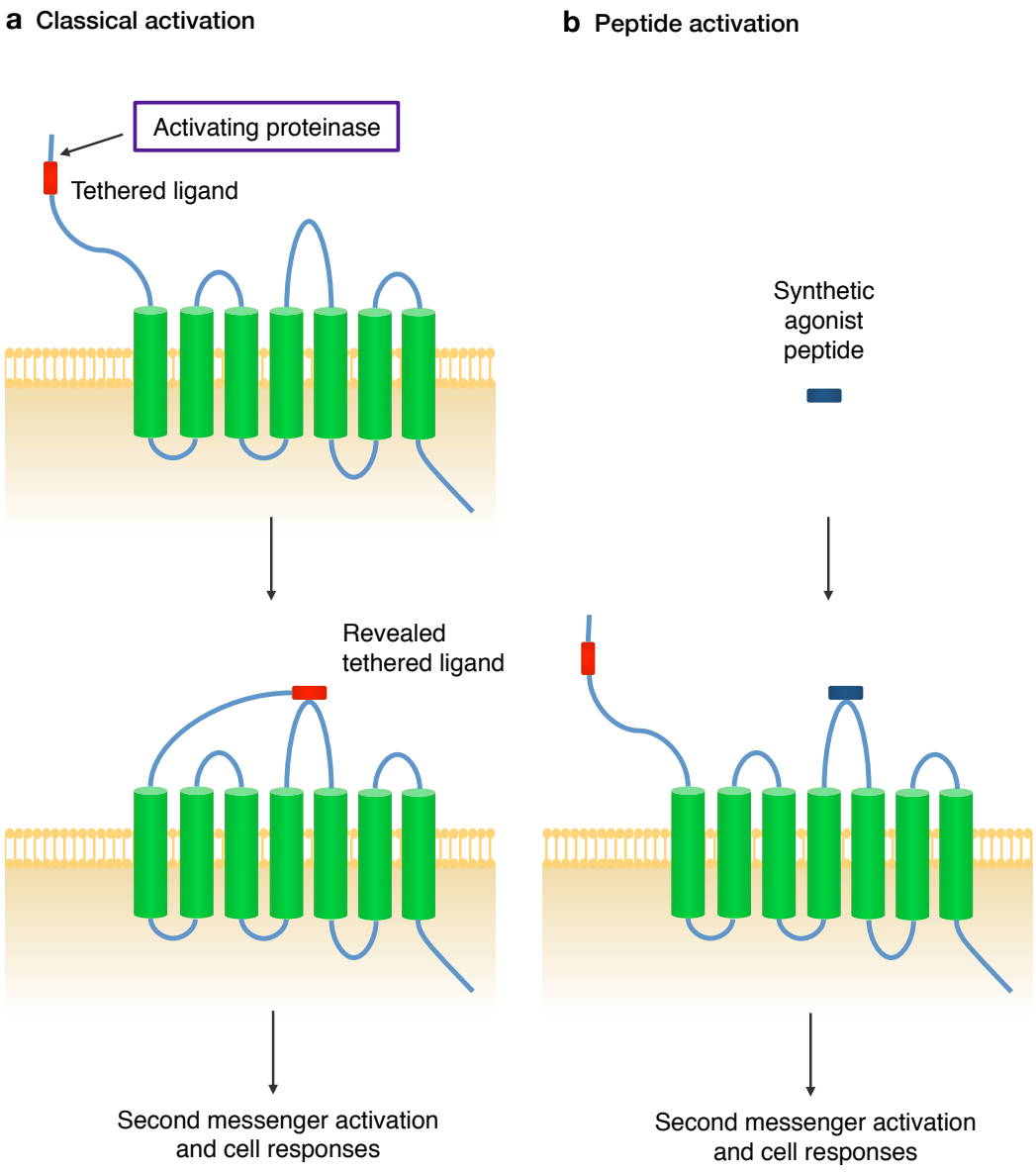


**Figure 3.1. Mechanism of protease-mediated receptor activation.** The figure depicts the activation of PARs by proteolytic cleavage and exposure of the tethered ligand to stimulate signalling (**a**). Activation of PARs can also be achieved by addition of synthetic agonist peptides in the absence of proteolytic unmasking of the tethered ligand (**b**).

### 3.2. Aims & Objectives

As described, PARs are involved in the regulation of a range of vascular mechanisms but their role in vasculogenesis is still not clear. Since these receptors can be selectively activated by small peptides, they may constitute a suitable target for promotion of vascularization using ECFCs if they are proven to positively influence the formation of blood vessels by these cells.

The aim of the work in this chapter is therefore to investigate the role of PARs in ECFC-driven vasculogenesis, which encompasses the following objectives:

- To establish the isolation of ECFCs and phenotypically characterize them.
- To confirm the expression of PAR-1 and PAR-2 in ECFCs.
- To test the effect of PAR stimulation on ECFC isolation.
- To assess the role of PAR activation on proliferation and tubular network formation by ECFCs and characterize signalling mechanisms.

## 3.3. Results

### 3.3.1 Characterisation of ECFCs

ECFCs can be isolated as cell colonies and expanded *ex vivo* from both umbilical cord blood mononuclear cells and adult peripheral blood mononuclear cells (PBMNCs) (Ingram et al., 2004). To establish the isolation of these cells as a routine method within our laboratory, hPBMNCs were harvested from healthy adults and the existing protocol developed by Ingram and colleagues (Ingram et al., 2004) was followed. Distinct colonies with cobblestone morphology could be observed among the adherent spindle-shaped hPBMNCs around 14-21 days after seeding (Figure 3.2). These colonies could be expanded for up to 8-10 passages with no obvious morphological alterations, while maintaining a colony-like growth.

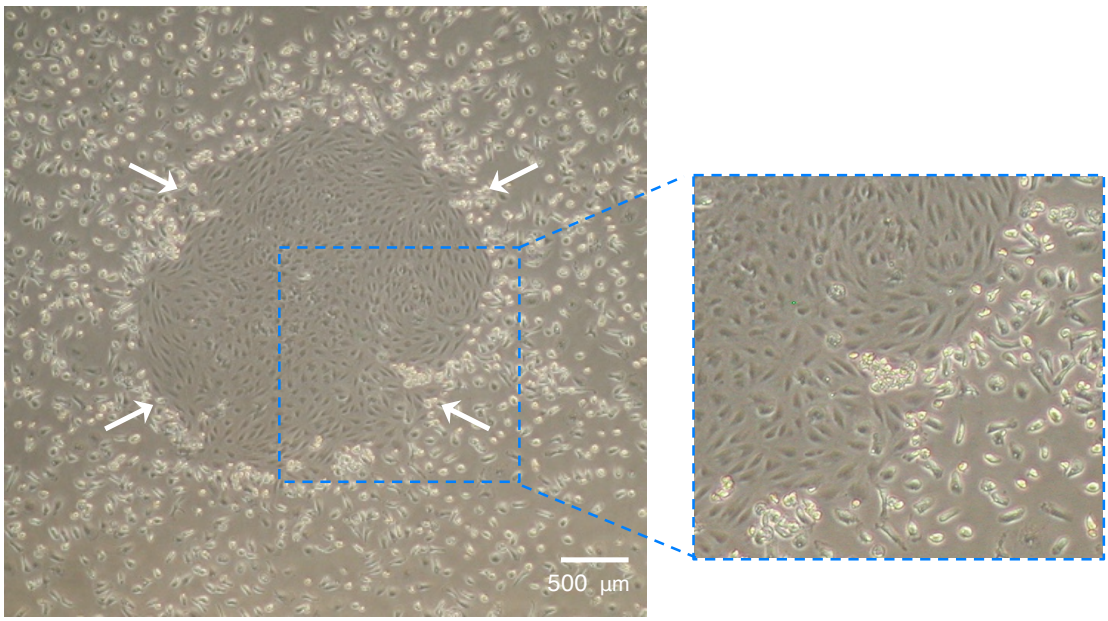


**Figure 3.2. Representative ECFC colony.** Photomicrograph of a typical ECFC colony appearing between 14 and 21 days following initial plating of hPBMNCs. Freshly isolated hPBMNCs were cultured on collagen type I-coated plates in EGM-2 medium and emerging colonies could be distinguished by their cobblestone morphology characteristic of endothelial cells.

The endothelial phenotype of the isolated cells was confirmed by immunoblotting for endothelial markers VEGFR-2, vWF, VE-Cad and CD31 (Figure 3.3A). While CD31 expression could be detected in both ECFCs and in the initial hPBMNC population (as expected due to the presence of leukocytes and platelets), specific endothelial markers such as VEGFR-2 and VE-Cad could only be detected in ECFCs. This phenotype was further confirmed by immunostaining for VE-Cad, (Figure 3.3B), denoting a typical localization pattern at the intercellular junctions, and for vWF, highlighting a punctate distribution compatible with the staining of the Weibel-Palade bodies (Figure 3.3C). Other hallmarks of an endothelial lineage were demonstrated, such as staining with FITC-conjugated Ulex europaeus lectin (FITC-UEA I) (Figure 3.3D), which binds to α-L-fucose-containing glycocompounds on the surface of these cells, and the ability to take up 1,1'-dioctadecyl–3,3,3',3'-tetramethyl-indocarbocyanine perchlorate-labelled acetylated low-density lipoprotein (DiI-Ac-LDL) (Figure 3.4).

Finally, cells treated with rhVEGF were grown on a layer of Growth Factor Reduced-Matrigel for up to 24 h (Arnaoutova and Kleinman, 2010). ECFCs organized into tubular networks in under 6 h in response to rhVEGF (Figure 3.5), suggestive of their ability to differentiate into mature endothelial cells and form capillary-like structures.

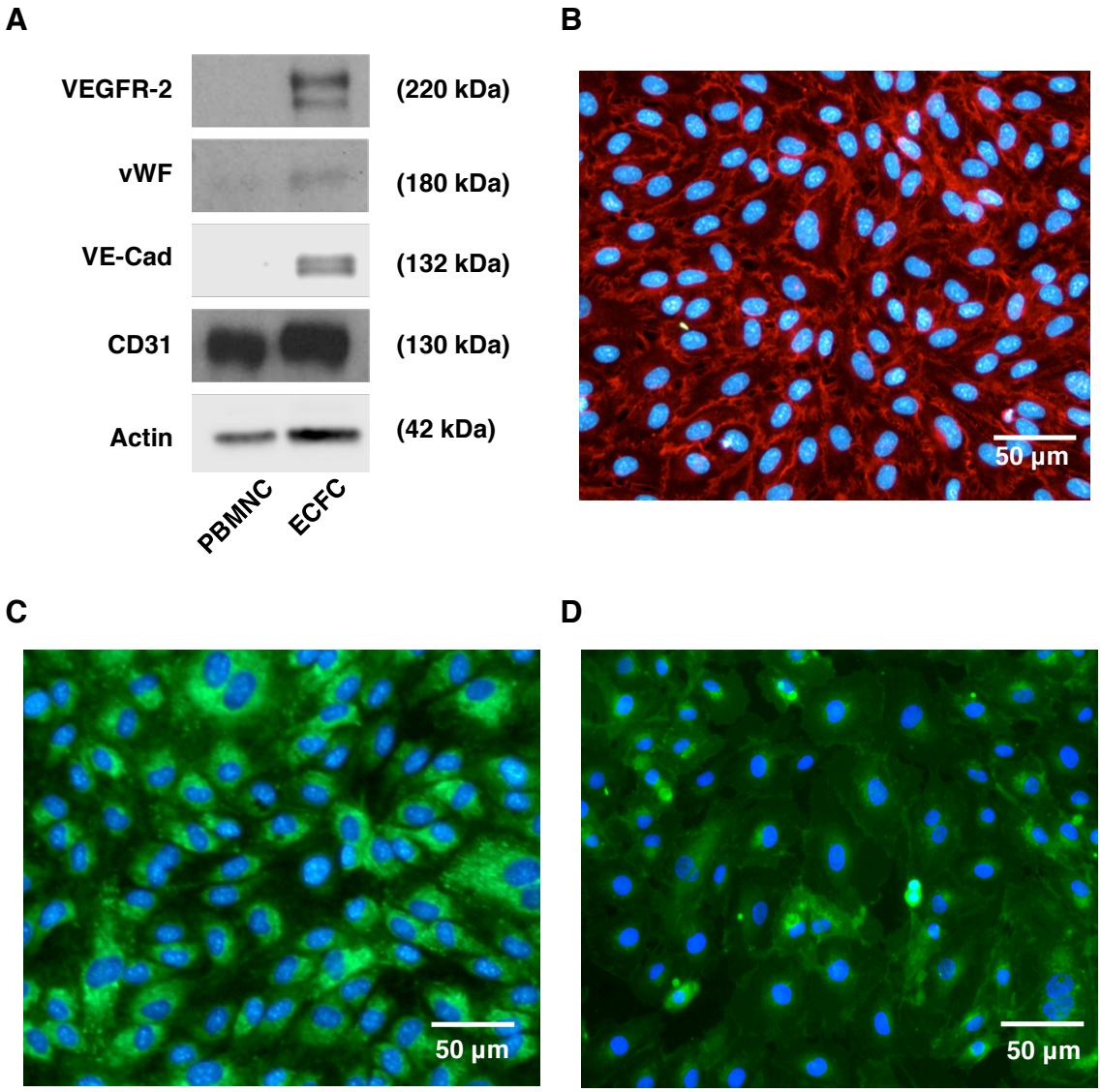


**Figure 3.3. Phenotypical characterisation of ECFCs.** (**A**) Immunoblotting for the endothelial markers VEGFR-2, vWF, VE-cadherin, the monocytic marker CD31 and actin (from top to bottom) in lysates of ECFCs and PBMNCs (day 0). (**B** and **C**) Immunofluorescence staining for VE-Cadherin and vWF. (**D**) Lectin staining with FITC-UEA 1. Nuclei were stained with DAPI. Blots and images are representative of three independent experiments.

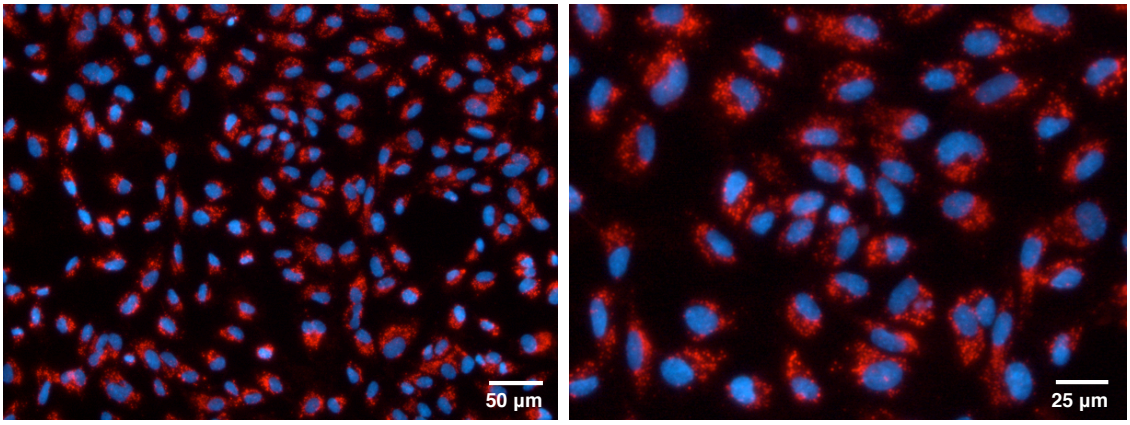


**Figure 3.4. Uptake of DiI-Ac-LDL by ECFCs.** Cells were pre-incubated with 10 µg/mL DiI-Ac-LDL (4 hours, 37 ºC, 5% $CO_2$). After fixation and permeabilisation, nuclei were stained with DAPI. Images were acquired with a Leica DMI4000B microscope. Images are representative of three independent experiments.

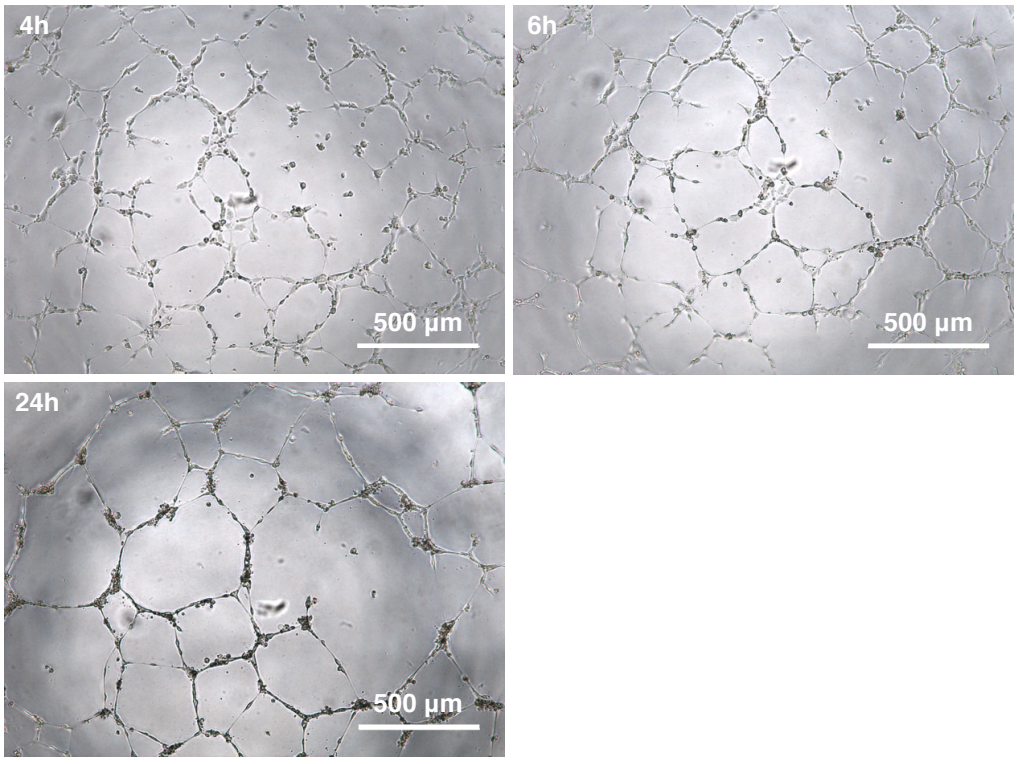


**Figure 3.5. Network formation by ECFCs.** ECFCs in growth factor reduced medium were seeded on a Growth Factor Reduced Matrigel™ matrix and incubated for up to 24 hours, and treated with rhVEGF (25 ng/mL). Tubes were already formed after 4 h, maturated by 6 h and started to remodel and regress by 24 h. Images are representative of three independent experiments.

### 3.3.2. Assessment of expression of protease-activated receptor (PAR)-1 and 2 in ECFCs

Both PBMNCs and ECFCs at day 0 were shown to express both PAR-1 and PAR-2, using N-19 and SAM-11 antibodies (Figure 3.6A-B). These antibodies have been shown to detect endogenous expression of PAR-1 and PAR-2 in primary cell lysates (Adams, Pagel, Mackie and Hooper, 2012). Platelet and HUVEC protein extracts were used as positive controls for PAR-1 and PAR-2, respectively. Their expression at mRNA level was then confirmed by qPCR and compared to other cell types known to express these receptors (lung fibroblasts, glomerular endothelial cells, myofibroblasts and HK2 cells) (Ortiz-Stern et al., 2012; Kumar Vr et al., 2016; Borensztajn et al., 2010; Grandaliano et al., 2000). In the case of PAR-2, expression in ECFCs was markedly higher compared to other cell types, suggesting it may have an important physiological role (Figure 3.6C-D). Finally, to further confirm the expression and assess the localization of these proteins in ECFCs, cells were stained with antibodies raised against PAR-1 and 2 and images acquired by confocal microscopy. The expression of both receptors was confirmed, with ECFCs exhibiting both membrane and cytoplasmic staining, a localization pattern similar to that observed previously in primary endothelial cells (Edlund, Andersson and Fried, 2004), with a minimal degree of co-localization (Figure 3.7).

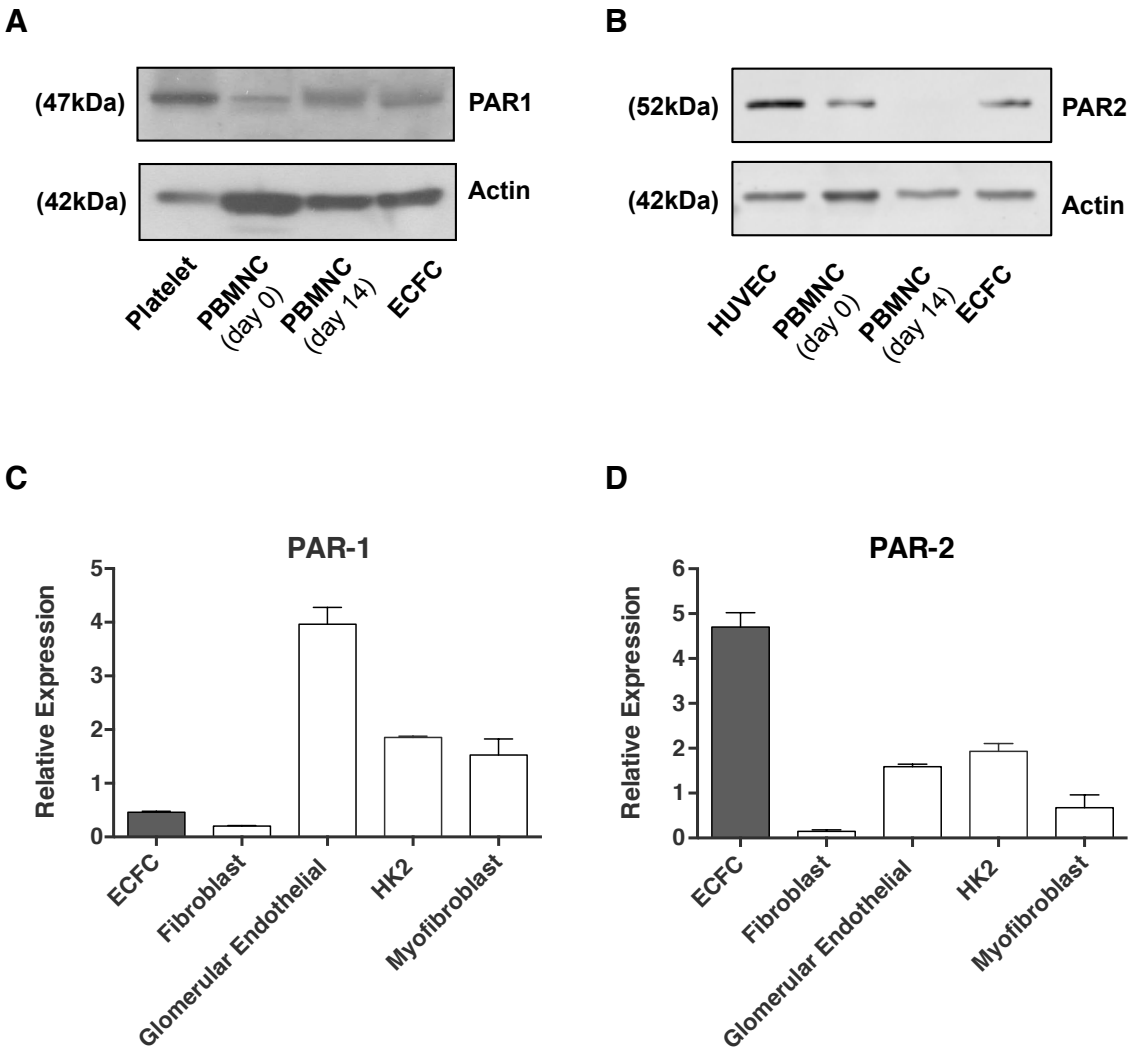


**Figure 3.6. ECFCs express PAR-1 and PAR-2**. The expression of (**A**) PAR-1 and (**B**) PAR-2 was tested in platelets or HUVECs (for PAR1 and PAR2 respectively), PBMNCs at days 0 and 14 and in ECFCs (from left to right) by immunoblotting using selective antibodies (N19 and SAM11, respectively). An actin-specific antibody was also utilized to detect the expression of a housekeeping gene in the different lysates. (**C**) Relative PAR-1 (**D**) PAR-2 expression in ECFCs, fibroblasts, myofibroblasts, glomerular endothelial and epithelial HK2 cells, was analysed by RT-qPCR using specific primers as described in Chapter 2.9. Data are normalized to GAPDH and are expressed as mean ± standard error of the means (SEM) (n=3).

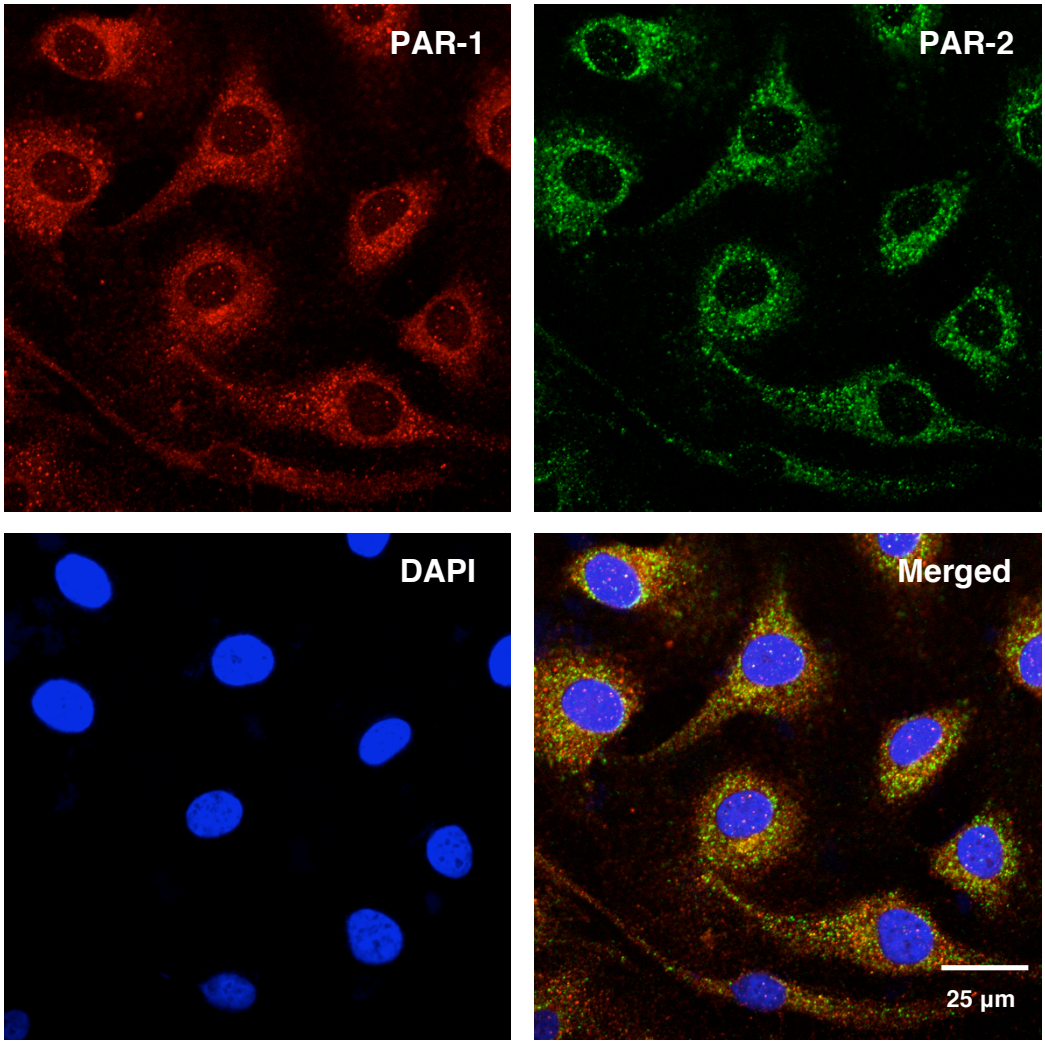


**Figure 3.7. Immunofluorescence staining of PAR-1 and PAR-2.** ECFCs were grown to near confluence were fixed in methanol. Expression and localization of PAR-1 and PAR-2 were assessed by immunostaining using specific antibodies combined with Alexa Fluor 488 Rabbit Anti-Mouse (green) and Alexa Fluor 546 Donkey Anti-Goat IgG (red) secondary antibodies. DAPI (blue) was used to localize cell nuclei. Superimposition of the three channels is shown in the lower right corner indicating co-localization of the receptors. Images are representative of three independent experiments.

### 3.3.3. Isolation of ECFCs under PAR-stimulation

As PAR activators such as thrombin and metalloproteases are abundant at sites of tissue injury, it was hypothesised that PAR-1 and/or PAR-2 may play a role in recruiting circulating progenitors or promoting their differentiation towards new endothelium. Therefore, the rate of ECFC colony formation *in vitro* was compared with or without PAR activation.

Selective activation of PAR-1 or PAR-2 was achieved by treating the cells with synthetic peptides (Table 3.1) displaying the sequence of the endogenous agonist peptide of the targeted receptor (Hollenberg et al., 1997). PAR-activating peptides were added at a concentration of 50 µM during every change of medium during the first 2 weeks of the isolation procedure. The number of colonies observed was then used to compare the isolation efficiency under PAR-stimulation versus the control condition. A peptide with a scrambled sequence was used as negative control. The sequences of the activating and scrambled peptides are detailed below:

***Table 3.1.*** *Sequences of synthetic agonist peptides*

| Targeted Receptor | Peptide Sequence |
|---|---|
| *PAR-1* | H-Thr-Phe-Leu-Leu-Arg-$NH_2$ |
| *PAR-2* | Ser-Leu-Ile-Gly-Lys-Val-$NH_2$ |
| *Scrambled control* | 2-Furoyl-Orn-Leu-Arg-Gly-Ile-Leu-$NH_2$ |

As shown in figure 3.8, the activation of either PAR-1 or PAR-2 did not significantly change the number of colonies obtained per mL of blood used for the isolation procedure.

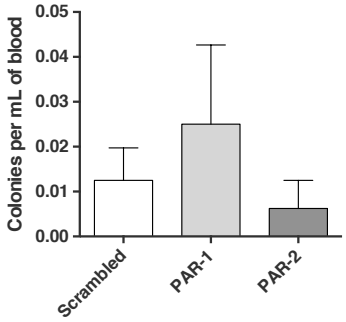


**Figure 3.8. Isolation of ECFCs under PAR-stimulation.** hPBMNCs from each 40 mL donation were divided and plated into collagen-coated 96-well plates. Cells were cultured in EGM-2 medium supplemented with either scrambled control peptide, PAR-1- or PAR-2-activating peptide (50 µM). Plates were inspected microscopically for the appearance of colonies and manually counted. No significant difference was observed using one-way ANOVA (n=4).

### 3.3.4. ERK activation by PAR-1 and -2 stimulation

As endothelial proliferation can be partly responsible for the angiogenic process, and as ERK1 and 2 are often associated with a proliferative response, it was investigated whether PAR-1 and/or PAR-2 are functionally coupled to the ERK1/2 pathway in ECFCs. For this purpose, cells were treated with synthetic agonist peptides and lysed after 30 min in buffer containing phosphatase inhibitors. By immunoblotting with specific antibodies for the total and phosphorylated forms of ERK1/2, followed by densitometric quantification, the level of ERK activation was assessed. In ECFCs, stimulation with both PAR-1 and PAR-2 activating peptides led to a significant increase in ERK1/2 phosphorylation (Figure 3.9).

These kinases and subsequent cascade can be inhibited *in vitro* with the compound PD98059 (Alessi et al., 1995). In order to determine the temporal profile of ERK activation via PAR-1 stimulation and validate PD98059 as an inhibitor of the ERK pathway, relevant to the network formation assay, cells were treated with PAR-1-activating peptide over a time course of 4 h and with PD98059. Phosphorylation was then assessed by immunoblotting with specific antibodies for the total and phosphorylated forms of ERK1/2. Stimulation of PAR-1 led to increased phosphorylation of ERK1/2 for up to 2 h, returning to basal levels at 4 h (Figure 3.10), in accordance with the timeframe of the angiogenesis assay. ERK phosphorylation was efficiently inhibited in the presence of 50 µM PD98059.

Due to the recognized role of ERKs in the regulation of EPC proliferation (Guo et al., 2012), the effect of PAR-1 or PAR-2 stimulation on cell proliferation was tested in our experimental conditions. ECFCs were grown for 24 h with scrambled, PAR-1- or PAR-2-activating peptides and their metabolic activity assessed using a resazurin-based assay (PrestoBlue). Despite the increased ERK1/2 activation in ECFCs, their metabolism did not appear to be affected by PAR-1/2 activation in either complete culture medium or growth factor reduced medium (i.e. complete medium diluted 1 in 5 in EBM-2 medium; Figure 3.11).

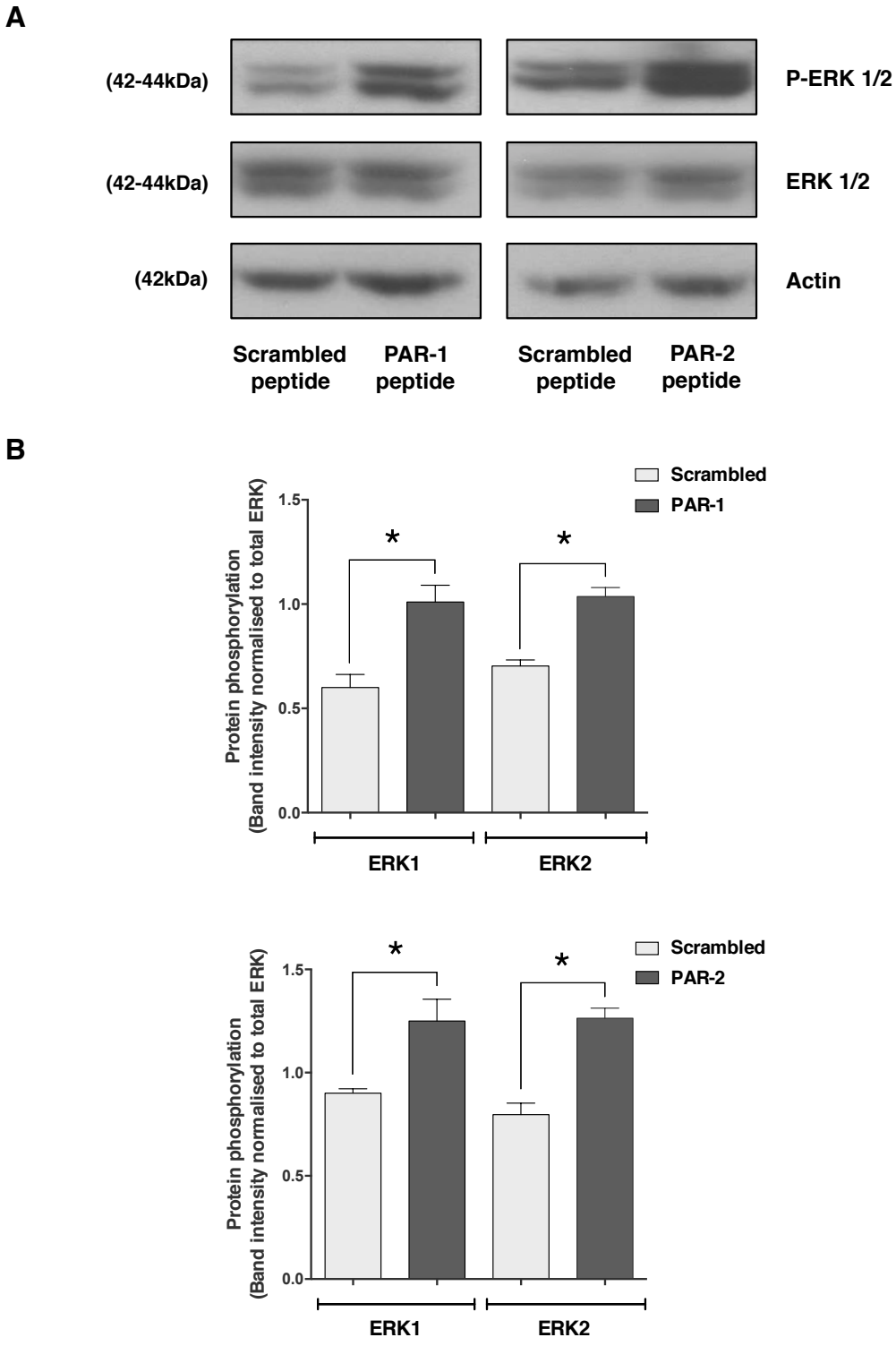


**Figure 3.9. ERK activation by PAR-1 and PAR-2 stimulation.** (**A**) Following treatment of ECFCs with 50 μM PAR-1- or PAR-2-activating peptide for 30 minutes, proteins were isolated in RIPA buffer containing phosphate inhibitors, as described in Chapter 2.7. A peptide with a scrambled sequence was used at a concentration of 50 μM as a negative control. Phospho-ERK1/2, total ERK1/2 and actin (from top to bottom) were detected by immunoblotting. (**B**) Densitometry analysis was performed using ImageJ. Graphs display the normalized intensities as arbitrary units for the phospho-ERK1 and phospho-ERK2. The data are mean ± SEM and the statistical significance of the difference was tested by Student's t-test (*=$p<0.05$; n=3).

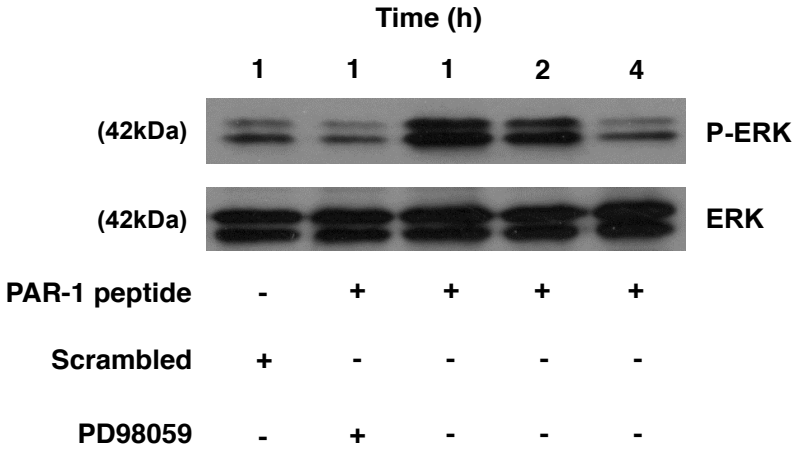


**Figure 3.10. Time course of ERK activation by stimulation of PAR-1.** Time-dependent activation of ERK1/2 by PAR-1-activating peptide (1, 2 and 4 hours) and its inhibition by 50 µM PD98059 were examined using phospho-specific ERK1/2 antibody and immunoblotting (n=3).

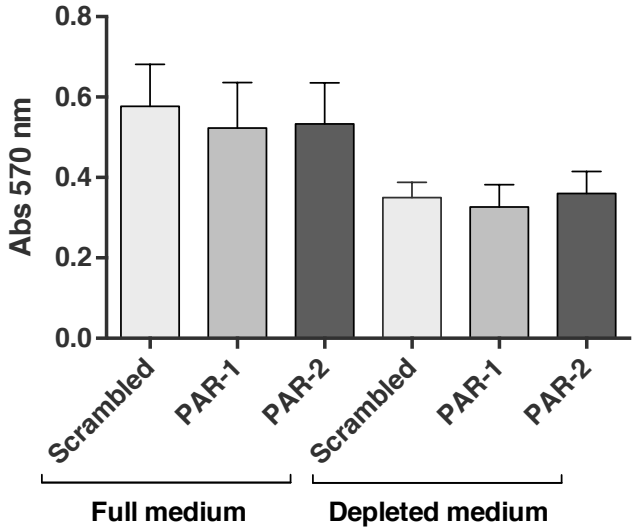


**Figure 3.11. No effect of PAR-1 or PAR-2 stimulation on ECFC proliferation and endothelial differentiation.** $2x10^5$ cells/well were seeded in 24-well plate in either complete culture medium or in depleted medium. Following 48 h incubation with 50 µM PAR-1- or PAR-2-activating peptide or 50 µM scrambled peptide, metabolic activity was quantified using the PrestoBlue assay. The data represent the mean ± SEM. No statistically significant difference was detected between treatments using one-way ANOVA (n=3).

### 3.3.5. Inhibition of network formation by ECFCs through activation of PAR-1

Next, the effect of PAR-1 and PAR-2 stimulation on the tubulogenic activity of ECFCs was investigated *in vitro* by monitoring network formation on Matrigel. This assay has been widely used to model the spatial reorganization of endothelial cells during angiogenesis and measures their ability to form tubular networks (devoid of a lumen, however). Thus, this assay has often been employed for the initial testing of potential pro- or anti-angiogenic compounds.

ECFCs were plated on Matrigel in basal endothelial medium (supplemented with 2% FBS to guarantee cell survival), and treated with 50 µM of PAR-activating peptide or scrambled control peptide. After 4 h incubation, wells were imaged under phase-contrast microscopy and network formation was quantified by measuring both the number of tubes as well as the total tube length, using a dedicated ImageJ plugin (Angiogenesis Analyzer). Unexpectedly, the stimulation of PAR-1, but not PAR-2 or treatment with scrambled peptide, strongly inhibited tube formation by ECFCs in this assay (Figure 3.12). Interestingly, treatment with ERK-inhibitor PD98059 did not affect basal tube formation by ECFCs and did not interfere with PAR-1-dependent inhibition of network formation, suggesting that ERK activation is not primarily involved in tube formation or responsible for its inhibition by PAR-1 agonist peptide.

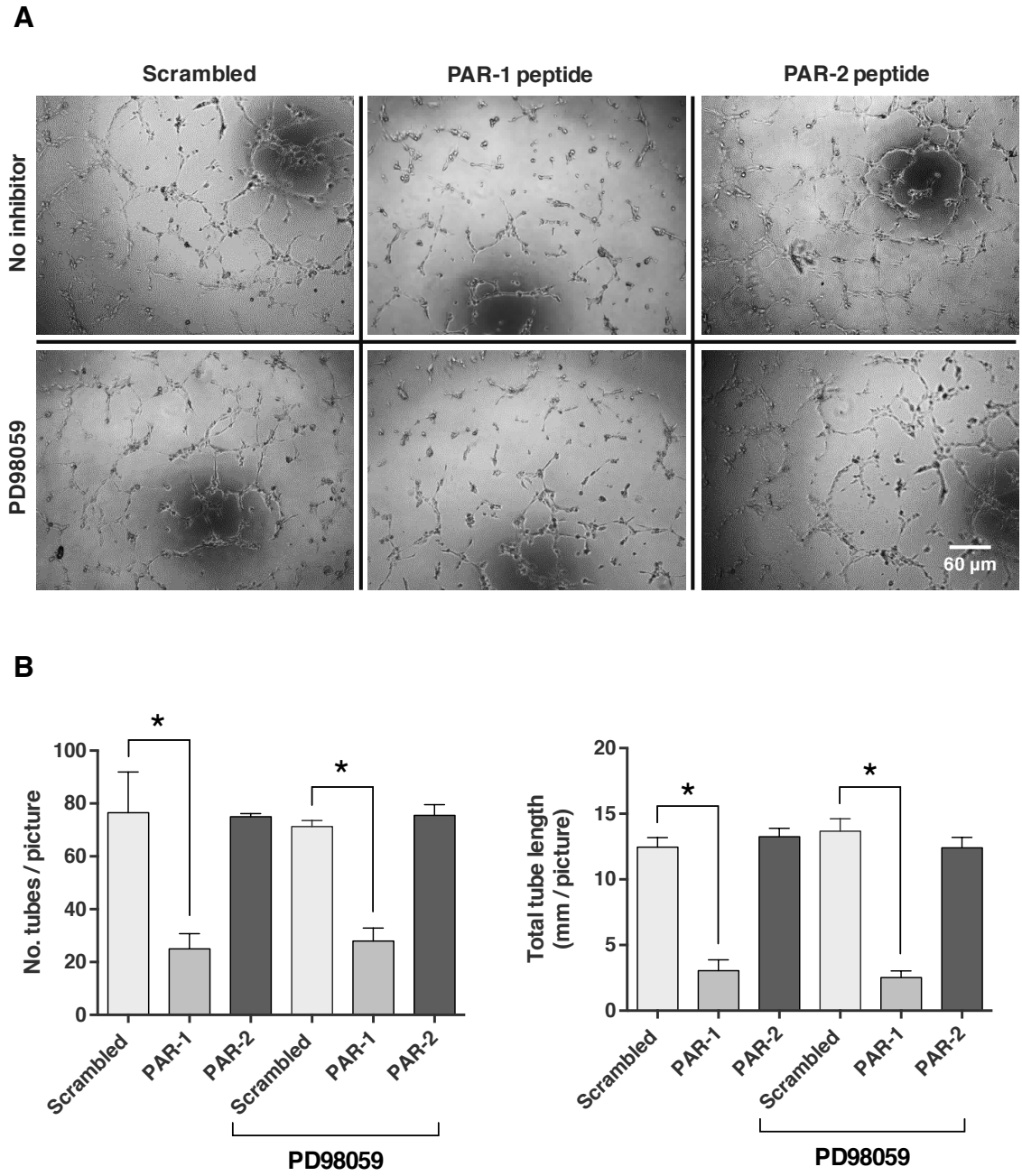


**Figure 3.12. The activation of PAR-1 inhibits network formation by ECFCs on Matrigel.** (**A**) 1x10$^4$ ECFCs/well were plated onto Matrigel matrix in basal medium (with 2% FBS). Cells were cultured with 50 µM scrambled control peptide, PAR-1-activating peptide or PAR-2-activating peptide in the absence or presence of 50 µM PD98059 (as indicated). Phase contrast images were acquired 4 h after seeding. (**B**) The number of tubes per image and the total tube length were quantified using the Angiogenesis Analyzer plugin for ImageJ. Means ± SEM from four independent experiments are shown. Statistical significance was tested by one-way ANOVA with Bonferroni's post-test (*=$p<0.05$) (n=4).

### 3.3.6. The effect of PAR-stimulation on gene expression in ECFCs

In view of the inhibitory effect of PAR-1 activation on network formation by ECFCs, the expression of a set of genes that are known to play a role in angiogenesis was evaluated. Among these are included both soluble factors, such as VEGF-A (Drake, LaRue, Ferrara and Little, 2000) and SDF-1 (Sbaa et al., 2006), and their receptors VEGFR-2 and CXCR4.

ECFCs were cultured under growth-arrested conditions for 24 h to unmask any effects produced by the growth factors in the complete culture medium and, in turn, highlight any change produced by the treatment with PAR-activating peptides. Cells were then treated with 50 µM of either PAR-activating peptides or scrambled control peptide, and total RNA was extracted at 1, 2, 4 and 8 hours. Relative gene expression was then analysed by RT-qPCR using specific primers.

While the expression of most genes analysed was not significantly affected following stimulation of PAR-1 or PAR-2 throughout the time course of the experiment, a significant decrease in VEGFR-2 expression was shown after 1 hour of treatment with PAR-1-activating peptide (Figure 3.13). Although not statistically significant, a trend towards down-regulation was visible at the 2 h time point with the expression levels of VEGFR-2 returning to control levels from 4 hours onwards post-treatment. Other changes included a trend for upregulation of IL-8 expression at shorter time points, and a marginally significant down-regulation for the expression of CD31 after 8 hours following PAR-1 stimulation ($p=0.05$).

In order to confirm the down-regulation of VEGFR-2 by PAR-1-stimulation, ECFCs were incubated with PAR-1-activating peptide for up to 4 hours, and the expression of VEGFR-2 was analysed by SDS-PAGE and immunoblotting. At the protein level, a significant down-regulation of VEGFR-2 was observed after 2 and 4 hours incubation, but not 1 hour (Figure 3.14A). This is in line with the previous results obtained by qPCR and matching the timeframe of tubulogenic inhibition observed on Matrigel. The densitometric analyses of VEGFR-2 immunoblots, with separate quantification of each of the two bands typically observed by western blot (representing two isoforms), are shown in Figure 3.14B.

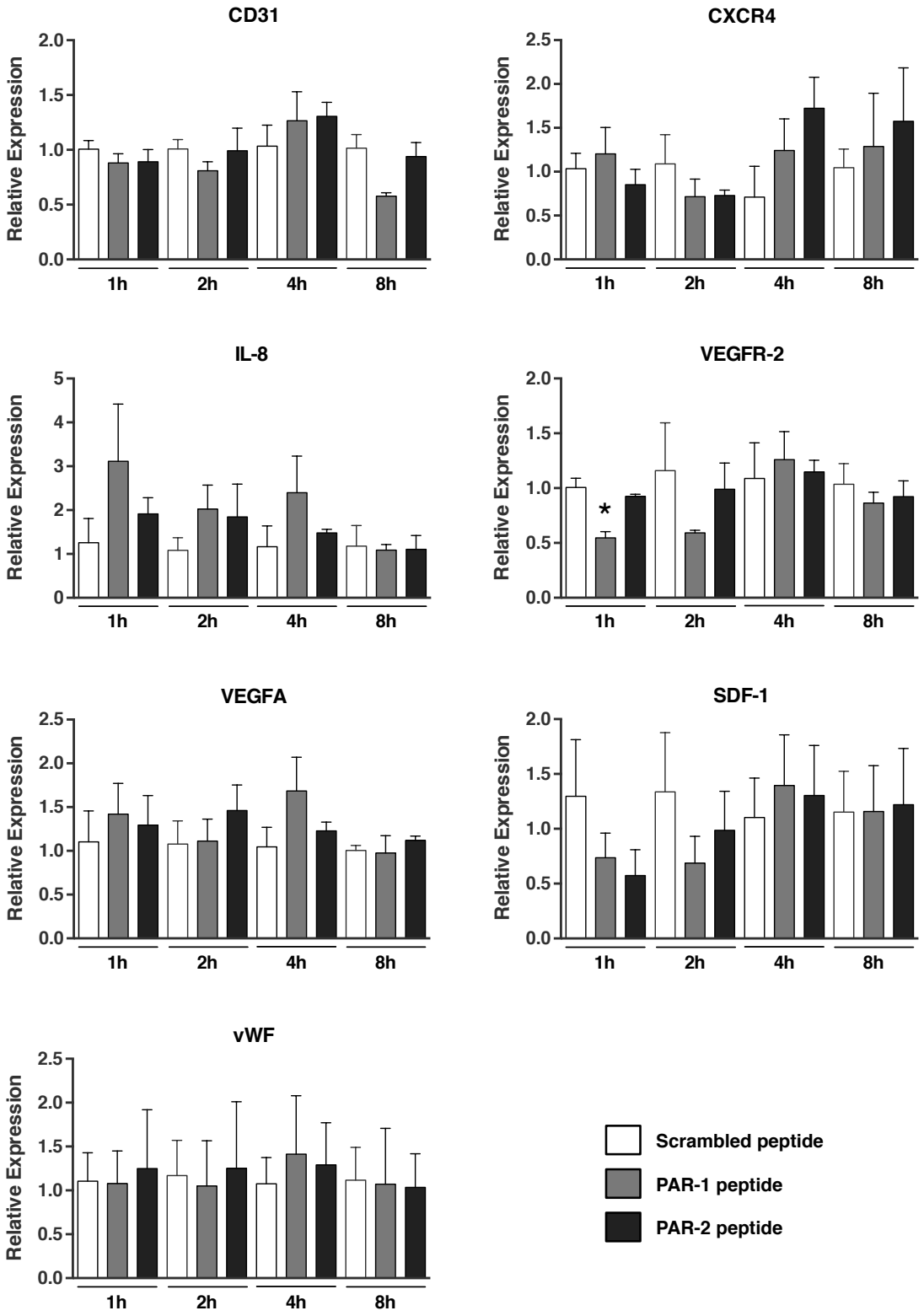


**Figure 3.13. Effect of PAR stimulation on expression of angiogenesis-related genes.** Total RNA was extracted at 1, 2, 4 and 8 hours after stimulation with 50 µM scrambled control peptide, PAR-1-activating peptide or PAR-2-activating peptide, and relative expression was analysed by RT-qPCR using specific primers as described in Chapter 2.9. Data are normalized to GAPDH and are expressed as mean ± SEM (n=3). Statistical significance was tested by one-way ANOVA with Bonferroni's post-test (*=$p<0.05$, compared to scrambled peptide treatment at matched time point).

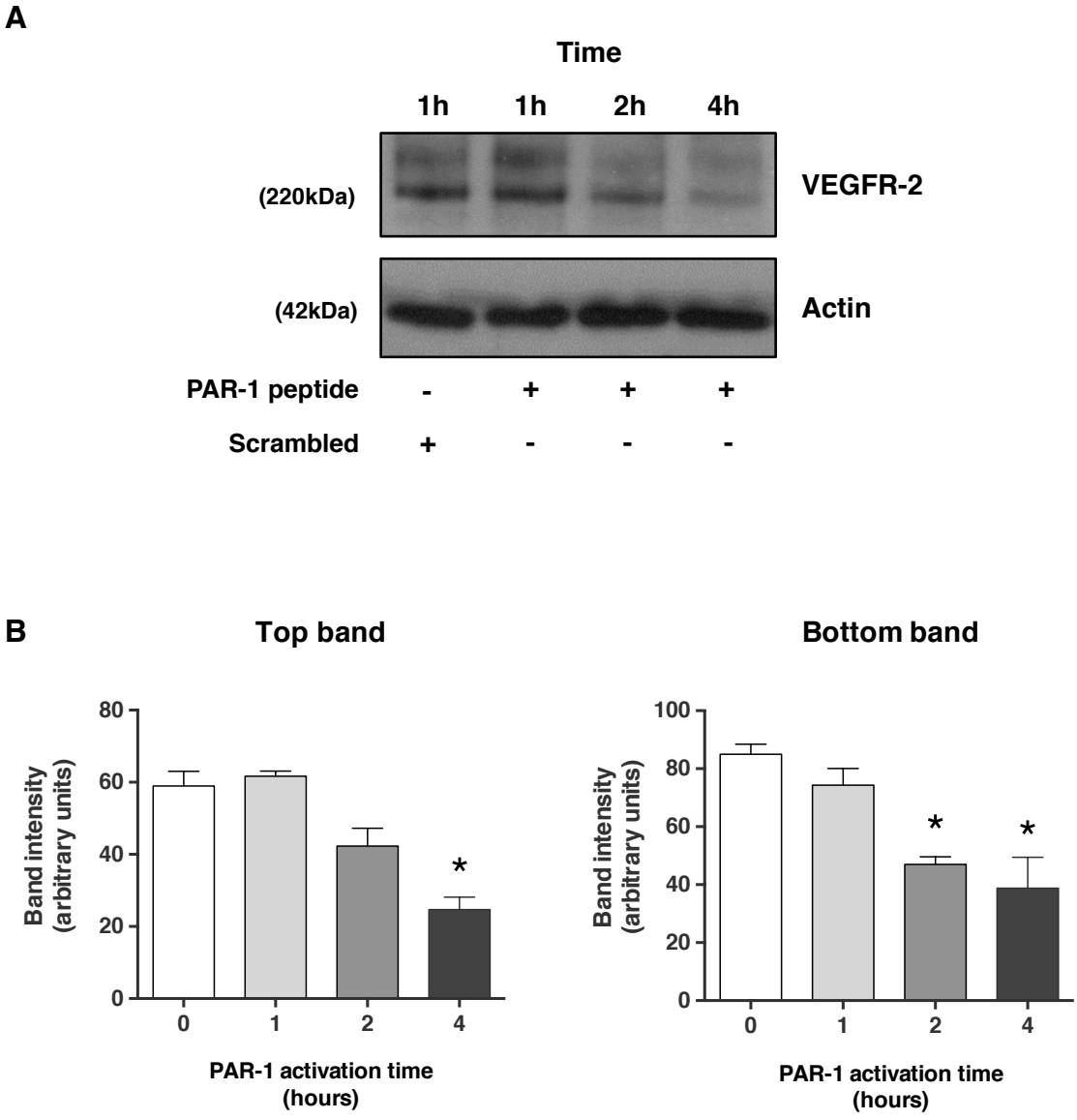


**Figure 3.14. Downregulation of VEGFR-2 by PAR-1 stimulation.** (**A**) Proteins were isolated from ECFCs as described in the Chapter 2.7 after treatment with 50 μM PAR-1-activating peptide for 0, 1, 2 and 4 hours. VEGFR-2 and actin were detected by SDS-PAGE and immunoblotting. (**B**) Densitometry analysis was performed with ImageJ. Graphs display the normalized intensities as arbitrary units for VEGFR-2's top and bottom band. The data are mean ± SEM and the statistical significance of the difference was tested by one-way ANOVA with Tukey's post-test (*=$p<0.05$) (n=3).

### 3.3.7. VEGF rescues the inhibitory effect of PAR-1 activation on network formation

The rescue of tubular network formation was attempted in the presence of PAR-1 stimulation through the addition of an excess of exogenous VEGF. Cells were plated onto Matrigel matrix and cultured with 50 μM scrambled control peptide or 50 μM PAR-1-activating peptide in the absence or presence of recombinant VEGF. After 4 hours, images were acquired by phase contrast microscopy (Figure 3.15A) and tube formation was quantified using ImageJ by measuring the number of tubes formed and total tube length.

As shown in Figure 3.15B, the addition of 50 or 100 ng/mL VEGF significantly reversed the inhibition of network formation induced by PAR-1-activating peptide, while no effect was seen in cells treated with scrambled peptide. As a control, the rescue of network formation with fibroblast growth factor (FGF) was also tested. As expected, FGF did not rescue tube formation in the presence of PAR-1-activating peptide at any of the tested concentrations (25, 50 and 100 ng/mL, Figure 3.16), and did not significantly increase tube formation in the absence of PAR-1-activating peptide.

In summary, these data suggest that PAR-1 inhibition of tubulogenesis is most likely happening through modulation of VEGFR-2 signalling rather than other GF receptors such as FGF receptors.

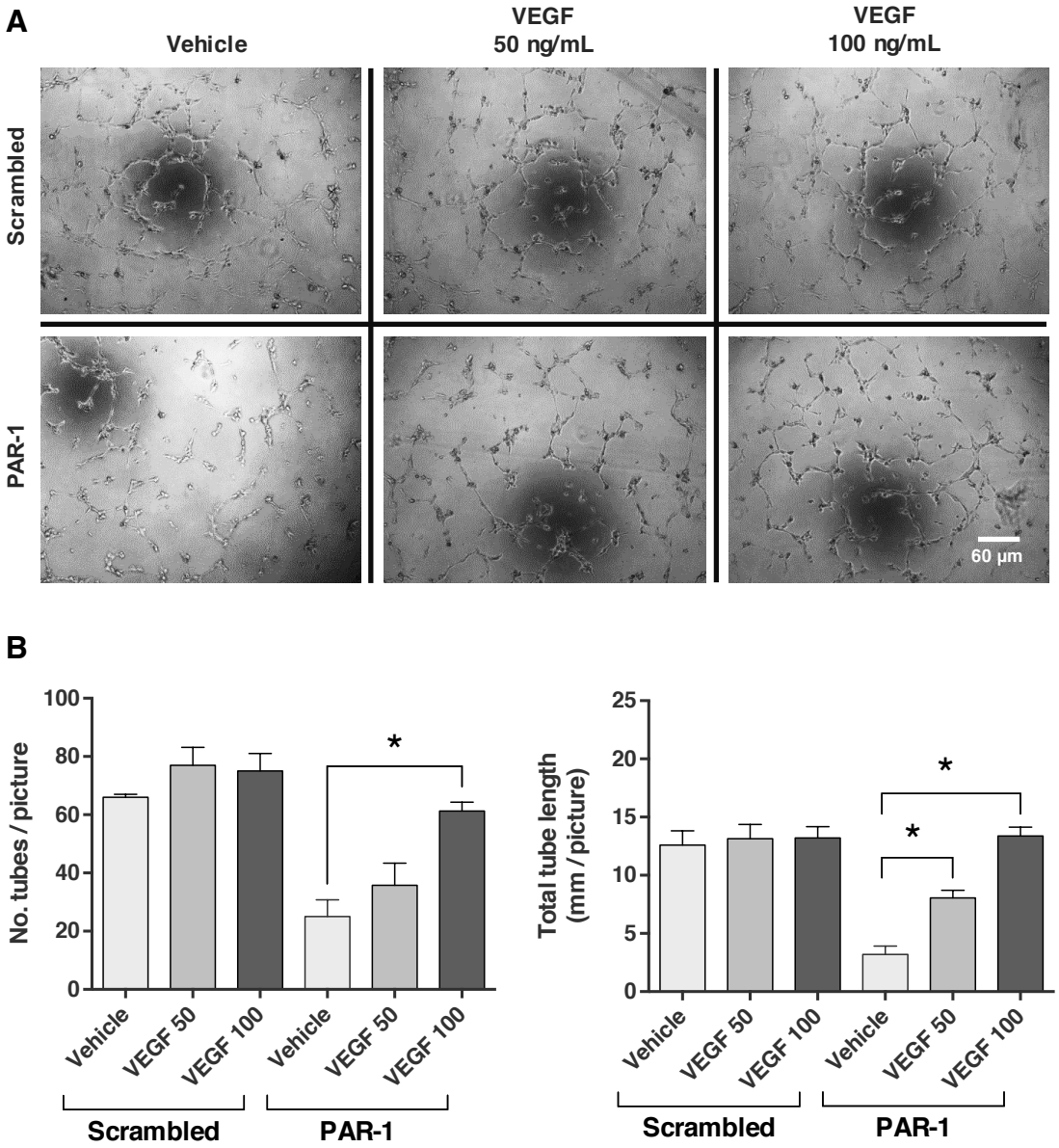


**Figure 3.15. Reversal of network formation inhibition due to PAR-1 activation by increasing concentrations of VEGF.** (**A**) 1x10$^4$ ECFCs/well were plated onto Matrigel matrix in basal medium (with 2% FBS). Cells were cultured with 50 µM scrambled control peptide or 50 µM PAR1-activating peptide in the absence or presence VEGF (50 and 100 ng/mL). Phase contrast images were acquired 4 h after seeding. (**B**) The number of tubes per image as well as the total tube length were quantified using the Angiogenesis Analyzer plugin for ImageJ. Data are mean ± SEM. Statistical significance was tested by one-way ANOVA with Bonferroni's post-test (*=$p<0.05$) (n=3).

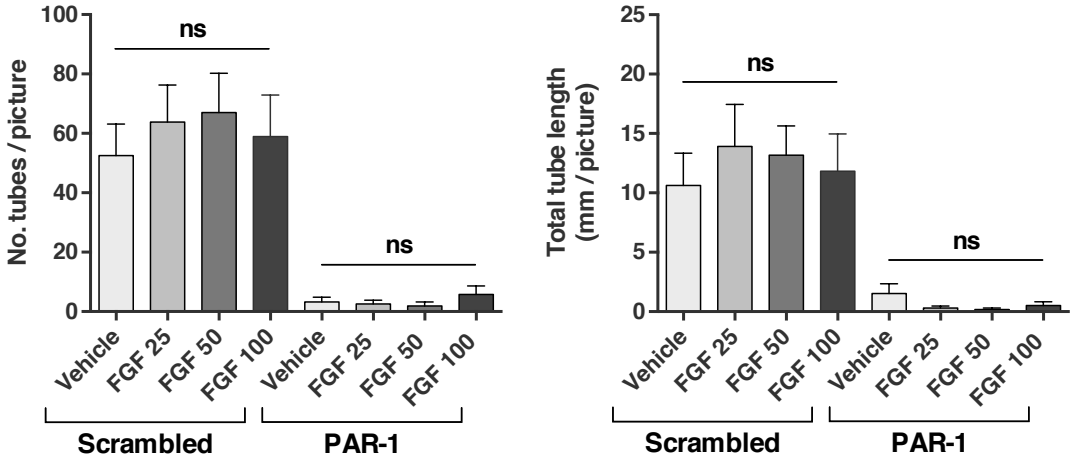


**Figure 3.16**. **Inhibition of network formation due to PAR-1 activation is not reversed by FGF.** 1x10$^4$ ECFCs/well were plated onto Matrigel matrix in basal medium (with 2% FBS). Cells were cultured with 50 µM scrambled control peptide or 50 µM PAR1-activating peptide in the absence or presence FGF (25, 50 and 100 ng/mL). Phase contrast images were acquired 4 h after seeding and the number of tubes per image as well as the total tube length were quantified the using the Angiogenesis Analyzer plugin for ImageJ. Data are expressed as mean ± SEM. No statistically significant difference was detected between treatments using one-way ANOVA (n=3).

### 3.4. Summary of results

- ECFCs can be routinely isolated, and express a typical endothelial phenotype.
- ECFCs express both PAR-1 and PAR-2.
- PAR stimulation does not promote endothelial colony formation.
- Activation of PAR-1 and PAR-2 leads to ERK1/2 phosphorylation, but does not have an effect on proliferation in ECFCs.
- Activation of PAR-1, but not PAR-2, inhibits network formation by ECFCs.
- The ERK pathway is not involved in this inhibition.
- VEGFR-2 is significantly down-regulated in response to PAR-1 stimulation.
- Exogenous VEGF, but not FGF, rescues PAR-1 mediated inhibition of tube formation.

### 3.5. Discussion

ECFCs are derived from a circulating source of vasculogenic progenitors with significant potential for tissue engineering (Tasev, Koolwijk and Hinsbergh, 2016). Following a well-established method (Ingram et al., 2004), ECFCs were successfully and routinely isolated from human peripheral blood. These cells, obtained as colonies, exhibited a cobblestone morphology, which is typical of the endothelial phenotype, and could be expanded for several passages (up to 10), as well as cryopreserved. Their phenotype was confirmed by a number of techniques. The simultaneous expression of CD31, VEGFR-2, VE-cadherin and vWF was demonstrated by immunoblotting, distinguishing them from the starting population of PBMNCs (Bogoslovsky et al., 2013; Van Craenenbroeck et al., 2008). The expression of VE-Cadherin and vWF was also confirmed by immunostaining, and the endothelial lineage was further validated by successful staining with fluorescent UEA-1 (Holthöfer et al., 1982) and uptake of DiI-Ac-LDL (Voyta, Via, Butterfield and Zetter, 1984). Additionally, ECFCs could form networks on basement membrane matrix in a shorter time then HUVECs (Arnaoutova and Kleinman, 2010), suggestive of their high vasculogenic potential.

The aim of this chapter was to determine if PAR-1 and PAR-2 are expressed, functionally active and involved in vasculogenesis in ECFCs. Mature endothelial cells have been shown to express all of the known protease-activated receptors (PAR-1 to PAR-4) (Camerer et al., 2002), but research has been mainly focused on the role of PAR-1 and PAR-2. These have been implicated in junctional remodelling and permeability (Feistritzer, Lenta and Riewald, 2005), paracrine activity (Garcia et al., 1993) and inflammatory response in endothelial cells in response to coagulation proteases, and as extensively reviewed by others (Alberelli and De Candia, 2014; Rezaie, 2014; Coughlin, 2005). Conversely, only the expression of PAR-1 had been previously reported in adult peripheral blood EPCs (Smadja et al., 2005; 2009).

The expression of both PAR-1 and PAR-2 was confirmed in adult peripheral blood ECFCs, detected by immunoblotting, qPCR and immunohistochemistry. The expression of PAR-2 was found to be particularly high in comparison to other cell types by qPCR, suggestive of a relevant physiological role. The constitutive activation of either PAR-1 or PAR-2 was investigated to ascertain whether it could promote the differentiation of the circulating progenitors into ECFCs, thereby increasing the number of colonies obtained. It is known that high amounts of thrombin are produced at sites of tissue injury during the coagulation cascade (Narayanan, 1999) resulting in the conversion of fibrinogen into fibrin and activation of platelets. Therefore, it is plausible

that circulating cells with regenerative potential could also be recruited via activation of PAR-1 by thrombin, with a subsequent increase in vasculogenesis at these sites of vascular damage. In a similar fashion, during the remodelling phases of tissue repair where several different proteases are released (Lu, Takai, Weaver and Werb, 2011), PAR-2 activation by trypsin-like proteases could constitute a mechanism by which endothelial progenitors participate in the generation of new blood vessels. If the addition of PAR-activating peptides had led to an increase in colony formation, this could have constituted a substantial improvement in the isolation of ECFCs without significantly aggravating the cost of this procedure. Unfortunately, despite a minor trend towards higher colony formation with added PAR-1-activating peptide, the addition of neither of the PAR-activating peptides resulted in a significant increase in the number of endothelial colonies after 2 weeks of culture, when compared to the standard protocol.

In isolated ECFCs, both PAR-1 and PAR-2 stimulation resulted in increased phosphorylation of ERK1/2. As this pathway is often linked to proliferation and differentiation (Mebratu and Tesfaigzi, 2009; Lian et al., 2014), the effect of PAR activation on ECFC proliferation was investigated. It has been previously reported that PAR-1 activation can lead to accelerated proliferation in ECFCs (Smadja et al., 2005; 2009). In contrast, no significant increase in ECFC proliferation was observed in our experiments. This discrepancy can be explained by several methodological differences between this study and those by Smadja *et al*. First, a different isolation protocol was adopted, which is likely to result in a significantly different phenotype in comparison with the cells used in the literature studies**.** Following the protocol established by Ingram *et al*., ECFCs were isolated from adult PBMNCs without pre-enrichment by magnetic-activated or fluorescence-activated cell sorting, while in the reports by Smadja *et al*, the authors isolated cells mostly from $CD34^+$-enriched cord blood populations. Albeit similar in most basic aspects, it is known that ECFCs isolated from cord blood have a genetic profile which is 20% different from those isolated from adult blood, with an overall lower expression of pro-thrombotic and pro-inflammatory genes (Nuzzolo et al., 2014), which could partly account for the differences observed between our study and those previously published. Other less relevant experimental differences include: 1) ECM coating of culture substrate (collagen type I in this study versus gelatin in (Smadja et al., 2005)) and 2) a different concentration of FBS in the culture medium (12% versus 2-5% in (Smadja et al., 2005)). Additionally, due to the extremely high proliferation rate of cells obtained with the protocol adopted in this thesis (Ingram et al.,

2004; Yoder et al., 2007; Hur et al., 2004), any further growth increase may be hard to assess. This growth profile supports previous suggestions for using ECFCs in tissue engineering (Fadini, Avogaro and Agostini, 2007). As with PAR-1, stimulation of PAR-2 did not have an effect on ECFC proliferation. Therefore, phosphorylation of ERK1/2 via PAR-stimulation in ECFCs appears to lead mainly to cellular events other than proliferation, such as transcription changes or cytoskeletal reorganization (Roskoski, 2012).

The role of PARs in vasculogenesis was then assessed. Converse to the initial hypothesis, network formation on Matrigel was strongly inhibited following PAR-1 activation and unaffected by PAR-2 activation. Again, this is in disagreement with the work by Smadja and colleagues (Smadja et al., 2005) in which PAR-1 activation was reported to have a pro-angiogenic effect using the same type of assay. The authors correlated this finding with the increased expression of pro-angiogenic chemokines IL-8 (Smadja et al., 2009), SDF-1 and its receptor CXCR4 (Smadja et al., 2005). Although a non-significant trend towards increased IL-8 was observed following PAR-1 activation (Figure 3.13), no relevant changes were detected in the expression of SDF-1 or CXCR4 following stimulation of either PAR-1 or PAR-2. As with the proliferation experiments, this discrepancy may again be due to the different starting population utilized for the isolation of ECFCs (i.e. non-selected PBMNCs in our study vs. cord blood $CD34^+$ cells in the study by Smadja *et al*), a hypothesis that is reinforced by the strikingly different timing of network formation between the two studies (4 hours vs. 18 hours of culture on Matrigel) (Smadja et al., 2005), possibly indicating a stronger vasculogenic response by the ECFCs used in this work. A similar inhibition of tubulogenesis on Matrigel in the presence of PAR-1-activating peptide or high concentrations of thrombin was previously shown using HUVECs (Chan, Merchan, Kale and Sukhatme, 2003) and with human microvessel endothelial cells (Blackburn and Brinckerhoff, 2008), respectively. This is in agreement with the results presented here with ECFCs. In addition, a swift down-regulation in VEGFR-2 by PAR-1 activation in ECFCs was observed by both qPCR and immunoblotting, corresponding to the timeframe of the inhibition seen on tube formation. Accordingly, network formation could be rescued by high concentrations of exogenous VEGF in the presence of PAR-1-activating peptide. This receptor is known to be crucial for proper vasculogenic responses by EPCs (Smadja et al., 2007), which suggests that PAR-1 stimulation could impair VEGF signalling by reducing VEGFR-2 density on the ECFC surface.

The inhibition of tube formation by PAR-1 activation was independent of activation of the ERK pathway, as the inhibitor PD98059 failed to affect tube formation, and PAR-2 stimulation activated ERKs without affecting tube formation. Of interest, recombinant VEGF failed to increase tube formation above basal levels, suggesting that the concentration of endogenously produced VEGF and, or that present in Matrigel, is sufficient to achieve a full response in the absence of PAR-1 stimulation (possibly because VEGFR-2 is expressed at a relatively high level). In contrast with the hypothesis presented here, i.e. that PAR-2 activation could promote vasculogenesis by ECFCs and despite similarities of the signal transduction of PAR-2 and PAR-1 (i.e. the MEK-ERK pathway) (Camerer et al., 2002; Syeda et al., 2006), no effect was seen on network formation or gene expression following treatment with a PAR-2-activating peptide. This hypothesis was based on previously published reports of angiogenic effects seen in mouse hindlimb ischaemia, where enhanced limb salvage was achieved through PAR-2-dependent reparative angiogenesis (Milia et al., 2002). Additionally, PAR-2 signalling appears to be essential for hypoxia-induced retinal angiogenesis (Uusitalo-Jarvinen et al., 2007) as well as in cancer-associated angiogenesis (Ruf, Yokota and Schaffner, 2010; Belting, Ahamed and Ruf, 2005). Although it cannot be excluded that basal levels of tube formation on Matrigel masked any effect of PAR-2, it is likely that the effects observed in the studies above are the consequence of secretion of paracrine growth factors or direct cell-to-cell interactions with other cell types. For example, it has been reported that PAR-2 increases the production of VEGF in both human adipose stem cells (hASCs) (Rasmussen et al., 2012) and in glioblastoma cell lines (Dutra-Oliveira, Monteiro and Mariano-Oliveira, 2012). Hence, it is plausible that the angiogenic outcome of PAR-2 activation seen *in vivo* is actually a result of an indirect action on endothelial cells.

As discussed by others (Staton, Reed and Brown, 2009; Auerbach et al., 2003), the assay that was adopted for this study, despite being one of the most widely used assays to study angiogenesis *in vitro* (Arnaoutova, George, Kleinman and Benton, 2009), does not accurately represent all of the different stages of blood vessel formation, including vascular lumen formation (Bikfalvi, Cramer, Tenza and Tobelem, 1991). In addition, the Matrigel assay has been suggested to be a poor approximation of the physiological extracellular environment and the three-dimensional environment of the extravascular space (Zimrin, Villeponteau and Maciag, 1995; Guo et al., 2014; Segura et al., 2002). It is commonly agreed that this assay is more representative of later stages of angiogenesis, such as differentiation and network reorganization rather

than sprouting (Staton, Reed and Brown, 2009). The data obtained with this assay are therefore informative of the formation of tight junctions between endothelial cells rather than a true representation of the angiogenic response (Auerbach et al., 2003). In accordance with this theory, a marginally significant down-regulation in expression of CD31 was observed after PAR-1 stimulation ($p=0.05$), which could contribute to the disruption of cell-cell junctions and consequent lack of interconnectivity. In a similar manner, it has been shown by others that PAR-1 activation by thrombin drastically reduces the expression of CD31 in ECFC monolayers, disturbing the intercellular adhesions and hampering the barrier function as a result (van den Biggelaar et al., 2014).

### 3.6. Conclusions

In conclusion, it was shown that PAR-1 and PAR-2 are both expressed in ECFCs and are functionally coupled to the ERK1/2 pathway. The anti-tubulogenic effect of PAR-1 in ECFCs was proposed to be a consequence of the down-regulation of VEGFR-2, which diminishes the responsiveness of these cells to VEGF. In spite of a previous report showing a beneficial effect on angiogenesis of PAR-2 activation *in vivo*, no evidence was found of a direct effect on ECFC-dependent tubulogenesis *in vitro*. Future studies that can expand the range of experimental techniques, including the use of more complete angiogenesis assays, would have the potential to shed light on the exact mechanism of reparative angiogenesis driven by PAR-2. Such findings could be of great interest for the modulation of the vasculogenic activity of ECFCs for cell therapy and tissue engineering purposes.

# Chapter 4: hPLG for expansion of ECFCs and microvascular network formation

## 4.1. Background

Insufficient vascularization is not only the main cause of chronic ischaemic diseases but also the main bottleneck towards the clinical implementation of tissue-engineered grafts (Novosel, Kleinhans and Kluger, 2011). In both situations, a shortage of an adequate extracellular matrix that can support blood vessel formation leads to a deficient regeneration of the host tissue (Lu et al., 2011), as cells that are further than 200 µm from a source of oxygen will become necrotic (Loffredo and Lee, 2008). Therefore, it is imperative to develop new ways of inducing tissue revascularization. The combined delivery of angiogenic growth factors (GFs) and endothelial progenitor cells (EPCs) within a supporting scaffold has been suggested as an approach capable of solving this challenge (Herrmann, Verrier and Alini, 2015). This approach aims at promoting the ingrowth of host vasculature into injectable scaffolds as well as through the generation of a vascular network from within the implanted construct (i.e. vasculogenesis).

For the formation of functional and stable new blood vessels, it is crucial that different cooperating cell types are recruited and prompted by a series of angiogenic signals to form new tubular structures (Stratman and Davis, 2012). Therapeutic approaches based on the delivery of a single GF, such as VEGF, usually fail to promote the formation of a healthy and lasting vasculature (Martino et al., 2015), one of the reasons being the failure to recruit perivascular cells that are capable of supporting endothelial cells (ECs) in the newly formed blood vessels (Stratman and Davis, 2012). However, the production of a set of GFs is extremely expensive and its clinical application is hardly feasible from an economical point of view. Furthermore, cells respond more efficiently to matrix-bound growth factors compared to soluble growth factors (Kang et al., 2011; Cybulsky, McTavish and Cyr, 1994; Swindle et al., 2001). This is due to the establishment of a spatial GF gradient which cells can sense and migrate towards, and also as a result of the essential crosstalk between integrins and GF receptors (Martino et al., 2015). While synthetic polymers have been extensively investigated for the delivery of GFs due to their off-the-shelf nature, these need to be modified in order to efficiently bind other molecules, such as GFs (Reed and Wu, 2014). Moreover, despite a few very recent examples (Lang et al., 2014), most synthetic polymers do not adhere efficiently to the target tissue and sometimes lack the ideal degradation profile. On the other hand, animal-derived biomaterials can naturally overcome these issues but their approval for clinical application is harder due to the risk of animal-borne disease transmission to the recipients and other adverse reactions

to animal products (Petter-Puchner et al., 2008; Doerr, Cinatl, Stürmer and Rabenau, 2003).

Platelets are a natural reservoir of angiogenic GFs and cytokines and are activated at sites of tissue injury, where they promote tissue repair, including revascularization, by releasing these GFs (Anitua et al., 2004; Kisucka et al., 2006). Therefore, through lysis of platelets, these GFs can be extracted, providing a less expensive and laborious alternative to recombinant production (Schallmoser and Strunk, 2009). Because platelet-enriched plasma (PRP) is already used systematically to treat patients with thrombocytopenia, it is widely available and can be easily approved for additional therapies. Furthermore, as these platelet concentrates are suspended in plasma, they also provide a source of ECM precursors, like fibrinogen, which can be quickly polymerized into fibrin at body temperature through the coagulation cascade. This can, in turn, bind to other scaffolding proteins present in plasma, such as fibronectin, or those originating from the disruption of platelets, like vitronectin (Seiffert and Schleef, 1996) (Figure 4.1A). These proteins are adhesive to collagen (Erat, Sladek, Campbell and Vakonakis, 2013) and other ECM components in injury sites and contain integrin-binding sites (e.g. RGD motifs), allowing for cell attachment. Importantly, the backbone of this natural polymer network, can be gradually degraded by the action of proteases produced by cells, such as plasmin and matrix metalloproteinases (MMPs), thus achieving full biodegradability and host integration (Ahmed, Ringuette, Wallace and Griffith, 2014). A further advantage of such approach compared to synthetic polymers is that these ECM proteins have a natural affinity for growth factors forgoing the need to be modified beforehand (Zhu and Clark, 2014).

The decision was taken to investigate the use of human platelets as the sole source of GFs and structural proteins for the generation of a complete animal product-free 3D cell culture support (Figure 4.1B). Previous studies on human stem cells demonstrated the possibility of fabricating scaffolds using human platelet lysates in conjugation with animal proteins (Walenda et al., 2012). Nonetheless, this approach has never been chosen for the culture of EPCs and, most importantly, no studies yet have focused on the ability of platelet lysate to support the formation of vascular capillaries by endothelial progenitors on their own.

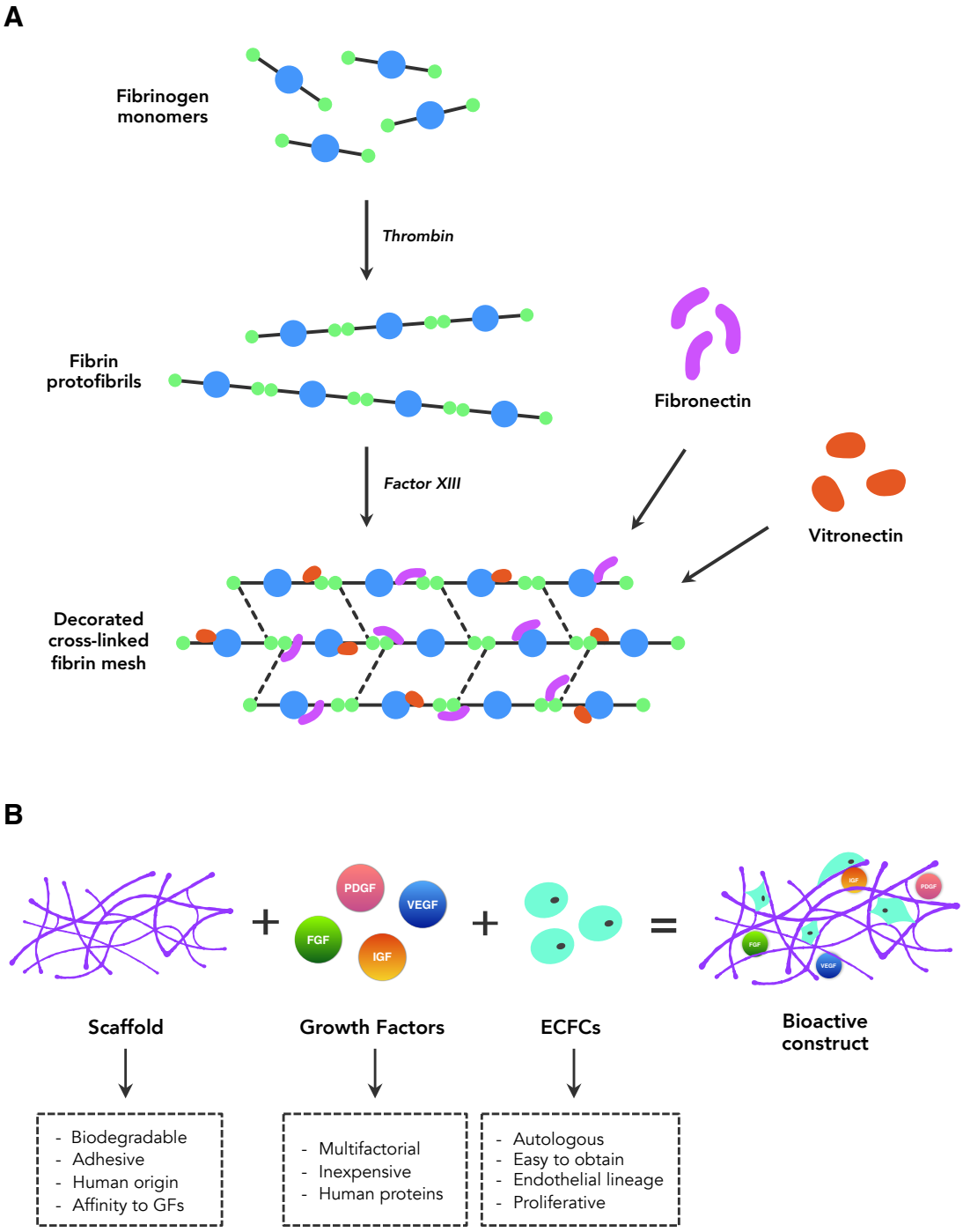


**Figure 4.1. Proposed mechanism of hPL polymerization and application rationale.** (**A**) hPLG is formed through a chain reaction, in which thrombin cleaves fibrinogen monomers to form fibrin protofibrils. Factor XIII then crosslinks these into a fibrin mesh, to which fibronectin and vitronectin bind at multiple sites. (**B**) By using hPLG as both a scaffold and a growth factor vehicle for encapsulation of ECFCs, a fully human angiogenic construct can be obtained.

### 4.2. Aims & Objectives

In spite of the interesting findings in the previous chapter regarding PAR-1 modulation of tubologenesis by ECFCs, there was no conclusive indication of a vasculogenic role played by PAR-2 in these cells, which could be exploited for tissue engineering purposes. Considering the need for developing alternative ways of promoting sustained blood vessel formation, the next chapter focused on the development of an animal-free multi-component system that can support ECFCs in this process.

The aim of the work in this chapter is therefore to create an angiogenic material derived from platelets as a fully human therapeutic approach for tissue revascularization by ECFCs. The objectives were defined as follows:

- To investigate if hPL could be gelled, and examine its structure and GF constitution.
- To test gelled hPL as a human substrate for *in vitro* expansion of ECFCs, characterizing their phenotype, gene expression profile and proliferation rate.
- To encapsulate ECFCs in the hPL matrix and evaluate their vasculogenic response.
- To evaluate the potential of gelled hPL to stimulate angiogenesis from existing vessels using an animal *ex vivo* assay.

## 4.3. Results

### 4.3.1. hPLG is dense fibrous scaffold containing plasma proteins and multiple angiogenic growth factors

The majority of ECM protein precursors in hPL, that allow it to be gelled, originate from its plasma component. Plasma is rich in soluble fibrinogen that can be quickly converted into an insoluble fibrin network, in a reaction catalysed by thrombin. Additionally, this mesh is also composed of fibronectin and vitronectin, which bind to the fibrin backbone. This conjugation of ECM proteins imports a number of advantages in using hPLG for cell delivery compared to the commercially available pure fibrin, such as improved structural stability, ability to bind growth factors and the number of cell binding sites. In order to evaluate the structure of hPLG and compare it against pure fibrin gels, samples of both were analysed by SEM. PRP was lyzed by ultrasonication to obtain hPL, as described in chapter 2.2, and gelled with and without encapsulated ECFCs.

hPLG was revealed to be composed of a fibrous matrix very similar to pure fibrin gels. However, fibrin gels were characterized as having a more unorganized structure and smooth texture, while hPLG was shown to have an abundant protein coating and more consistently organized fibres. This protein layer appears to be mostly released or digested over the period of 3 days, though a remainder of it still visible on the surface of fibres (Figure 4.2).

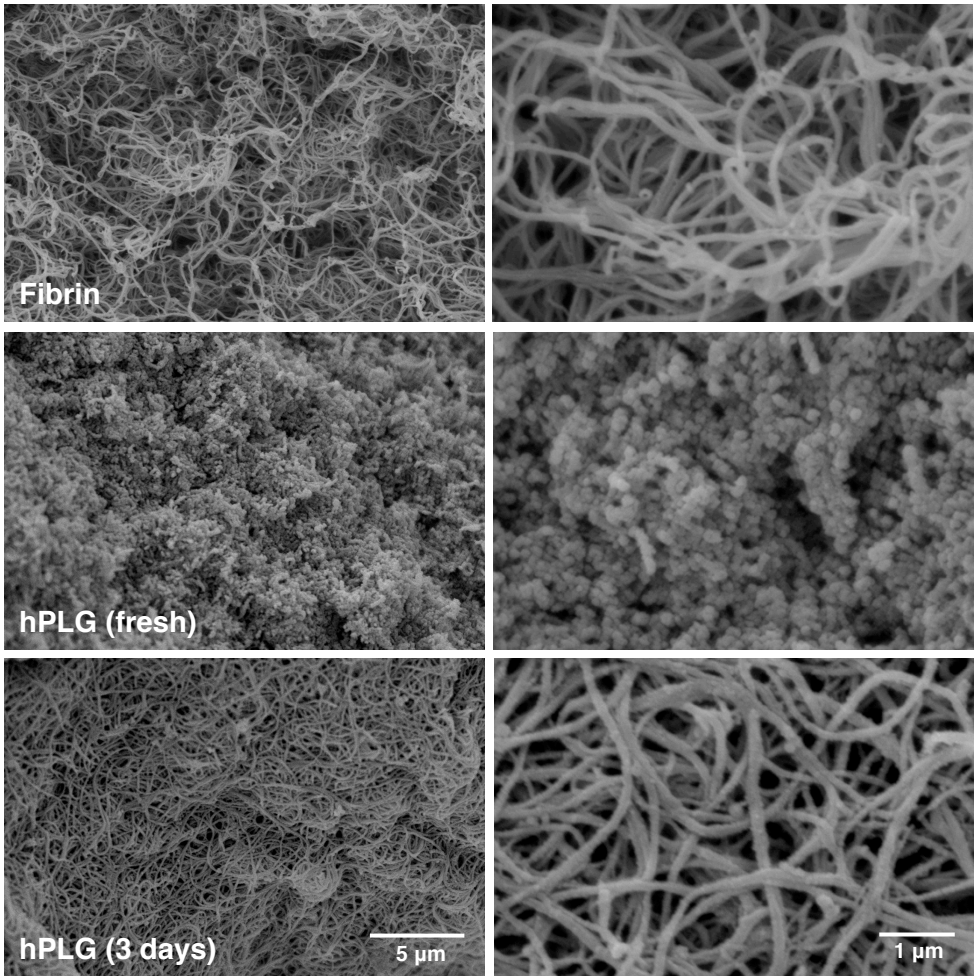


**Figure 4.2. Microscopic structure of fibrin and hPLG.** Scanning electron microscopy images of fresh fibrin (top), fresh hPLG (middle) and hPLG after 3 days incubation (bottom) at 5,000x (left) and 20,000x (right) magnification.

Additionally, hPL produced by freeze-thaw methods has been shown to contain a variety of GFs with angiogenic profiles (Fekete et al., 2012; Burnouf et al., 2016). To confirm that ultra sonication could be equally efficient in disruption of platelets, the identity and concentrations of some of these GFs was determined in hPL produced by this method. Data obtained by ELISA showed that hPLG contains significant amounts of VEGF (77±50 pg/mL), EGF (545±49 pg/mL), PDGF-BB (2,293±20 pg/mL) and FGF-2 (318±10 pg/mL) (Figure 4.3A), which are in line with the previously reported values in the literature for platelet lysates produced by the more conventional freeze-thaw method. The release of these GFs from hPLG was then analysed in culture medium. Gels were incubated at 37 ºC in basal medium and samples of medium were collected at 1, 3 and 5 days from different replicates (i.e. data are non-cumulative). Only VEGF-A, EGF and PDGF-BB appeared to be efficiently released, with the latter being the GF detected in highest quantities (Figure 4.3B).

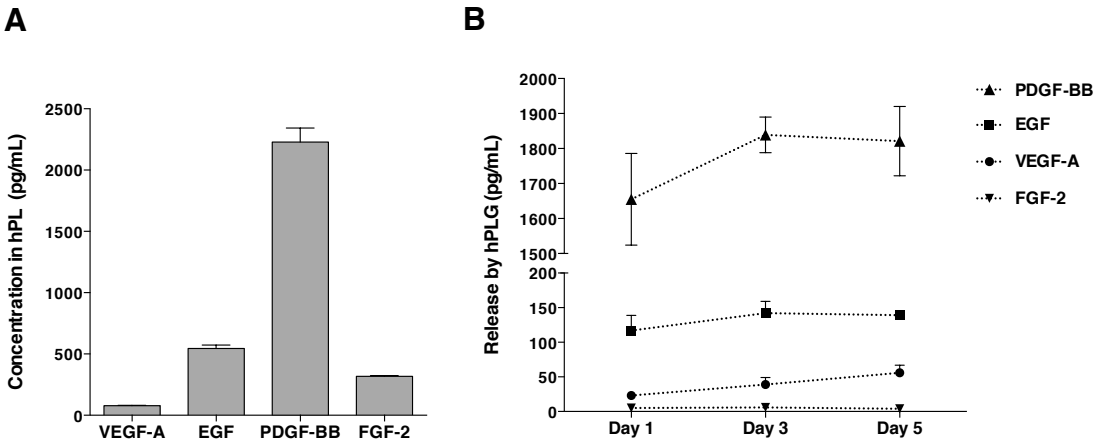


**Figure 4.3. Initial concentration and release of GFs by hPLG.** (**A**) Growth factor concentrations in fresh hPL (20% v/v) and (**B**) released from hPLG after 1, 3 and 5 days of incubation at 37 ºC were determined by ELISA. Data are expressed as mean ± SEM (n=3).

### 4.3.2. Culture of ECFCs on hPLG stimulates cell proliferation in a GF-dependent manner

The suitability of hPLG as a substitute to rat collagen I coating (i.e. traditional surface coating) in the continuous culture of ECFCs was assessed by immunofluorescence for endothelial markers CD31 and vWF (Figure 4.4). Cells were seeded on both substrates and cultured for 2 days until being fixed and stained. The endothelial phenotype of ECFCs was retained when cultured on hPLG, exhibiting typical cobblestone morphology with CD31 localized to intracellular junctions and identical punctate cytoplasmic distribution of vWF protein, denoting the existence of Weibel-Palade bodies.

Additionally, the phenotype of ECFCs cultured on hPLG was also confirmed by gene expression analysis of a broader series of endothelial markers. In this case, cells were cultured on each of the substrates for 24 h, at which point total RNA was extracted and analyzed by RT-qPCR. The relative expression of CD31, eNOS, FGFR-1, VE-cadherin and vWF remained unchanged in comparison to that of ECFCs grown on collagen (Figure 4.5). Interestingly, the expression of a series pro-angiogenic molecules and receptors such as angiogenin, PDGFR-β, SDF-1 and VEGFR-2 were significantly upregulated in ECFCs grown on hPLG compared to collagen I coating (Figure 4.5).

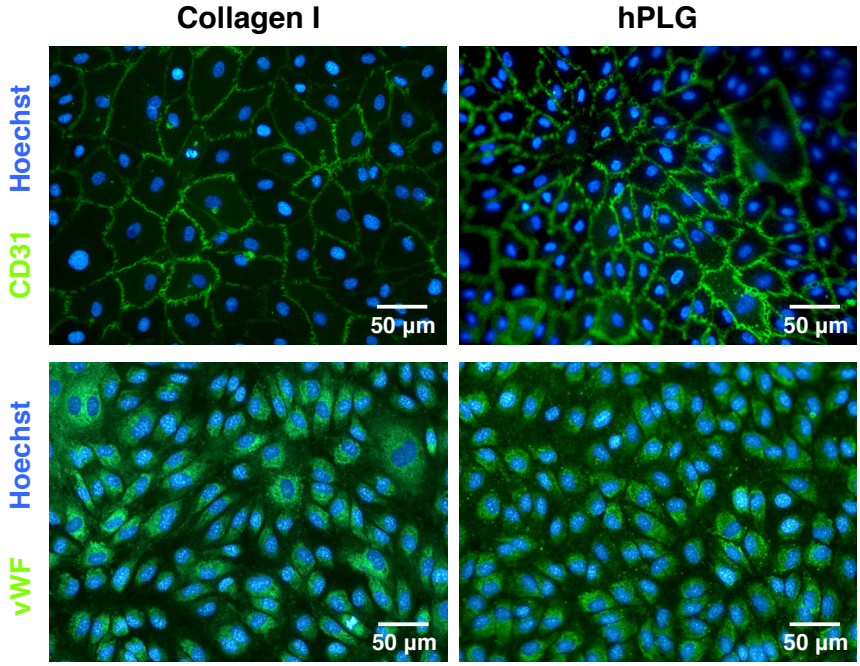


**Figure 4.4. ECFC morphology and phenotype on collagen I vs hPLG.** ECFCs grown on collagen-coated plastic and hPLG were stained with antibodies for specific endothelial markers CD31 and vWF to confirm their morphology and phenotype (n=3).

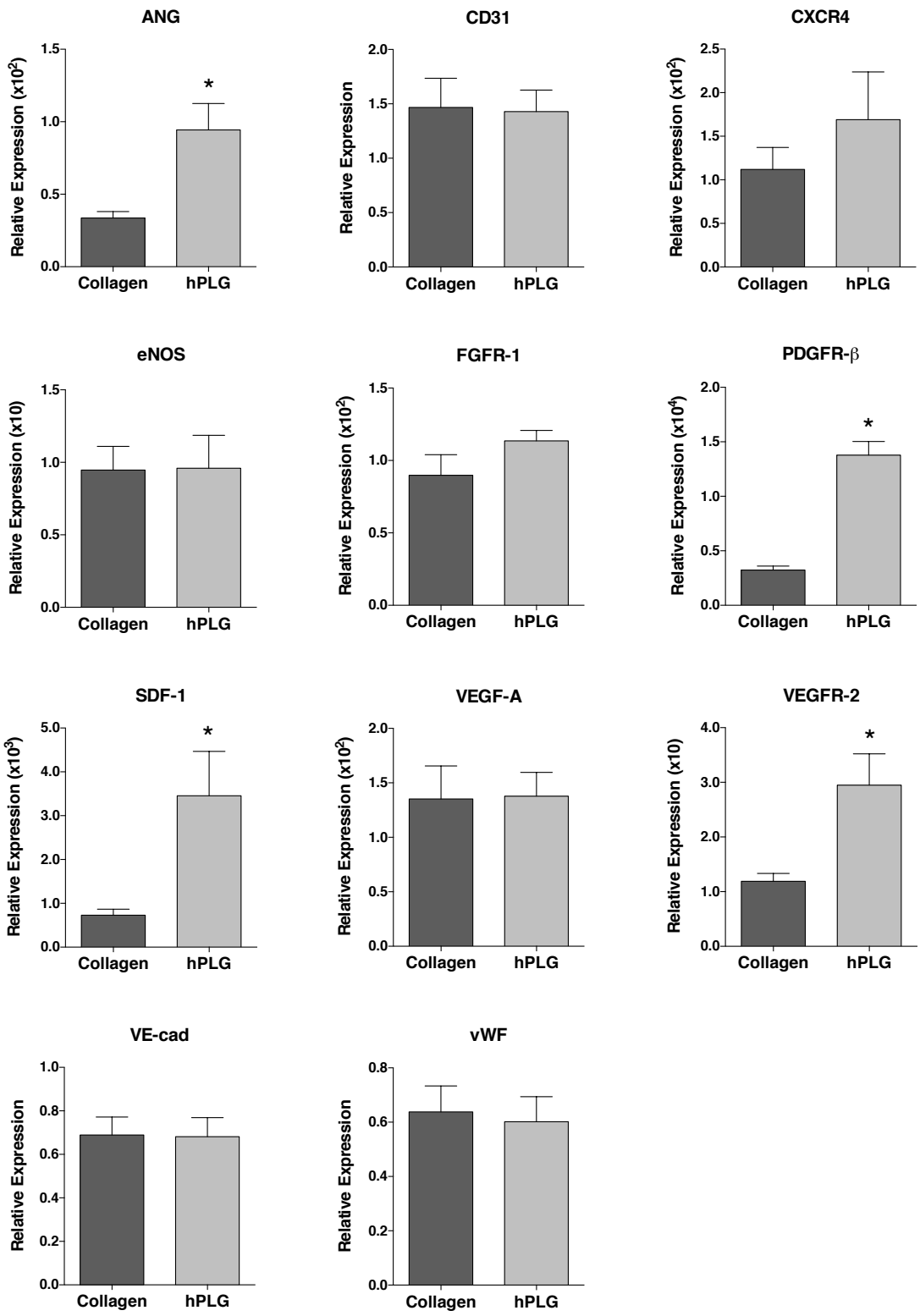


**Figure 4.5. Gene expression of endothelial markers and pro-angiogenic genes by ECFCs on hPLG.** Total RNA was extracted from ECFCs cultured on collagen-coated plastic and hPLG for 24 h. Relative expression of selected genes was analysed by RT-qPCR using specific primers as described in Methods chapter 2.9. Data are normalized to GAPDH and are expressed as mean ± SEM (n=3). Statistical significance was tested using Mann-Whitney U-test (*=$p<0.05$).

Considering the observations on GF concentrations in hPLG and overexpression of some of their receptors by ECFCs when cultured on this substrate, the proliferation rate of these cells was assessed over a 24 h period on hPLG in comparison to the traditional coating, while maintaining all the other normal culture conditions (i.e. culture in full medium). Additionally, the role of GF signalling as well as the activation of ERK1/2 and CXCR4 on proliferation was determined through the addition of specific inhibitors. Because this gel was found to interfere with most commonly used metabolic activity assays, such as MTS or resazurin-based assays, as well as with dsDNA quantification assays due to residual amounts of DNA originating from contaminating leukocytes in PRP, a different method had to be employed. Cells were fixed and their nuclei stained with Hoechst 33342, followed by epifluorescence imaging. Nuclei were then manually counted and expressed as the relative increase versus the number of cells seeded. The proliferation of ECFCs on hPLG was significantly higher than on collagen-coated plastic (Figure 4.6A) and this difference was associated with the activity of several GFs. A decrease in proliferation on hPLG was seen with the non-specific growth factor receptor blocker pazopanib, without significantly affecting growth on collagen. In the presence of VEGF receptor specific inhibitors Ki8751 and tivozanib or PDGFRβ/VEGFR inhibitor brivanib, ECFC proliferation was nearly halted on both surfaces. Additionally, in agreement with the gene expression data, the increased proliferation on hPLG was partially related to SDF-1/CXCR4 signalling as the CXCR4 antagonist AMD3100 significantly reduced proliferation, while no significant effect was observed on collagen I (Figure 4.6B). As expected due to its role in GF signalling and cell proliferation, ERK1/2 inhibition with PD98058 suppressed proliferation on hPLG but not the traditional collagen coating (Figure 4.6B).

In order to determine whether the GFs contained in hPL were responsible on their own for the higher proliferation observed on hPLG, experiments were performed with hPL as a liquid supplement to the culture medium. In addition to collagen coating and hPLG, pure fibrin was also tested as a substrate for ECFCs. Data showed that the addition of the same quantity of liquid hPL per well as that used for the generation of hPLG did not lead to the same improvement in proliferation in as observed for ECFCs growing on hPLG (Figure 4.6C and D).

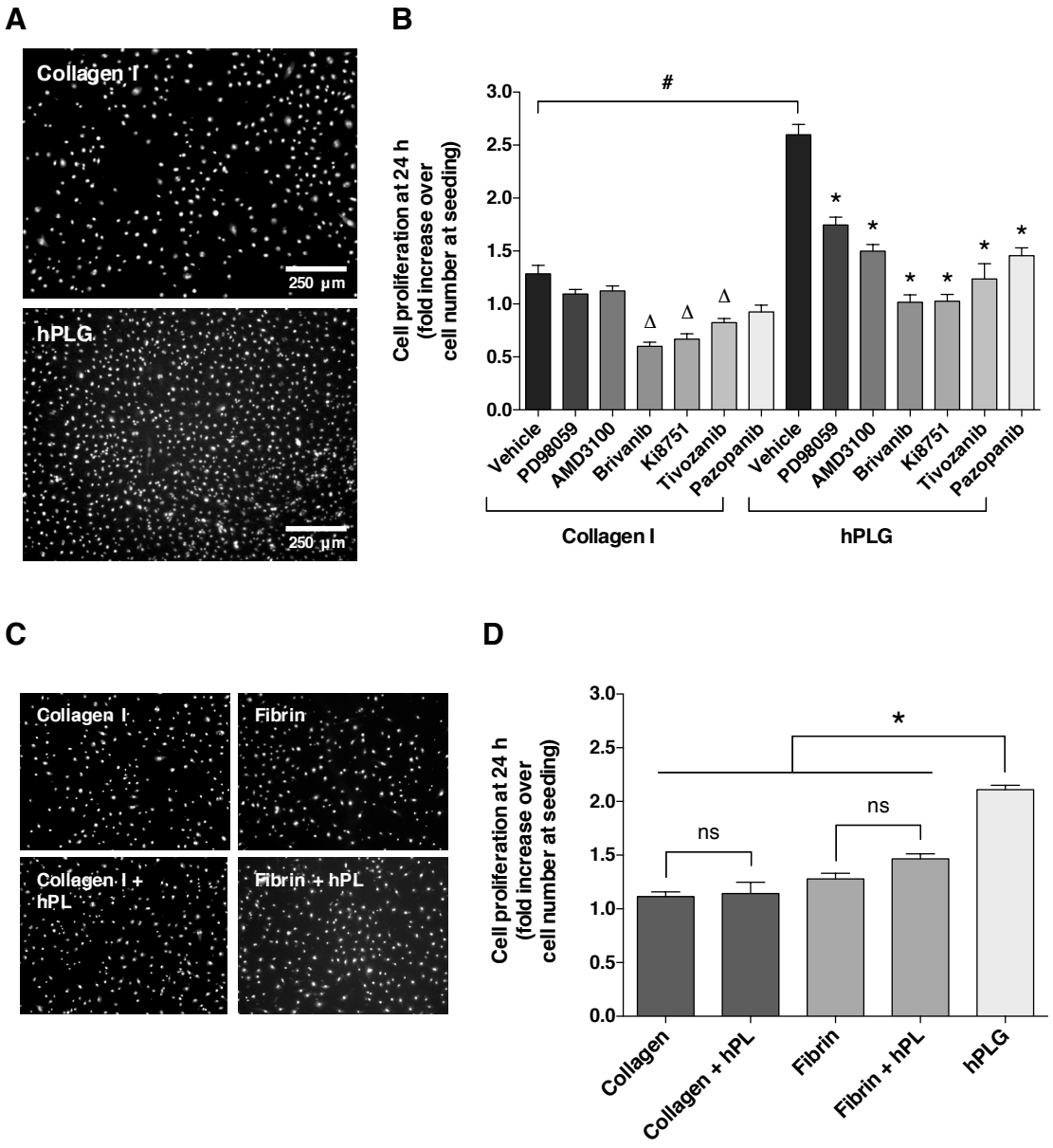


**Figure 4.6. Stimulation of ECFC proliferation on hPLG.** (**A**) 12,000 ECFCs/well were seeded on collagen-coated plastic and hPLG and cultured for 24 h in complete culture medium before being fixed and nuclear-stained with Hoechst 33342 (in blue). (**B**) ECFCs were incubated with PD98059 (50 µM), AMD3100 (10 µg/mL), Brivanib (10 µM), Ki8751 (100 nM), Tivozanib (1 µM), Pazopanib (20 µg/mL) on both collagen-coated plastic and hPLG. The number of cells per $mm^2$ was quantified by microscopy and expressed as fold increase, as described in chapter 2.11.1. Data show mean ± SEM. Statistical significance was tested by one-way ANOVA with Bonferroni's post-test test to compare different inhibitors against the control conditions (Δ and * indicate statistical differences against the collagen I and hPLG controls respectively) (*=$p<0.05$) (n=6). ECFC proliferation was also tested in 2D cultures on collagen-coated plastic and fibrin gels with soluble hPL provided as a source of extra GFs. Representative pictures are shown in (**C**) and quantitative analysis is shown in (**D**). Data are mean ± SEM. Statistical significance was tested using one-way ANOVA with Tukey's post-test (*=$p<0.05$) (n=6).

In view of the demonstrated role of ERK1/2 in the promotion of ECFC proliferation, it was decided to investigate the time frame of ERK activation elicited by hPLG. ECFCs were seeded on both hPLG or control collagen-coated plastic, and phosphorylation was assessed after 1 h and 6 h by immunoblotting using specific antibodies for total ERK1/2 and the respective phosphorylated forms. At both time points, these kinases were found to be robustly activated on hPLG (Figure 4.7). Because hPLG contains considerable amounts of platelet cytoplasmic proteins, actin could not be used as an additional loading control and for proper intensity quantification it was necessary to take in account the contribution of ERK1/2 from hPLG devoid of ECFCs, which is not phosphorylated (far right lanes).

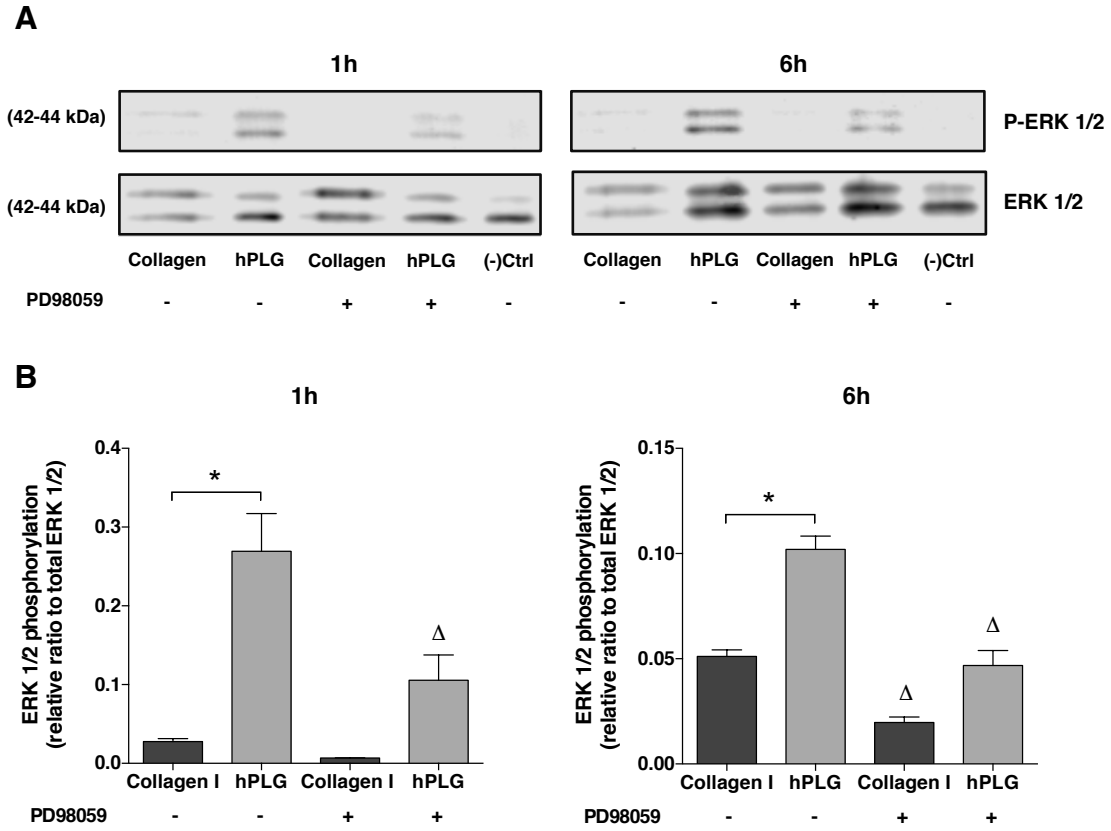


**Figure 4.7. Culture of ECFCs on hPLG continually activates ERK1/2.** (**A**) Activation of ERK1/2 by contact with hPLG versus rat collagen I-coating (1 and 6 hours incubation) and its inhibition by 50 µM PD98059. ERK1/2 phosphorylation was assessed using phospho-specific ERK1/2 antibodies and immunoblotting. Last lane demonstrates expression but no phosphorylation of ERK1/2 from platelets in hPLG (in the absence of ECFCs). (**B**) Densitometry analysis was performed using ImageStudio (LICOR). Graphs display the normalized intensities as arbitrary units for the phospho-ERK1 and phospho-ERK2. Data show mean ± SEM. Statistical significance was tested using one-way ANOVA with Tukey's post-test (*=$p<0.05$). Δ indicates significance relative to the condition without ERK inhibitor on the same substrate (n=3).

The contribution of VEGF signalling to this elevated ERK1/2 activation was then assessed by inhibition of VEGFR-2 with the specific inhibitor Ki8751. At both time points, no decrease in ERK activation was observed when VEGFR-2 was inhibited, suggesting that either VEGF is not connected to the increased ERK phosphorylation or that this pathway is redundantly activated by the different growth factors in hPLG (Figure 4.8).

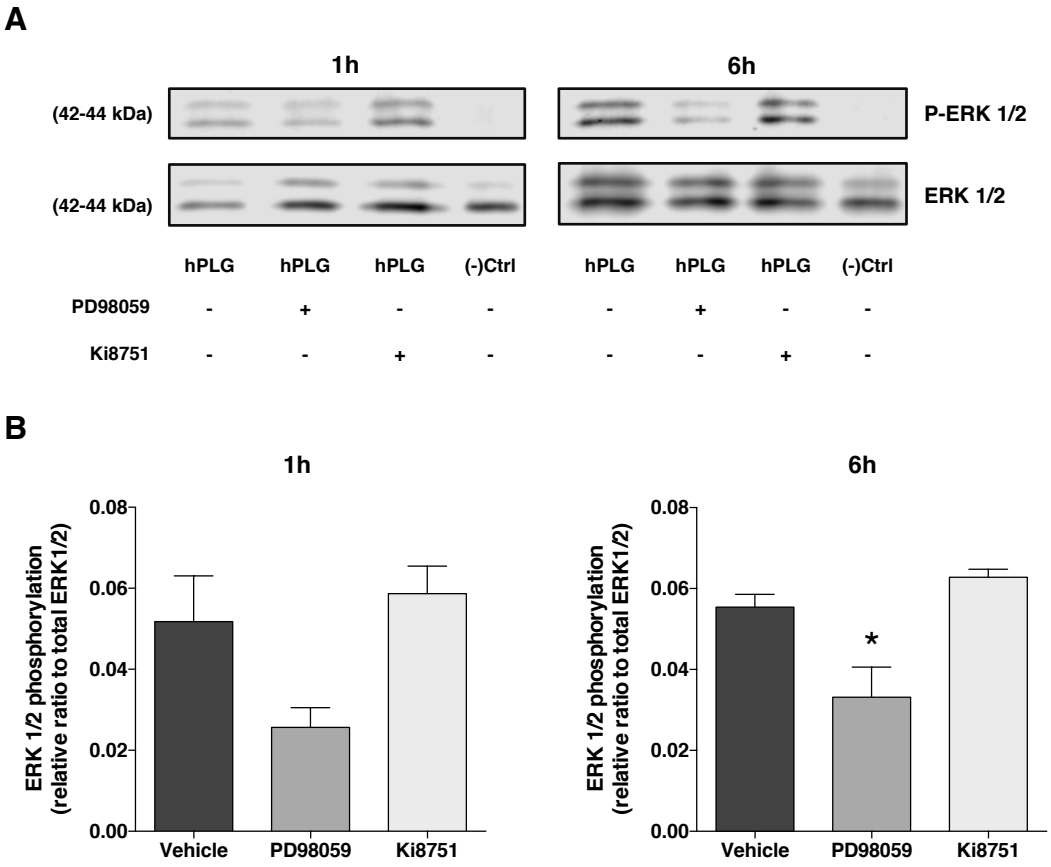


**Figure 4.8. Activation of ERK pathway by culture on hPLG is not VEGF dependent.** (**A**) Effect of inhibition of VEGFR-2 on ERK activation in ECFCs cultured on hPLG was tested by incubating cells with 100 nM Ki8751 or 50 μM PD98059 (1 and 6 hours incubation). ERK1/2 phosphorylation was assessed using phospho-specific ERK1/2 antibodies and immunoblotting. Last lane demonstrates expression but no phosphorylation of ERK1/2 from platelets in hPLG (in the absence of ECFCs). (**B**) Densitometry analysis was performed using ImageStudio (LICOR). Graphs display the normalized intensities as arbitrary units for the combined phospho-ERK1/2. Data show mean ± SEM. Statistical significance was tested using one-way ANOVA with Tukey's post-test (*=$p<0.05$) (n=3).

### 4.3.3. 3D culture of ECFCs in hPLG promotes capillary vascular network formation

Due to the possibility of gelling hPLG *in situ* by the simple addition of thrombin, it has great potential to become an off-the-shelf means of delivering cells for tissue regeneration, especially for the promotion of vascularization. Therefore, the potential of hPLG as a supportive scaffold for the formation of fully human endothelial networks was investigated. For that purpose, ECFCs were encapsulated in hPLG and their response compared with ECFCs in collagen I and fibrin gels, the two gold standards for 3D angiogenic assays (di Blasio, Bussolino and Primo, 2015). Cells in hPLG were cultured in serum-free basal medium, while complete medium (i.e. 10% FBS plus recombinant GFs) was used for cells in collagen or fibrin gels in order to ensure cell viability and angiogenic response. To visualize and measure the degree of network formation, cells were either fixed and stained with fluorescent lectin or live imaged following loading with calcein AM.

Over a 3 day period, ECFCs within hPLG rapidly established a *de novo* endothelial network as evidenced by dual staining with FITC-UEA I and Hoechst 33342 (Figure 4.9A). Conversely, in collagen I or fibrin gels there was negligible formation of an interconnected capillary network, as shown by quantitative image analysis (Figure 4.9B). Again, as for ERK phosphorylation in 2D cultures, the activation of VEGFR-2 was not essential for network formation in 3D, as no significant effect was observed using the specific inhibitor Ki8751 (Figure 4.10). The cell-permeant dye calcein AM was then used to clearly distinguish lumens lined by endothelial cells as part of the capillary structures in hPLG. Both epifluorescence (Figure 4.11A) and confocal microscopy were used (Figure 4.11B). Confocal images are shown with orthogonal views obtained by z-stacking, which clearly show the presence of a lumen in the capillaries. The formation of capillaries with lumens by ECFCs cultured in hPLG was also confirmed by TEM (Figure 4.12A). Through this technique it was possible to detect the different stages by which a capillary lumen is typically formed, including the emergence of small vacuoles inside individual cells and their gradual fusion to give origin to continuous multicellular hollow tubes. Although the lumens of the capillaries reached a considerable size, due to limitations in TEM technique (i.e. grid size and data acquisition), only capillaries with lumens smaller than 30 µm can be frequently captured in one scan. Larger capillaries can be detected and displayed by building a composite picture made of several scans, as in Figure 4.12B.

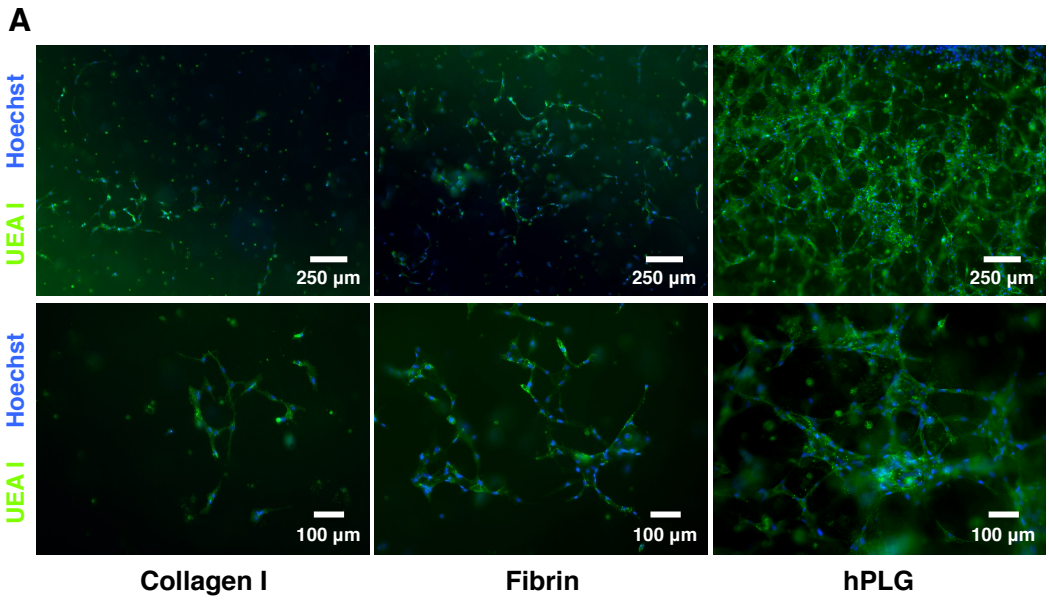


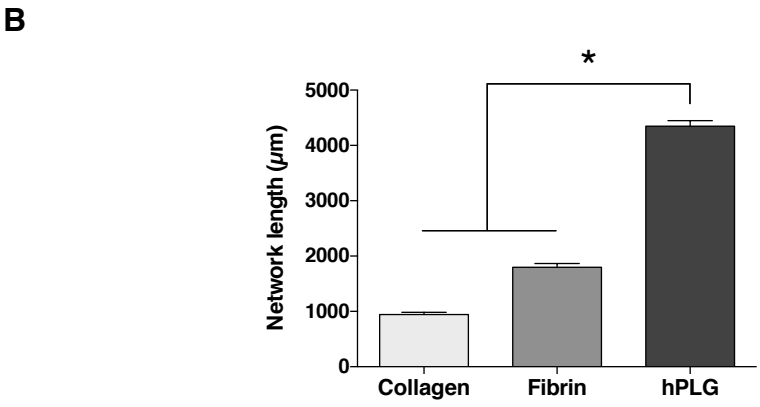


**Figure 4.9. Network formation by ECFCs in different matrices.** (**A**) ECFCs were encapsulated in collagen I, fibrin or hPLG and cultured for 3 days at 37 ºC. Constructs were fixed and stained with FITC-conjugated Ulex europaeus lectin (FITC-UEA I) which binds to α-L-fucose-containing glycocompounds on the surface of endothelial cells and with Hoechst 33342 to localize cell nuclei. Images were captured with an EVOS FL microscope at 4x (top row) and 10x magnifications (bottom row). (**B**) Total length of capillary network was manually measured using ImageJ. Data are mean ± SEM. Statistical significance was tested using one-way ANOVA with Tukey's post-test (*=$p<0.05$) (n=3).

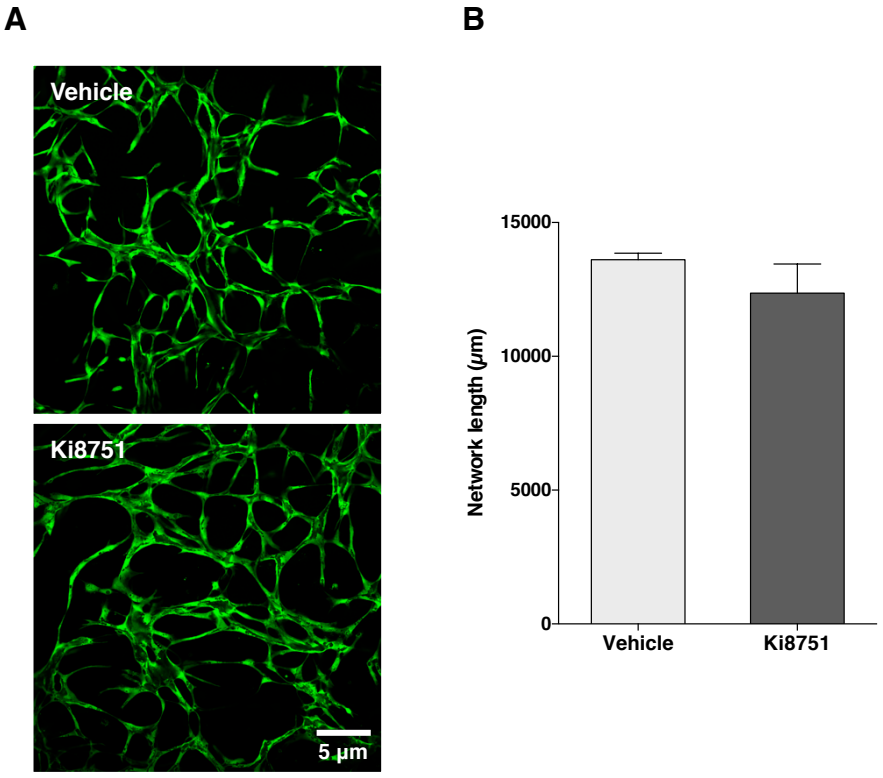


**Figure 4.10. hPLG supports network formation in a VEGFR-2 independent manner.** (**A**) ECFCs were embedded in hPLG and treated daily with Ki8751 solution (100 nM) or vehicle solution. Cells were live stained after 3 days of the start of the experiment. Fluorescent calcein AM was used to stain the cytoplasm of viable cells. Confocal images were acquired using a Zeiss LSM 510 META microscope (10x objective). (**B**) Total length of the capillary network in the different conditions was manually measured using ImageJ. Data are mean ± SEM. Statistical significance was tested using Student's t-test (n=3).

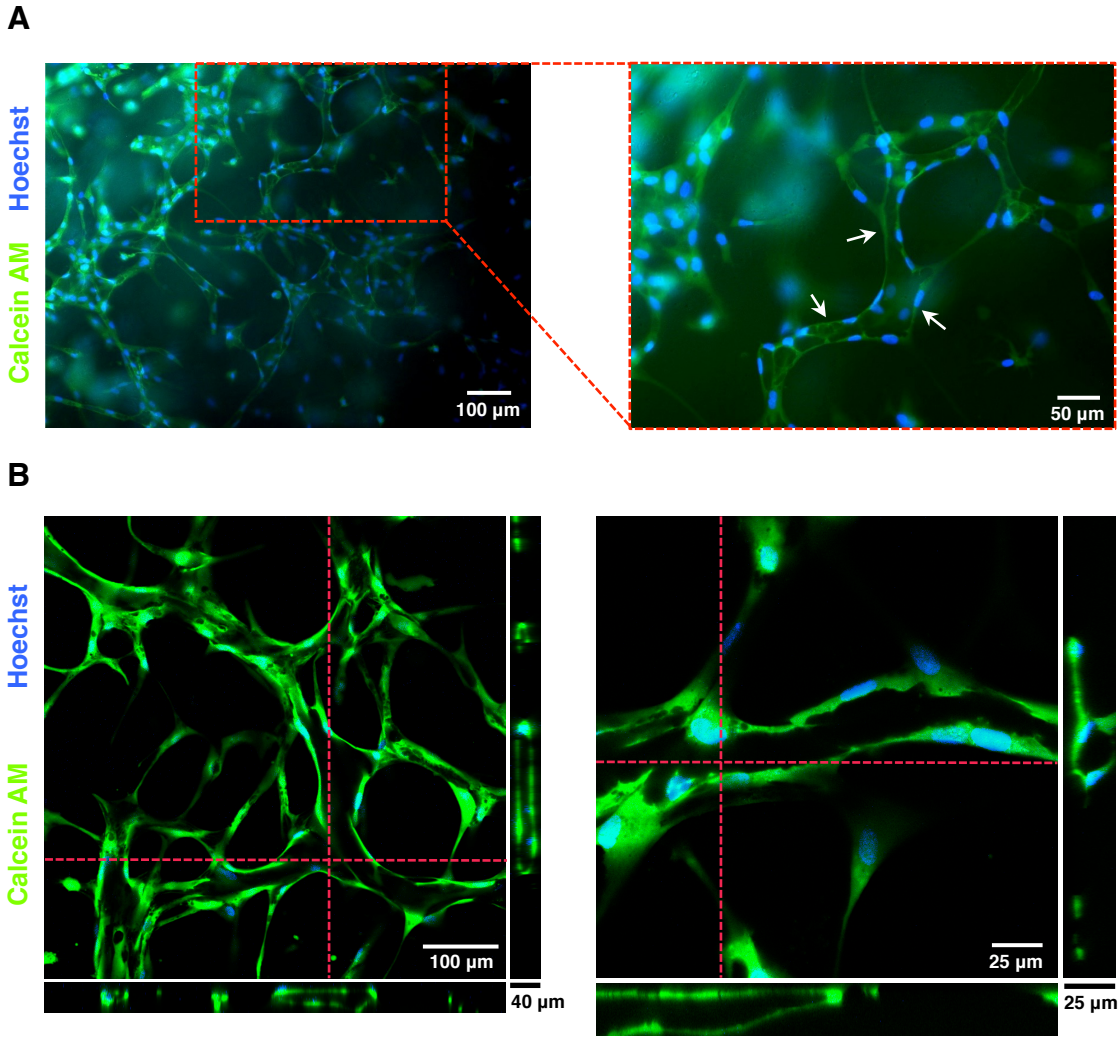


**Figure 4.11. Detection of lumenized capillary networks by ECFCs encapsulated in hPLG using fluorescence microscopy.** hPLG-encapsulated ECFCs were live stained 3 days after the start of the experiment. Fluorescent calcein AM was used to stain the cytoplasm of viable cells, while Hoechst 33342 was used to localize cell nuclei. (**A**) Images show multiple ECFCs organized into primitive vascular structures with a lumen (white arrows). Epifluorescence images were obtained using an EVOS FL microscope (10x and 20x objectives). (**B**) Z-stack images were acquired using a Zeiss LSM 510 META confocal microscope (20x and 40x objectives).

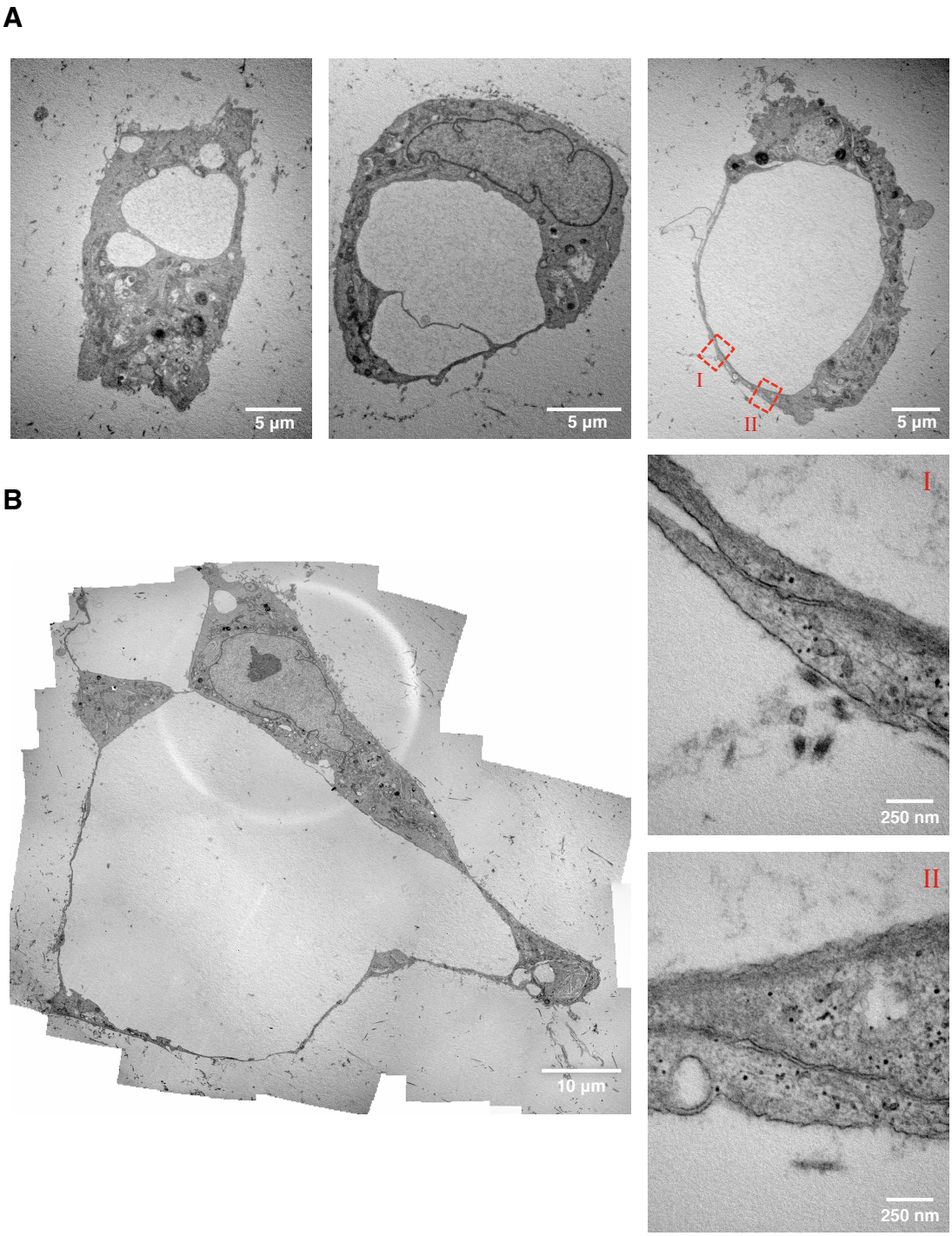


**Figure 4.12. Detection of lumenized capillary networks formed by ECFCs encapsulated in hPLG using transmission electron microscopy (TEM).** (**A**) TEM was used to confirm the existence of a lumen in tubular structures by ECFCs in hPLG. Different stages of lumen formation can be observed: from the initial vacuolization within individual cells, to the fusion of vacuoles from neighbouring cells forming continuous multicellular tubes (, left to right). Tight junctions formed between connecting cells at sites of overlap can be seen in I and II (right side panel) while a larger lumen delimited by multiple cells is shown in (**B**) (stitched composition of several electron micrographs).

### 4.3.4. hPLG stimulation of pre-existing vessels in an *ex vivo* model

As a proof of concept for the application of hPLG as an injectable scaffold and cell carrier, a previously developed *ex vivo* animal assay was adapted to demonstrate the ability of this biomaterial to promote angiogenesis through sprouting of existing blood vessels, while allowing for anastomosis between these and the network newly formed by injected ECFCs.

Rat aortic ring sections were encapsulated in hPLG and compared with collagen I and fibrin gels. While for hPLG, culture was performed in basal medium, for collagen and fibrin matrices 2% FBS was added to guarantee cell survival. In spite of the unfavourable conditions, a swift and robust response was seen in hPLG, with sprouts reaching close to 600 μm on average into the gel matrix, while negligible sprouting was observed in collagen and fibrin gels during the 3 day period (Figure 4.13). Then, to simulate *in vitro* the delivery of ECFCs in hPLG into an ischaemic site as closely as possible, these cells were co-encapsulated with rat aortic rings and cultured for 3 days. Rat capillaries sprouting from the aortic tissue were stained with TRITC-conjugated Isolectin B4 (IB4), which binds terminal α-galactosyl residues expressed on non-primate ECs, and human ECFCs were stained with FITC-UEA I as previously. Again, on a short time scale, extensive sprouting from the aortic rings was observed, closely surrounded by a capillary network of ECFCs (Figure 4.14A). Additionally, despite the xenogeneic nature of this assay, points of interaction between human and rat vasculature were identified already at this early time point (white arrows in Figure 4.14B), which suggests the ability of ECFC capillaries to anastomose with the “host's” vascular network after implantation.

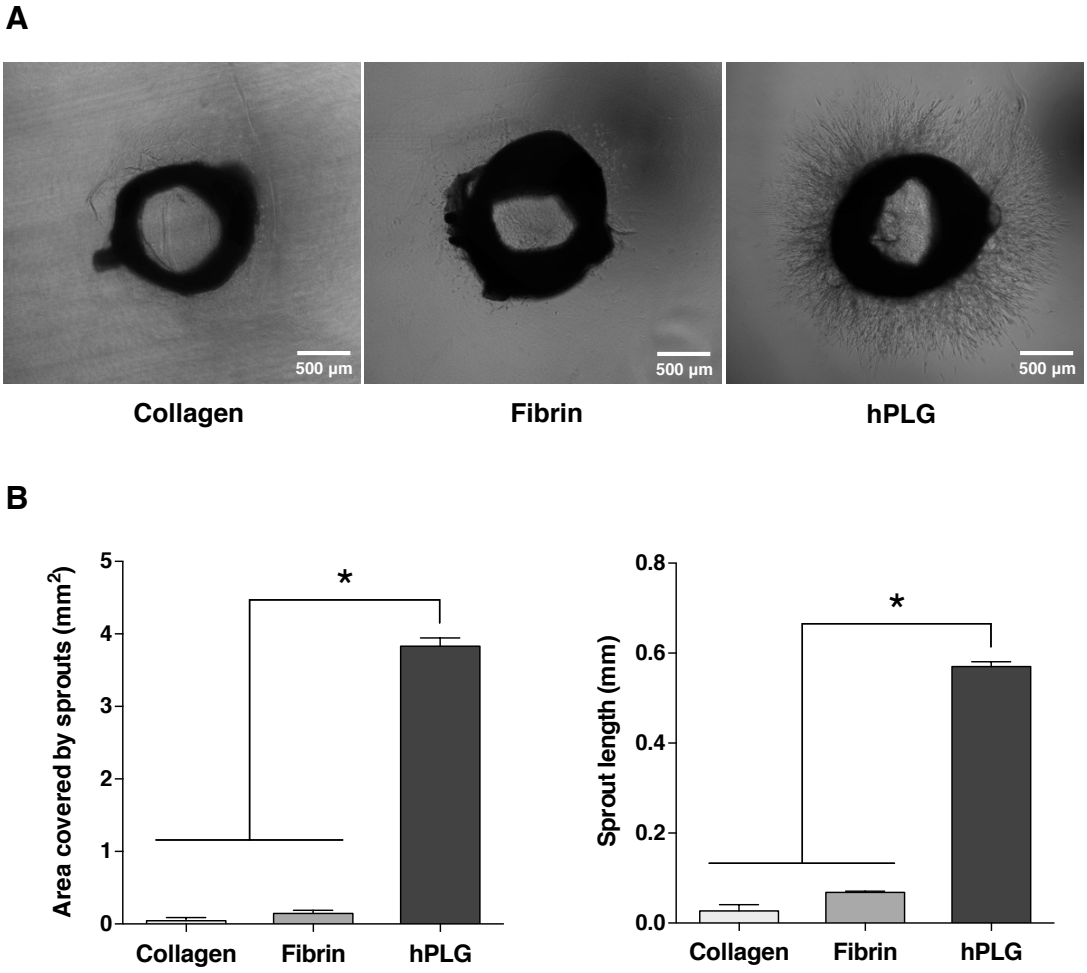


**Figure 4.13. hPLG induces robust aortic ring sprouting.** (**A**) Cross sections of rat aorta were encapsulated in collagen I, fibrin or hPLG for 3 days at 37 ºC. Aortic rings were fixed and images captured with an EVOS FL microscope (4x objective, stitched images). (**B**) Angiogenesis was quantified as total sprouting area and average length of sprouts, measured using ImageJ. Data show mean ± SEM. Statistical significance was tested by one-way ANOVA with Tukey's post-test (*=$p<0.05$) (n=3).

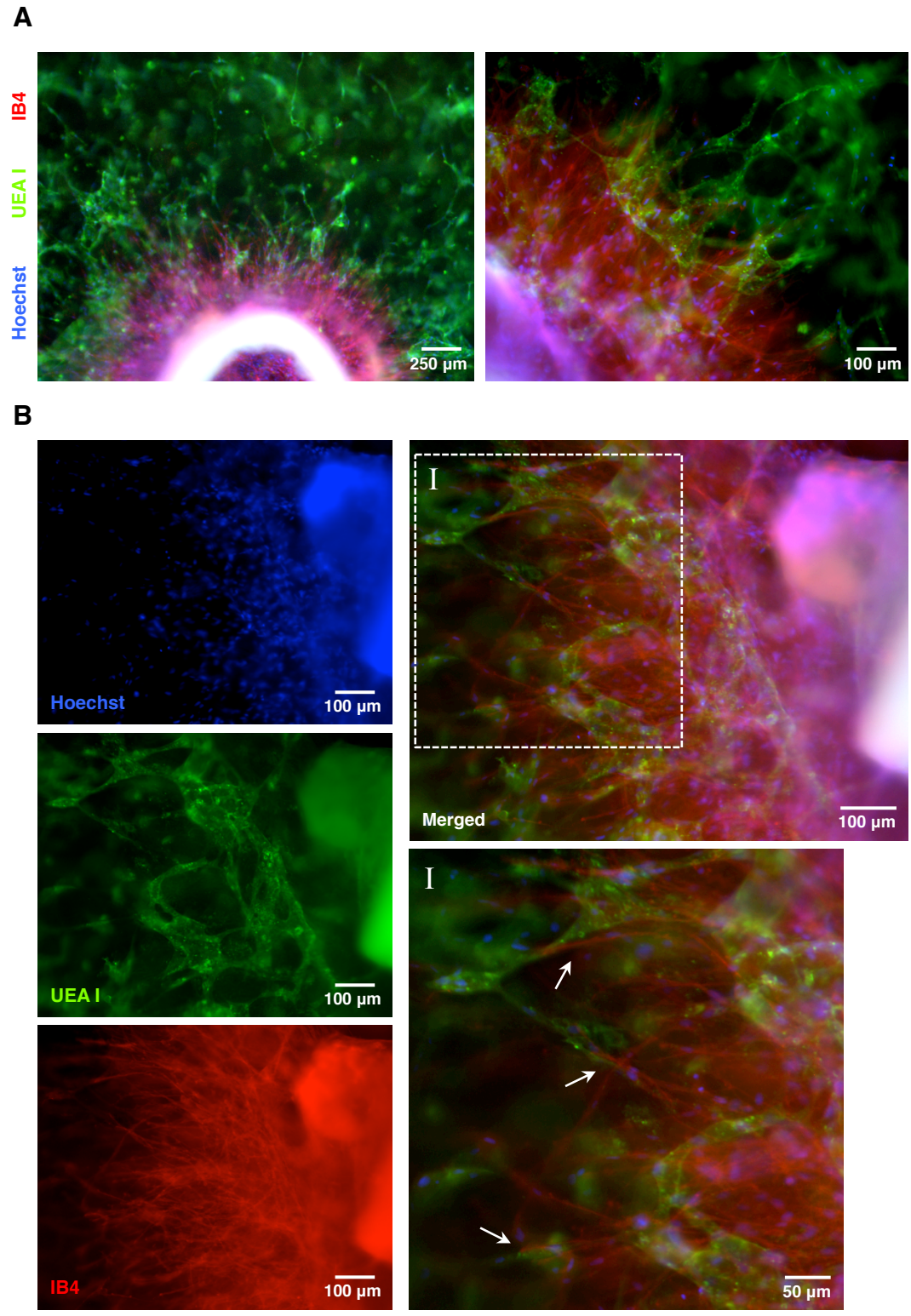


**Figure 4.14. Interaction between ECFC capillary network with rat aortic sprouts in hPLG.** (**A**) Cross sections of rat aorta were co-encapsulated with ECFCs in hPLG and cultured in serum-free basal medium, leading to robust sprout formation. After 3 days of incubation, gels were fixed and stained with FITC-conjugated Ulex europaeus lectin (FITC-UEA I) to specifically label human endothelial cells (ECs) and with TRITC-conjugated Isolectin B4 (IB4) which binds terminal α-galactosyl residues expressed on non-primate ECs, in addition to Hoechst 33342 for nuclear staining. (**B**) White arrows indicate sites of close interaction between rat ECs and network formed by human ECFCs. Images were obtained with an EVOS FL microscope (4x, 10x and 20x objectives).

### 4.4. Summary of results

- hPLG consists of a fibrin-based matrix containing several angiogenic GFs.
- Significant upregulation of the angiogenic markers angiogenin, PDGFR-β, VEGFR-2 and SDF-1 on hPLG.
- hPLG stimulates ECFCs proliferation, while maintaining the endothelial phenotype.
- ECFC proliferation is mainly dependent on VEGFR-2.
- Prolonged ERK activation on hPLG vs collagen I.
- Encapsulation of ECFCs in hPLG promotes the formation of morphologically complete capillaries in 3D cultures.
- hPLG induces robust sprouting of rat aortic sections, which interact with ECFC networks.

## 4.5. Discussion

The delivery of EPCs and angiogenic growth factors (GFs) has been proposed as a viable approach for vascularization of tissue-engineered grafts as well as for the treatment of ischaemic conditions through therapeutic vasculogenesis (Herrmann, Verrier and Alini, 2015; Martino et al., 2015; Kuroda et al., 2014; Levengood et al., 2011; Lesman et al., 2011). In light of this, there is a need to develop a multi-component system comprising a source of autologous endothelial cells, a cocktail of human growth factors that can induce cell survival and blood vessel formation, and a biodegradable scaffold that can be used to deliver and help retain both at the target site. Human Platelet Lysate Gel (hPLG) was investigated as a potential injectable scaffold that is enriched in several angiogenic GFs to expand and deliver human ECFCs.

To obtain a plasma-derived gel-based scaffold enriched in platelet-derived growth factors, we have opted for lysing platelet-rich plasma by ultrasonication. This method disrupts platelets and their alpha-granules through cavitation, diminishing the possible impact of repeated freeze-thaw methods (Arakawa, Prestrelski, Kenney and Carpenter, 2001), often used by others (Schallmoser and Strunk, 2012; Doucet et al., 2005), on the bioactivity of GFs. It was shown that significant amounts of VEGF-A, EGF, PDGF-BB and FGF-2 can be obtained in this manner (Figure 4.3A). This panel is further complemented by ANGPT-1, IGF-1, PDGF-AB and TGFβ-1, as previously demonstrated (Leotot et al., 2013; Fekete et al., 2012; Doucet et al., 2005). These growth factors have been shown to play a role in tissue repair through promotion of angiogenesis, due to their chemotactic, mitogenic and anti-apoptotic effects on both endothelial cells and perivascular cells (pericytes and smooth muscle cells) (Mazzucco, Borzini and Gope, 2010; Rozman and Bolta, 2007). Most of these GFs have a natural affinity for ECM proteins found in hPLG, such as fibrin (Sahni and Francis, 2000; Martino et al., 2013), fibronectin (Rahman et al., 2005; Wijelath et al., 2002; Lin et al., 2011; Martino and Hubbell, 2010) and vitronectin (Rahman et al., 2005; Upton et al., 2008), and are slowly released due to the action of proteases that cleave the ECM or the ECM-binding domains of GFs (Ferrara, 2010). In our experiments, the quantification of growth factor release from hPLG into the medium was performed in the absence of cells and only PDGF-BB reached concentrations above 1 ng/mL over 5 days (Figure 4.3B). It is likely that the majority of the growth factor content remains bound to the hPLG matrix and it's only released in higher amounts due to cell activity. The ultrastructure of this matrix appeared more organized than that of pure fibrin gels

(Figure 4.2). This difference can be mainly attributed to presence of plasma fibronectin, which is known to bind to fibrin (Makogonenko, Tsurupa, Ingham and Medved, 2002). Such binding has been reported to lead to the formation of thicker and denser fibres (Procyk and King, 1990; Carr, Gabriel and McDonagh, 1987), as well as in the stiffening of the protofibril bundles by additional linkage of the α chains, with a subsequent increase of its elastic modulus (Kamykowski, Mosher, Lorand and Ferry, 1981). In addition to higher elasticity, hPLG should also benefit from the incorporation of vitronectin from a structural point of view. Although not investigated in our study, vitronectin has been found to inhibit fibrinolysis by modulating the action of Type 1 plasminogen activator inhibitor (PAI-1) (Podor et al., 2000), while its deficiency has been associated with increased wound fibrinolysis and decreased microvascular angiogenesis in animal models (Jang, Tsou, Gibran and Isik, 2000). Fibrin gels used in surgical settings (i.e. fibrin glue) require the addition of aprotinin to slow down its degradation (Thompson, Letassy and Thompson, 1988). This bovine protein has been associated with serious allergic reactions, especially in the case of repeated exposure (Scheule et al., 1998; Beierlein et al., 2000). Therefore, the use of hPLG as an alternative to fibrin glue in certain clinical procedures has the potential to dispense with the use of aprotinin, as vitronectin should produce the same effect without any adverse effects.

We focused on the use of hPLG for culture and vascular network formation by ECFCs. The standard isolation protocol for ECFCs initially developed by Ingram *et al.* (2004) requires the coating of wells with collagen I from rat-tail to increase the adhesion and proliferation of these cells. The use of rat collagen or other animal products raises safety issues and hinders clinical applications of these cells. As mentioned above, in addition to the high GF content, hPLG contains high amounts of ECM proteins, which facilitate integrin interactions and result in higher cell adhesion and proliferation, while avoiding the use of animal proteins. Culture of ECFCs on hPLG did not lead to significant changes in morphology or expression of endothelial markers when compared to the traditional collagen I coating. On both substrates, ECFCs organized into a monolayer with cobblestone morphology with CD31 localized at the tight intercellular junctions, as well as vWF pinpointing Weibel–Palade bodies, typical of functional endothelial cells (Figure 4.4). The preservation of their structure and function was further confirmed by the unchanged gene expression of VE-cad, which plays an essential role in the maintenance of a restrictive endothelial barrier, and eNOS, which is involved in the regulation of vascular tone and platelet aggregation (Figure 4.5).

Despite this, hPLG greatly increased the proliferation rate of ECFCs when compared to the standard collagen I (Figure 4.6). This effect appeared to be correlated with the simultaneous activation of EGFR, FGFR, VEGFR-2 and PDGFR-β, since the multiple inhibition of these receptors decreased cell growth to the same extent as single VEGFR-2 inhibition. As reviewed by Mazzucco *et al.*, it is known that the two main downstream targets shared by all of these receptors are ERK and PI3K (Mazzucco, Borzini and Gope, 2010). Accordingly, the prolonged activation of ERK1/2 pathway was observed in ECFCs cultured on hPLG (Figure 4.7), yet the inhibition of VEGF signalling did not decrease ERK phosphorylation on its own (Figure 4.8). This is probably due to the synergistic effect of the different GFs on ERK activation and the enhanced integrin binding on hPLG's ECM, which further stimulates this mechanism (Wang and Milner, 2006). As observed in our study, the phosphorylation of ERK1/2 proteins is often linked to cell proliferation but, in fact, its end result cannot be dissociated from the effect of the simultaneously activated PI3K pathway on cell migration (Graupera et al., 2008; Huang and Sheibani, 2008; Lai et al., 2011), protein synthesis (Viñals, Chambard and Pouysségur, 1999) and inhibition of apoptosis (Gerber et al., 1998; Dai, Zheng and Fu, 2008). Therefore, it is plausible that although VEGFR-2 is not solely responsible for increased ERK phosphorylation, by acting as a biological checkpoint for endothelial cell survival via PI3K (Zhuang et al., 2013; Fujio and Walsh, 1999), its complete inhibition can have such a dramatic effect on proliferation. In agreement, even on collagen, the inhibition of VEGFR-2 completely halted any degree of proliferation. On the other hand, inhibition of ERK1/2 decreased cell proliferation only partially when compared to blocking of VEGFR-2, further demonstrating the multiple pathways through which this receptor can have an effect on cell growth. Likewise, inhibition of the SDF-1/CXCR4 axis, which is known for playing a role in migration and cell survival (Zheng et al., 2008; Pi et al., 2009; Mirshahi et al., 2000; Yun and Jo, 2003), resulted in a partial decrease in proliferation. Additionally, the superior proliferation observed on hPLG vs collagen I is not simply due to its content in GFs but can also be explained by the interplay between these and ECM, integrins and respective GF receptors. The presentation of an ECM-bound GF generates a protracted signalling on the target cell, when compared to a liquid-phase GF, by delaying GF receptor internalization (Kang et al., 2011; Swindle et al., 2001; Cybulsky, McTavish and Cyr, 1994). Also, the proximity of GF-binding domains and integrin-binding sites in ECM proteins facilitates the formation of focal adhesion complexes and regulates the activity of associated GF receptors (Zhu and Clark, 2014; Kim, Turnbull and Guimond, 2011). For example, VEGF signalling in endothelial cells is impaired

when the binding of αvβ3 integrin to RGD motifs in vitronectin is blocked (Montenegro et al., 2012) and angiogenesis regulated by FGF-2 is dependent on binding of integrin α5β1 to fibronectin (Kim, Bell, Mousa and Varner, 2000).

Interestingly, for the first time a coordinated upregulation of a set of genes involved in angiogenesis by endothelial cells was reported in response to a platelet-derived biomaterial (Figure 4.5). The expression of both VEGFR-2 and PDGFR-β by ECFCs was in fact significantly upregulated on hPLG after 24 h, which suggests increased sensitivity to VEGF and PDGF by ECFCs in these culture conditions. One plausible hypothesis is that the binding of a set of integrins to fibrin and other ECM proteins in hPLG may initiate a cascade of events that lead to an increase in the transcription levels of these receptors. Indeed, it is known, for example, that the attachment to RGD motifs via αvβ3 and α5β1 integrins is required for endothelial cell morphogenesis in fibrin matrices (Bayless, Salazar and Davis, 2000). In addition, the expression of the secretable molecules SDF-1 and angiogenin was also significantly upregulated at the same time point. The first is known to stimulate the recruitment of pro-angiogenic hematopoietic cells (Ascione et al., 2015) as well as the migration of endothelial cells (Zheng, Fu, Dai and Huang, 2007; Mai et al., 2014; Pi et al., 2009) which might explain the decrease in ECFC proliferation when its receptor CXCR4 is inhibited. Although SDF-1 is already present in hPLG (Rafii et al., 2015), it appears to be further produced by ECFCs, likely also promoting proliferation in an autocrine manner. Finally, angiogenin is a ribonuclease essential for focal adhesion formation (Wei et al., 2011) and plasmin generation (Hu and Riordan, 1993), but perhaps more important in this context is its role in inhibition of apoptosis (Li, Yu and Hu, 2012; Li, Yu, Kishikawa and Hu, 2010) and cell proliferation induced by other growth factors, namely VEGF, EGF and FGF (Kishimoto et al., 2005). Additionally, it has been reported that angiogenin can lead to ERK1/2 phosphorylation in endothelial cells on its own (Liu et al., 2001), contributing to the prolonged activation of this kinase observed in our study. Taken together, the combined effect of direct receptor activation by synergistic matrix-bound GFs, enhanced integrin binding and crosstalk between these GF receptors in addition to the consequential upregulation of pro-angiogenic genes is likely responsible for the superior proliferation of ECFCs on hPLG.

It was also demonstrated that hPLG can support the formation of a profuse microvascular network by human ECFCs. The 3D network formed *in vitro* was not only far superior to those formed in collagen I and fibrin gels (Figure 4.9), but also exhibited a well-defined lumen generated in a period of just 3 days (Figures 4.11 and 4.12), with

diameter similar to that of native human capillaries (Hansen et al., 2013). As a point of comparison, other groups have reported the formation of networks by HUVECs in collagen/fibrin gels requiring between 7 and 14 days (Peterson et al., 2014). The short time frame of our approach is believed to be optimal for the regeneration of tissues by scaffold implantation, where it is vital to avoid tissue necrosis due to an initial lack of blood supply. Therefore, hPLG is ideally suited for the *in vivo* delivery of ECFCs and possibly of other pro-angiogenic cells. Such a combinatorial approach has the advantage of not requiring the production and delivery of any recombinant GFs, like in other proposed methods (Chu and Wang, 2012; Bai et al., 2013). While the delivery of high amounts of rhVEGF has been extensively attempted to promote *in situ* angiogenesis, it is now known that this leads to aberrant blood vessel formation (Ozawa et al., 2004) and the combined delivery of VEGF and PDGF-BB is necessary to induce normal angiogenesis (Banfi et al., 2012). By using this platelet-derived gel both these GFs, plus others, can be delivered, and more efficiently induce the formation of healthy blood vessels. Interestingly, the inhibition of VEGF receptors did not diminish network formation in our 3D model (Figure 4.10), in contrast to what was seen for 2D proliferation, suggesting that morphogenesis into lumenized structures is not as dependent on VEGF signalling and can still happen due to the variety of GFs in hPLG. Also, due to its properties, the initial cell density needed for the development of a network is on average 10 times less than that previously reported in other vasculogenic approaches (Koh et al., 2008; Allen, Melero-Martin and Bischoff, 2011; Sieminski, Hebbel and Gooch, 2012). In a clinical setting, these aspects greatly improve the feasibility of delivering *ex vivo* expanded ECFCs for regenerative purposes, as less time and resources would be needed to obtain the necessary cells and produce a bioactive scaffold.

Furthermore, the prompt formation of a capillary network by administered cells must be able to anastomose with the host's vasculature at the earliest possible. For this purpose, a scaffold should simultaneously promote the sprouting of existing blood vessels into it, including perivascular cells to stabilize the newly formed network (Aguilera and Brekken, 2014; Stratman and Davis, 2012; Evensen et al., 2009). As PDGF-BB is considered the main driver of pericyte migration and proliferation (Campagnolo et al., 2010; Stratman, Schwindt, Malotte and Davis, 2010; Hellberg, Ostman and Heldin, 2010), hPLG should be particularly efficient at recruiting these cells. In our *ex vivo* model system, hPLG exhibited an unsurpassed angiogenic activity, using the rat aortic ring assay (Figure 4.13). While an angiogenic response only starts

around day 3 in fibrin and collagen I matrices, at the same time point an extensive sprouting network can already be observed in hPLG. While the addition of recombinant GFs is known to improve this response (Aplin and Nicosia, 2015), no equivalent outcome has been reported before in such a short period. In addition, by combining this *ex vivo* assay with the encapsulation of ECFCs, it is believed that the *in vivo* conditions of delivering ECFCs into a tissue using hPLG can be mimicked. Although this assay lacks some of the more dynamic and physiological components (e.g. blood flow), it can accurately depict the timing of formation of the human endothelial network and the concurrent sprouting from vascular tissue sections, as well as the interactions between the two. In this regard, due to the swiftness of sprout formation and despite the xenogeneic nature of the assay, an initial association between both can already be observed after 3 days (Figure 4.14). Considering the gelling properties of this biomaterial, these preliminary findings demonstrate its potential for a wide range of applications, such as cell-sheet technologies for skin regeneration or as an injectable cell carrier for bone tissue engineering, where a swift vascular connection is essential.

### 4.6. Conclusions

In conclusion, it was shown that hPLG can support the formation of *in vitro* endothelial networks by ECFCs and strongly promotes the proliferation of these cells by upregulating several angiogenic genes. Vitally, it was also shown that hPLG has the ability to promote sprouting of existing vessels and the subsequent formation of cellular bridges with the ECFC-generated vascular network. Current tissue engineering and regenerative medicine strategies are severely hampered by poor integration of implanted scaffolds and tissues with the host vasculature (Novosel, Kleinhans and Kluger, 2011). The use of hPLG as a combined scaffold and cell delivery vehicle has the potential to overcome this barrier. Thus, we propose the use of hPLG as a human-derived method for the expansion and delivery of endothelial progenitors to promote tissue revascularization for therapeutic purposes.

# Chapter 5: Combination of surface-treated electrospun scaffolds and ECFCs for tissue engineering

## 5.1. Background

The swift and effective endothelisation of grafts has been suggested as a possible method of preventing the thrombogenic and fibrotic response seen in earlier synthetic scaffolds for vascular replacement (Sato, Abdel-Wahab and Richardt, 2015; Sreerekha and Krishnan, 2006). Endothelial cells are known for their role inhibiting platelet aggregation and activation of immune cells, thus facilitating the continuous flow of blood. Being easily obtained, ECFCs constitute a suitable source of autologous cells for this purpose (Fioretta et al., 2012). As demonstrated in the previous chapter or shown by others, platelet lysate in its gel form (i.e. hPLG) or as culture supplement (Reinisch et al., 2009) strongly promotes ECFC proliferation while avoiding the use of animal proteins. To impart these properties onto artificial scaffolds for vascular tissue engineering, the decision was taken to develop a method of adsorbing the different components of hPL onto electrospun scaffolds.

Electrospinning was first developed as a way of generating relatively flat 3D matrices of synthetic fibres with diameters that could not be manufactured by other methods (Tucker et al., 2012). Briefly, a polymer is dissolved in a volatile solvent (usually an organic solvent or an acid) and is then slowly extruded from a syringe at the same time as a high voltage current is applied. Instead of giving rise to droplets, extremely fine fibres are continuously produced and collected on a conductive metallic surface with a desired shape. The architecture of these fibres mimics the fibrillar nature of the extracellular matrix, allowing for its use as a scaffold for cell growth (Kai, Liow and Loh, 2014; Braghirolli, Steffens and Pranke, 2014). In recent years, this technique has been also adopted for the development of scaffolds with a tubular shape, with different approaches being pursued, such as the use of synthetic and natural polymers, the engraftment of different moieties to promote vascularization or the incorporation of antithrombotic drugs (Ercolani, Del Gaudio and Bianco, 2013).

The polymers chosen for this study, polylactic-co-glycolic acid (PLGA) and polycaprolactone (PCL), are two synthetic, FDA-approved, biodegradable polymers of relatively low-cost that have been extensively used in the biomedical field for both tissue engineering and drug delivery (Martina and Hutmacher, 2006). Their biocompatibility is mainly due to their degradation mechanisms, which confers them low cytotoxicity. PLGA is degraded relatively quickly (a few days to months) by hydrolysis into its original monomers, lactic acid and glycolic acid, which are common by-products of various metabolic pathways, hence can be easily dealt by the body (Makadia and Siegel, 2011). On the other hand, PCL takes considerably longer to be

degraded (up to a few years), being slowly broken into smaller MW fragments followed by hydrolysis. During this process it is completely secreted via the kidneys and is not accumulated in any tissues (Sun et al., 2006).

Nevertheless, these two polymers share a common drawback with many of the synthetic polymers used in tissue engineering – an inherently very hydrophobic profile (Martina and Hutmacher, 2006). This feature hinders cell adhesion and proliferation on their surface, as cells usually respond better to hydrophilic surfaces (van Wachem et al., 1985). Additionally, synthetic polymers lack integrin-binding sites, such as RGD repeats, hence cell adhesion to these materials relies mostly on an interfacial protein layer being established (Wilson, Clegg, Leavesley and Pearcy, 2005; Duque Sánchez et al., 2016). However, in line with their poor wettability, a number of these synthetic polymers are also characterized by a weak ability to adsorb proteins. With the aim of improving both of these traits, many research groups have turned to chemical plasma treatment in order to modify the surface of these polymers without compromising their inner structure and physical properties (Jokinen, Suvanto and Franssila, 2012). This treatment is based on the ionisation of a low-pressure gas by an oscillating electric field, creating radicals that interact with the surface of the polymer (Aziz, De Geyter and Morent, 2015). While the most common surface modification is the introduction of functional groups, it can also be used to alter its roughness, induce crosslinking or deposit polymer coatings (Poncin-Epaillard and Legeay, 2003). As a result of the increased wettability and surface polarity (Duque Sánchez et al., 2016), several cases of increased cell adhesion, proliferation and differentiation into a number of target phenotypes have been reported (Sankar et al., 2014; Uppanan et al., 2015), including endothelial (Ramires et al., 2000; De et al., 2005).

Many of these studies have employed rather expensive or dangerous gases, such as oxygen, hydrogen or acetylene (Yan et al., 2013; Girard-Lauriault et al., 2009), which grant less control over the simultaneous etching of the material's surface than less reactive gases (Huang and Weigand, 2008). However, in this work the use of safer nitrogen gas plasma is proposed for the improvement of surface properties of PLGA/PCL blended scaffolds. By improving the ability of the electrospun fibres to be coated with hPL proteins, their biocompatibility towards ECFCs should be greatly improved due to the interfacial bridge that is created.

## 5.2. Aims & Objectives

An important endeavour of investigation in vascular tissue engineering is the development of artificial vascular grafts. Considering that electrospinning of synthetic polymers is one of the preferred methods of scaffold fabrication for this purpose, new methods that can increase the adhesion and proliferation of endothelial progenitors onto these substrates are obviously of great interest to the field. In the previous chapter, the potent effect of hPLG on ECFC proliferation was demonstrated. Therefore, the decision was taken to explore a method to improve hPL absorption to electrospun fibre-based scaffolds. This approach could potentially become usable for the manufacture of polymers with improved ability to stimulate endothelial cell adhesion and growth and the generation of artificial vascular grafts with superior patency.

The work is this section of the project was therefore divided into the following objectives:

- Design and test a new method for the fabrication of tubular scaffolds by electrospinning.
- Investigate the structure and morphology of electrospun scaffolds produced from different PLGA/PCL blends.
- Analyse the effect of $N_2$ gas plasma treatment on the surface properties of these scaffolds, including topography, chemical nature, wettability and adsorption of hPL proteins.
- Assess the effect on ECFC proliferation onto these scaffolds as a result of the plasma treatment and incubation in hPL.
- Examine the morphology and cellular organization of ECFCs on the different scaffolds.

## 5.3. Results

### 5.3.1. Characterisation of electrospun scaffolds

Tubular scaffolds were produced using a novel method, as described in chapter 2.4. Briefly, PLGA and PCL were blended together in three different ratios in an organic solvent mixture and electrospun into an ethanol (non-solvent) bath. Individual fibres coalesced soon after wetting in ethanol, giving rise to bundles of polymer fibres, which were collected by winding onto a rotating tubular Teflon mould. The ethanol was then eluted from the scaffolds allowing the maintenance of the cylindrical shape, which is necessary for the generation of bioengineered vascular grafts (Figure 5.1A). Considering the scope of this study, scaffolds with a rather wide diameter (1 cm) were produced in order that relatively flat samples of the tube walls could be obtained for subsequent experiments (e.g. cell staining).

For the assessment of fibre morphology, samples of each scaffold were examined by SEM and analysed regarding fibre diameter using ImageJ software (Figure 5.1B). At lower magnification, it is sometimes possible to observe the juxtaposition or overlap of the fibres bundles (top row) with little degree of alignment of individual fibres (bottom row). Fibre diameter increased with increasing concentration of PCL relative to PLGA, with an average size of 0.87±0.03 µm for PLGA 75:25 PCL, 1.25±0.02 µm for PLGA 50:50 PCL and 2.80±0.05 µm for PLGA 25:75 PCL (Figure 5.2). This last mixture ratio was also characterized for having the larger spread in this parameter, with a standard deviation approximately double of the other blends (Figure 5.2).

**A**

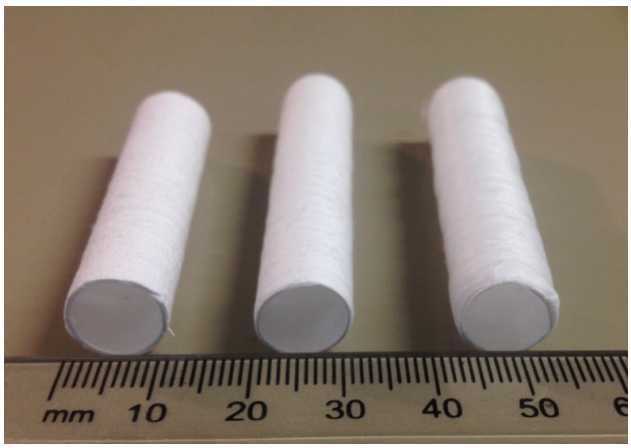


**B**

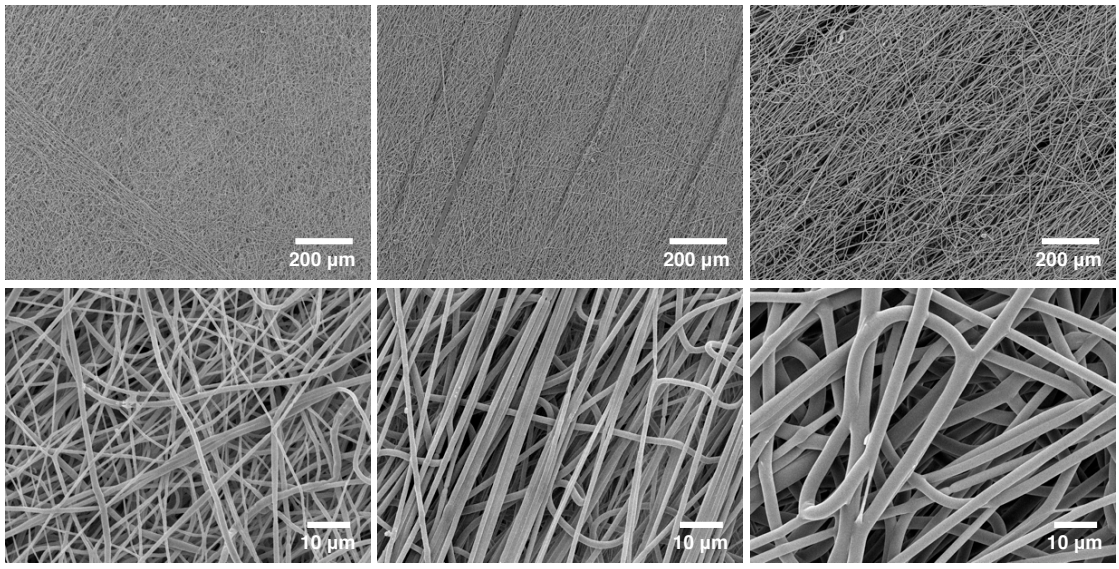


**Figure 5.1. Macro- and microscopic imaging of electrospun scaffolds.** (**A**) Tubular scaffolds were produced by electrospinning from PLGA 75:25 PCL, PLGA 50:50 PCL and PLGA 25:75 PCL polymer blends (left to right). (**B**) Fibre morphology was evaluated by SEM at 100x (top) and 1,500x (bottom) magnification.

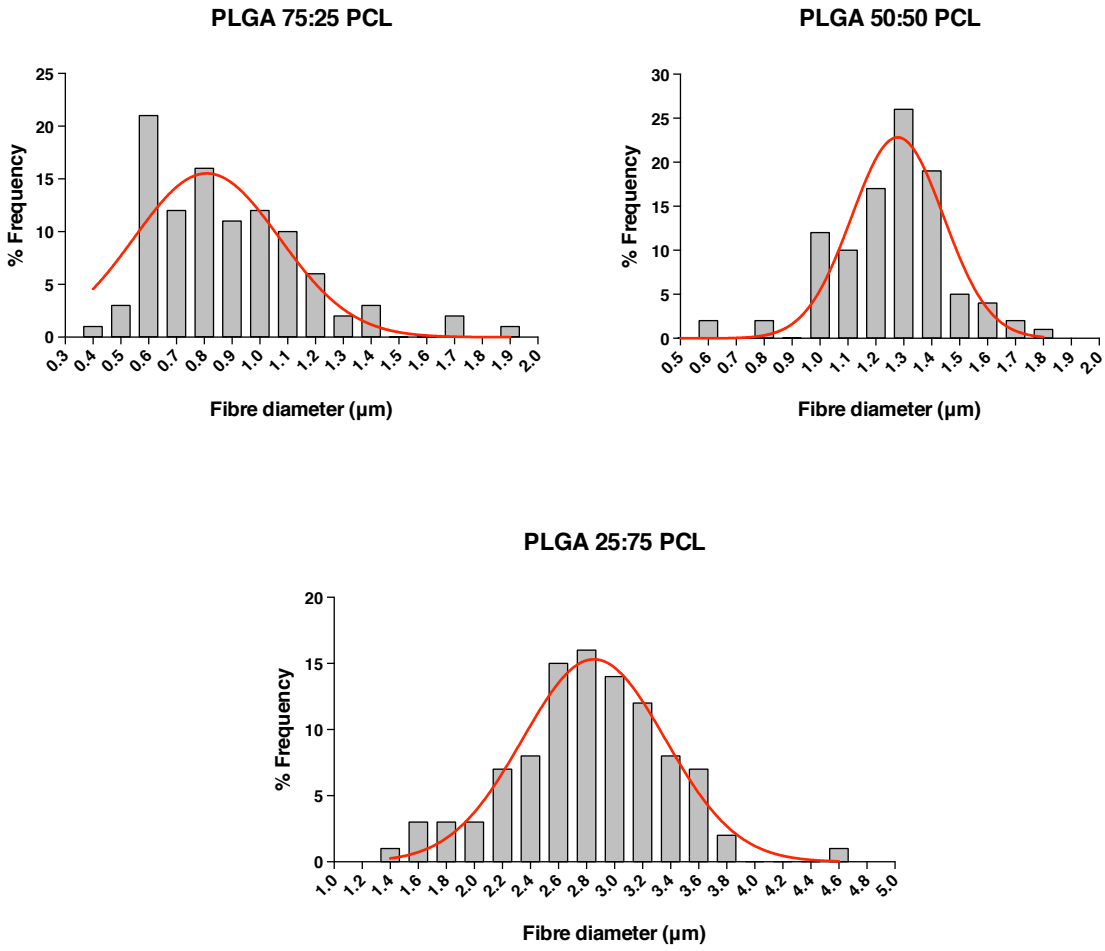


**Figure 5.2. Fibre size distribution.** Diameter of individual fibres from the three different PLGA/PCL blends was manually measured using ImageJ from SEM images at 1,500x and 3,000x magnification (100 fibres per sample).

### 5.3.2. Effect of plasma treatment on surface properties of electrospun scaffolds

PLGA and PCL are naturally hydrophobic polymers and characterized by a limited ability to adsorb proteins on their surface, which consequently hinders cell adhesion and growth (van Wachem et al., 1985). In an attempt to increase both the hydrophilicity and protein adsorption of the scaffolds in this study, they were treated with $N_2$ gas plasma. In theory, this procedure should render the surface of each fibre rich in nitrogen-based groups (e.g. amines), without affecting the bulk of the polymer so that inherent physicochemical and mechanical properties are preserved (Sanchis et al., 2008).

SEM was used to compare the morphology and texture between untreated and plasma-treated (60 s) scaffolds. As expected, no obvious differences were observed between the two conditions within the resolution permitted by the SEM equipment and defined by the grain size of the conductive gold layer (Figure 5.3A). Most importantly, plasma treatment with $N_2$ gas did not result in any evident surface etching, as is often common when other gases are employed (Hirotsu, Nakayama and Tsujisaka, 2002; Tsujisaka, Masuda and Nakayama, 2000).

Subsequently, scaffold samples were plasma-treated for increasingly longer periods (up to 120 s) and analysed by Fourier transform infrared spectroscopy (FTIR). This technique is based on the interaction of an oscillating electromagnetic field with molecules in the sample. A particular structural group reveals infrared absorption bands within characteristic regions on the spectrum. Therefore, it provides information on the nature of functional groups with a depth penetration of up to several microns (Kazarian and Chan, 2006). Although the formation of groups such as primary amines (usually detected above 3,000 $cm^{-1}$) was expected, we could not observe any traces of this even at the longest treatment times (120 s, Figure 5.3B). This suggests that the plasma treatment may have only marginal effects polymer chemistry or that the changes are limited to the superficial layers of the polymer fibres (i.e. nanometre range).

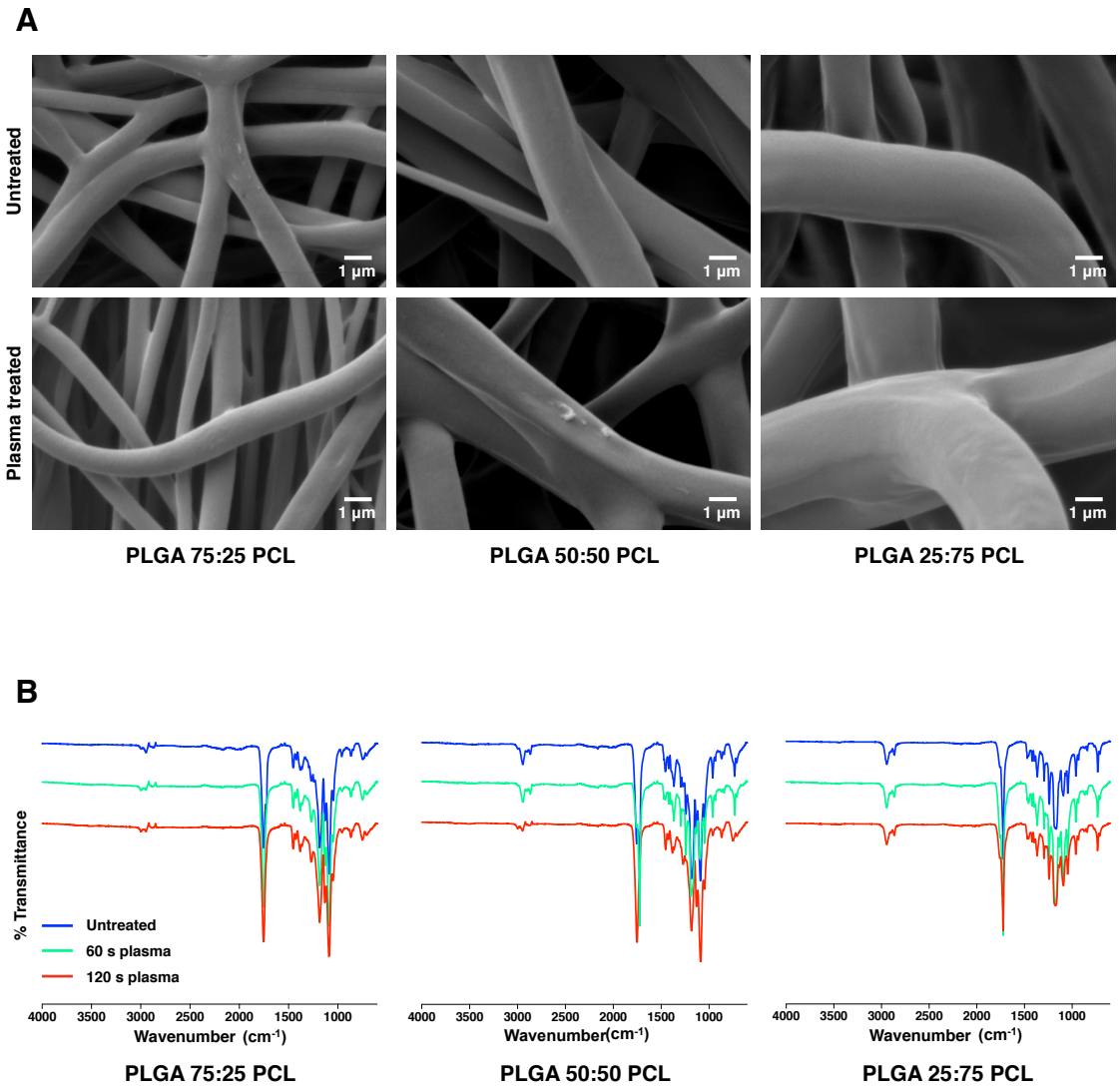


**Figure 5.3. Coarse surface examination of plasma-treated scaffolds by SEM and FTIR.** Electrospun scaffolds were surface treated with $N_2$ gas plasma for up to 120 s. Changes to the surface texture of polymer fibres due to the plasma treatment were evaluated by SEM at 10,000x magnification (**A**). Surface chemical group functionalization was analysed by FTIR (**B**). No differences were detected with either technique.

In order to analyse the surface chemistry of the scaffolds, samples of scaffolds treated for the maximum duration (120 s) were analysed by X-Ray Photoelectron Spectroscopy (XPS). When using this technique, samples are irradiated with a beam of X-rays, while the kinetic energy and electrons that are emitted from the superficial layers of the sample (i.e. 1-10 nm) is measured, producing a photoelectron spectrum. Figure 5.4 shows that the incorporation of nitrogen atoms is dependent on the amount of PLGA in the scaffolds. Survey spectra are characterized by two pronounced peaks at 531 eV and 285 eV, corresponding to the oxygen and carbon elements of PLGA and PCL chains (Figure 5.4A). Following plasma treatment, a nitrogen peak at 400 eV can be detected in the spectrum of PLGA 75:25 PCL and, to a smaller degree, in that of PLGA 50:50 PCL. For PLGA 75:25 PCL scaffolds, a high-resolution spectrum of $N_{1s}$ more clearly demonstrates the characteristic peak arising from the incorporation of nitrogen (Figure 5.4B). Deconvolution of this peak further reveals two narrower peaks at 399.9 eV and 401.6 eV, which are likely due to the formation of N-H and C-N bonds, respectively (Figure 5.4C). Quantification of the constituent elements shows a relevant increase in the percentage of nitrogen as a result of plasma treatment, especially in the case of PLGA 75:25 PCL scaffolds, while none could be detected in PLGA 25:75 PCL (Table 5.1). Interestingly, the carbon content was reduced in all plasma-treated scaffolds compared to the untreated ones, accompanied by an increase in the oxygen content. This indicates that treated scaffolds reacted with oxygen in the atmosphere, becoming oxidized. Furthermore, $O_{1s}$ spectra suggest that the oxygen moieties were likely to be incorporated through the formation of C=O bonds, as seen by the proportionally bigger peak at 531.2 eV relative to the C-O peak at 533.5 eV (Figure 5.5).

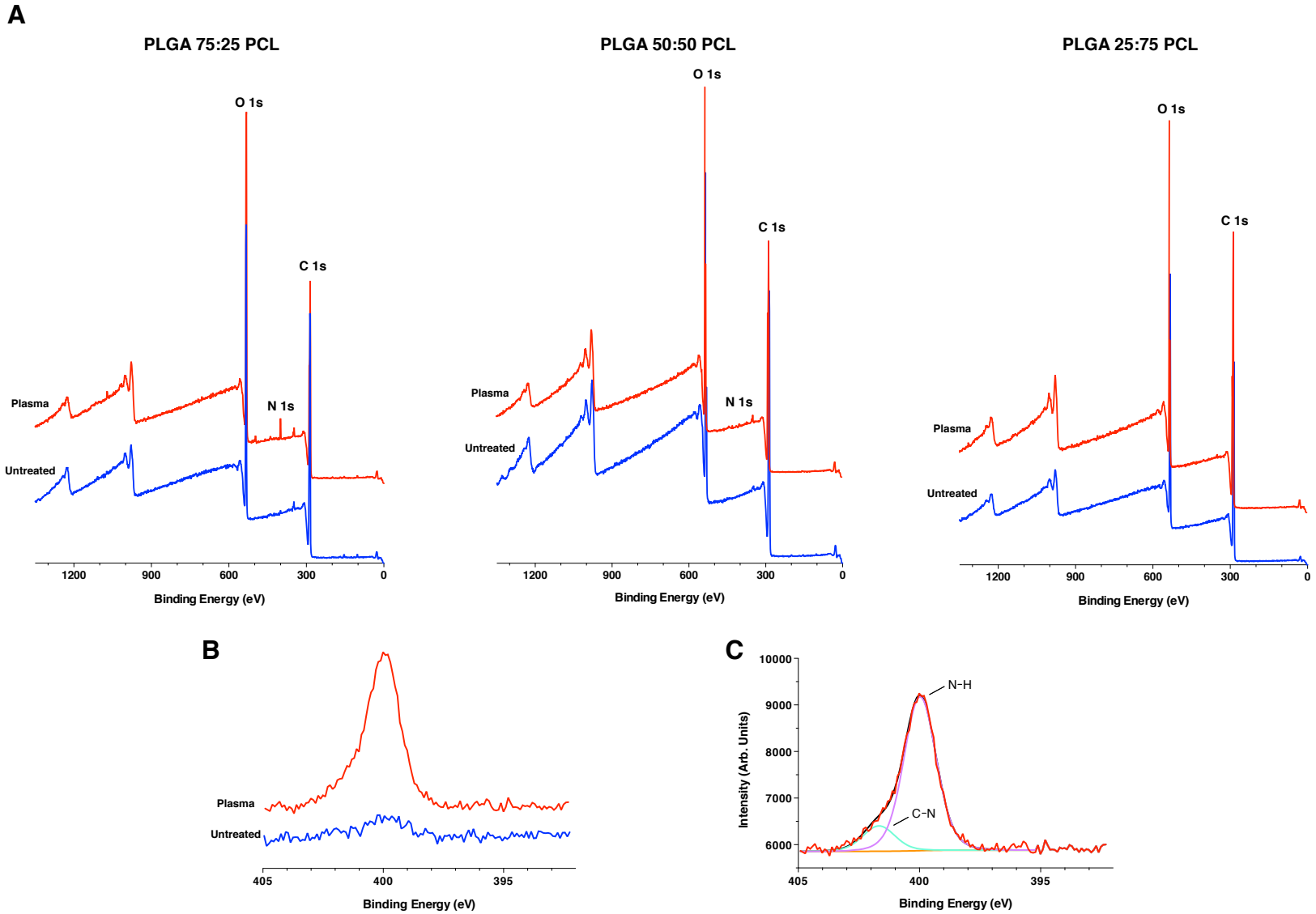


**Figure 5.4. XPS analysis of untreated and $N_2$ plasma-treated scaffolds.** (**A**) XPS survey spectra of untreated (blue) and $N_2$ gas plasma-treated (red) scaffolds. (**B**) $N_{1s}$ scan of PLGA 75:25 PCL scaffolds and (**C**) deconvoluted spectrum of plasma-treated PLGA 75:25 PCL.

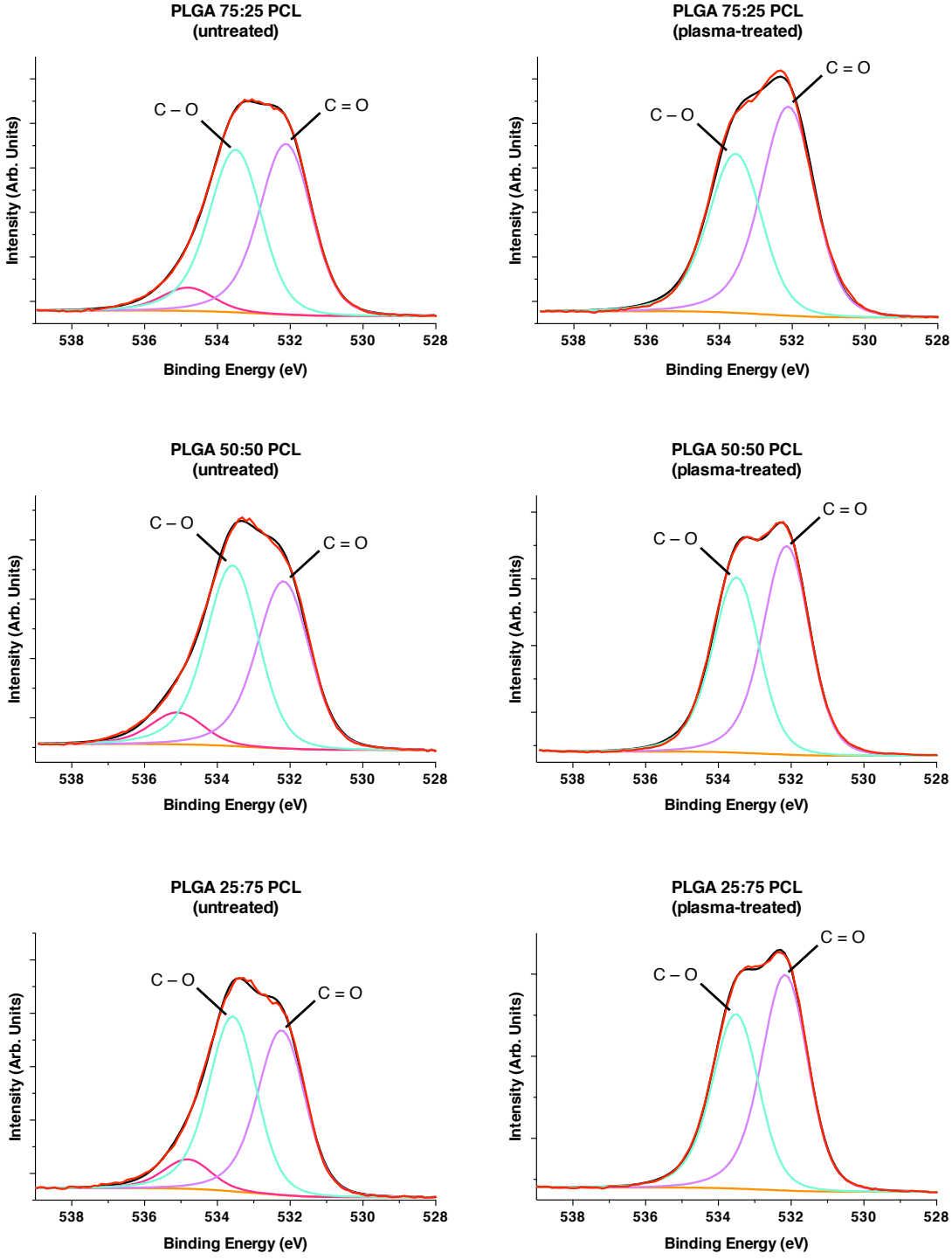


**Figure 5.5. High-resolution XPS analysis of oxygen spectra of untreated and $N_2$ plasma-treated scaffolds.** $O_{1s}$ deconvoluted spectra of the different untreated (left) and plasma-treated (right) scaffolds.

***Table 5.1.*** *XPS quantification of elemental composition of scaffolds before and after plasma treatment.*

| | | C | O | N |
|---|---|---|---|---|
| *PLGA 75:25 PCL* | Untreated | 71.47 | 27.23 | 0.24 |
| | Plasma | 64.22 | 32.37 | 2.24 |
| *PLGA 50:50 PCL* | Untreated | 66.30 | 33.28 | * |
| | Plasma | 64.02 | 35.50 | 0.19 |
| *PLGA 25:75 PCL* | Untreated | 72.12 | 27.88 | * |
| | Plasma | 68.08 | 31.84 | * |

Wettability of the scaffolds was then characterized as a function of the duration of plasma treatment. Samples of the different PLGA/PCL blend scaffolds were left untreated or treated for either 30 s, 60 s or 120 s and water contact angle analysis was performed using a semi-automated system (see chapter 2.15). A drop of distilled water was dispensed onto each sample and recorded over a period of 60 s (Figure 5.6). The contact angle was then measured using the proprietary software. If the contact angle was smaller than 90º, the surface was considered hydrophilic, and hydrophobic if larger than 90º (Sanchis et al., 2008). All untreated scaffolds were found to be very hydrophobic, with initial contact angles above 120º and no droplets were absorbed by the matrices within the recorded period (Tables 5.2-5.4). Plasma treatment reduced contact angles more strongly with increasing PLGA content in the scaffolds, with PLGA 72:25 PCL being the only scaffold type that became hydrophilic at all treatment durations tested. This suggests that PLGA is more sensitive to plasma treatment than PCL. Of relevance, treatment for 60 s was enough to efficiently reverse the hydrophobicity of all scaffolds and led to droplet absorption within 1 min.

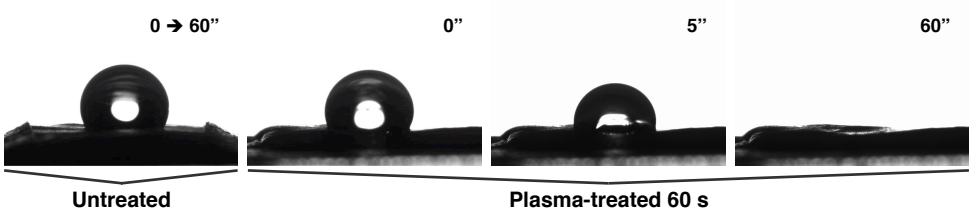


**Figure 5.6. Water contact angles of untreated and plasma-treated scaffolds as a function of time.** Wetting of electrospun scaffolds over the period of 1 min was assessed using a semi-automated contact angle analysis system as described in chapter 2.15. Plasma treatment reduces scaffold hydrophobicity as shown for PLGA 50:50 PCL (60 s treatment) and water droplet is no longer repelled.

***Table 5.2.*** *Water contact angles of untreated and plasma-treated PLGA 75:25 PCL scaffolds.*

| | PLGA 75:25 PCL | | | |
|---|---|---|---|---|
| | **Untreated** | **Plasma 30 s** | **Plasma 60 s** | **Plasma 120 s** |
| 0” | 128.9 ± 2.0 | 110.0 ± 2.3 | 104.2 ± 4.5 | 84.9 ± 24.9 |
| 5” | 128.5 ± 1.7 | 99.2 ± 6.5 | 35.0 ± 0.8 | * |
| 10” | 128.4 ± 1.7 | 59.1 ± 23.6 | * | * |
| 20” | 128.4 ± 1.7 | * | * | * |
| 40” | 128.2 ± 1.7 | * | * | * |
| 60” | 128.2 ± 1.7 | * | * | * |

* Absorbed

***Table 5.3.*** *Water contact angles of untreated and plasma-treated PLGA 50:50 PCL scaffolds.*

| | PLGA 50:50 PCL | | | |
|---|---|---|---|---|
| | **Untreated** | **Plasma 30 s** | **Plasma 60 s** | **Plasma 120 s** |
| 0” | 123.0 ± 1.4 | 101.7 ± 3.9 | 118.2 ± 1.6 | 97.9 ± 2.0 |
| 5” | 121.6 ± 0.8 | 102.1 ± 3.5 | 98.1 ± 3.0 | * |
| 10” | 120.9 ± 1.5 | 102.1 ± 3.5 | * | * |
| 20” | 120.8 ± 1.5 | 101.9 ± 3.5 | * | * |
| 40” | 121.5 ± 0.9 | 101.7 ± 3.5 | * | * |
| 60” | 120.6 ± 1.6 | 101.4 ± 3.6 | * | * |

* Absorbed

***Table 5.4.*** *Water contact angles of untreated and plasma-treated PLGA 25:75 PCL scaffolds.*

| | PLGA 25:75 PCL | | | |
|---|---|---|---|---|
| | **Untreated** | **Plasma 30 s** | **Plasma 60 s** | **Plasma 120 s** |
| 0” | 125.8 ± 4.2 | 128.2 ± 0.9 | 117.1 ± 1.1 | * |
| 5” | 125.0 ± 4.6 | 128.3 ± 0.8 | 111.6 ± 2.8 | * |
| 10” | 124.9 ± 4.5 | 128.2 ± 0.8 | 106.8 ± 3.1 | * |
| 20” | 124.8 ± 4.5 | 127.9 ± 0.9 | 53.8 ± 28.0 | * |
| 40” | 124.7 ± 4.6 | 127.8 ± 0.9 | * | * |
| 60” | 124.6 ± 4.6 | 127.7 ± 0.9 | * | * |

* Absorbed

Next, the effect of plasma treatment on the adsorption of proteins from hPL onto the scaffolds was investigated by protein quantification and spectroscopy. Scaffold samples were treated with $N_2$ gas plasma for 30 s, 60 s or 120 s and incubated in hPL (diluted 1:1 in PBS) for 1 h at room temperature, then washed to remove any unbound protein as described in chapter 2.17. For quantification of protein adsorbed to scaffolds, binding proteins were eluted with RIPA buffer, and total protein was measured using the micro BCA assay. Interestingly, and contrary to the trend observed by contact angle analysis, baseline adsorption was dependent on the ratio of PCL in scaffolds, with untreated PLGA 25:75 PCL adsorbing approximately double the amount of protein of the other untreated polymer blends (Figure 5.7). Plasma treatment for all the tested durations significantly improved protein adsorption onto all scaffolds except for PLGA 25:75 PCL treated for 30 s.

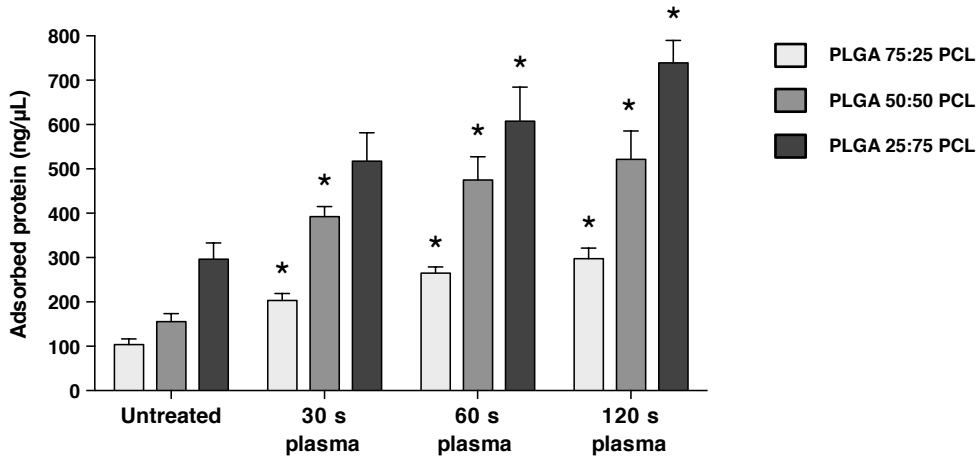


**Figure 5.7. Quantification of hPL protein adsorption by scaffolds.** Scaffolds of the different PLGA/PCL blends were plasma-treated for 30 s, 60 s or 120 s, or left untreated, and incubated with hPL. Protein was eluted from scaffolds and quantified by micro BCA assay. Data are mean ± SEM. Statistical significance was tested by one-way ANOVA with Bonferroni's post-test (* indicates statistical difference against "Untreated") (*=$p<0.05$) (n=3).

Scaffolds treated similarly to the BCA analysis described above (i.e. plasma treatment for 30, 60 and 120 s, followed by hPL incubation) were then freeze-dried after the washing step and examined by FTIR. Additionally, hPL was analysed to provide a reference spectrum. Plasma treatment increased hPL protein adsorption onto all polymer blends proportionally with increasing treatment duration (Figure 5.8). The main absorbance peaks seen in the hPL spectrum (dashed lines) could also be detected in the spectra of all scaffold types incubated with hPL, except for untreated PLGA 75:25 PCL. Such peaks are characteristic of amide groups in proteins and are due to the different stretches in these groups. Wide peaks between 3100 and 3500 $cm^{-1}$ correspond to N-H bonds, while peaks around 2900 $cm^{-1}$ and 1600 $cm^{-1}$ indicate the presence of C-H and C=O bonds, respectively. Amongst the three polymer blends, PLGA 25:75 PCL adsorbed the highest amount of protein prior to plasma treatment but also benefited the most from the plasma treatment.

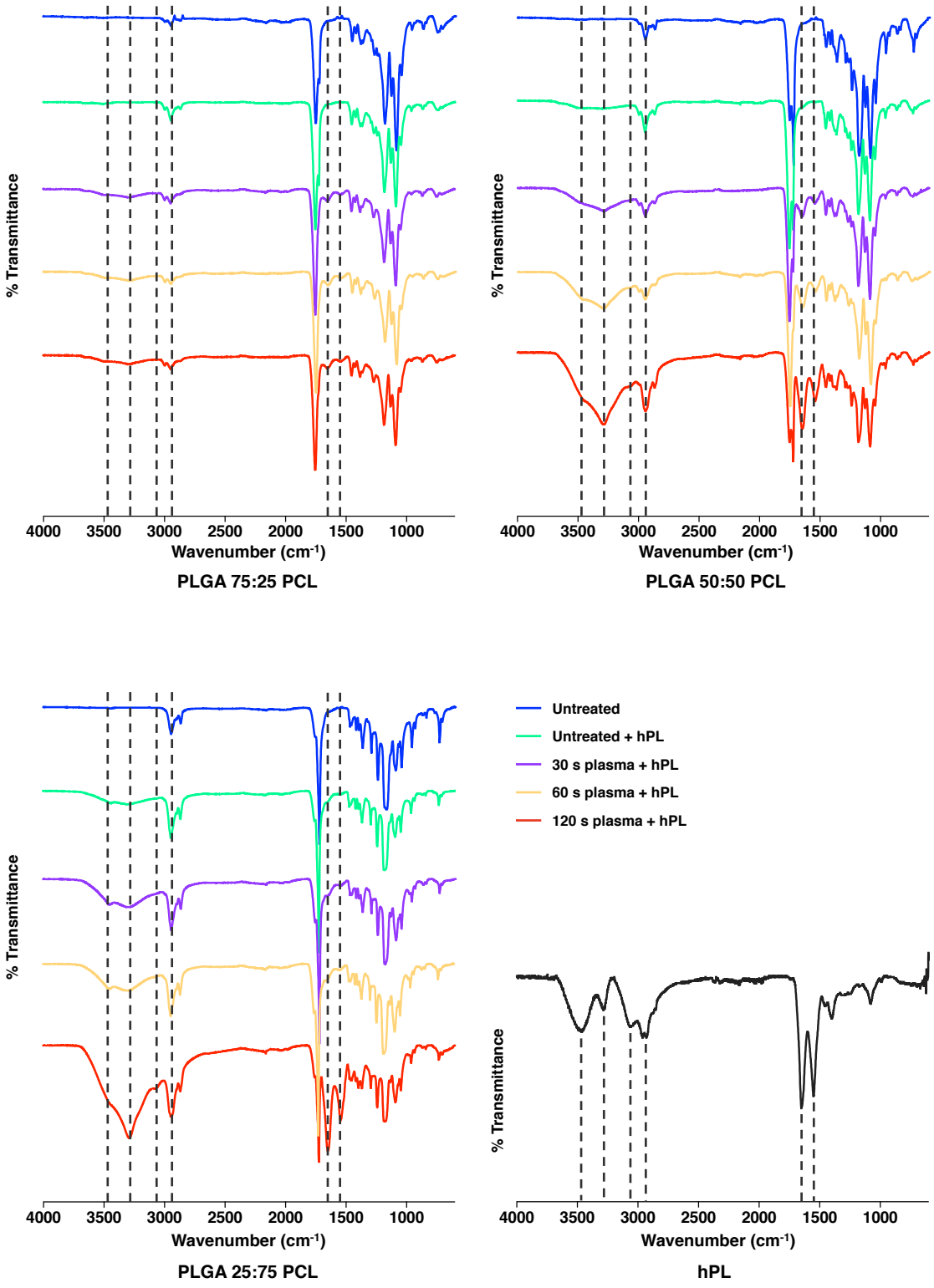


**Figure 5.8. Characterisation of protein adsorption by FTIR.** Scaffolds of the different PLGA/PCL blends were plasma-treated for 30 s, 60 s or 120 s, or left untreated, and incubated with hPL. Spectra were obtained by FTIR on freeze-dried scaffold samples and on liquid hPL. Dashed lines indicate the wavenumber of the main peaks detected in hPL spectrum. Such peaks are characteristic of amide groups in proteins and are due to the different stretches in these groups (between 3100 and 3500 $cm^{-1}$ for N-H, around 2900 $cm^{-1}$ for C-H and around 1600 $cm^{-1}$ for C=O).

### 5.3.3. Adhesion and growth of ECFCs on electrospun PLGA/PCL scaffolds

The increased hydrophilicity and ability to adsorb proteins from hPL conferred by $N_2$ gas plasma treatment was expected to promote the adhesion and proliferation of seeded cells on to electrospun PLGA/PCL scaffolds. To test this hypothesis, scaffold samples of equal sizes were left untreated or plasma-treated and incubated with FBS (acting as a control) or with hPL. Treatment was performed for 60 s as this was shown to be sufficient time to improve the surface properties in an efficient manner and considering that longer treatment periods might impart an excess of surface energy, which might hinder cell proliferation (Kennedy, Washburn, Simon and Amis, 2006).

Proliferation was measured using the metabolic assay of resazurin conversion (i.e. PrestoBlue) at days 1, 3 and 5, returning samples to culture after each time point. Across all polymer blends, plasma treatment led to significantly increased metabolic rates after 1 and 3 days for both FBS- and hPL-incubated scaffolds versus untreated control samples (Figure 5.9A). Although overall metabolic levels had decreased by day 5, in the case of PLGA 25:75 PCL proliferation was still significantly higher in samples treated with $N_2$ gas plasma plus hPL. Additionally, this synergistic combination proved to be more effective than FBS incubation of treated scaffolds at day 3 for the same polymer blend (bottom graph).

At the end of the time course, samples were lyzed and dsDNA was quantified using the PicoGreen assay, as a measure of absolute cell density. The amount of retrieved dsDNA was repeatedly higher for plasma treatment samples with either of the protein solutions, except in the case of PLGA 25:75 PCL (bottom graph), where only hPL incubation produced such an effect (Figure 5.9B).

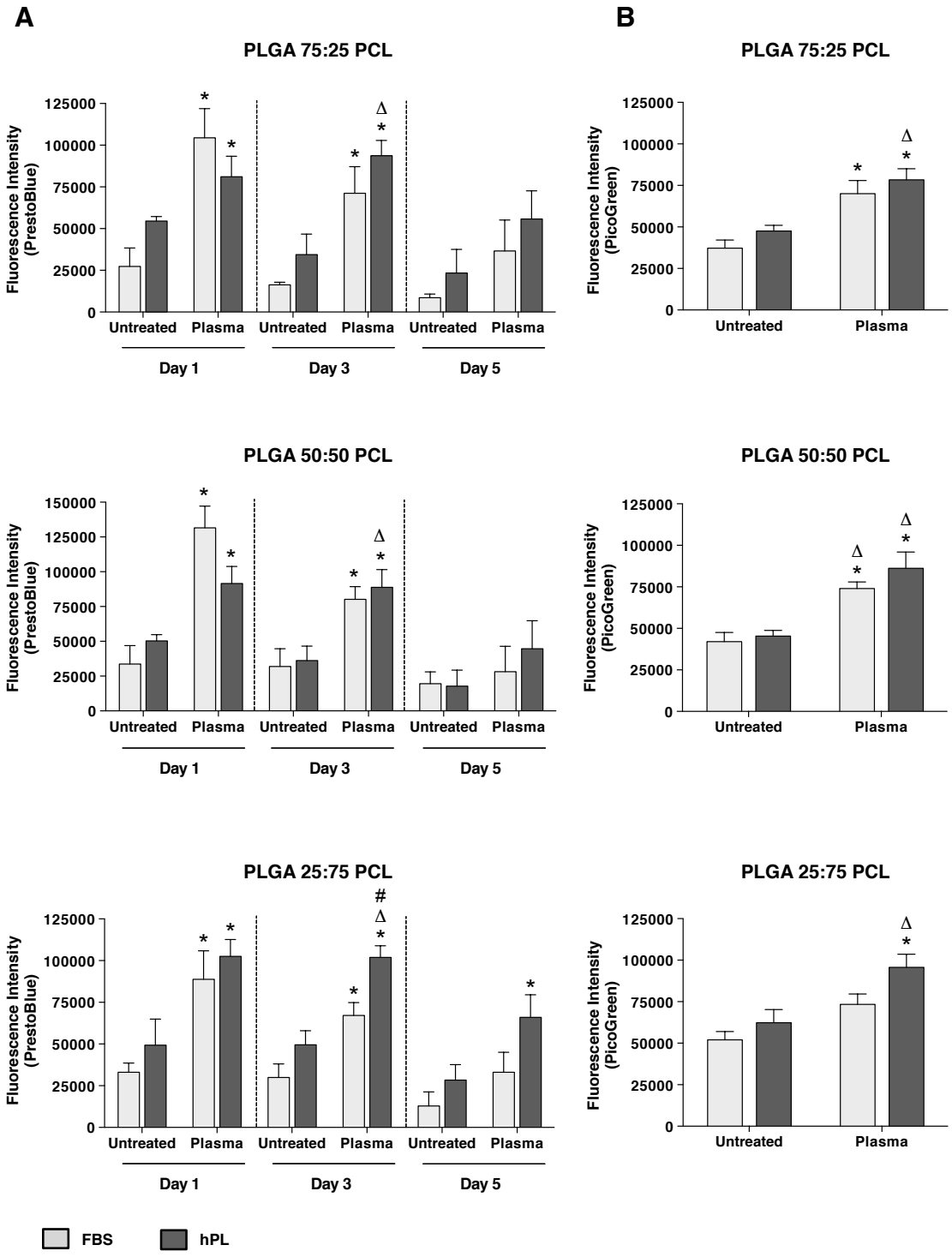


**Figure 5.9. Proliferation of ECFCs on electrospun scaffolds.** Untreated and plasma-treated (60 s) samples of PLGA/PCL scaffolds were incubated with either FBS or hPL for 1 h at room temperature. 7,000 ECFCs were seeded per scaffold and (**A**) metabolic rate was assessed by PrestoBlue assay at 1, 3 and 5 days, (**B**) followed by lysis for quantification of dsDNA amount on each sample using PicoGreen assay. Data are mean ± SEM. Statistical significance was tested using two-way ANOVA with Tukey's post-test. (* indicates statistical difference against "Untreated FBS", Δ against "Untreated hPL" and # against "Plasma FBS") (*=$p<0.05$) (n=4).

To qualitatively assess the viability and coverage of cells on the different scaffolds, constructs were live/dead stained after 5 days of seeding with calcein AM and EthD-III to label healthy cells and necrotic cells, respectively. This demonstrated that scaffolds exposed to hPL or FBS without prior $N_2$ plasma treatment supported a highly viable cell population, but cells were much sparser and less well spread in comparison to plasma-treated scaffolds (Figure 5.10). The latter supported a confluent layer of viable cells, with hPL and FBS being very comparable to one another.

Taken together, these data suggest that treatment of PLGA/PCL electrospun scaffolds with $N_2$ plasma followed by incubation with hPL constitutes a facile method of improving the biocompatibility of these scaffolds for endothelial cell seeding, without the use of animal protein coatings.

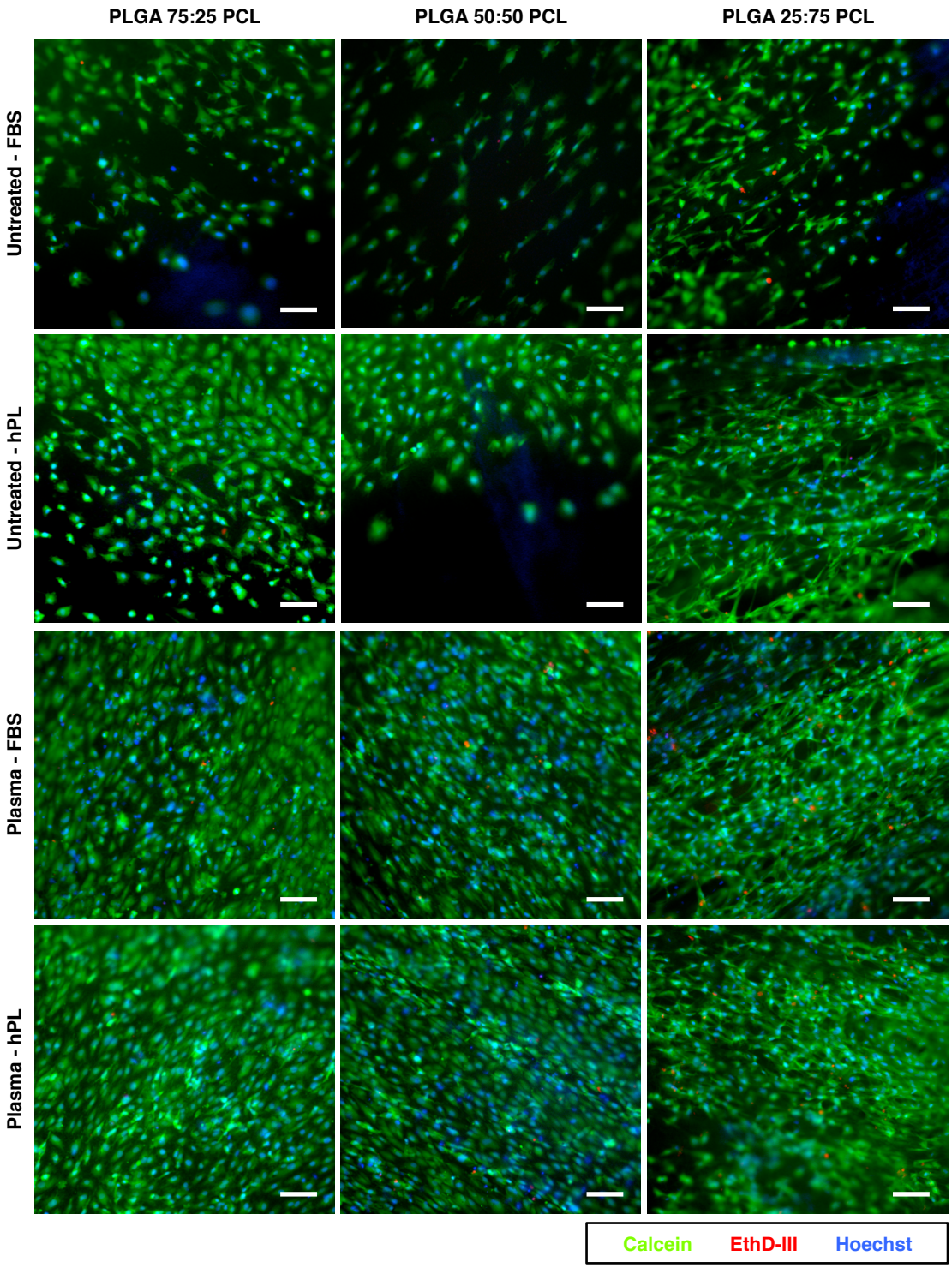


**Figure 5.10. Viability of ECFCs grown on electrospun scaffolds.** Live/Dead assay was used to assess viability and coverage of ECFCs on different scaffolds. Untreated and plasma-treated (60 s) samples of PLGA/PCL scaffolds were incubated with either FBS or hPL for 1 h at room temperature. 7,000 ECFCs were seeded onto each scaffold and after 5 days incubated with Calcein AM/EthD-III to fluorescently label viable and necrotic cells respectively, and with Hoechst 33342 to localize cell nuclei. Images were acquired with a Leica DMI4000B microscope (n=3). Scale bars represent 100 µm.

### 5.3.4. ECFC morphology on plasma-treated scaffolds

In order to mimic the endothelial lining of a blood vessel, a vascular graft should allow the formation of monolayer of tightly packed endothelial cells (i.e. cobblestone morphology) to provide a smooth barrier surface for the flowing blood. The specific fibre size and associated porosity of scaffolds produced using the different PLGA/PCL blends may give origin to distinct three-dimensional cellular arrangements. To determine the morphology and cytoskeletal organization of ECFCs on the different scaffold types, scaffolds were seeded and cultured for 5 days after $N_2$ gas plasma treatment and hPL adsorption. Following fixation, samples were either prepared for SEM analysis or stained with DAPI and phalloidin to respectively label nuclei and the actin cytoskeleton. By SEM, it was possible to observe the formation of a thin ECFC monolayer on both PLGA 75:25 PCL and PLGA 50:50 PCL scaffolds, while on PLGA 25:75 PCL cells were found mostly wrapped around fibres and did not form a continuous endothelial layer (Figure 5.11). During the preparation of samples for SEM, constructs were dried which led to shrinking of the cellular content, revealing where some of the intercellular junctions were located and exposing the fibres underneath (Figure 5.11, top and middle rows). The same pattern was also observed by imaging of fluorescently stained cells (Figure 5.12). On PLGA 75:25 PCL and PLGA 50:50 PCL scaffolds, ECFCs existed in a monolayer with typical endothelial morphology, exhibiting a cytoskeleton mostly organized in close association with intercellular junctions. On PLGA 25:75 PCL (Figure 5.12, bottom row), cells failed to form a continuous barrier and were found deeper inside the scaffolds. Their cytoskeletons displayed a mixed profile, with filamentous actin fibres aligned along the polymer fibres as well as perpendicular to these. These data indicate that PLGA 25:75 PCL scaffolds do not provide enough anchoring points for ECFCs to grow into a monolayer, as they are unable to come in contact with each other to the same extent as in the other polymer blends.

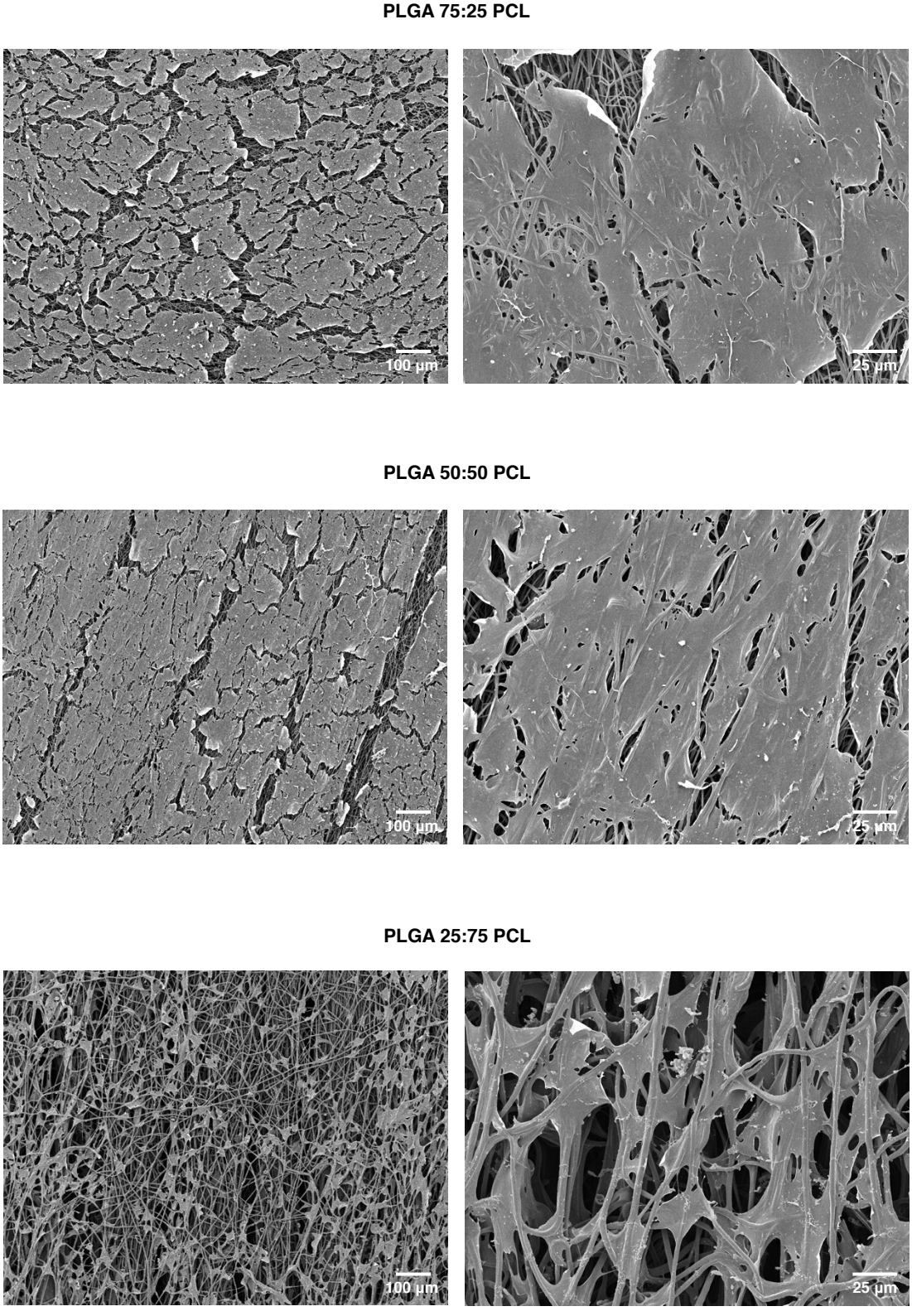


**Figure 5.11. Assessment of ECFC morphology grown on electrospun scaffolds by SEM.** Electrospun scaffolds treated by $N_2$ plasma for 60 s and incubated with hPL were seeded with 7,000 ECFCs and cultured for 5 days. Constructs were fixed and imaged by SEM at 100x (left) and 500x magnification (right).

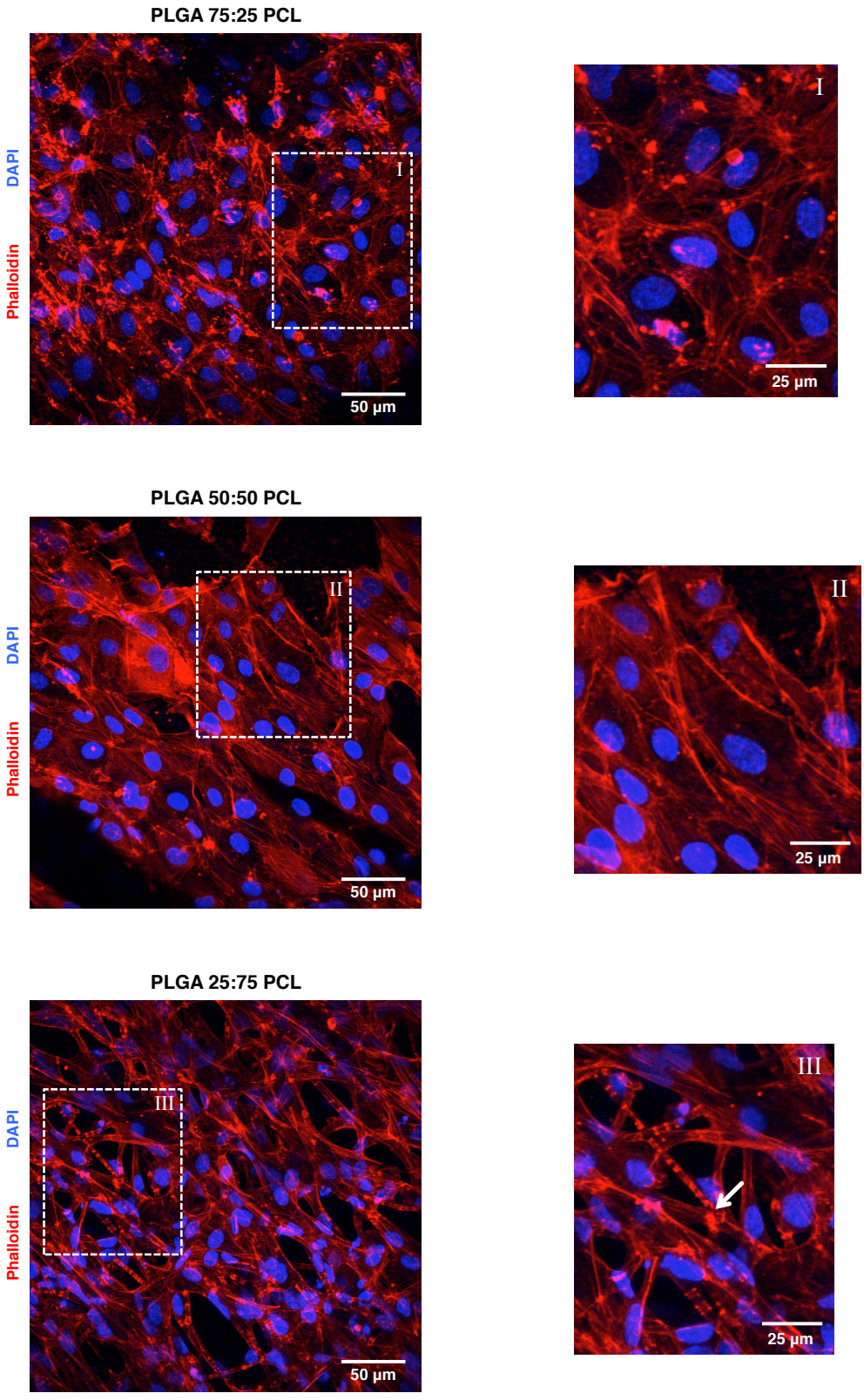


**Figure 5.12. Assessment of morphology and cytoskeleton arrangement by confocal microscopy.** Electrospun scaffolds treated by $N_2$ plasma for 60 s and incubated with hPL were seeded with 7,000 ECFCs and cultured for 5 days. After fixation, TRITC-conjugated phalloidin was used to stain F-actin cytoskeleton and DAPI to localize nuclei. Z-stack images were acquired using a Zeiss LSM 510 META confocal microscope (20x objective). Maximum intensity Z-projections were obtained with ImageJ (left). Zoomed in images (right) show the cytoskeleton arrangement of ECFCs on different size fibre scaffolds. White arrow pinpoints an example of actin fibres organized perpendicularly to the polymer fibres.

### 5.4. Summary of results

- Scaffolds were successfully produced by wet-electrospinning using different blends of PLGA and PCL.
- Fibre diameter increased with increasing PCL content.
- $N_2$ gas plasma treatment led to incorporation of nitrogen-based groups in PLGA 75:25 PCL and PLGA 50:50 PCL matrices, as well as oxidation of all scaffold types.
- Plasma treatment efficiently reduced hydrophobicity of scaffolds and increased adsorption of proteins from hPL.
- Plasma-treated scaffolds promoted higher proliferation of ECFCs, especially when coated with hPL proteins.
- ECFC growth into a confluent monolayer was dependent on fibre size, only occurring on $N_2$ plasma-treated PLGA 75:25 PCL and PLGA 50:50 PCL scaffolds.

## 5.5. Discussion

While electrospinning has been previously adapted to produce tubular scaffolds (Vaz, van Tuijl, Bouten and Baaijens, 2005), the most commonly used method for doing so suffers from a number of drawbacks. The method consists of electrospinning the chosen polymer(s) directly onto an earthed rotating metallic mandrel instead of a flat collector. Efficient capture of the fibres requires a continuously conductive surface but, after some time, the collector becomes gradually insulated by the polymer fibres themselves, hindering the process and limiting the thickness of scaffolds that can be generated by this method (Migliaresi, Ruffo, Volpato and Zeni, 2012). Additionally, at least one more technical issue is usually reported when following this approach. Because fibres are tightly held onto the collector, removal of the whole scaffold without damaging it has proven to be very difficult (Errico et al., 2011). Some groups have overcome this issue by spinning an initial sacrificial layer of a polymer with a different solubility onto the collector followed by the polymer intended for use as a scaffold (Inoguchi et al., 2006). The inner layer is then dissolved in a solvent that does not affect the outer layer, allowing for its subsequent removal. While this might be a valid solution in some instances, due to the solubility requirements, the combinations of polymers that can be employed are very limited. Moreover, it has the potential of considerably aggravating the previously mentioned issue of collector insulation. To circumvent these issues, a new method that does not require the direct collection of the fibres onto a conductive mandrel was developed in this work for the fabrication of tubular scaffolds by combining wet-electrospinning (Yang et al., 2013) with yarn spinning (Teo et al., 2007; Smit, Buttner and Sanderson, 2005). As, in this approach, fibres were instead indirectly collected onto a Teflon tube, there is no practical limit to the desired wall thickness, and the scaffold can be removed from the mould with ease. In this study, tubular scaffolds were successfully produced from PLGA/PCL blends (ranging between 25% and 75% of each polymer) using this method (Figure 5.1A).

Each different polymer can only be properly electrospun into a very narrow range of fibre sizes, determined mainly by the flow-rate, the voltage applied, the solvent used and the solution's viscosity and conductivity (Li and Wang, 2013). Hence, for the same solvent and electrospinning conditions, the two polymers can give rise to differently sized fibres. Moreover, PLGA is known for its brittleness and relatively fast degradation rates, while PCL is more elastic and can take up to a few years to be degraded once implanted (Sa and Kim, 2013). By mixing these two polymers in different ratios, it is possible to tailor the fibre size, degradation rate and mechanical properties to

conveniently create a scaffold with the optimal characteristics for a vascular graft. This study focused on the initial adhesion and proliferation of endothelial cells under static conditions, thus emphasis was placed only on investigating the effect of fibre diameter on cell behaviour rather than looking at the degradation rates or mechanical properties of the different scaffolds. As expected, the fibre size varied with the ratio of PLGA and PCL in the initial solution (Figure 5.2), providing a range of fibre topographies for the study of endothelial growth patterns.

$N_2$ gas plasma treatment was used to modify the surface of the electrospun scaffolds, with the aim of simultaneously reducing their hydrophobicity and increasing their ability to adsorb proteins. As hoped, the treatment with this gas plasma did not damage or chemically modify the bulk of the fibres (Figure 5.3A), as observed by SEM and FTIR, but was efficient at improving their surface properties (Figures 5.6-5.7). Conversely, plasma generated using other gases, such as oxygen, has been reported to etch the surface of PLGA fibres and structurally degrade them (Park et al., 2007). Other groups have used atomic force microscopy (AFM) to examine the surface of films and found an increase in roughness at the lower nanometre scale following $N_2$ plasma treatment of polymers, such as polypropylene (Mortazavi, Ghoranneviss and Sari, 2011; Morent et al., 2008) or polyethylene terephthalate (Junkar et al., 2009) for example. It is possible that the same texture modification is imparted to the PLGA/PCL scaffolds however, technical issues arise when this method is used with fibre scaffolds as the AFM tip becomes jammed in the nanofibres instead of passing over them (Verdonck, Calíope, Hernandez and da Silva, 2006). Next, it was demonstrated that $N_2$ plasma treatment results in increased nitrogen content at the surface of scaffolds when the PLGA ratio was at least 50% (Figure 5.4A) and was especially clear in the case of PLGA 75:25 PCL samples (Figure 5.4A-C). This increase in nitrogen incorporation with increasing PLGA concentration, suggests that PLGA is more amenable to this process than PCL. It can also be speculated that, the increased surface area conferred by the smaller fibre diameter in these scaffolds allows for more polymer chains to be exposed to chemical modification by the plasma and attachment of nitrogen-based groups. Although, the specific nature of these groups cannot be precisely determined without further empirical evidence, these would be most likely amine groups ($-NH_2$) as pinpointed by the predicted N-H and C-N peaks detected in the deconvoluted $N_{1s}$ spectrum (Figure 5.4C). In a similar manner, other researchers have detected the formation of amine groups on the surface of polymers following treatment with ammonia gas plasma (Marasescu and Wertheimer, 2008). Interestingly, all scaffolds

were shown to become oxidized, independently of the polymer blend, as indicated by the increased relative amount of oxygen at their surface (Table 5.1). As suggested by others, this increase is probably due to the scission of C-H bonds from the polymer chains, which then induces the formation of free radicals (Correia, Ribeiro, Botelho and Borges, 2016). After the treatment and upon exposure to atmospheric oxygen, these radicals give rise to C=O groups (Figure 5.5), via an intermediate step where highly unstable hydroperoxides are formed. Polar groups such as $–NH_2$ and C=O groups are known to increase the surface energy and, as a consequence, also the hydrophilicity of polymer surfaces (Ferreira et al., 2009). Accordingly, the wettability of all electrospun scaffolds was greatly increased as a result of the plasma treatment, proportional to the duration of the treatment (Figure 5.6). Again, the increased surface area of PLGA 75:25 PCL scaffolds might explain why shorter treatments were more effective on these substrates than on PLGA 25:75 PCL. However, the amine groups detected on the former may also contribute significantly to this outcome. Another advantage of grafting amine groups onto the surface of the scaffolds is that these are usually positively charged at physiological pH. Since most proteins carry a net negative charge, this chemical modification should favour the interaction between these and the polymer surface.

Plasma treatment, produced with a variety of gases, has been widely shown to enhance protein adsorption on different polymers (Alves et al., 2008; Yang, Bei and Wang, 2002; Nandakumar et al., 2013). These reports usually focus on the adsorption of animal or recombinant proteins, while improving the adsorption of a complex mixture of human proteins, such as platelet lysates, has never been described before. In line with the findings regarding contact angle, it was demonstrated that the adsorption of proteins from hPL was significantly increased after plasma treatment (Figure 5.7). Surprisingly, of all the blends PLGA 25:75 PCL was the most efficient at this process in its native state and this difference was also seen with the treated scaffolds. Of relevance, the FTIR profile of the adsorbed proteins on treated scaffolds was similar across all blends, although all the peaks were once again detected more strongly with increasing PCL content (Figure 5.8). Therefore, it can be presumed that plasma treatment improves this phenomenon even when amine groups were not apparently formed at the surface of the polymers. Additionally, this adsorption profile was shown to be identical to that of pure PCL scaffolds incubated with platelet-rich plasma (PRP), as previously reported by (Diaz-Gomez et al., 2014), suggesting a similar protein constitution and adsorption specificity. For the coating of scaffolds with protein mixtures

rich in GFs, as in the case hPL (Fortunato et al., 2016), it is vital that this adsorption process can happen as quickly as possible so that the integrity and bioactivity of GFs is preserved. While several other tissue engineering studies have been published with incubation of scaffolds in protein solutions being performed for long periods of time, including overnight (Oliveira et al., 2014; Woo, Chen and Ma, 2003) and often at 37 ºC (Salvay et al., 2008), $N_2$ plasma treatment, as described in this study, permits the swift adsorption of proteins at room temperature. As a result, the shorter incubation period required for the coating of scaffolds when this treatment is employed should help preserving the integrity of the hPL proteins.

The increase of hydrophilicity and protein adsorption by treating the scaffolds with $N_2$ gas plasma was shown to significantly promote the initial adhesion and proliferation of ECFCs onto these scaffolds (Figure 5.9). Although across all polymer blends, the incubation with either FBS or hPL led to comparable metabolic rates 1 day after seeding, on PLGA 25:75 PCL scaffolds hPL coating further stimulated ECFC proliferation above FBS levels at day 3, as assessed by the PrestoBlue assay (Figure 5.9A). A similar effect was seen at the end of the time course using the PicoGreen assay (Figure 5.9B), which is considered a more accurate method of determining the differences in cell numbers (Ng, Leong and Hutmacher, 2005; Sittampalam et al., 2004). The fact that only on plasma-treated PLGA 25:75 PCL a significant difference is seen between FBS and hPL coating may be due to the greater ability of PCL to adsorb hPL proteins, compared to the other blends. As shown in the previous chapter, this protein mix is rich ECM proteins and angiogenic growth-factors (Fortunato et al., 2016), which once adsorbed to scaffolds should greatly increase the ECFC adhesion via integrins and subsequent proliferation. Worth noting, an overall decrease in the metabolic rate was seen by the last day of the time course, especially for PLGA 75:25 PCL and PLGA 50:50 PCL. Although, the measurement of the metabolism of cells is often used as an indicator of their proliferative rate, it is likely that the repeated exposure to resazurin for long incubation periods led to a toxic effect on the cells. Indeed, changes of cell morphology after only a few hours of incubation have been reported before, which suggest that this compound interferes with normal cell function by reducing the amount of ATP measured as a marker of cell viability (Sittampalam et al., 2004). Additionally, the accuracy of this assay as a method of determining the actual cell number has been debated, as metabolism can obviously be affected by cellular processes other than mitosis, leading to a lack of correlation between the values obtained by this assay and those of more absolute methods (i.e.

cell counting or dsDNA quantification) (Quent et al., 2010). This issue is even more prominent in the case of the measurement of cell proliferation in three-dimensional substrates over time, with inconsistent or even inverse results to those obtained by PicoGreen assay being reported (Ng, Leong and Hutmacher, 2005). It is also possible that ECFCs have a lower basal metabolism as they are cultured under static rather than dynamic conditions, unlike endothelial cells in a living blood vessel, and because these have already reached confluence and stopped dividing by day 5. Corroborating this hypothesis, the reduction in metabolism was not as pronounced on PLGA 25:75 PCL scaffolds, which may be due to their wider fibre diameter. This results in a higher porosity, allowing cells to infiltrate the scaffolds and grow for longer periods of time. In agreement, ECFCs were shown to grow into a confluent monolayer on the surface of both PLGA 75:25 PCL and PLGA 50:50 PCL in just 5 days, but appeared to be spread deeper inside PLGA 25:75 PCL scaffolds (Figures 5.10 and 5.11). This morphology was confirmed by staining the actin cytoskeleton and confocal imaging. On the smaller and intermediate size fibres, the ECFCs arranged into monolayers and exhibited cytoskeletons organized at the periphery of cells (Figure 5.12), in similarity to what was reported in another study regarding the morphology of HUVECs seeded on sub-micron fibres (Whited and Rylander, 2014). Likewise, Fioretta and colleagues have observed a monolayer type of growth by ECFCs seeded on electrospun fibres with a diameter less than 2 μm and a penetrating growth pattern on larger diameter fibres (Fioretta et al., 2014). Interestingly, on these latter fibres, the same authors described a cytoskeleton organization that was strictly in alignment with the polymer fibres, which is not in agreement with our observations characterised by a mixed type of arrangement, with F-actin filaments circumferentially aligned as well as in the same direction as the fibres.

## 5.6. Conclusions

In this chapter, a novel method for the generation of tubular electrospun scaffolds of PLGA and PCL polymers was described, and their modification via plasma treatment was investigated with the final purpose of improving the adhesion and proliferation of ECFCs. It was shown that gas plasma treatment using $N_2$ gas modified the surface of the polymer fibres by addition of different oxygen and nitrogen functionalities in a controlled manner. This surface treatment was responsible for a decrease in the hydrophobicity of the scaffolds and an improvement in their ability to adsorb proteins from hPL. As a consequence, these effects synergistically enhanced ECFC proliferation on these scaffolds. Future work should investigate the ratio of formation of specific chemical groups and determine the specificity of the protein adsorption mechanism.

It was also demonstrated that ECFCs exhibited a different morphology and intercellular organization depending on the average diameter of the substrate fibres, pinpointing a fibre size threshold between 1.3 μm and 2.7 μm, and respective porosity, for the transition between an endothelial-like cobblestone monolayer type of growth and a more invasive one. Considering the need to establish a single layer of endothelial cells on the luminal side of a bioengineered graft, these findings provide useful information regarding the ideal polymer blend to be used in the different layers of a vascular scaffold. Future work should assess the marker expression by ECFCS on these scaffolds to appraise their phenotype. In addition, it would be of interest to expand the cell types being tested on these scaffolds (e.g. smooth muscle cells) to include cells that can give origin to the remaining layers of the blood vessels.

Taken together, the combination of $N_2$ plasma treatment and hPL incubation described here provides a novel approach for the improvement of ECFC adhesion and proliferation onto synthetic electrospun scaffolds. The off-the-shelf nature of the polymers as well as the human origin of the proteins used, coupled with the simplicity of the scaffold's fabrication process and surface treatment constitutes a promising first step for the future development of artificial vascular grafts for clinical use.

# Chapter 6: Conclusions & future directions

## 6.1. Conclusions

ECFCs are a promising cell population for vascular tissue engineering, from minute capillary networks up to arterial-sized vessels. Several approaches based on the application of ECFCs were explored in this project.

The first aim of the work in this thesis was to assess the role of PAR-1 and PAR-2 in ECFCs from a vasculogenesis perspective. The stimulation of PAR-1 in ECFCs was shown to lead to inhibition of *in vitro* tubulogenesis, as a likely consequence of VEGFR-2 down-regulation. On the contrary, exogenous activation of PAR-2 did not alter the vasculogenic response of these cells, despite being both functionally couple to the ERK1/2 pathway. In view of these results, PARs did not prove to be a suitable target in the promotion of vascularization by ECFCs and was not pursued any further.

In a second line of investigation, human platelets were utilized to develop an ECM-based hydrogel rich in angiogenic growth factors. Culturing of ECFCs on hPLG induced the proliferation and maturation of ECFCs through the upregulation of several angiogenic genes. It was also shown for the first time that this material can support the formation of microvascular networks *in vitro* solely by ECFCs and simultaneously promote the sprouting of existing vessels from arterial explants. Therefore, hPLG exhibits a considerable potential as a both a substrate for the expansion of ECFCs, as well as for the delivery of endothelial progenitors to promote tissue revascularization via existing vessel angiogenesis, ECFC-driven vasculogenesis and anastomosis of these two vascular networks. An additional advantage of hPLG is the elimination of animal products from ECFC culture and delivery methods.

Finally, in chapter 5, a series of novel PLGA and PCL tubular scaffolds with a wide range of fibre diameters were developed using a variant of the electrospinning technique. The chemical modification of these scaffolds using $N_2$ plasma treatment was shown to introduce new oxygen and nitrogen moieties, which drastically altered the physical properties of these conduits. Most importantly, the adsorption of proteins from platelet lysate was greatly improved as a result, revealing a facile method of accelerating the coating of biomaterials with human proteins. In this case, the combination of plasma treatment and coating with platelet proteins greatly increased the adhesion and proliferation of ECFCs on these scaffolds. Furthermore, cells exhibited a markedly different infiltration and morphology depending on the fibre size in each scaffold. These findings provide useful information regarding the ideal scaffold properties necessary to regulate endothelial growth and organization. In addition, it

was demonstrated that the bioactive properties of platelet-derived factors can be successfully imparted onto synthetic scaffolds and constitutes a reliable method of promoting the endothelisation of scaffolds for tissue engineering.

## 6.2. Future directions

The initial aims of this work were to investigate and develop novel biomaterial-based approaches for the promotion of vasculogenesis and endothelisation of vascular grafts by ECFCs. Although successful approaches were created for these two tissue engineering avenues, a deeper understanding of the mechanisms that govern endothelial cell behaviour on these materials would be necessary in order to bring a significant contribution to the field.

### 6.2.1. Short-term targets

While tubular scaffolds have been fabricated before via electrospinning (Ercolani, Del Gaudio and Bianco, 2013), the novel method described in this thesis can give origin to scaffolds with new microscopic structures that may also lead to different mechanical and biological properties. More specifically, the organization of the polymer fibres into circumferentially aligned bundles may mimic the orientation of smooth muscle cells (SMCs) and collagen fibrils in the media layer of the blood vessels providing the added mechanical strength needed to withstand the circulatory pressures. In the short term, it would be of relevance to compare the mechanical properties of tubular scaffolds produce by previous methods versus those fabricated using this new technique. As discussed before, PLGA and PCL are degraded at considerably different speeds and vascular scaffolds should degrade in tune with the simultaneous growth of new tissue to prevent graft failure. Thus, it would be important to characterize the degradation profiles of scaffolds produced from each of the different polymer blends. Additionally, aspects of scaffold micro-architecture, such as fibre diameter or anisotropy, are known to play a major role on cell differentiation and ECM deposition. Specifically, the effect of fibre size and alignment on the maintenance of an anti-thrombotic phenotype by the endothelial cells would be further investigated. Finally, although the coating of electrospun scaffolds with proteins from hPL was shown to promote ECFC growth, the exact reason for this effect is still unknown. For this purpose, it would be crucial to determine the nature of the adsorbed proteins that are responsible for this effect.

### 6.2.2. Medium to long-term targets

Considering the robust pro-vasculogenic response of ECFCs in hPLG *in vitro* and its potential as an injectable cell-delivery method, it would be of the utmost relevance to assess the ability of ECFCs to form functional blood vessels *in vivo* as a proof of concept towards its future application in humans. Among the different therapeutic targets that could benefit from such approach, chronic wound healing and bone fracture repair are likely the most relevant. For the first, this would be initially investigated using animal models of chronic skin wounds using an immunodeficient diabetic mouse strain to assess the ability of human ECFCs and hPLG in reversing the impairment in revascularization and reepithelization that is common in diabetic patients. The potential increase in capillary formation, coupled with the recognized anti-inflammatory and anti-bacterial effect of platelet preparations (Bendinelli et al., 2010) (Drago et al., 2013), could synergistically lead to a measurable improvement in wound rate closure. Nevertheless, mouse skin is considerably thinner than the human skin and exhibits a predominantly contractile wound-healing phenotype due to significant structural differences, resulting in limited resemblance to the human response following injury (Dunn et al., 2013). Therefore, it would be also imperative to perform a similar study using large animal models, such as the porcine, since the skin's stratification, ECM, turnover time and content in immune cells in these animals is more similar to that of the human skin (Seaton, Hocking and Gibran, 2015). Additionally, hPLG could also be investigated as a delivery method for other cell types that, unlike ECFCS, can be quickly obtained and contribute as well to enhanced angiogenesis (e.g. circulating $CD34^+$ cells or MSCs). While the utilization of ECFCs can only be envisaged for the treatment of less urgent medical conditions (due to the time required for ECFC isolation and expansion), such studies could also demonstrate the ability of hPLG to promote revascularization on its own by sprouting of existing vessels and recruitment of tissue progenitors, as hinted by the results presented in Chapter 4. Due to the negligible immunogenic risk, this more simplistic approach could expand the range of suitable applications of hPLG to include those of a more acute character, such as skin burns, and greatly accelerate its translation to the clinic.

# References

Abu El-Asrar, A.M., Alam, K., Nawaz, M.I., Mohammad, G., Van den Eynde, K., Siddiquei, M.M., Mousa, A., Hertogh, G.D. and Opdenakker, G., 2016. Upregulation of Thrombin/Matrix Metalloproteinase-1/Protease-Activated Receptor-1 Chain in Proliferative Diabetic Retinopathy. *Current eye research*, pp.1–11.

Adams, M.N., Pagel, C.N., Mackie, E.J. and Hooper, J.D., 2012. Evaluation of antibodies directed against human protease-activated receptor-2. *Naunyn-Schmiedeberg's archives of pharmacology*, 385(9), pp.861–873.

Aguilera, K.Y. and Brekken, R.A., 2014. Recruitment and retention: factors that affect pericyte migration. *Cellular and molecular life sciences : CMLS*, 71(2), pp.299–309.

Ahmed, T.A.E., Ringuette, R., Wallace, V.A. and Griffith, M., 2014. Autologous fibrin glue as an encapsulating scaffold for delivery of retinal progenitor cells. *Frontiers in bioengineering and biotechnology*, 2, p.85.

Alberelli, M.A. and De Candia, E., 2014. Functional role of protease activated receptors in vascular biology. *Vascular pharmacology*, 62(2), pp.72–81.

Alessi, D.R., Cuenda, A., Cohen, P., Dudley, D.T. and Saltiel, A.R., 1995. PD 098059 is a specific inhibitor of the activation of mitogen-activated protein kinase kinase in vitro and in vivo. *The Journal of biological chemistry*, 270(46), pp.27489–27494.

Allen, P., Melero-Martin, J. and Bischoff, J., 2011. Type I collagen, fibrin and PuraMatrix matrices provide permissive environments for human endothelial and mesenchymal progenitor cells to form neovascular networks. *Journal of Tissue Engineering and Regenerative Medicine*, 5(4), pp.e74–86.

Alves, C.M., Yang, Y., Marton, D., Carnes, D.L., Ong, J.L., Sylvia, V.L., Dean, D.D., Reis, R.L. and Agrawal, C.M., 2008. Plasma surface modification of poly(D,L-lactic acid) as a tool to enhance protein adsorption and the attachment of different cell types. *Journal of biomedical materials research. Part B, Applied biomaterials*, 87(1), pp.59–66.

Andía, I. and Maffulli, N., 2013. Platelet-rich plasma for managing pain and inflammation in osteoarthritis. *Nature reviews. Rheumatology*, 9(12), pp.721–730.

Anitua, E., Andía, I., Ardanza, B., Nurden, P. and Nurden, A.T., 2004. Autologous platelets as a source of proteins for healing and tissue regeneration. *Thrombosis and Haemostasis*, 91(1), pp.4–15.

Aplin, A.C. and Nicosia, R.F., 2015. The rat aortic ring model of angiogenesis. *Methods in molecular biology (Clifton, N.J.)*, 1214, pp.255–264.

Arakawa, T., Prestrelski, S.J., Kenney, W.C. and Carpenter, J.F., 2001. Factors affecting short-term and long-term stabilities of proteins. *Advanced Drug Delivery Reviews*, 46(1-3), pp.307–326.

Ardehali, A. and Ports, T.A., 1990. Myocardial oxygen supply and demand. *Chest*, 98(3), pp.699–705.

Arnaoutova, I. and Kleinman, H.K., 2010. In vitro angiogenesis: endothelial cell tube formation on gelled basement membrane extract. *Nature protocols*, 5(4), pp.628–635.

Arnaoutova, I., George, J., Kleinman, H.K. and Benton, G., 2009. The endothelial cell tube formation assay on basement membrane turns 20: state of the science and the art. *Angiogenesis*, 12(3), pp.267–274.

Asahara, T., Murohara, T., Sullivan, A., Silver, M., van der Zee, R., Li, T., Witzenbichler, B., Schatteman, G. and Isner, J.M., 1997. Isolation of putative progenitor endothelial cells for angiogenesis. *Science*, 275(5302), pp.964–967.

Ascione, R., Rowlinson, J., Avolio, E., Katare, R., Meloni, M., Spencer, H.L., Mangialardi, G., Norris, C., Kränkel, N., Spinetti, G., Emanueli, C. and Madeddu, P., 2015. Migration towards SDF-1 selects angiogenin-expressing bone marrow monocytes endowed with cardiac reparative activity in patients with previous myocardial infarction. *Stem cell research & therapy*, 6, p.53.

Astete, C.E. and Sabliov, C.M., 2006. Synthesis and characterization of PLGA nanoparticles. *Journal of biomaterials science. Polymer edition*, 17(3), pp.247–289.

Auerbach, R., Lewis, R., Shinners, B., Kubai, L. and Akhtar, N., 2003. Angiogenesis assays: a critical overview. *Clinical chemistry*, 49(1), pp.32–40.

Aziz, G., De Geyter, N. and Morent, R., 2015. Incorporation of primary amines via plasma technology on biomaterials. *Advances in bioengineering*.

Bai, Y., Yin, G., Huang, Z., Liao, X., Chen, X., Yao, Y. and Pu, X., 2013. Localized delivery of growth factors for angiogenesis and bone formation in tissue engineering. *International immunopharmacology*, 16(2), pp.214–223.

Bajpai, V.K., Mistriotis, P., Loh, Y.-H., Daley, G.Q. and Andreadis, S.T., 2012. Functional vascular smooth muscle cells derived from human induced pluripotent stem cells via mesenchymal stem cell intermediates. *Cardiovascular Research*, 96(3), pp.391–400.

Balaji, S., King, A., Crombleholme, T.M. and Keswani, S.G., 2013. The Role of Endothelial Progenitor Cells in Postnatal Vasculogenesis: Implications for Therapeutic Neovascularization and Wound Healing. *Advances in wound care*, 2(6), pp.283–295.

Ballerio, R., Brambilla, M., Colnago, D., Parolari, A., Agrifoglio, M., Camera, M., Tremoli, E. and Mussoni, L., 2007. Distinct roles for PAR1- and PAR2-mediated vasomotor modulation in human arterial and venous conduits. *Journal of thrombosis and haemostasis : JTH*, 5(1), pp.174–180.

Banfi, A., Degenfeld, von, G., Gianni Barrera, R., Reginato, S., Merchant, M.J., McDonald, D.M. and Blau, H.M., 2012. Therapeutic angiogenesis due to balanced single-vector delivery of VEGF and PDGF-BB. *FASEB journal : official publication of the Federation of American Societies for Experimental Biology*, 26(6), pp.2486–2497.

BaoLin, G. and Ma, P.X., 2014. Synthetic biodegradable functional polymers for tissue engineering: a brief review. *Science China. Chemistry*, 57(4), pp.490–500.

Bayless, K.J., Salazar, R. and Davis, G.E., 2000. RGD-dependent vacuolation and lumen formation observed during endothelial cell morphogenesis in three-dimensional fibrin matrices involves the alpha(v)beta(3) and alpha(5)beta(1) integrins. *The American journal of pathology*, 156(5), pp.1673–1683.

Beierlein, W., Scheule, A.M., Antoniadis, G., Braun, C. and Schosser, R., 2000. An immediate, allergic skin reaction to aprotinin after reexposure to fibrin sealant. *Transfusion*, 40(3), pp.302–305.

Belting, M., Ahamed, J. and Ruf, W., 2005. Signaling of the tissue factor coagulation pathway in angiogenesis and cancer. *Arteriosclerosis, Thrombosis, and Vascular Biology*, 25(8), pp.1545–1550.

Belting, M., Dorrell, M.I., Sandgren, S., Aguilar, E., Ahamed, J., Dorfleutner, A., Carmeliet, P., Mueller, B.M., Friedlander, M. and Ruf, W., 2004. Regulation of angiogenesis by tissue factor cytoplasmic domain signaling. *Nature medicine*, 10(5), pp.502–509.

Benam, K.H., Dauth, S., Hassell, B., Herland, A., Jain, A., Jang, K.-J., Karalis, K., Kim, H.J., MacQueen, L., Mahmoodian, R., Musah, S., Torisawa, Y.-S., van der Meer, A.D., Villenave, R., Yadid, M., Parker, K.K. and Ingber, D.E., 2015. Engineered In Vitro Disease Models. *Annual Review of Pathology: Mechanisms of Disease*, 10(1), pp.195–262.

Benavides, O.M., Brooks, A.R., Cho, S.K., Petsche Connell, J., Ruano, R. and Jacot, J.G., 2015. In situ vascularization of injectable fibrin/poly(ethylene glycol) hydrogels by human amniotic fluid-derived stem cells. *Journal of Biomedical Materials Research Part A*, 103(8), pp.2645–2653.

Bendinelli, P., Matteucci, E., Dogliotti, G., Corsi, M.M., Banfi, G., Maroni, P. and Desiderio, M.A., 2010. Molecular basis of anti-inflammatory action of platelet-rich plasma on human chondrocytes: mechanisms of NF-κB inhibition via HGF. *Journal of cellular physiology*, 225(3), pp.757–766.

Bennion, R.S., Williams, R.A., Stabile, B.E., Fox, M.A., Owens, M.L. and Wilson, S.E., 1985. Patency of autogenous saphenous vein versus polytetrafluoroethylene grafts in femoropopliteal bypass for advanced ischemia of the extremity. *Surgery, gynecology & obstetrics*, 160(3), pp.239–242.

Berthiaume, F., Maguire, T.J. and Yarmush, M.L., 2011. Tissue engineering and regenerative medicine: history, progress, and challenges. *Annual review of chemical and biomolecular engineering*, 2, pp.403–430.

Bikfalvi, A., Cramer, E.M., Tenza, D. and Tobelem, G., 1991. Phenotypic modulations of human umbilical vein endothelial cells and human dermal fibroblasts using two angiogenic assays. *Biology of the cell / under the auspices of the European Cell Biology Organization*, 72(3), pp.275–278.

Binns, R.L., Ku, D.N., Stewart, M.T., Ansley, J.P. and Coyle, K.A., 1989. Optimal graft diameter: effect of wall shear stress on vascular healing. *Journal of vascular surgery*, 10(3), pp.326–337.

Birla, R.K., Borschel, G.H., Dennis, R.G. and Brown, D.L., 2005. Myocardial engineering in vivo: formation and characterization of contractile, vascularized three-

dimensional cardiac tissue. *Tissue engineering*, 11(5-6), pp.803–813.

Blackburn, J.S. and Brinckerhoff, C.E., 2008. Matrix metalloproteinase-1 and thrombin differentially activate gene expression in endothelial cells via PAR-1 and promote angiogenesis. *The American journal of pathology*, 173(6), pp.1736–1746.

Bogoslovsky, T., Wang, D., Maric, D., Scattergood-Keepper, L., Spatz, M., Auh, S. and Hallenbeck, J., 2013. Cryopreservation and Enumeration of Human Endothelial Progenitor and Endothelial Cells for Clinical Trials. *Journal of blood disorders & transfusion*, 4(5).

Bonani, W., Maniglio, D., Motta, A., Tan, W. and Migliaresi, C., 2011. Biohybrid nanofiber constructs with anisotropic biomechanical properties. *Journal of biomedical materials research. Part B, Applied biomaterials*, 96(2), pp.276–286.

Boquest, A.C., Noer, A., Sørensen, A.L., Vekterud, K. and Collas, P., 2007. CpG methylation profiles of endothelial cell-specific gene promoter regions in adipose tissue stem cells suggest limited differentiation potential toward the endothelial cell lineage. *STEM CELLS*, 25(4), pp.852–861.

Borensztajn, K., Bresser, P., van der Loos, C., Bot, I., van den Blink, B., Bakker, den, M.A., Daalhuisen, J., Groot, A.P., Peppelenbosch, M.P., Thüsen, von der, J.H. and Spek, C.A., 2010. Protease-activated receptor-2 induces myofibroblast differentiation and tissue factor up-regulation during bleomycin-induced lung injury: potential role in pulmonary fibrosis. *The American journal of pathology*, 177(6), pp.2753–2764.

Bouten, C.V.C., Dankers, P.Y.W., Driessen-Mol, A., Pedron, S., Brizard, A.M.A. and Baaijens, F.P.T., 2011. Substrates for cardiovascular tissue engineering. *Advanced Drug Delivery Reviews*, 63(4-5), pp.221–241.

Braghirolli, D.I., Steffens, D. and Pranke, P., 2014. Electrospinning for regenerative medicine: a review of the main topics. *Drug discovery today*, 19(6), pp.743–753.

Brooks, S.A. and Hall, D.M.S., 2012. Lectin histochemistry to detect altered glycosylation in cells and tissues. *Methods in molecular biology (Clifton, N.J.)*, 878, pp.31–50.

Burnouf, T., Goubran, H.A., Chen, T.-M., Ou, K.-L., El-Ekiaby, M. and Radosevic, M., 2013. Blood-derived biomaterials and platelet growth factors in regenerative medicine. *Blood reviews*, 27(2), pp.77–89.

Burnouf, T., Strunk, D., Koh, M.B.C. and Schallmoser, K., 2016. Human platelet lysate: Replacing fetal bovine serum as a gold standard for human cell propagation? *Biomaterials*, 76, pp.371–387.

Camerer, E., Kataoka, H., Kahn, M., Lease, K. and Coughlin, S.R., 2002. Genetic evidence that protease-activated receptors mediate factor Xa signaling in endothelial cells. *The Journal of biological chemistry*, 277(18), pp.16081–16087.

Campagnolo, P., Cesselli, D., Haj Zen, Al, A., Beltrami, A.P., Kränkel, N., Katare, R., Angelini, G., Emanueli, C. and Madeddu, P., 2010. Human adult vena saphena contains perivascular progenitor cells endowed with clonogenic and proangiogenic potential. *Circulation*, 121(15), pp.1735–1745.

Carr, M.E., Gabriel, D.A. and McDonagh, J., 1987. Influence of factor XIII and fibronectin on fiber size and density in thrombin-induced fibrin gels. *The Journal of laboratory and clinical medicine*, 110(6), pp.747–752.

Case, J., Mead, L.E., Bessler, W.K., Prater, D., White, H.A., Saadatzadeh, M.R., Bhavsar, J.R., Yoder, M.C., Haneline, L.S. and Ingram, D.A., 2007. Human CD34+AC133+VEGFR-2+ cells are not endothelial progenitor cells but distinct, primitive hematopoietic progenitors. *Experimental Hematology*, 35(7), pp.1109–1118.

Castro-Manrreza, M.E. and Montesinos, J.J., 2015. Immunoregulation by mesenchymal stem cells: biological aspects and clinical applications. *Journal of immunology research*, 2015, p.394917.

Ceccarelli, J. and Putnam, A.J., 2014. Sculpting the blank slate: how fibrin's support of vascularization can inspire biomaterial design. *Acta Biomaterialia*, 10(4), pp.1515–1523.

Chan, B., Merchan, J.R., Kale, S. and Sukhatme, V.P., 2003. Antiangiogenic property of human thrombin. *Microvascular research*, 66(1), pp.1–14.

Chao, T.-H., Chen, I.-C., Lee, C.-H., Chen, J.-Y., Tsai, W.-C., Li, Y.-H., Tseng, S.-Y., Tsai, L.-M. and Tseng, W.-K., 2016. Cilostazol Enhances Mobilization of Circulating Endothelial Progenitor Cells and Improves Endothelium-Dependent Function in Patients at High Risk of Cardiovascular Disease. *Angiology*, 67(7), pp.638–646.

Chatterjee, M., Huang, Z., Zhang, W., Jiang, L., Hultenby, K., Zhu, L., Hu, H., Nilsson, G.P. and Li, N., 2011. Distinct platelet packaging, release, and surface expression of proangiogenic and antiangiogenic factors on different platelet stimuli. *Blood*, 117(14), pp.3907–3911.

Chavakis, E. and Dimmeler, S., 2002. Regulation of endothelial cell survival and apoptosis during angiogenesis. *Arteriosclerosis, Thrombosis, and Vascular Biology*, 22(6), pp.887–893.

Cheung, C., Bernardo, A.S., Trotter, M.W.B., Pedersen, R.A. and Sinha, S., 2012. Generation of human vascular smooth muscle subtypes provides insight into embryological origin-dependent disease susceptibility. *Nature biotechnology*, 30(2), pp.165–173.

Chlupác, J., Filová, E. and Bacáková, L., 2009. Blood vessel replacement: 50 years of development and tissue engineering paradigms in vascular surgery. *Physiological research / Academia Scientiarum Bohemoslovaca*, 58 Suppl 2, pp.S119–39.

Chu, H. and Wang, Y., 2012. Therapeutic angiogenesis: controlled delivery of angiogenic factors. *Therapeutic Delivery*, 3(6), pp.693–714.

Correia, D.M., Ribeiro, C., Botelho, G. and Borges, J., 2016. Superhydrophilic poly (l-lactic acid) electrospun membranes for biomedical applications obtained by argon and oxygen plasma treatment. *Applied Surface ….*

Corselli, M., Crisan, M., Murray, I.R., West, C.C., Scholes, J., Codrea, F., Khan, N. and Péault, B., 2013. Identification of perivascular mesenchymal stromal/stem cells by flow cytometry. *Cytometry. Part A : the journal of the International Society for Analytical Cytology*, 83(8), pp.714–720.

Coughlin, S.R., 2005. Protease-activated receptors in hemostasis, thrombosis and vascular biology. *Journal of thrombosis and haemostasis : JTH*, 3(8), pp.1800–1814.

Covas, D.T., Piccinato, C.E., Orellana, M.D., Siufi, J.L.C., Silva, W.A., Proto-Siqueira, R., Rizzatti, E.G., Neder, L., Silva, A.R.L., Rocha, V. and Zago, M.A., 2005. Mesenchymal stem cells can be obtained from the human saphena vein. *Experimental cell research*, 309(2), pp.340–344.

Critser, P.J. and Yoder, M.C., 2010. Endothelial colony-forming cell role in neoangiogenesis and tissue repair. *Current opinion in organ transplantation*, 15(1), pp.68–72.

Critser, P.J., Kreger, S.T., Voytik-Harbin, S.L. and Yoder, M.C., 2010. Collagen matrix physical properties modulate endothelial colony forming cell-derived vessels in vivo. *Microvascular research*, 80(1), pp.23–30.

Cybulsky, A.V., McTavish, A.J. and Cyr, M.D., 1994. Extracellular matrix modulates epidermal growth factor receptor activation in rat glomerular epithelial cells. *The Journal of clinical investigation*, 94(1), pp.68–78.

da Silva Meirelles, L., Caplan, A.I. and Nardi, N.B., 2008. In search of the in vivo identity of mesenchymal stem cells. *STEM CELLS*, 26(9), pp.2287–2299.

Daculsi, G., Uzel, A.P., Weiss, P., Goyenvalle, E. and Aguado, E., 2010. Developments in injectable multiphasic biomaterials. The performance of microporous biphasic calcium phosphate granules and hydrogels. *Journal of materials science. Materials in medicine*, 21(3), pp.855–861.

Dai, T., Zheng, H. and Fu, G.-S., 2008. Hypoxia confers protection against apoptosis via the PI3K/Akt pathway in endothelial progenitor cells. *Acta pharmacologica Sinica*, 29(12), pp.1425–1431.

de Mel, A., Cousins, B.G. and Seifalian, A.M., 2012. Surface modification of biomaterials: a quest for blood compatibility. *International journal of biomaterials*, 2012, p.707863.

De, S., Sharma, R., Trigwell, S., Laska, B., Ali, N., Mazumder, M.K. and Mehta, J.L., 2005. Plasma treatment of polyurethane coating for improving endothelial cell growth and adhesion. *Journal of biomaterials science. Polymer edition*, 16(8), pp.973–989.

Deng, C., Zhang, P., Vulesevic, B., Kuraitis, D., Li, F., Yang, A.F., Griffith, M., Ruel, M. and Suuronen, E.J., 2010. A collagen–chitosan hydrogel for endothelial differentiation and angiogenesis. *Tissue Engineering Part A*, 16(10), pp.3099–3109.

di Blasio, L., Bussolino, F. and Primo, L., 2015. Three-dimensional in vitro assay of endothelial cell invasion and capillary tube morphogenesis. *Methods in molecular biology (Clifton, N.J.)*, 1214, pp.41–47.

Diaz-Gomez, L., Alvarez-Lorenzo, C., Concheiro, A., Silva, M., Dominguez, F., Sheikh, F.A., Cantu, T., Desai, R., Garcia, V.L. and Macossay, J., 2014. Biodegradable electrospun nanofibers coated with platelet-rich plasma for cell adhesion and proliferation. *Materials science & engineering. C, Materials for biological applications*, 40, pp.180–188.

Doerr, H.W., Cinatl, J., Stürmer, M. and Rabenau, H.F., 2003. Prions and orthopedic surgery. *Infection*, 31(3), pp.163–171.

Dorrucci, V., Griselli, F., Petralia, G., Spinamano, L. and Adornetto, R., 2008. Heparin-bonded expanded polytetrafluoroethylene grafts for infragenicular bypass in patients with critical limb ischemia: 2-year results. *The Journal of cardiovascular surgery*, 49(2), pp.145–149.

Doucet, C., Ernou, I., Zhang, Y., Llense, J.-R., Begot, L., Holy, X. and Lataillade, J.-J., 2005. Platelet lysates promote mesenchymal stem cell expansion: a safety substitute for animal serum in cell-based therapy applications. *Journal of cellular physiology*, 205(2), pp.228–236.

Drago, L., Bortolin, M., Vassena, C., Taschieri, S. and Del Fabbro, M., 2013. Antimicrobial activity of pure platelet-rich plasma against microorganisms isolated from oral cavity. *BMC microbiology*, 13, p.47.

Drake, C.J., LaRue, A., Ferrara, N. and Little, C.D., 2000. VEGF regulates cell behavior during vasculogenesis. *Developmental Biology*, 224(2), pp.178–188.

Dunn, C.J. and Goa, K.L., 1999. Fibrin sealant: a review of its use in surgery and endoscopy. *Drugs*, 58(5), pp.863–886.

Dunn, L., Prosser, H.C.G., Tan, J.T.M., Vanags, L.Z., Ng, M.K.C. and Bursill, C.A., 2013. Murine model of wound healing. *Journal of visualized experiments : JoVE*, (75), p.e50265.

Duque Sánchez, L., Brack, N., Postma, A., Pigram, P.J. and Meagher, L., 2016. Surface modification of electrospun fibres for biomedical applications: A focus on radical polymerization methods. *Biomaterials*, 106(C), pp.24–45.

Dutra-Oliveira, A., Monteiro, R.Q. and Mariano-Oliveira, A., 2012. Protease-activated receptor-2 (PAR2) mediates VEGF production through the ERK1/2 pathway in human glioblastoma cell lines. *Biochemical and biophysical research communications*, 421(2), pp.221–227.

Edelblute, C.M., Donate, A.L., Hargrave, B.Y. and Heller, L.C., 2015. Human platelet gel supernatant inactivates opportunistic wound pathogens on skin. *Platelets*, 26(1), pp.13–16.

Edlund, M., Andersson, E. and Fried, G., 2004. Progesterone withdrawal causes endothelin release from cultured human uterine microvascular endothelial cells. *Human reproduction (Oxford, England)*, 19(6), pp.1272–1280.

El-Sherbiny, I.M. and Yacoub, M.H., 2013. Hydrogel scaffolds for tissue engineering: Progress and challenges. *Global cardiology science & practice*, 2013(3), pp.316–342.

Erat, M.C., Sladek, B., Campbell, I.D. and Vakonakis, I., 2013. Structural analysis of collagen type I interactions with human fibronectin reveals a cooperative binding mode. *The Journal of biological chemistry*, 288(24), pp.17441–17450.

Ercolani, E., Del Gaudio, C. and Bianco, A., 2013. Vascular tissue engineering of small-diameter blood vessels: reviewing the electrospinning approach. *Journal of Tissue Engineering and Regenerative Medicine*, 9(8), pp.861–888.

Errico, C., Detta, N., Puppi, D., Piras, A.M., Chiellini, F. and Chiellini, E., 2011. Polymeric nanostructured items electrospun on a cylindrical template: a simple procedure for their removal. *Polymer International*, [online] 60(8), pp.1162–1166. Available at: <http://onlinelibrary.wiley.com/doi/10.1002/pi.3060/full>.

Etulain, J., Mena, H.A., Negrotto, S. and Schattner, M., 2015. Stimulation of PAR-1 or PAR-4 promotes similar pattern of VEGF and endostatin release and pro-angiogenic responses mediated by human platelets. *Platelets*, 26(8), pp.799–804.

Evensen, L., Micklem, D.R., Blois, A., Berge, S.V., Aarsæther, N., Littlewood-Evans, A., Wood, J. and Lorens, J.B., 2009. Mural cell associated VEGF is required for organotypic vessel formation. *PLoS ONE*, 4(6), p.e5798.

Fadini, G.P., Avogaro, A. and Agostini, C., 2007. Critical assessment of putative endothelial progenitor phenotypes. *Experimental Hematology*, 35(10), pp.1479–80– author reply 1481–2.

Fadini, G.P., Losordo, D. and Dimmeler, S., 2012. Critical reevaluation of endothelial progenitor cell phenotypes for therapeutic and diagnostic use. *Circulation research*, 110(4), pp.624–637.

Feistritzer, C., Lenta, R. and Riewald, M., 2005. Protease-activated receptors-1 and -2 can mediate endothelial barrier protection: role in factor Xa signaling. *Journal of thrombosis and haemostasis : JTH*, 3(12), pp.2798–2805.

Fekete, N., Gadelorge, M., Fürst, D., Maurer, C., Dausend, J., Fleury-Cappellesso, S., Mailänder, V., Lotfi, R., Ignatius, A., Sensebé, L., Bourin, P., Schrezenmeier, H. and Rojewski, M.T., 2012. Platelet lysate from whole blood-derived pooled platelet concentrates and apheresis-derived platelet concentrates for the isolation and expansion of human bone marrow mesenchymal stromal cells: production process, content and identification of active components. *Cytotherapy*, 14(5), pp.540–554.

Ferrara, N., 2010. Binding to the extracellular matrix and proteolytic processing: two key mechanisms regulating vascular endothelial growth factor action. *Molecular biology of the cell*, 21(5), pp.687–690.

Ferreira, B., Pinheiro, L., Nascente, P., Ferreira, M.J. and Duek, E., 2009. Plasma surface treatments of poly (l-lactic acid)(PLLA) and poly (hydroxybutyrate-co-hydroxyvalerate)(PHBV). *Materials Science & Engineering C*, 29(3), pp.806–813.

Fiedler, T., Belova, I.V., Murch, G.E., Poologasundarampillai, G., Jones, J.R., Roether, J.A. and Boccaccini, A.R., 2014. A comparative study of oxygen diffusion in tissue engineering scaffolds. *Journal of materials science. Materials in medicine*, 25(11), pp.2573–2578.

Fioretta, E.S., Fledderus, J.O., Burakowska-Meise, E.A., Baaijens, F.P.T., Verhaar, M.C. and Bouten, C.V.C., 2012. Polymer-based scaffold designs for in situ vascular tissue engineering: controlling recruitment and differentiation behavior of endothelial colony forming cells. *Macromolecular Bioscience*, 12(5), pp.577–590.

Fioretta, E.S., Simonet, M., Smits, A.I.P.M., Baaijens, F.P.T. and Bouten, C.V.C., 2014. Differential response of endothelial and endothelial colony forming cells on electrospun scaffolds with distinct microfiber diameters. *Biomacromolecules*, 15(3), pp.821–829.

Fortunato, T.M., Beltrami, C., Emanueli, C., De Bank, P.A. and Pula, G., 2016. Platelet lysate gel and endothelial progenitors stimulate microvascular network formation in vitro: tissue engineering implications. *Scientific Reports*, 6, pp.25326 EP–.

Fujio, Y. and Walsh, K., 1999. Akt mediates cytoprotection of endothelial cells by vascular endothelial growth factor in an anchorage-dependent manner. *The Journal of biological chemistry*, 274(23), pp.16349–16354.

Gabriel, M., Niederer, K., Becker, M., Raynaud, C.M., Vahl, C.-F. and Frey, H., 2016. Tailoring Novel PTFE Surface Properties: Promoting Cell Adhesion and Antifouling Properties via a Wet Chemical Approach. *Bioconjugate chemistry*, 27(5), pp.1216–1221.

Garcia, J.G., Patterson, C., Bahler, C., Aschner, J., Hart, C.M. and English, D., 1993. Thrombin receptor activating peptides induce Ca2+ mobilization, barrier dysfunction, prostaglandin synthesis, and platelet-derived growth factor mRNA expression in cultured endothelium. *Journal of cellular physiology*, 156(3), pp.541–549.

Gerber, H.P., McMurtrey, A., Kowalski, J., Yan, M., Keyt, B.A., Dixit, V. and Ferrara, N., 1998. Vascular endothelial growth factor regulates endothelial cell survival through the phosphatidylinositol 3'-kinase/Akt signal transduction pathway. Requirement for Flk-1/KDR activation. *The Journal of biological chemistry*, 273(46), pp.30336–30343.

Ginsberg, M., James, D., Ding, B.-S., Nolan, D., Geng, F., Butler, J.M., Schachterle, W., Pulijaal, V.R., Mathew, S., Chasen, S.T., Xiang, J., Rosenwaks, Z., Shido, K., Elemento, O., Rabbany, S.Y. and Rafii, S., 2012. Efficient direct reprogramming of mature amniotic cells into endothelial cells by ETS factors and TGFβ suppression. *Cell*, 151(3), pp.559–575.

Girard-Lauriault, P.-L., Truica-Marasescu, F., Petit, A., Wang, H.T., Desjardins, P., Antoniou, J., Mwale, F. and Wertheimer, M.R., 2009. Adhesion of human U937 monocytes to nitrogen-rich organic thin films: novel insights into the mechanism of cellular adhesion. *Macromolecular Bioscience*, 9(9), pp.911–921.

Golebiewska, E.M. and Poole, A.W., 2015. Platelet secretion: From haemostasis to wound healing and beyond. *Blood reviews*, 29(3), pp.153–162.

Gong, Z. and Niklason, L.E., 2008. Small-diameter human vessel wall engineered from bone marrow-derived mesenchymal stem cells (hMSCs). *FASEB journal : official publication of the Federation of American Societies for Experimental Biology*, 22(6), pp.1635–1648.

Gordillo, G.M. and Sen, C.K., 2003. Revisiting the essential role of oxygen in wound healing. *American journal of surgery*, 186(3), pp.259–263.

Grandaliano, G., Monno, R., Ranieri, E., Gesualdo, L., Schena, F.P., Martino, C. and Ursi, M., 2000. Regenerative and proinflammatory effects of thrombin on human proximal tubular cells. *Journal of the American Society of Nephrology : JASN*, 11(6), pp.1016–1025.

Graupera, M., Guillermet-Guibert, J., Foukas, L.C., Phng, L.-K., Cain, R.J., Salpekar, A., Pearce, W., Meek, S., Millan, J., Cutillas, P.R., Smith, A.J.H., Ridley, A.J., Ruhrberg, C., Gerhardt, H. and Vanhaesebroeck, B., 2008. Angiogenesis selectively requires the p110alpha isoform of PI3K to control endothelial cell migration. *Nature*,

453(7195), pp.662–666.

Greppi, N., Mazzucco, L., Galetti, G., Bona, F., Petrillo, E., Smacchia, C., Raspollini, E., Cossovich, P., Caprioli, R., Borzini, P., Rebulla, P. and Marconi, M., 2011. Treatment of recalcitrant ulcers with allogeneic platelet gel from pooled platelets in aged hypomobile patients. *Biologicals : journal of the International Association of Biological Standardization*, 39(2), pp.73–80.

Guo, H., Jia, Y., Shang, M., Zhang, Y., Xie, F., Wang, H., Yuan, M., Yuan, L. and Ye, J., 2014. Comparison of two in vitro angiogenesis assays for evaluating the effects of netrin-1 on tube formation. *Acta Biochimica et Biophysica Sinica*, 46(9), pp.810–816.

Guo, S., Yu, L., Cheng, Y., Li, C., Zhang, J., An, J., Wang, H., Yan, B., Zhan, T., Cao, Y., Zheng, H. and Li, Z., 2012. PDGFRβ triggered by bFGF promotes the proliferation and migration of endothelial progenitor cells via p-ERK signalling. *Cell Biology International*, 36(10), pp.945–950.

Hamilton, J.R., Nguyen, P.B. and Cocks, T.M., 1998. Atypical protease-activated receptor mediates endothelium-dependent relaxation of human coronary arteries. *Circulation research*, 82(12), pp.1306–1311.

Hansen, C.G., Shvets, E., Howard, G., Riento, K. and Nichols, B.J., 2013. Deletion of cavin genes reveals tissue-specific mechanisms for morphogenesis of endothelial caveolae. *Nature communications*, 4, p.1831.

Hansmann, J., Groeber, F., Kahlig, A., Kleinhans, C. and Walles, H., 2013. Bioreactors in tissue engineering - principles, applications and commercial constraints. *Biotechnology journal*, 8(3), pp.298–307.

Harris, L.J., Abdollahi, H., Zhang, P., McIlhenny, S., Tulenko, T.N. and DiMuzio, P.J., 2011. Differentiation of adult stem cells into smooth muscle for vascular tissue engineering. *The Journal of surgical research*, 168(2), pp.306–314.

Heidari, B., Shirazi, A., Akhondi, M.M., Hassanpour, H., Behzadi, B., Naderi, M.M., Sarvari, A. and Borjian, S., 2013. Comparison of proliferative and multilineage differentiation potential of sheep mesenchymal stem cells derived from bone marrow, liver, and adipose tissue. *Avicenna journal of medical biotechnology*, 5(2), pp.104–117.

Hellberg, C., Ostman, A. and Heldin, C.-H., 2010. PDGF and vessel maturation. *Recent results in cancer research. Fortschritte der Krebsforschung. Progrès dans les recherches sur le cancer*, 180, pp.103–114.

Herrmann, M., Verrier, S. and Alini, M., 2015. Strategies to Stimulate Mobilization and Homing of Endogenous Stem and Progenitor Cells for Bone Tissue Repair. *Frontiers in bioengineering and biotechnology*, 3, p.79.

Heydarkhan-Hagvall, S., Schenke-Layland, K., Yang, J.Q., Heydarkhan, S., Xu, Y., Zuk, P.A., MacLellan, W.R. and Beygui, R.E., 2008. Human adipose stem cells: a potential cell source for cardiovascular tissue engineering. *Cells, tissues, organs*, 187(4), pp.263–274.

Hirotsu, T., Nakayama, K. and Tsujisaka, T., 2002. Plasma surface treatments of melt-extruded sheets of poly (L-lactic acid). *Polymer Engineering ….*

Hirschi, K.K., Ingram, D.A. and Yoder, M.C., 2008. Assessing identity, phenotype, and fate of endothelial progenitor cells. *Arteriosclerosis, Thrombosis, and Vascular Biology*, 28(9), pp.1584–1595.

Hollenberg, M.D., Saifeddine, M., Al-Ani, B. and Kawabata, A., 1997. Proteinase-activated receptors: structural requirements for activity, receptor cross-reactivity, and receptor selectivity of receptor-activating peptides. *Canadian journal of physiology and pharmacology*, 75(7), pp.832–841.

Holthöfer, H., Virtanen, I., Kariniemi, A.L., Hormia, M., Linder, E. and Miettinen, A., 1982. Ulex europaeus I lectin as a marker for vascular endothelium in human tissues. *Laboratory investigation; a journal of technical methods and pathology*, 47(1), pp.60–66.

Hu, G. and Riordan, J.F., 1993. Angiogenin enhances actin acceleration of plasminogen activation. *Biochemical and biophysical research communications*, 197(2), pp.682–687.

Huang, H., Zhao, X., Chen, L., Xu, C., Yao, X., Lu, Y., Dai, L. and Zhang, M., 2006. Differentiation of human embryonic stem cells into smooth muscle cells in adherent monolayer culture. *Biochemical and biophysical research communications*, 351(2), pp.321–327.

Huang, Q. and Sheibani, N., 2008. High glucose promotes retinal endothelial cell migration through activation of Src, PI3K/Akt1/eNOS, and ERKs. *American journal of physiology. Cell physiology*, 295(6), pp.C1647–57.

Huang, R. and Weigand, M., 2008. Plasma etch properties of organic BARCs. *Advances in Resist Materials and Processing Technology XXV*, 6923.

Hur, J., Yoon, C.-H., Kim, H.-S., Choi, J.-H., Kang, H.-J., Hwang, K.-K., Oh, B.-H., Lee, M.-M. and Park, Y.-B., 2004. Characterization of two types of endothelial progenitor cells and their different contributions to neovasculogenesis. *Arteriosclerosis, Thrombosis, and Vascular Biology*, 24(2), pp.288–293.

Ingram, D.A., Mead, L.E., Tanaka, H., Meade, V., Fenoglio, A., Mortell, K., Pollok, K., Ferkowicz, M.J., Gilley, D. and Yoder, M.C., 2004. Identification of a novel hierarchy of endothelial progenitor cells using human peripheral and umbilical cord blood. *Blood*, 104(9), pp.2752–2760.

Inoguchi, H., Kwon, I.K., Inoue, E., Takamizawa, K., Maehara, Y. and Matsuda, T., 2006. Mechanical responses of a compliant electrospun poly(L-lactide-co-epsilon-caprolactone) small-diameter vascular graft. *Biomaterials*, 27(8), pp.1470–1478.

Isenberg, B.C., Williams, C. and Tranquillo, R.T., 2006. Small-diameter artificial arteries engineered in vitro. *Circulation research*, 98(1), pp.25–35.

Italiano, J.E., Lecine, P., Shivdasani, R.A. and Hartwig, J.H., 1999. Blood platelets are assembled principally at the ends of proplatelet processes produced by differentiated megakaryocytes. *The Journal of Cell Biology*, 147(6), pp.1299–1312.

Jang, Y.C., Tsou, R., Gibran, N.S. and Isik, F.F., 2000. Vitronectin deficiency is associated with increased wound fibrinolysis and decreased microvascular angiogenesis in mice. *Surgery*, 127(6), pp.696–704.

Johnson, T.D. and Christman, K.L., 2013. Injectable hydrogel therapies and their delivery strategies for treating myocardial infarction. *Expert opinion on drug delivery*, 10(1), pp.59–72.

Jokinen, V., Suvanto, P. and Franssila, S., 2012. Oxygen and nitrogen plasma hydrophilization and hydrophobic recovery of polymers. *Biomicrofluidics*, 6(1), pp.16501–1650110.

Junkar, I., Vesel, A., Cvelbar, U., Mozetič, M. and Strnad, S., 2009. Influence of oxygen and nitrogen plasma treatment on polyethylene terephthalate (PET) polymers. *Vacuum*, (1), pp.83–85.

Kai, D., Liow, S.S. and Loh, X.J., 2014. Biodegradable polymers for electrospinning: towards biomedical applications. *Materials science & engineering. C, Materials for biological applications*, 45(C), pp.659–670.

Kalka, C., Masuda, H., Takahashi, T., Kalka-Moll, W.M., Silver, M., Kearney, M., Li, T., Isner, J.M. and Asahara, T., 2000. Transplantation of ex vivo expanded endothelial progenitor cells for therapeutic neovascularization. *Proceedings of the National Academy of Sciences of the United States of America*, 97(7), pp.3422–3427.

Kamykowski, G.W., Mosher, D.F., Lorand, L. and Ferry, J.D., 1981. Modification of shear modulus and creep compliance of fibrin clots by fibronectin. *Biophysical chemistry*, 13(1), pp.25–28.

Kang, T.-Y., Lee, J.H., Kim, B.J., Kang, J.-A., Hong, J.M., Kim, B.S., Cha, H.J., Rhie, J.-W. and Cho, D.-W., 2015. In vivo endothelization of tubular vascular grafts through in situ recruitment of endothelial and endothelial progenitor cells by RGD-fused mussel adhesive proteins. *Biofabrication*, 7(1), p.015007.

Kang, Y.S., Kim, W., Huh, Y.H., Bae, J., Kim, J.S. and Song, W.K., 2011. P130Cas attenuates epidermal growth factor (EGF) receptor internalization by modulating EGF-triggered dynamin phosphorylation. *PLoS ONE*, 6(5), p.e20125.

Karamariti, E., Margariti, A., Winkler, B., Wang, X., Hong, X., Baban, D., Ragoussis, J., Huang, Y., Han, J.-D.J., Wong, M.M., Sag, C.M., Shah, A.M., Hu, Y. and Xu, Q., 2013. Smooth muscle cells differentiated from reprogrammed embryonic lung fibroblasts through DKK3 signaling are potent for tissue engineering of vascular grafts. *Circulation research*, 112(11), pp.1433–1443.

Katabathina, V., Menias, C.O., Pickhardt, P., Lubner, M. and Prasad, S.R., 2016. Complications of Immunosuppressive Therapy in Solid Organ Transplantation. *Radiologic clinics of North America*, 54(2), pp.303–319.

Katare, R., Riu, F., Mitchell, K., Gubernator, M., Campagnolo, P., Cui, Y., Fortunato, O., Avolio, E., Cesselli, D., Beltrami, A.P., Angelini, G., Emanueli, C. and Madeddu, P., 2011. Transplantation of human pericyte progenitor cells improves the repair of infarcted heart through activation of an angiogenic program involving micro-RNA-132. *Circulation research*, 109(8), pp.894–906.

Kazarian, S.G. and Chan, K.L.A., 2006. Applications of ATR-FTIR spectroscopic imaging to biomedical samples. *Biochimica et biophysica acta*, 1758(7), pp.858–867.

Kelaini, S., Cochrane, A. and Margariti, A., 2014. Direct reprogramming of adult cells:

avoiding the pluripotent state. *Stem cells and cloning : advances and applications*, 7, pp.19–29.

Kennedy, S.B., Washburn, N.R., Simon, C.G. and Amis, E.J., 2006. Combinatorial screen of the effect of surface energy on fibronectin-mediated osteoblast adhesion, spreading and proliferation. *Biomaterials*, 27(20), pp.3817–3824.

Kern, S., Eichler, H., Stoeve, J., Klüter, H. and Bieback, K., 2006. Comparative analysis of mesenchymal stem cells from bone marrow, umbilical cord blood, or adipose tissue. *STEM CELLS*, 24(5), pp.1294–1301.

Kim, B.S. and Mooney, D.J., 1998. Development of biocompatible synthetic extracellular matrices for tissue engineering. *Trends in biotechnology*, 16(5), pp.224–230.

Kim, C., 2014. Disease modeling and cell based therapy with iPSC: future therapeutic option with fast and safe application. *Blood research*, 49(1), pp.7–14.

Kim, M.J., Kim, J.-H., Yi, G., Lim, S.H., Hong, Y.S. and Chung, D.J., 2008. In vitro and in vivo application of PLGA nanofiber for artificial blood vessel. *Macromolecular research*, 16(4), pp.345–352.

Kim, S., Bell, K., Mousa, S.A. and Varner, J.A., 2000. Regulation of angiogenesis in vivo by ligation of integrin alpha5beta1 with the central cell-binding domain of fibronectin. *The American journal of pathology*, 156(4), pp.1345–1362.

Kim, S.-H., Turnbull, J. and Guimond, S., 2011. Extracellular matrix and cell signalling: the dynamic cooperation of integrin, proteoglycan and growth factor receptor. *The Journal of endocrinology*, 209(2), pp.139–151.

Kishimoto, K., Liu, S., Tsuji, T., Olson, K.A. and Hu, G.-F., 2005. Endogenous angiogenin in endothelial cells is a general requirement for cell proliferation and angiogenesis. *Oncogene*, 24(3), pp.445–456.

Kisucka, J., Butterfield, C.E., Duda, D.G., Eichenberger, S.C., Saffaripour, S., Ware, J., Ruggeri, Z.M., Jain, R.K., Folkman, J. and Wagner, D.D., 2006. Platelets and platelet adhesion support angiogenesis while preventing excessive hemorrhage. *Proceedings of the National Academy of Sciences of the United States of America*, 103(4), pp.855–860.

Klouda, L., Perkins, K.R., Watson, B.M., Hacker, M.C., Bryant, S.J., Raphael, R.M., Kasper, F.K. and Mikos, A.G., 2011. Thermoresponsive, in situ cross-linkable hydrogels based on N-isopropylacrylamide: fabrication, characterization and mesenchymal stem cell encapsulation. *Acta Biomaterialia*, 7(4), pp.1460–1467.

Koh, W., Stratman, A.N., Sacharidou, A. and Davis, G.E., 2008. In vitro three dimensional collagen matrix models of endothelial lumen formation during vasculogenesis and angiogenesis. *Methods in enzymology*, 443, pp.83–101.

Koria, P., 2012. Delivery of growth factors for tissue regeneration and wound healing. *BioDrugs : clinical immunotherapeutics, biopharmaceuticals and gene therapy*, 26(3), pp.163–175.

Kumar Vr, S., Darisipudi, M.N., Steiger, S., Devarapu, S.K., Tato, M., Kukarni, O.P.,

Mulay, S.R., Thomasova, D., Popper, B., Demleitner, J., Zuchtriegel, G., Reichel, C., Cohen, C.D., Lindenmeyer, M.T., Liapis, H., Moll, S., Reid, E., Stitt, A.W., Schott, B., Gruner, S., Haap, W., Ebeling, M., Hartmann, G. and Anders, H.-J., 2016. Cathepsin S Cleavage of Protease-Activated Receptor-2 on Endothelial Cells Promotes Microvascular Diabetes Complications. *Journal of the American Society of Nephrology : JASN*, 27(6), pp.1635–1649.

Kumar, A. and Starly, B., 2015. Large scale industrialized cell expansion: producing the critical raw material for biofabrication processes. *Biofabrication*, 7(4), p.044103.

Kuroda, R., Matsumoto, T., Kawakami, Y., Fukui, T., Mifune, Y. and Kurosaka, M., 2014. Clinical impact of circulating CD34-positive cells on bone regeneration and healing. *Tissue engineering. Part B, Reviews*, 20(3), pp.190–199.

Kurpinski, K., Lam, H., Chu, J., Wang, A., Kim, A., Tsay, E., Agrawal, S., Schaffer, D.V. and Li, S., 2010. Transforming growth factor-beta and notch signaling mediate stem cell differentiation into smooth muscle cells. *STEM CELLS*, 28(4), pp.734–742.

Lai, D., Wang, Y., Sun, J., Chen, Y., Li, T., Wu, Y., Guo, L. and Wei, C., 2015. Derivation and characterization of human embryonic stem cells on human amnion epithelial cells. *Scientific Reports*, 5, p.10014.

Lai, Y., Shen, Y., Liu, X.-H., Zhang, Y., Zeng, Y. and Liu, Y.-F., 2011. Interleukin-8 induces the endothelial cell migration through the activation of phosphoinositide 3-kinase-Rac1/RhoA pathway. *International journal of biological sciences*, 7(6), pp.782–791.

Lang, N., Pereira, M.J., Lee, Y., Friehs, I., Vasilyev, N.V., Feins, E.N., Ablasser, K., O'Cearbhaill, E.D., Xu, C., Fabozzo, A., Padera, R., Wasserman, S., Freudenthal, F., Ferreira, L.S., Langer, R., Karp, J.M. and del Nido, P.J., 2014. A blood-resistant surgical glue for minimally invasive repair of vessels and heart defects. *Science translational medicine*, 6(218), p.218ra6.

Laschke, M.W. and Menger, M.D., 2016. Prevascularization in tissue engineering: Current concepts and future directions. *Biotechnology Advances*, 34(2), pp.112–121.

Lebois, M. and Josefsson, E.C., 2016. Regulation of platelet lifespan by apoptosis. *Platelets*, 27(6), pp.497–504.

Leotot, J., Coquelin, L., Bodivit, G., Bierling, P., Hernigou, P., Rouard, H. and Chevallier, N., 2013. Platelet lysate coating on scaffolds directly and indirectly enhances cell migration, improving bone and blood vessel formation. *Acta Biomaterialia*, 9(5), pp.6630–6640.

Lesman, A., Koffler, J., Atlas, R., Blinder, Y.J., Kam, Z. and Levenberg, S., 2011. Engineering vessel-like networks within multicellular fibrin-based constructs. *Biomaterials*, 32(31), pp.7856–7869.

Levenberg, S., Golub, J.S., Amit, M., Itskovitz-Eldor, J. and Langer, R., 2002. Endothelial cells derived from human embryonic stem cells. *Proceedings of the National Academy of Sciences of the United States of America*, 99(7), pp.4391–4396.

Levengood, S.K.L., Poellmann, M.J., Clark, S.G., Ingram, D.A., Yoder, M.C. and Johnson, A.J.W., 2011. Human endothelial colony forming cells undergo

vasculogenesis within biphasic calcium phosphate bone tissue engineering constructs. *Acta Biomaterialia*, 7(12), pp.4222–4228.

Li, S., Sengupta, D. and Chien, S., 2014. Vascular tissue engineering: from in vitro to in situ. *Wiley interdisciplinary reviews. Systems biology and medicine*, 6(1), pp.61–76.

Li, S., Yu, W. and Hu, G.-F., 2012. Angiogenin inhibits nuclear translocation of apoptosis inducing factor in a Bcl-2-dependent manner. *Journal of cellular physiology*, 227(4), pp.1639–1644.

Li, S., Yu, W., Kishikawa, H. and Hu, G.-F., 2010. Angiogenin prevents serum withdrawal-induced apoptosis of P19 embryonal carcinoma cells. *The FEBS journal*, 277(17), pp.3575–3587.

Li, Z. and Wang, C., 2013. *One-Dimensional nanostructures*. Springer Science & Business Media.

Li, Z., Hu, S., Ghosh, Z., Han, Z. and Wu, J.C., 2011. Functional characterization and expression profiling of human induced pluripotent stem cell- and embryonic stem cell-derived endothelial cells. *Stem cells and development*, 20(10), pp.1701–1710.

Lian, X., Bao, X., Al-Ahmad, A., Liu, J., Wu, Y., Dong, W., Dunn, K.K., Shusta, E.V. and Palecek, S.P., 2014. Efficient differentiation of human pluripotent stem cells to endothelial progenitors via small-molecule activation of WNT signaling. *Stem cell reports*, 3(5), pp.804–816.

Lim, S.H., Cho, S.-W., Park, J.-C., Jeon, O., Lim, J.M., Kim, S.-S. and Kim, B.-S., 2008. Tissue-engineered blood vessels with endothelial nitric oxide synthase activity. *Journal of biomedical materials research. Part B, Applied biomaterials*, 85(2), pp.537–546.

Lin, F., Ren, X.-D., Pan, Z., Macri, L., Zong, W.-X., Tonnesen, M.G., Rafailovich, M., Bar-Sagi, D. and Clark, R.A.F., 2011. Fibronectin growth factor-binding domains are required for fibroblast survival. *The Journal of investigative dermatology*, 131(1), pp.84–98.

Lin, R.-Z., Moreno-Luna, R., Zhou, B., Pu, W.T. and Melero-Martin, J.M., 2012. Equal modulation of endothelial cell function by four distinct tissue-specific mesenchymal stem cells. *Angiogenesis*, 15(3), pp.443–455.

Lin, Y., Weisdorf, D.J., Solovey, A. and Hebbel, R.P., 2000. Origins of circulating endothelial cells and endothelial outgrowth from blood. *The Journal of clinical investigation*, 105(1), pp.71–77.

Liu, S., Yu, D., Xu, Z.-P., Riordan, J.F. and Hu, G.-F., 2001. Angiogenin Activates Erk1/2 in Human Umbilical Vein Endothelial Cells. *Biochemical and biophysical research communications*, 287(1), pp.305–310.

Livak, K.J. and Schmittgen, T.D., 2001. Analysis of relative gene expression data using real-time quantitative PCR and the 2(-Delta Delta C(T)) Method. *Methods (San Diego, Calif.)*, 25(4), pp.402–408.

Loffredo, F. and Lee, R.T., 2008. Therapeutic vasculogenesis: it takes two. *Circulation research*, 103(2), pp.128–130.

Lu, P., Takai, K., Weaver, V.M. and Werb, Z., 2011. Extracellular matrix degradation and remodeling in development and disease. *Cold Spring Harbor perspectives in biology*, 3(12).

Mai, J., Wang, F., Qiu, Q., Tang, B., Lin, Y., Luo, N., Yuan, W., Wang, X., Chen, Q., Wang, J. and Chen, Y., 2014. Tachycardia pacing induces myocardial neovascularization and mobilizes circulating endothelial progenitor cells partly via SDF-1 pathway in canines. *Heart and vessels*, 31(2), pp.230–240.

Majka, S.M., Beutz, M.A., Hagen, M., Izzo, A.A., Voelkel, N. and Helm, K.M., 2005. Identification of novel resident pulmonary stem cells: form and function of the lung side population. *STEM CELLS*, 23(8), pp.1073–1081.

Makadia, H.K. and Siegel, S.J., 2011. Poly Lactic-co-Glycolic Acid (PLGA) as Biodegradable Controlled Drug Delivery Carrier. *Polymers*, 3(3), pp.1377–1397.

Makogonenko, E., Tsurupa, G., Ingham, K. and Medved, L., 2002. Interaction of fibrin(ogen) with fibronectin: further characterization and localization of the fibronectin-binding site. *Biochemistry*, 41(25), pp.7907–7913.

Marasescu, F. and Wertheimer, M., 2008. Nitrogen-Rich Plasma-Polymer Films for Biomedical Applications. *Plasma processes and polymers*, 5(1), pp.44–57.

Margariti, A., Winkler, B., Karamariti, E., Zampetaki, A., Tsai, T.-N., Baban, D., Ragoussis, J., Huang, Y., Han, J.-D.J., Zeng, L., Hu, Y. and Xu, Q., 2012. Direct reprogramming of fibroblasts into endothelial cells capable of angiogenesis and reendothelialization in tissue-engineered vessels. *Proceedings of the National Academy of Sciences of the United States of America*, 109(34), pp.13793–13798.

Marklein, R.A. and Burdick, J.A., 2010. Controlling stem cell fate with material design. *Advanced materials (Deerfield Beach, Fla.)*, 22(2), pp.175–189.

Martin, J., Helm, K., Ruegg, P., Varella-Garcia, M., Burnham, E. and Majka, S., 2008. Adult lung side population cells have mesenchymal stem cell potential. *Cytotherapy*, 10(2), pp.140–151.

Martin, P. and Nunan, R., 2015. Cellular and molecular mechanisms of repair in acute and chronic wound healing. *The British journal of dermatology*, 173(2), pp.370–378.

Martina, M. and Hutmacher, D.W., 2006. Biodegradable polymers applied in tissue engineering research: a review. *Polymer International*, [online] 56(2), pp.145–157. Available at: <http://onlinelibrary.wiley.com/doi/10.1002/pi.2108/full>.

Martino, M.M. and Hubbell, J.A., 2010. The 12th-14th type III repeats of fibronectin function as a highly promiscuous growth factor-binding domain. *FASEB journal : official publication of the Federation of American Societies for Experimental Biology*, 24(12), pp.4711–4721.

Martino, M.M., Briquez, P.S., Ranga, A., Lutolf, M.P. and Hubbell, J.A., 2013. Heparin-binding domain of fibrin(ogen) binds growth factors and promotes tissue repair when incorporated within a synthetic matrix. *Proceedings of the National Academy of Sciences of the United States of America*, 110(12), pp.4563–4568.

Martino, M.M., Brkic, S., Bovo, E., Burger, M., Schaefer, D.J., Wolff, T., Gürke, L.,

Briquez, P.S., Larsson, H.M., Gianni Barrera, R., Hubbell, J.A. and Banfi, A., 2015. Extracellular matrix and growth factor engineering for controlled angiogenesis in regenerative medicine. *Frontiers in bioengineering and biotechnology*, 3, p.45.

Martínez, C.E., Smith, P.C. and Palma Alvarado, V.A., 2015. The influence of platelet-derived products on angiogenesis and tissue repair: a concise update. *Frontiers in physiology*, 6, p.290.

Mazzucco, L., Borzini, P. and Gope, R., 2010. Platelet-derived factors involved in tissue repair-from signal to function. *Transfusion medicine reviews*, 24(3), pp.218–234.

McClure, M.J., Sell, S.A., Ayres, C.E., Simpson, D.G. and Bowlin, G.L., 2009. Electrospinning-aligned and random polydioxanone-polycaprolactone-silk fibroin-blended scaffolds: geometry for a vascular matrix. *Biomedical materials (Bristol, England)*, 4(5), p.055010.

McKee, J.A., Banik, S.S.R., Boyer, M.J., Hamad, N.M., Lawson, J.H., Niklason, L.E. and Counter, C.M., 2003. Human arteries engineered in vitro. *EMBO reports*, 4(6), pp.633–638.

Mead, L.E., Prater, D., Yoder, M.C. and Ingram, D.A., 2008. Isolation and characterization of endothelial progenitor cells from human blood. *Current protocols in stem cell biology*, Chapter 2, p.Unit 2C.1.

Mebratu, Y. and Tesfaigzi, Y., 2009. How ERK1/2 activation controls cell proliferation and cell death: Is subcellular localization the answer? *Cell cycle (Georgetown, Tex.)*, 8(8), pp.1168–1175.

Medina, R.J., O'Neill, C.L., Humphreys, M.W., Gardiner, T.A. and Stitt, A.W., 2010a. Outgrowth endothelial cells: characterization and their potential for reversing ischemic retinopathy. *Investigative ophthalmology & visual science*, 51(11), pp.5906–5913.

Medina, R.J., O'Neill, C.L., O'Doherty, T.M., Wilson, S.E.J. and Stitt, A.W., 2012. Endothelial progenitors as tools to study vascular disease. *Stem cells international*, 2012, p.346735.

Medina, R.J., O'Neill, C.L., Sweeney, M., Guduric-Fuchs, J., Gardiner, T.A., Simpson, D.A. and Stitt, A.W., 2010b. Molecular analysis of endothelial progenitor cell (EPC) subtypes reveals two distinct cell populations with different identities. *BMC medical genomics*, 3, p.18.

Melero-Martin, J.M., De Obaldia, M.E., Kang, S.-Y., Khan, Z.A., Yuan, L., Oettgen, P. and Bischoff, J., 2008. Engineering robust and functional vascular networks in vivo with human adult and cord blood-derived progenitor cells. *Circulation research*, 103(2), pp.194–202.

Migliaresi, C., Ruffo, G.A., Volpato, F.Z. and Zeni, D., 2012. Advanced Electrospinning Setups and Special Fibre and Mesh Morphologies. Electrospinning for Advanced Biomedical Applications and Therapies, pp.23–68.

Milia, A.F., Salis, M.B., Stacca, T., Pinna, A., Madeddu, P., Trevisani, M., Geppetti, P. and Emanueli, C., 2002. Protease-activated receptor-2 stimulates angiogenesis and accelerates hemodynamic recovery in a mouse model of hindlimb ischemia. *Circulation research*, 91(4), pp.346–352.

Mirshahi, F., Pourtau, J., Li, H., Muraine, M., Trochon, V., Legrand, E., Vannier, J., Soria, J., Vasse, M. and Soria, C., 2000. SDF-1 activity on microvascular endothelial cells: consequences on angiogenesis in in vitro and in vivo models. *Thrombosis research*, 99(6), pp.587–594.

Mirza, A., Hyvelin, J.-M., Rochefort, G.Y., Lermusiaux, P., Antier, D., Awede, B., Bonnet, P., Domenech, J. and Eder, V., 2008. Undifferentiated mesenchymal stem cells seeded on a vascular prosthesis contribute to the restoration of a physiologic vascular wall. *Journal of vascular surgery*, 47(6), pp.1313–1321.

Mitchell, S.L. and Niklason, L.E., 2003. Requirements for growing tissue-engineered vascular grafts. *Cardiovascular pathology : the official journal of the Society for Cardiovascular Pathology*, 12(2), pp.59–64.

Mo, M., Wang, S., Zhou, Y., Li, H. and Wu, Y., 2016. Mesenchymal stem cell subpopulations: phenotype, property and therapeutic potential. *Cellular and molecular life sciences : CMLS*, 73(17), pp.3311–3321.

Molino, M., Barnathan, E.S., Numerof, R., Clark, J., Dreyer, M., Cumashi, A., Hoxie, J.A., Schechter, N., Woolkalis, M. and Brass, L.F., 1997. Interactions of mast cell tryptase with thrombin receptors and PAR-2. *The Journal of biological chemistry*, 272(7), pp.4043–4049.

Montenegro, C.F., Salla-Pontes, C.L., Ribeiro, J.U., Machado, A.Z., Ramos, R.F., Figueiredo, C.C., Morandi, V. and Selistre-de-Araujo, H.S., 2012. Blocking alphavbeta3 integrin by a recombinant RGD disintegrin impairs VEGF signaling in endothelial cells. *Biochimie*, 94(8), pp.1812–1820.

Montini-Ballarin, F., Calvo, D., Caracciolo, P.C., Rojo, F., Frontini, P.M., Abraham, G.A. and V Guinea, G., 2016. Mechanical behavior of bilayered small-diameter nanofibrous structures as biomimetic vascular grafts. *Journal of the Mechanical Behavior of Biomedical Materials*, 60, pp.220–233.

Morent, R., De Geyter, N., Gengembre, L., Leys, C., Payen, E., Van Vlierberghe, S. and Schacht, E., 2008. Surface treatment of a polypropylene film with a nitrogen DBD at medium pressure. *The European Physical Journal Applied Physics*, 43(3), pp.289–294.

Mortazavi, S.H., Ghoranneviss, M. and Sari, A.H., 2011. Low Pressure Hexamethyldisiloxane (HMDSO)/Nitrogen Plasma Treatment on the Wettability and Surface Free Energy of Biaxial-Oriented Polypropylene (BOPP) Films. *Journal of Fusion Energy*, 30, pp.83–88.

Munarin, F., Petrini, P., Bozzini, S. and Tanzi, M.C., 2012. New perspectives in cell delivery systems for tissue regeneration: natural-derived injectable hydrogels. *Journal of applied biomaterials & functional materials*, 10(2), pp.67–81.

Mund, J.A., Estes, M.L., Yoder, M.C., Ingram, D.A. and Case, J., 2012. Flow cytometric identification and functional characterization of immature and mature circulating endothelial cells. *Arteriosclerosis, Thrombosis, and Vascular Biology*, 32(4), pp.1045–1053.

Nakagami, H., Nakagawa, N., Takeya, Y., Kashiwagi, K., Ishida, C., Hayashi, S.-I., Aoki, M., Matsumoto, K., Nakamura, T., Ogihara, T. and Morishita, R., 2006. Model of

vasculogenesis from embryonic stem cells for vascular research and regenerative medicine. *Hypertension (Dallas, Tex. : 1979)*, 48(1), pp.112–119.

Nandakumar, A., Tahmasebi Birgani, Z., Santos, D., Mentink, A., Auffermann, N., van der Werf, K., Bennink, M., Moroni, L., van Blitterswijk, C. and Habibovic, P., 2013. Surface modification of electrospun fibre meshes by oxygen plasma for bone regeneration. *Biofabrication*, 5(1), p.015006.

Narayanan, S., 1999. Multifunctional roles of thrombin. *Annals of clinical and laboratory science*, 29(4), pp.275–280.

Ng, K.W., Leong, D.T.W. and Hutmacher, D.W., 2005. The challenge to measure cell proliferation in two and three dimensions. *Tissue engineering*, 11(1-2), pp.182–191.

Nicosia, R.F. and Ottinetti, A., 1990. Growth of microvessels in serum-free matrix culture of rat aorta. A quantitative assay of angiogenesis in vitro. *Laboratory investigation; a journal of technical methods and pathology*, 63(1), pp.115–122.

Nieponice, A., Soletti, L., Guan, J., Deasy, B.M., Huard, J., Wagner, W.R. and Vorp, D.A., 2008. Development of a tissue-engineered vascular graft combining a biodegradable scaffold, muscle-derived stem cells and a rotational vacuum seeding technique. *Biomaterials*, 29(7), pp.825–833.

Novosel, E.C., Kleinhans, C. and Kluger, P.J., 2011. Vascularization is the key challenge in tissue engineering. *Advanced Drug Delivery Reviews*, 63(4-5), pp.300–311.

Nurden, A.T., 2011. Platelets, inflammation and tissue regeneration. *Thrombosis and Haemostasis*, 105 Suppl 1, pp.S13–33.

Nuzzolo, E.R., Capodimonti, S., Martini, M., Iachininoto, M.G., Bianchi, M., Cocomazzi, A., Zini, G., Leone, G., Larocca, L.M. and Teofili, L., 2014. Adult and cord blood endothelial progenitor cells have different gene expression profiles and immunogenic potential. *Blood transfusion = Trasfusione del sangue*, 12 Suppl 1, pp.s367–74.

Nystedt, S., Emilsson, K., Wahlestedt, C. and Sundelin, J., 1994. Molecular cloning of a potential proteinase activated receptor. *Proceedings of the National Academy of Sciences of the United States of America*, 91(20), pp.9208–9212.

Oliveira, C., Costa-Pinto, A.R., Reis, R.L., Martins, A. and Neves, N.M., 2014. Biofunctional nanofibrous substrate comprising immobilized antibodies and selective binding of autologous growth factors. *Biomacromolecules*, 15(6), pp.2196–2205.

Orlando, G., Soker, S. and Stratta, R.J., 2013. Organ bioengineering and regeneration as the new Holy Grail for organ transplantation. *Annals of surgery*, 258(2), pp.221–232.

Orlova, V.V., Drabsch, Y., Freund, C., Petrus-Reurer, S., van den Hil, F.E., Muenthaisong, S., Dijke, P.T. and Mummery, C.L., 2014. Functionality of endothelial cells and pericytes from human pluripotent stem cells demonstrated in cultured vascular plexus and zebrafish xenografts. *Arteriosclerosis, Thrombosis, and Vascular Biology*, 34(1), pp.177–186.

Ortiz-Stern, A., Deng, X., Smoktunowicz, N., Mercer, P.F. and Chambers, R.C., 2012. PAR-1-dependent and PAR-independent pro-inflammatory signaling in human lung

fibroblasts exposed to thrombin. *Journal of cellular physiology*, 227(11), pp.3575–3584.

Owens, C.D., Wake, N., Conte, M.S., Gerhard-Herman, M. and Beckman, J.A., 2009. In vivo human lower extremity saphenous vein bypass grafts manifest flow mediated vasodilation. *Journal of vascular surgery*, 50(5), pp.1063–1070.

Ozawa, C.R., Banfi, A., Glazer, N.L., Thurston, G., Springer, M.L., Kraft, P.E., McDonald, D.M. and Blau, H.M., 2004. Microenvironmental VEGF concentration, not total dose, determines a threshold between normal and aberrant angiogenesis. *The Journal of clinical investigation*, 113(4), pp.516–527.

Park, H., Lee, K.Y., Lee, S.J., Park, K.E. and Park, W.H., 2007. Plasma-treated poly (lactic-co-glycolic acid) nanofibers for tissue engineering. *Macromolecular research*, 15(3), pp.238–243.

Pektok, E., Nottelet, B., Tille, J.-C., Gurny, R., Kalangos, A., Moeller, M. and Walpoth, B.H., 2008. Degradation and healing characteristics of small-diameter poly(epsilon-caprolactone) vascular grafts in the rat systemic arterial circulation. *Circulation*, 118(24), pp.2563–2570.

Perets, A., Baruch, Y., Weisbuch, F., Shoshany, G., Neufeld, G. and Cohen, S., 2003. Enhancing the vascularization of three-dimensional porous alginate scaffolds by incorporating controlled release basic fibroblast growth factor microspheres. *Journal of Biomedical Materials Research Part A*, 65(4), pp.489–497.

Perry, B.C., Zhou, D., Wu, X., Yang, F.-C., Byers, M.A., Chu, T.-M.G., Hockema, J.J., Woods, E.J. and Goebel, W.S., 2008. Collection, cryopreservation, and characterization of human dental pulp-derived mesenchymal stem cells for banking and clinical use. *Tissue Engineering Part C: Methods*, 14(2), pp.149–156.

Petersen, S., Strohbach, A., Busch, R., Felix, S.B., Schmitz, K.-P. and Sternberg, K., 2014. Site-selective immobilization of anti-CD34 antibodies to poly(l-lactide) for endovascular implant surfaces. *Journal of biomedical materials research. Part B, Applied biomaterials*, 102(2), pp.345–355.

Peterson, A.W., Caldwell, D.J., Rioja, A.Y., Rao, R.R., Putnam, A.J. and Stegemann, J.P., 2014. Vasculogenesis and Angiogenesis in Modular Collagen-Fibrin Microtissues. *Biomaterials science*, 2(10), pp.1497–1508.

Peterson, J.E., Zurakowski, D., Italiano, J.E., Michel, L.V., Fox, L., Klement, G.L. and Folkman, J., 2010. Normal ranges of angiogenesis regulatory proteins in human platelets. *American journal of hematology*, 85(7), pp.487–493.

Petter-Puchner, A.H., Fortelny, R.H., Walder, N., Mittermayr, R., Öhlinger, W., van Griensven, M. and Redl, H., 2008. Adverse effects associated with the use of porcine cross-linked collagen implants in an experimental model of incisional hernia repair. *The Journal of surgical research*, 145(1), pp.105–110.

Pi, X., Wu, Y., Ferguson, J.E., Portbury, A.L. and Patterson, C., 2009. SDF-1alpha stimulates JNK3 activity via eNOS-dependent nitrosylation of MKP7 to enhance endothelial migration. *Proceedings of the National Academy of Sciences of the United States of America*, 106(14), pp.5675–5680.

Piccin, A., Di Pierro, A.M., Canzian, L., Primerano, M., Corvetta, D., Negri, G.,

Mazzoleni, G., Gastl, G., Steurer, M., Gentilini, I., Eisendle, K. and Fontanella, F., 2016. Platelet gel: a new therapeutic tool with great potential. *Blood transfusion = Trasfusione del sangue*, pp.1–8.

Podor, T.J., Peterson, C.B., Lawrence, D.A., Stefansson, S., Shaughnessy, S.G., Foulon, D.M., Butcher, M. and Weitz, J.I., 2000. Type 1 plasminogen activator inhibitor binds to fibrin via vitronectin. *The Journal of biological chemistry*, 275(26), pp.19788–19794.

Poncin-Epaillard, F. and Legeay, G., 2003. Surface engineering of biomaterials with plasma techniques. *Journal of biomaterials science. Polymer edition*, 14(10), pp.1005–1028.

Procyk, R. and King, R.G., 1990. The elastic modulus of fibrin clots and fibrinogen gels: the effect of fibronectin and dithiothreitol. *Biopolymers*, 29(3), pp.559–565.

Quent, V.M.C., Loessner, D., Friis, T., Reichert, J.C. and Hutmacher, D.W., 2010. Discrepancies between metabolic activity and DNA content as tool to assess cell proliferation in cancer research. *Journal of cellular and molecular medicine*, 14(4), pp.1003–1013.

Rafii, S., Cao, Z., Lis, R., Siempos, I.I., Chavez, D., Shido, K., Rabbany, S.Y. and Ding, B.-S., 2015. Platelet-derived SDF-1 primes the pulmonary capillary vascular niche to drive lung alveolar regeneration. *Nature cell biology*, 17(2), pp.123–136.

Rahman, S., Patel, Y., Murray, J., Patel, K.V., Sumathipala, R., Sobel, M. and Wijelath, E.S., 2005. Novel hepatocyte growth factor (HGF) binding domains on fibronectin and vitronectin coordinate a distinct and amplified Met-integrin induced signalling pathway in endothelial cells. *BMC cell biology*, 6(1), p.8.

Ramires, P.A., Mirenghi, L., Romano, A.R., Palumbo, F. and Nicolardi, G., 2000. Plasma-treated PET surfaces improve the biocompatibility of human endothelial cells. *Journal of Biomedical Materials Research Part A*, 51(3), pp.535–539.

Rasmussen, J.G., Riis, S.E., Frøbert, O., Yang, S., Kastrup, J., Zachar, V., Simonsen, U. and Fink, T., 2012. Activation of protease-activated receptor 2 induces VEGF independently of HIF-1. *PLoS ONE*, 7(9), p.e46087.

Reed, S. and Wu, B., 2014. Sustained growth factor delivery in tissue engineering applications. *Annals of biomedical engineering*, 42(7), pp.1528–1536.

Reinisch, A., Hofmann, N.A., Obenauf, A.C., Kashofer, K., Rohde, E., Schallmoser, K., Flicker, K., Lanzer, G., Linkesch, W., Speicher, M.R. and Strunk, D., 2009. Humanized large-scale expanded endothelial colony-forming cells function in vitro and in vivo. *Blood*, 113(26), pp.6716–6725.

Rezaie, A.R., 2014. Protease-activated receptor signalling by coagulation proteases in endothelial cells. *Thrombosis and Haemostasis*, 112(5), pp.876–882.

Rhee, J.-S., Black, M., Schubert, U., Fischer, S., Morgenstern, E., Hammes, H.-P. and Preissner, K.T., 2004. The functional role of blood platelet components in angiogenesis. *Thrombosis and Haemostasis*, 92(2), pp.394–402.

Rodríguez, L.V., Alfonso, Z., Zhang, R., Leung, J., Wu, B. and Ignarro, L.J., 2006.

Clonogenic multipotent stem cells in human adipose tissue differentiate into functional smooth muscle cells. *Proceedings of the National Academy of Sciences of the United States of America*, 103(32), pp.12167–12172.

Rohde, E., Malischnik, C., Thaler, D., Maierhofer, T., Linkesch, W., Lanzer, G., Guelly, C. and Strunk, D., 2006. Blood monocytes mimic endothelial progenitor cells. *STEM CELLS*, 24(2), pp.357–367.

Roskoski, R., 2012. ERK1/2 MAP kinases: structure, function, and regulation. *Pharmacological research*, 66(2), pp.105–143.

Rouwkema, J. and Khademhosseini, A., 2016. Vascularization and Angiogenesis in Tissue Engineering: Beyond Creating Static Networks. *Trends in biotechnology*, 34(9), pp.733–745.

Roy, S., Driggs, J., Elgharably, H., Biswas, S., Findley, M., Khanna, S., Gnyawali, U., Bergdall, V.K. and Sen, C.K., 2011. Platelet-rich fibrin matrix improves wound angiogenesis via inducing endothelial cell proliferation. *Wound repair and regeneration : official publication of the Wound Healing Society [and] the European Tissue Repair Society*, 19(6), pp.753–766.

Roy, S.S., Saifeddine, M., Loutzenhiser, R., Triggle, C.R. and Hollenberg, M.D., 1998. Dual endothelium-dependent vascular activities of proteinase-activated receptor-2-activating peptides: evidence for receptor heterogeneity. *British journal of pharmacology*, 123(7), pp.1434–1440.

Rozman, P. and Bolta, Z., 2007. Use of platelet growth factors in treating wounds and soft-tissue injuries. *Acta dermatovenerologica Alpina, Pannonica, et Adriatica*, 16(4), pp.156–165.

Ruf, W., Yokota, N. and Schaffner, F., 2010. Tissue factor in cancer progression and angiogenesis. *Thrombosis research*, 125 Suppl 2, pp.S36–8.

Rufaihah, A.J. and Seliktar, D., 2016. Hydrogels for therapeutic cardiovascular angiogenesis. *Advanced Drug Delivery Reviews*, 96, pp.31–39.

Sa, M.W. and Kim, J.Y., 2013. Effect of various blending ratios on the cell characteristics of PCL and PLGA scaffolds fabricated by polymer deposition system. *International Journal of Precision Engineering and Manufacturing*, 14(4), pp.649–655.

Sahni, A. and Francis, C.W., 2000. Vascular endothelial growth factor binds to fibrinogen and fibrin and stimulates endothelial cell proliferation. *Blood*, 96(12), pp.3772–3778.

Salvay, D.M., Rives, C.B., Zhang, X., Chen, F., Kaufman, D.B., Lowe, W.L. and Shea, L.D., 2008. Extracellular matrix protein-coated scaffolds promote the reversal of diabetes after extrahepatic islet transplantation. *Transplantation*, 85(10), pp.1456–1464.

Sanchis, M.R., Calvo, O., Fenollar, O., Garcia, D. and Balart, R., 2008. Characterization of the surface changes and the aging effects of low-pressure nitrogen plasma treatment in a polyurethane film. *Polymer Testing*, 27(1), pp.75–83.

Sankar, D., Shalumon, K.T., Chennazhi, K.P., Menon, D. and Jayakumar, R., 2014.

Surface plasma treatment of poly(caprolactone) micro, nano, and multiscale fibrous scaffolds for enhanced osteoconductivity. *Tissue Engineering Part A*, 20(11-12), pp.1689–1702.

Sato, T., Abdel-Wahab, M. and Richardt, G., 2015. Very late thrombosis observed on optical coherence tomography 22 months after the implantation of a polymer-based bioresorbable vascular scaffold. *European Heart Journal*, 36(20), p.1273.

Sbaa, E., Dewever, J., Martinive, P., Bouzin, C., Frérart, F., Balligand, J.-L., Dessy, C. and Feron, O., 2006. Caveolin plays a central role in endothelial progenitor cell mobilization and homing in SDF-1-driven postischemic vasculogenesis. *Circulation research*, 98(9), pp.1219–1227.

Schallmoser, K. and Strunk, D., 2009. Preparation of pooled human platelet lysate (pHPL) as an efficient supplement for animal serum-free human stem cell cultures. *Journal of visualized experiments : JoVE*, (32).

Schallmoser, K. and Strunk, D., 2012. Generation of a Pool of Human Platelet Lysate and Efficient Use in Cell Culture. In: *Methods in Molecular Biology*, Methods in Molecular Biology. Totowa, NJ: Humana Press, pp.349–362.

Schallmoser, K., Bartmann, C., Rohde, E., Reinisch, A., Kashofer, K., Stadelmeyer, E., Drexler, C., Lanzer, G., Linkesch, W. and Strunk, D., 2007. Human platelet lysate can replace fetal bovine serum for clinical-scale expansion of functional mesenchymal stromal cells. *Transfusion*, 47(8), pp.1436–1446.

Scheule, A.M., Beierlein, W., Wendel, H.P., Eckstein, F.S., Heinemann, M.K. and Ziemer, G., 1998. Fibrin sealant, aprotinin, and immune response in children undergoing operations for congenital heart disease. *The Journal of thoracic and cardiovascular surgery*, 115(4), pp.883–889.

Schwartz, S.D., Regillo, C.D., Lam, B.L., Eliott, D., Rosenfeld, P.J., Gregori, N.Z., Hubschman, J.-P., Davis, J.L., Heilwell, G., Spirn, M., Maguire, J., Gay, R., Bateman, J., Ostrick, R.M., Morris, D., Vincent, M., Anglade, E., Del Priore, L.V. and Lanza, R., 2015. Human embryonic stem cell-derived retinal pigment epithelium in patients with age-related macular degeneration and Stargardt's macular dystrophy: follow-up of two open-label phase 1/2 studies. *Lancet (London, England)*, 385(9967), pp.509–516.

Seaton, M., Hocking, A. and Gibran, N.S., 2015. Porcine models of cutaneous wound healing. *ILAR journal*, 56(1), pp.127–138.

Segura, I., Serrano, A., De Buitrago, G.G., González, M.A., Abad, J.L., Clavería, C., Gómez, L., Bernad, A., Martínez-A, C. and Riese, H.H., 2002. Inhibition of programmed cell death impairs in vitro vascular-like structure formation and reduces in vivo angiogenesis. *FASEB journal : official publication of the Federation of American Societies for Experimental Biology*, 16(8), pp.833–841.

Seiffert, D. and Schleef, R.R., 1996. Two functionally distinct pools of vitronectin (Vn) in the blood circulation: identification of a heparin-binding competent population of Vn within platelet alpha-granules. *Blood*, 88(2), pp.552–560.

Seifu, D.G., Purnama, A., Mequanint, K. and Mantovani, D., 2013. Small-diameter vascular tissue engineering. *Nature reviews. Cardiology*, 10(7), pp.410–421.

Serra, R., Buffone, G., Dominijanni, A., Molinari, V., Montemurro, R. and de Franciscis, S., 2013. Application of platelet-rich gel to enhance healing of transmetatarsal amputations in diabetic dysvascular patients. *International wound journal*, 10(5), pp.612–615.

Shan, G.-Q., Zhang, Y.-N., Ma, J., Li, Y.-H., Zuo, D.-M., Qiu, J.-L., Cheng, B. and Chen, Z.-L., 2013. Evaluation of the effects of homologous platelet gel on healing lower extremity wounds in patients with diabetes. *The international journal of lower extremity wounds*, 12(1), pp.22–29.

Sieminski, A.L., Hebbel, R.P. and Gooch, K.J., 2012. Improved microvascular network in vitro by human blood outgrowth endothelial cells relative to vessel-derived endothelial cells. *Tissue engineering*, 11(9-10), pp.1332–1345.

Sim, X., Poncz, M., Gadue, P. and French, D.L., 2016. Understanding platelet generation from megakaryocytes: implications for in vitro-derived platelets. *Blood*, 127(10), pp.1227–1233.

Sittampalam, G.S., Coussens, N.P., Nelson, H., Arkin, M., Auld, D., Austin, C., Bejcek, B., Glicksman, M., Inglese, J., Iversen, P.W., Li, Z., McGee, J., McManus, O., Minor, L., Napper, A., Peltier, J.M., Riss, T., Trask, O.J., Weidner, J., Riss, T.L., Moravec, R.A., Niles, A.L., Benink, H.A., Worzella, T.J. and Minor, L., 2004. Cell Viability Assays.

Skottman, H. and Hovatta, O., 2006. Culture conditions for human embryonic stem cells. *Reproduction (Cambridge, England)*, 132(5), pp.691–698.

Smadja, D.M., Bièche, I., Helley, D., Laurendeau, I., Simonin, G., Muller, L., Aiach, M. and Gaussem, P., 2007. Increased VEGFR2 expression during human late endothelial progenitor cells expansion enhances in vitro angiogenesis with up-regulation of integrin alpha(6). *Journal of cellular and molecular medicine*, 11(5), pp.1149–1161.

Smadja, D.M., Bièche, I., Susen, S., Mauge, L., Laurendeau, I., d'Audigier, C., Grelac, F., Emmerich, J., Aiach, M. and Gaussem, P., 2009. Interleukin 8 is differently expressed and modulated by PAR-1 activation in early and late endothelial progenitor cells. *Journal of cellular and molecular medicine*, 13(8B), pp.2534–2546.

Smadja, D.M., Bièche, I., Uzan, G., Bompais, H., Muller, L., Boisson-Vidal, C., Vidaud, M., Aiach, M. and Gaussem, P., 2005. PAR-1 activation on human late endothelial progenitor cells enhances angiogenesis in vitro with upregulation of the SDF-1/CXCR4 system. *Arteriosclerosis, Thrombosis, and Vascular Biology*, 25(11), pp.2321–2327.

Smit, E., Buttner, U. and Sanderson, R.D., 2005. Continuous yarns from electrospun fibers. *Polymer*, 46(8), pp.2419–2423.

Soletti, L., Hong, Y., Guan, J., Stankus, J.J., El-Kurdi, M.S., Wagner, W.R. and Vorp, D.A., 2010. A bilayered elastomeric scaffold for tissue engineering of small diameter vascular grafts. *Acta Biomaterialia*, 6(1), pp.110–122.

Sommeling, C.E., Heyneman, A., Hoeksema, H., Verbelen, J., Stillaert, F.B. and Monstrey, S., 2013. The use of platelet-rich plasma in plastic surgery: a systematic review. *Journal of plastic, reconstructive & aesthetic surgery : JPRAS*, 66(3), pp.301–311.

Spadaccio, C., Rainer, A., Barbato, R., Chello, M. and Meyns, B., 2013. The fate of

large-diameter Dacron® vascular grafts in surgical practice: are we really satisfied? *International journal of cardiology*, 168(5), pp.5028–5029.

Spencer, H.L., Slater, S.C., Rowlinson, J., Morgan, T., Culliford, L.A., Guttridge, M., Emanueli, C., Angelini, G. and Madeddu, P., 2015. A journey from basic stem cell discovery to clinical application: the case of adventitial progenitor cells. *Regenerative medicine*, 10(1), pp.39–47.

Squillaro, T., Peluso, G. and Galderisi, U., 2016. Clinical Trials With Mesenchymal Stem Cells: An Update. *Cell Transplantation*, 25(5), pp.829–848.

Sreerekha, P.R. and Krishnan, L.K., 2006. Cultivation of endothelial progenitor cells on fibrin matrix and layering on dacron/polytetrafluoroethylene vascular grafts. *Artificial organs*, 30(4), pp.242–249.

Starzl, T.E., Demetris, A.J., Trucco, M., Murase, N., Ricordi, C., Ildstad, S., Ramos, H., Todo, S., Tzakis, A. and Fung, J.J., 1993. Cell migration and chimerism after whole-organ transplantation: the basis of graft acceptance. *Hepatology (Baltimore, Md.)*, 17(6), pp.1127–1152.

Staton, C.A., Reed, M.W.R. and Brown, N.J., 2009. A critical analysis of current in vitro and in vivo angiogenesis assays. *International journal of experimental pathology*, 90(3), pp.195–221.

Stratman, A.N. and Davis, G.E., 2012. Endothelial cell-pericyte interactions stimulate basement membrane matrix assembly: influence on vascular tube remodeling, maturation, and stabilization. *Microscopy and microanalysis : the official journal of Microscopy Society of America, Microbeam Analysis Society, Microscopical Society of Canada*, 18(1), pp.68–80.

Stratman, A.N., Schwindt, A.E., Malotte, K.M. and Davis, G.E., 2010. Endothelial-derived PDGF-BB and HB-EGF coordinately regulate pericyte recruitment during vasculogenic tube assembly and stabilization. *Blood*, 116(22), pp.4720–4730.

Su, L.-C., Xu, H., Tran, R.T., Tsai, Y.-T., Tang, L., Banerjee, S., Yang, J. and Nguyen, K.T., 2014. In situ re-endothelialization via multifunctional nanoscaffolds. *ACS nano*, 8(10), pp.10826–10836.

Sun, H., Mei, L., Song, C., Cui, X. and Wang, P., 2006. The in vivo degradation, absorption and excretion of PCL-based implant. *Biomaterials*, 27(9), pp.1735–1740.

Sun, J., Xie, J., Kang, L., Ferro, A., Dong, L. and Xu, B., 2016. Amlodipine Ameliorates Ischemia-Induced Neovascularization in Diabetic Rats through Endothelial Progenitor Cell Mobilization. *BioMed research international*, 2016, p.3182764.

Sur, S., Sugimoto, J.T. and Agrawal, D.K., 2014. Coronary artery bypass graft: why is the saphenous vein prone to intimal hyperplasia? *Canadian journal of physiology and pharmacology*, 92(7), pp.531–545.

Swindle, C.S., Tran, K.T., Johnson, T.D., Banerjee, P., Mayes, A.M., Griffith, L. and Wells, A., 2001. Epidermal growth factor (EGF)-like repeats of human tenascin-C as ligands for EGF receptor. *The Journal of Cell Biology*, 154(2), pp.459–468.

Syeda, F., Grosjean, J., Houliston, R.A., Keogh, R.J., Carter, T.D., Paleolog, E. and

Wheeler-Jones, C.P.D., 2006. Cyclooxygenase-2 induction and prostacyclin release by protease-activated receptors in endothelial cells require cooperation between mitogen-activated protein kinase and NF-kappaB pathways. *The Journal of biological chemistry*, 281(17), pp.11792–11804.

Takahashi, K. and Yamanaka, S., 2006. Induction of pluripotent stem cells from mouse embryonic and adult fibroblast cultures by defined factors. *Cell*, 126(4), pp.663–676.

Tannenbaum, S.E., Tako Turetsky, T., Singer, O., Aizenman, E., Kirshberg, S., Ilouz, N., Gil, Y., Berman-Zaken, Y., Perlman, T.S., Geva, N., Levy, O., Arbell, D., Simon, A., Ben-Meir, A., Shufaro, Y., Laufer, N. and Reubinoff, B.E., 2012. Derivation of Xeno-Free and GMP-Grade Human Embryonic Stem Cells – Platforms for Future Clinical Applications. *PLoS ONE*, 7(6), p.e35325.

Tasev, D., Koolwijk, P. and Hinsbergh, V.W.M.V., 2016. Therapeutic Potential of Human-Derived Endothelial Colony-Forming Cells in Animal Models. *Tissue engineering. Part B, Reviews*, p.ten.teb.2016.0050.

Teo, W.-E., Gopal, R., Ramaseshan, R., Fujihara, K. and Ramakrishna, S., 2007. A dynamic liquid support system for continuous electrospun yarn fabrication. *Polymer*, 48(12), pp.3400–3405.

Thompson, D.F., Letassy, N.A. and Thompson, G.D., 1988. Fibrin glue: a review of its preparation, efficacy, and adverse effects as a topical hemostat. *Drug intelligence & clinical pharmacy*, 22(12), pp.946–952.

Tian, H., Tang, Z., Zhuang, X., Chen, X. and Jing, X., 2012. Biodegradable synthetic polymers: preparation, functionalization and biomedical application. *Progress in Polymer Science*.

Timmermans, F., Van Hauwermeiren, F., De Smedt, M., Raedt, R., Plasschaert, F., De Buyzere, M.L., Gillebert, T.C., Plum, J. and Vandekerckhove, B., 2007. Endothelial outgrowth cells are not derived from CD133+ cells or CD45+ hematopoietic precursors. *Arteriosclerosis, Thrombosis, and Vascular Biology*, 27(7), pp.1572–1579.

Tsujisaka, T., Masuda, T. and Nakayama, K., 2000. Plasma surface treatments and biodegradation of poly (butylene succinate) sheets. *Journal of Applied Polymer Science*, 78(5), pp.1121–1129.

Tucker, N., Stanger, J.J., Staiger, M.P., Razzaq, H. and Hofman, K., 2012. The History of the Science and Technology of Electrospinning from 1600 to 1995. *Journal of Engineered Fibers and Fabrics*, 7, pp.63–73.

Tura, O., Skinner, E.M., Barclay, G.R., Samuel, K., Gallagher, R.C.J., Brittan, M., Hadoke, P.W.F., Newby, D.E., Turner, M.L. and Mills, N.L., 2013. Late outgrowth endothelial cells resemble mature endothelial cells and are not derived from bone marrow. *STEM CELLS*, 31(2), pp.338–348.

Uppanan, P., Thavornyutikarn, B., Kosorn, W., Kaewkong, P. and Janvikul, W., 2015. Enhancement of chondrocyte proliferation, distribution, and functions within polycaprolactone scaffolds by surface treatments. *Journal of Biomedical Materials Research Part A*, 103(7), pp.2322–2332.

Upton, Z., Cuttle, L., Noble, A., Kempf, M., Topping, G., Malda, J., Xie, Y., Mill, J.,

Harkin, D.G., Kravchuk, O., Leavesley, D.I. and Kimble, R.M., 2008. Vitronectin: growth factor complexes hold potential as a wound therapy approach. *The Journal of investigative dermatology*, 128(6), pp.1535–1544.

Uusitalo-Jarvinen, H., Kurokawa, T., Mueller, B.M., Andrade-Gordon, P., Friedlander, M. and Ruf, W., 2007. Role of protease activated receptor 1 and 2 signaling in hypoxia-induced angiogenesis. *Arteriosclerosis, Thrombosis, and Vascular Biology*, 27(6), pp.1456–1462.

Van Craenenbroeck, E.M.F., Conraads, V.M.A., Van Bockstaele, D.R., Haine, S.E., Vermeulen, K., Van Tendeloo, V.F., Vrints, C.J. and Hoymans, V.Y., 2008. Quantification of circulating endothelial progenitor cells: a methodological comparison of six flow cytometric approaches. *Journal of Immunological Methods*, 332(1-2), pp.31–40.

van den Biggelaar, M., Hernández-Fernaud, J.R., van den Eshof, B.L., Neilson, L.J., Meijer, A.B., Mertens, K. and Zanivan, S., 2014. Quantitative phosphoproteomics unveils temporal dynamics of thrombin signaling in human endothelial cells. *Blood*, 123(12), pp.e22–36.

van der Pouw Kraan, T.C.T.M., van der Laan, A.M., Piek, J.J. and Horrevoets, A.J.G., 2012. Surfing the data tsunami, a bioinformatic dissection of the proangiogenic monocyte. *Vascular pharmacology*, 56(5-6), pp.297–305.

van Wachem, P.B., Beugeling, T., Feijen, J., Bantjes, A., Detmers, J.P. and van Aken, W.G., 1985. Interaction of cultured human endothelial cells with polymeric surfaces of different wettabilities. *Biomaterials*, 6(6), pp.403–408.

Vats, A., Tolley, N.S., Bishop, A.E. and Polak, J.M., 2005. Embryonic stem cells and tissue engineering: delivering stem cells to the clinic. *Journal of the Royal Society of Medicine*, 98(8), pp.346–350.

Vaz, C.M., van Tuijl, S., Bouten, C.V.C. and Baaijens, F.P.T., 2005. Design of scaffolds for blood vessel tissue engineering using a multi-layering electrospinning technique. *Acta Biomaterialia*, 1(5), pp.575–582.

Verdonck, P., Calíope, P.B., Hernandez, E. and da Silva, A.N.R., 2006. Plasma etching of electrospun polymeric nanofibres. *Thin Solid Films*.

Viñals, F., Chambard, J.C. and Pouysségur, J., 1999. p70 S6 kinase-mediated protein synthesis is a critical step for vascular endothelial cell proliferation. *The Journal of biological chemistry*, 274(38), pp.26776–26782.

Voyta, J.C., Via, D.P., Butterfield, C.E. and Zetter, B.R., 1984. Identification and isolation of endothelial cells based on their increased uptake of acetylated-low density lipoprotein. *The Journal of Cell Biology*, 99(6), pp.2034–2040.

Vu, T.K., Hung, D.T., Wheaton, V.I. and Coughlin, S.R., 1991. Molecular cloning of a functional thrombin receptor reveals a novel proteolytic mechanism of receptor activation. *Cell*, 64(6), pp.1057–1068.

Walenda, G., Hemeda, H., Schneider, R.K., Merkel, R., Hoffmann, B. and Wagner, W., 2012. Human platelet lysate gel provides a novel three dimensional-matrix for enhanced culture expansion of mesenchymal stromal cells. *Tissue Engineering Part C:*

*Methods*, 18(12), pp.924–934.

Wang, A., Tang, Z., Li, X., Jiang, Y., Tsou, D.A. and Li, S., 2012. Derivation of smooth muscle cells with neural crest origin from human induced pluripotent stem cells. *Cells, tissues, organs*, 195(1-2), pp.5–14.

Wang, J. and Milner, R., 2006. Fibronectin promotes brain capillary endothelial cell survival and proliferation through alpha5beta1 and alphavbeta3 integrins via MAP kinase signalling. *Journal of neurochemistry*, 96(1), pp.148–159.

Wang, Y., Gallant, R.C. and Ni, H., 2016. Extracellular matrix proteins in the regulation of thrombus formation. *Current Opinion in Hematology*, 23(3), pp.280–287.

Wang, Y., Hu, J., Jiao, J., Liu, Z., Zhou, Z., Zhao, C., Chang, L.-J., Chen, Y.E., Ma, P.X. and Yang, B., 2014a. Engineering vascular tissue with functional smooth muscle cells derived from human iPS cells and nanofibrous scaffolds. *Biomaterials*, 35(32), pp.8960–8969.

Wang, Z., Cui, Y., Wang, J., Yang, X., Wu, Y., Wang, K., Gao, X., Li, D., Li, Y., Zheng, X.-L., Zhu, Y., Kong, D. and Zhao, Q., 2014b. The effect of thick fibers and large pores of electrospun poly(ε-caprolactone) vascular grafts on macrophage polarization and arterial regeneration. *Biomaterials*, 35(22), pp.5700–5710.

Wang, Z.Z., Au, P., Chen, T., Shao, Y., Daheron, L.M., Bai, H., Arzigian, M., Fukumura, D., Jain, R.K. and Scadden, D.T., 2007. Endothelial cells derived from human embryonic stem cells form durable blood vessels in vivo. *Nature biotechnology*, 25(3), pp.317–318.

Wei, Q., Becherer, T., Angioletti-Uberti, S., Dzubiella, J., Wischke, C., Neffe, A.T., Lendlein, A., Ballauff, M. and Haag, R., 2014. Protein interactions with polymer coatings and biomaterials. *Angewandte Chemie (International ed. in English)*, 53(31), pp.8004–8031.

Wei, S., Gao, X., Du, J., Su, J. and Xu, Z., 2011. Angiogenin enhances cell migration by regulating stress fiber assembly and focal adhesion dynamics. *PLoS ONE*, 6(12), p.e28797.

Whited, B.M. and Rylander, M.N., 2014. The influence of electrospun scaffold topography on endothelial cell morphology, alignment, and adhesion in response to fluid flow. *Biotechnology and Bioengineering*, 111(1), pp.184–195.

Wijelath, E.S., Murray, J., Rahman, S., Patel, Y., Ishida, A., Strand, K., Aziz, S., Cardona, C., Hammond, W.P., Savidge, G.F., Rafii, S. and Sobel, M., 2002. Novel vascular endothelial growth factor binding domains of fibronectin enhance vascular endothelial growth factor biological activity. *Circulation research*, 91(1), pp.25–31.

Wilson, C.J., Clegg, R.E., Leavesley, D.I. and Pearcy, M.J., 2005. Mediation of biomaterial-cell interactions by adsorbed proteins: a review. *Tissue engineering*, 11(1-2), pp.1–18.

Woo, K.M., Chen, V.J. and Ma, P.X., 2003. Nano-fibrous scaffolding architecture selectively enhances protein adsorption contributing to cell attachment. *Journal of Biomedical Materials Research Part A*, 67(2), pp.531–537.

Woodruff, M.A. and Hutmacher, D.W., 2010. The return of a forgotten polymer—polycaprolactone in the 21st century. *Progress in Polymer Science*, 35(10), pp.1217–1256.

Xie, C.-Q., Zhang, J., Villacorta, L., Cui, T., Huang, H. and Chen, Y.E., 2007. A highly efficient method to differentiate smooth muscle cells from human embryonic stem cells. *Arteriosclerosis, Thrombosis, and Vascular Biology*, 27(12), pp.e311–2.

Xu, Z., Wan, L. and Huang, X., 2009. Surface Modification by Graft Polymerization. In: *link.springer.com*, Advanced Topics in Science and Technology in China. Berlin, Heidelberg: Springer Berlin Heidelberg, pp.80–149.

Yan, D., Jones, J., Yuan, X.Y., Xu, X.H., Sheng, J., Lee, J.C.M., Ma, G.Q. and Yu, Q.S., 2013. Plasma treatment of electrospun PCL random nanofiber meshes (NFMs) for biological property improvement. *Journal of Biomedical Materials Research Part A*, 101(4), pp.963–972.

Yang, J., Bei, J. and Wang, S., 2002. Enhanced cell affinity of poly (D,L-lactide) by combining plasma treatment with collagen anchorage. *Biomaterials*, 23(12), pp.2607–2614.

Yang, W., Yang, F., Wang, Y., Both, S.K. and Jansen, J.A., 2013. In vivo bone generation via the endochondral pathway on three-dimensional electrospun fibers. *Acta Biomaterialia*, 9(1), pp.4505–4512.

Yin, Y., Huang, L., Zhao, X., Fang, Y., Yu, S., Zhao, J. and Cui, B., 2007. AMD3100 mobilizes endothelial progenitor cells in mice, but inhibits its biological functions by blocking an autocrine/paracrine regulatory loop of stromal cell derived factor-1 in vitro. *Journal of cardiovascular pharmacology*, 50(1), pp.61–67.

Yoder, M.C., 2009. Defining human endothelial progenitor cells. *Journal of thrombosis and haemostasis : JTH*, 7 Suppl 1, pp.49–52.

Yoder, M.C., Mead, L.E., Prater, D., Krier, T.R., Mroueh, K.N., Li, F., Krasich, R., Temm, C.J., Prchal, J.T. and Ingram, D.A., 2007. Redefining endothelial progenitor cells via clonal analysis and hematopoietic stem/progenitor cell principals. *Blood*, 109(5), pp.1801–1809.

Yoo, H.S., Kim, T.G. and Park, T.G., 2009. Surface-functionalized electrospun nanofibers for tissue engineering and drug delivery. *Advanced Drug Delivery Reviews*, 61(12), pp.1033–1042.

Yoon, C.-H., Hur, J., Park, K.-W., Kim, J.-H., Lee, C.-S., Oh, I.-Y., Kim, T.-Y., Cho, H.-J., Kang, H.-J., Chae, I.-H., Yang, H.-K., Oh, B.-H., Park, Y.-B. and Kim, H.-S., 2005. Synergistic neovascularization by mixed transplantation of early endothelial progenitor cells and late outgrowth endothelial cells: the role of angiogenic cytokines and matrix metalloproteinases. *Circulation*, 112(11), pp.1618–1627.

Young, H.E., Steele, T.A., Bray, R.A., Hudson, J., Floyd, J.A., Hawkins, K., Thomas, K., Austin, T., Edwards, C., Cuzzourt, J., Duenzl, M., Lucas, P.A. and Black, A.C., 2001. Human reserve pluripotent mesenchymal stem cells are present in the connective tissues of skeletal muscle and dermis derived from fetal, adult, and geriatric donors. *The Anatomical record*, 264(1), pp.51–62.

Yun, H.-J. and Jo, D.-Y., 2003. Production of stromal cell-derived factor-1 (SDF-1)and expression of CXCR4 in human bone marrow endothelial cells. *Journal of Korean medical science*, 18(5), pp.679–685.

Zambon, J.P., de Sá Barretto, L.S., Nakamura, A.N.S.E., Duailibi, S., Leite, K., Magalhaes, R.S., Orlando, G., Ross, C.L., Peloso, A. and Almeida, F.G., 2014. Histological changes induced by Polyglycolic-Acid (PGA) scaffolds seeded with autologous adipose or muscle-derived stem cells when implanted on rabbit bladder. *Organogenesis*, 10(2), pp.278–288.

Zanotelli, M.R., Ardalani, H., Zhang, J., Hou, Z., Nguyen, E.H., Swanson, S., Nguyen, B.K., Bolin, J., Elwell, A., Bischel, L.L., Xie, A.W., Stewart, R., Beebe, D.J., Thomson, J.A., Schwartz, M.P. and Murphy, W.L., 2016. Stable engineered vascular networks from human induced pluripotent stem cell-derived endothelial cells cultured in synthetic hydrogels. *Acta Biomaterialia*, 35, pp.32–41.

Zheng, H., Dai, T., Zhou, B., Zhu, J., Huang, H., Wang, M. and Fu, G., 2008. SDF-1alpha/CXCR4 decreases endothelial progenitor cells apoptosis under serum deprivation by PI3K/Akt/eNOS pathway. *Atherosclerosis*, 201(1), pp.36–42.

Zheng, H., Fu, G., Dai, T. and Huang, H., 2007. Migration of endothelial progenitor cells mediated by stromal cell-derived factor-1alpha/CXCR4 via PI3K/Akt/eNOS signal transduction pathway. *Journal of cardiovascular pharmacology*, 50(3), pp.274–280.

Zhu, J. and Clark, R.A.F., 2014. Fibronectin at select sites binds multiple growth factors and enhances their activity: expansion of the collaborative ECM-GF paradigm. *The Journal of investigative dermatology*, 134(4), pp.895–901.

Zhu, J. and Marchant, R.E., 2011. Design properties of hydrogel tissue-engineering scaffolds. *Expert review of medical devices*, 8(5), pp.607–626.

Zhuang, G., Yu, K., Jiang, Z., Chung, A., Yao, J., Ha, C., Toy, K., Soriano, R., Haley, B., Blackwood, E., Sampath, D., Bais, C., Lill, J.R. and Ferrara, N., 2013. Phosphoproteomic analysis implicates the mTORC2-FoxO1 axis in VEGF signaling and feedback activation of receptor tyrosine kinases. *Science signaling*, 6(271), p.ra25.

Zimrin, A.B., Villeponteau, B. and Maciag, T., 1995. Models of in vitro angiogenesis: endothelial cell differentiation on fibrin but not matrigel is transcriptionally dependent. *Biochemical and biophysical research communications*, 213(2), pp.630–638.

# Appendix

## Publications

**Fortunato T.M.**, Beltrami C., Emanueli C., De Bank P.A., Pula G., 2016. Platelet lysate gel and endothelial progenitors stimulate capillary formation in vitro: implications for tissue engineering. *Scientific Reports*. 6**,** 25326

**Fortunato T.M.**, Vara D.S., Wheeler-Jones C.P., Pula G., 2014. Expression of protease-activated receptor 1 and 2 and anti-tubulogenic activity of protease-activated receptor 1 in human endothelial colony-forming cells. *PLOS ONE*, 9 (10), e109375.

## Conference proceedings

Pula G., **Fortunato T.M.**, De Bank P.A., 2015. Human platelet lysate gel (hPLG) supports and stimulates endothelial progenitor cell-driven vasculogenesis. *Journal of Thrombosis and Haemostasis*. 13 (Suppl. 2), 271

**Fortunato T.M.**, De Bank P.A., Pula G., 2015. Human Platelet Lysate Gel as a Substrate for Isolation and Delivery of Endothelial Colony-Forming Cells. *Journal of Vascular Research*, 52 (Suppl. 1), 12

## Awards

Images of Research 2016 – Best Overall Entry - University of Bath (2016)

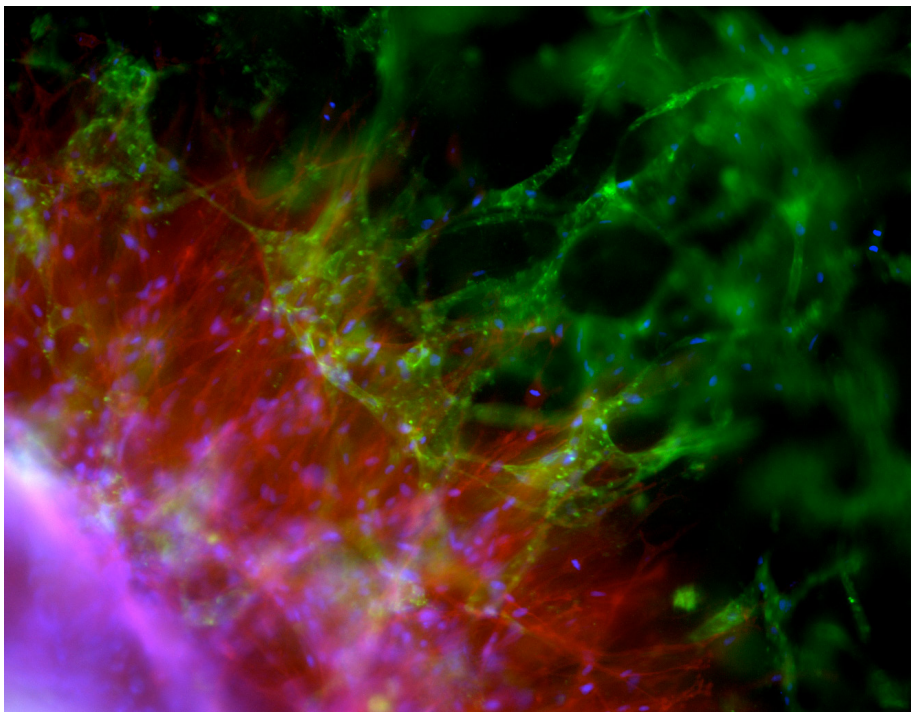

# Touch base

Tiago Fortunato, Department of Pharmacy & Pharmacology
Dr Paul De Bank, Department of Pharmacy & Pharmacology
Dr Giordano Pula, Department of Pharmacy & Pharmacology

When it comes to regenerating tissues, time is of the essence and promiscuity is a must - networking is all that matters. The recent emergence of lab-grown tissues and organs has posed a new challenge; their survival after implantation into the human body. It is vital to establish a swift connection between the host blood vessels and the implant.

In our lab, we are studying ways of promoting this “speed dating” of vascular networks by harnessing our own bodies’ tools. We have developed an injectable hydrogel derived from human blood platelets to stimulate and support this biological tête-à-tête, creating an off-the-shelf and animal-free approach.

Here, lab-engineered human capillaries (in green) derived from stem cells are caught in the act of “making contact” with the sprouts protruding from a rat aorta (in red) in a bed of platelet hydrogel, documenting the, not so shy, first stages of recognition and interaction.

research matters

UNIVERSITY OF BATH
go.bath.ac.uk/ior